

**Studies on the role of peroxisome proliferators:
in liver growth and neurodegenerative disorders**

By

Fikry A. A. Abushofa B.Sc., M.Sc.

Thesis submitted to the University of Nottingham for the degree of
Doctor of Philosophy

September 2013

DEDICATION

I would like to dedicate this thesis to the memory of my father, Ali Abushofa, who sadly passed away in 2011 during the course of my studies, and my supervisor Terry Parker who also very sadly passed away in the final months of my PhD studies.

Abstract

This thesis is divided into two main chapters. The first chapter relates to studies undertaken to gain insights into the mechanism of action on liver growth by the peroxisome proliferator (PP) ciprofibrate and the chemical cyproterone acetate (CPA) in rodents. Peroxisome proliferators are a class of chemicals that have diverse effects in rats and mice including increased DNA synthesis and peroxisome proliferation. Peroxisome proliferators include herbicides, plasticisers, hypolipidemic drugs and synthetic fatty acids. These chemicals act through ligand activation of nuclear membrane receptors termed 'peroxisome-proliferator-activated receptors' (PPARs), which ultimately activate nuclear transcription.

PPs induce a cellular process in liver characterised by dramatic increases in the size and number of peroxisomes, correlated with both hepatocyte hypertrophy (i.e. an increase in the size of liver cells) and hyperplasia (i.e. an increase in the number of liver cells during replicative DNA synthesis and cell division). However, the mechanism of action of increased hepatocyte growth is not currently understood. Understanding the mechanism by which increased liver growth is induced by PPs in rodents will hopefully provide insights into how natural liver growth occurs and might have medical benefits for human health if the mechanism of PP toxicity can be overcome. Knowledge gained from the mechanism of PP activation might also then be applied to other chemical carcinogens. Therefore, firstly the mode of action of the peroxisome proliferator ciprofibrate was investigated. Previous work had indicated that two successive doses of ciprofibrate treatment separated by 24hr led to two rounds of liver cell replication, but it was not clear whether the same or different hepatocytes were involved in this growth response. To study this phenomenon, histochemical experimental work was undertaken to assess whether the same or different hepatocyte cells were stained during the two rounds of cell division following ciprofibrate treatment. The two histochemical stains used were EdU and BrdU, which are both base-pair analogues that stain nuclei undergoing DNA replication. It was hypothesized that if EdU was used to stain cells at 24 hr and then

BrdU at 48 hr, that if the same cells were responding to ciprofibrate treatment then cells would be co-stained by both dyes, whereas if different cells were responding then there would be little or no double staining of hepatocyte cells. It was found that different cells were stained by the two dyes, indicating that ciprofibrate treatment was targeting different cells. Secondly, the mode of action of the carcinogen cyproterone acetate (CPA) on hepatocyte growth was investigated. Previous work had investigated the effects of CPA on hepatocyte growth in male and female rats and had suggested differences in response between the sexes. In the present study female rats were treated with CPA, to assess whether differences in labelling indices were present compared to previous male results. Female F-344/NHsd rats, aged 14-15 weeks, were treated with CPA and then injected with BrdU at 22 hr, and rats were killed 2 hr later. Results confirmed that the female rats had a considerably higher labelling index (50%) compared to male rats (6%). This suggested that upregulation of gene expression in female rats was much higher, which might provide an exciting opportunity to identify sets of genes involved in carcinogenic responses. To investigate whether there was any overlap between genes induced by ciprofibrate and CPA treatment a preliminary study was designed where female rats were gavaged with CPA and then killed 3 hr later. Real-time PCR analysis of a small number of target genes showed no consistent changes in expression between the present CPA and previous ciprofibrate treatment results, suggesting largely different modes of action of these chemicals.

The second chapter of this thesis relates to studies undertaken to gain insights into neurodegenerative disorders. Neurodegeneration is a gradual loss of structure or function of neurons, which may lead to neuronal death. Neurodegenerative diseases including Parkinson's, Alzheimer's, and Huntington's occur as a result of neurodegenerative changes. Several studies have suggested that PPARs have critical roles in reducing the brain inflammation which in turn might have a significant effect on reducing the fundamental processes involved. Work was performed using a mouse model of dementia with lewy body disease ($Psmc^{1fl/fl}$; $CaMKII\alpha$ -Cre) to represent neurodegenerative disorder, and involved parallel, *in vivo* and *in vitro* investigations to determine whether the development of neurodegenerative diseases occurs at the same rate *in vitro* and *in vivo* i.e. a comparison of rapidity of

pathogenicity progression was made. Astrocytes were used to track the development of disease, given that these play a key role in neurological disorders, using an immunohistochemistry approach. A PPAR- γ analogue was used to investigate the role of PPARs in reducing astrocytes proliferation. To optimise the validity of the results, four controls were used including an antagonist T0070907 which abolished the effect of rosiglitazone treatment alone. The results on the effect of PPAR- γ agonist and rosiglitazone, after a week of treatment, showed that the PPAR- γ agonist inhibited astrocytes activation in both the cortex and hippocampus of the mutant mice organotypic slice culture. The number of GFAP⁺ve astrocytes was significantly decreased in mutant mice with 100 μ M rosiglitazone in both areas, whereas 50 μ M rosiglitazone showed a decrease in the number of astrocytes in the cortex, but the effect was less in the region of the hippocampus. This finding suggests that PPs such as rosiglitazone may have potential uses as therapeutic drugs to inhibit neurodegeneration.

Acknowledgments

I would like to thank my former supervisor Dr. David Bell who has helped and supported me during the first 15 months of the project.

I would also like to express my sincere thanks to my supervisor Dr. Terry Parker who took over supervision responsibilities after David Bell left.

I would like to thank Dr. Paul Dyer who took responsibility for supervision during the period between the leaving of Dr. Bell and the start of actual supervision by Dr. Parker, and assisted with preparation of the thesis. I wish to acknowledge Dr. Lynn Bedford my second supervisor for her supporting of me and provide the mice model.

Also many thanks to Annabelle Chambers for her help with proofreading of part II of my thesis. In addition I wish to thank my thesis examiners, Profs. Dave Kendall and Helen Fillmore for their comments and assistance with amendment of the thesis.

Special thanks also go to Declan Brady and Sue (the lab's technicians) for all of their help. Further thanks go to my university (University of Zawia) that supported my project financially.

Finally, I would like to thank my family, my wife, my kids and my colleagues (PhD students).

DECLARATION

I declare, that this work has been achieved in the duration of my PhD studies at the University of Nottingham, and is my original effort unless otherwise stated. Information from other resources has been fully recognized.

No part of this thesis has been submitted for assessment leading to another degree.

FIKRY ALI ABUSHOFA

Table of Contents

Part 1	32
The role of peroxisome proliferators in liver growth.....	32
1. Introduction - Review of Literature	33
1.1 The Liver	33
1.1.1 Liver cells.....	33
1.1.2 The liver cell cycle	35
1.1.3 Liver growth and its regeneration	37
1.1.4 Control of liver growth.....	37
1.2 Peroxisome proliferation.....	38
1.2.1 Peroxisomes	38
1.2.2 Peroxisome proliferators	38
1.2.3 Cyproterone acetate.....	40
1.2.4 Ciprofibrate (peroxisome proliferators) compared to Cyproterone acetate (CPA)	42
1.2.5 Induction of hepatic DNA synthesis by cyproterone acetate	43
1.2.6 Inducing the expression of hepatic Cytochrome P ₄₅₀	43
1.2.7 Effect of CPA (PXR) ligands on hepatic DNA synthesis.....	45
1.2.8 Hepatic CYP450 gene expression by Peroxisome proliferators and cyproterone acetate.....	46
1.3 Previous Work Leading to the Present Study	47
1.4 The hypotheses and aims of the first part of the current project: liver cell growth	50
2. Materials and methods	52
2.1 Materials	52

2.1.1	Animals	52
2.1.2	Chemicals	52
2.1.3	EdU chemistry materials	54
2.1.4	Total RNA isolation	55
2.1.5	Other chemicals and instruments	56
2.2	Methods	57
2.2.1	Experimental Design	57
2.2.2	Time course protocol of effects of 50 mg/kg/day ciprofibrate	59
2.2.3	Measuring dual labelling of liver hepatocytes	63
2.2.4	Time course protocol of effects 100 mg/kg CPA	64
2.2.5	Tissue processing	66
2.2.6	Detecting DNA synthesis and cell cycle population.....	66
2.2.7	Statistics	67
2.2.8	Real – time PCR materials	67
3.	Results	70
3.1	Validation of Methodology	70
3.1.1	Detection of EdU and BrdU	70
3.1.2	Optimisation of the dose of EdU to monitor hepatic DNA synthesis	74
3.1.3	Investigation of EdU doses to monitor hepatic DNA synthesis.....	77
3.1.4	Preliminary work for dual labelling of treated cells.....	79
3.1.4	Induction of hepatic DNA synthesis by ciprofibrate in male F-344/NHsd rats	82
3.1.5	Using base analogue stains EdU and BrdU.....	87
3.1.6	Comparison of induction of DNA synthesis by EdU and BrdU staining .	90
3.1.7	Use of both EdU and BrdU to distinguish if the two peaks of cell division are related	97

3.1.8	Percentage of hepatocytes labelled with EdU and BrdU after induction with 50 mg/kg ciprofibrate.....	102
3.2	Induction of DNA synthesis induced by CPA (PXR).....	103
3.2.1	Effect of CPA (PXR) ligands on hepatic DNA synthesis in female Fischer rats	104
3.2.2	Early induction of DNA synthesis by CPA in female F-344 /NHsd rats	107
3.2.3	Real time PCR results of CPA induction	109
3.2.4	Effects of CPA on <i>CY3A1</i> gene expression	112
3.2.5	Effects of CPA on sterol-coenzyme A - desaturase 1 (<i>Scd1</i>) gene expression.....	113
3.2.6	Effects of CPA on cyclin D1 (<i>Ccnd1</i>) gene expression.....	114
3.2.7	Effects of CPA on expression of <i>G0s2</i> gene involved with G0/G1 switching	115
4.	Discussion	116
4.2	Rationale and method validation.....	116
4.1.1	Optimisation of Hoechst dye concentration.....	116
4.1.2	Assessment of immunohistochemistry protocol	117
4.1.3	Optimisation of the dose of the EdU.....	118
4.1.4	Using base analogue stains EdU and BrdU.....	119
4.1.5	Use of both EdU and BrdU to distinguish if the two peaks of DNA replication and cell division are related	119
4.1.6	Percentage of labelled hepatocytes in liver.....	120
4.2.1	Effect of PXR ligands on hepatic DNA synthesis in female rats dosed with CPA:.....	120
4.2.2	Induction of hepatic DNA synthesis by CPA (PXR).....	121
4.2.3	Effect of PXR ligands on hepatic DNA synthesis in female Fisher rats.	122
4.2.4	Effect of CPA on <i>CYP3A1</i> gene expression	123

4.2.5 Effect of CPA on <i>Scd1</i>	124
4.2.6 Effect of CPA on <i>Ccnd1</i>	124
4.2.7 Effect of CPA on <i>G0s2</i>	126
5. CONCLUSION	127
Part 2	130
The role of peroxisome proliferators in a model of a neurodegenerative disorder..	130
6. Introduction - Review of Literature	131
6.1 Introduction to part two.....	131
6.1.1 The nervous system.....	132
6.2.1 Neuroglia (glial cells).....	138
6.2.2 Fundamental functions of astrocytes.....	141
6.2.3 Gliosis	142
6.2.4 Mechanism of action of gliosis (proliferation of astrocytes)	142
6.2.5 Role of astrocyte in promotes neuronal survival.....	144
6.2.6 Reactivation of astrocytes during CNS injury	144
6.3 Neurodegenerative diseases	145
6.3.1 Anti-Inflammatory role of PPARs in neurodegenerative disorders.....	145
6.3.2 Neuro-inflammation in parkinsons' disease (PD), Alzheimer (AD) and Sclerosis	146
6.4 Peroxisome proliferator-activated receptors (PPARs) in the brain.....	149
6.5 Aims of project part 2	151
7. Materials and method.....	152
7.1Materials.....	152
7.1.1Animals	152
7.1.2 Immunohistochemistry materials.....	154
7.1.3 Culture mediums	154

7.1.4	Chemicals and instruments	154
7.1.5	Inserts and slide types	155
7.1.6	Mounting medium.....	155
7.1.7	Peroxisome proliferator-activated receptor gamma (PPAR- γ) agonist and antagonist	156
7.1.8	Microscopes	156
7.1.9	Statistics	156
7.2	Methodology	157
7.2.1	Sample preparation.....	157
7.2.2	Determination of area of interest using a box dividing protocol	158
7.2.3	Organotypic Slice Culture.....	159
7.2.4	Tissue fixation of organotypic slices.....	161
7.2.5	H&E staining.....	161
7.2.6	Distinguishing between a mutant and control animals using DNAreleasey technique to release gDNA	162
7.2.7	Immunohistochemistry.....	164
7.3.1	Image-J program for calculating the number of astrocytes.....	167
7.4.1	Resazurin cell viability assay	170
7.5.1	Effect of PPAR- γ agonist rosiglitazone on the reduction of astrocyte proliferation.....	170
8.	Results	172
8.1	Immunohistochemistry validation.....	172
8.1.1	Validation of GFAP marker to stain astrocytes of paraffin sections	172
8.1.2	Optimising GFAP primary antibodies to stain astrocytes of rat and mouse paraffin sections	175

8.1.3 Examining the impact of gasket thickness on clarity of image resolution for organotypic slice cultures	177
8.2.1 The differences between the staining of astrocytes in the brains of mice between fluorescent with fluorescent Rhodamine and DAB markers	179
8.3.1 Determining the genotype of mouse pups.....	182
8.4.1 Astrocyte detection in organotypic slice cultures technique.....	183
8.4.2 Optimisations to improve immunohistochemical protocol.....	186
8.4.3 Validation of the use organotypic slice cultures to observe astrocytes, and detect proliferation.	187
8.5.1 Creating cryostat and paraffin sections from organotypic slice culture..	193
8.5.2 Morphology of brain tissue in paraffin sections using haematoxylin and eosin staining.....	197
8.6 Neurodegenerative disease.....	199
8.6.1 Progression of neurological disease <i>in vivo</i>	199
8.6.2 Effect of PPAR- γ agonist on astrocyte population in Dementia with Lewy Body Model.....	207
8.6.3 Expressing astrocyte numbers as a percentage of the controls	226
9. Discussion	230
9.1 Methodology validation	230
9.1.1 Assessment of the use of immunohistochemistry to detect astrocytes ...	230
9.1.2 The development of neurodegenerative diseases <i>in vivo</i>	231
9.1.3 Evaluating the use of organotypic slice cultures study neurodegenerative diseases.....	232
9.2 Peroxisome proliferator activated receptor- γ agonists.....	235
9.2.1 Rosiglitazone (Peroxisome proliferator activated receptor- γ agonist) may be effective in the treatment of human diseases.....	235
9.3 Conclusion	238

Part 3	239
GENERAL DISCUSSION.....	239
10. General discussion	240
10.1 Role of peroxisome proliferators in liver growth.....	240
10.2 Role of peroxisome proliferators in neurodegenerative disorders	242
11. Future work	243
11.1 Studies on PP and CPA toxicity and mode of action.....	243
11.2 Studies on role of PPs in neurodegenerative disorders	243
12. References	245
13. Appendixes.....	269

List of Figures

Figure 1-1 Illustration of the arrangement of liver cells in a lobule:	34
Figure 1-2 Cartoon illustration of cell cycle:	36
Figure 1-3 Chemical formula and structure of cyproterone acetate.....	41
Figure 1-4; Diagram showing the mechanism of action of various P450 transcription factors.....	44
Figure 1-5 Schematic diagram of PXR binding to DNA as a heterodimer with RXR:	45
Figure 1-6 Time course showing change in labelling index following treatment with 50 mg/kg/day ciprofibrate compared to labelling index of control corn oil treatment.	49
Figure 2-1 Enzyme-labelled secondary antibody reaction with primary antibody bound to tissue antigen.....	53
Figure 2-2 Schematic of the click reaction for detecting EdU incorporated into cellular DNA.	54
Figure 2-3 Schematic showing different injection treatments, either BrdU or EdU, and relative time of killing of animals.	58
Figure 2-4 Time course of the effects of control corn oil treatment on hepatic DNA synthesis in male F-344/NHsd rats aged 14-15 weeks.	60
Figure 2-5 Time course of procedures for treatment of rats in control vehicle group 3	61
Figure 2-6, A and B: Time course of effects of treatment with 50 mg/kg ciprofibrate on hepatic DNA synthesis in male F-344/NHsd rats aged 14-15 weeks.	61
Figure 2-7 C: Time course of effects of treatment with 50 mg/kg ciprofibrate on hepatic DNA synthesis in male F-344/NHsd rats aged 14-15 weeks in treatment group 3.	62
Figure 2-8; A and B Time course of effects of 100 mg/kg CPA treatment on hepatic DNA synthesis in female F-344/NHds rats aged 14-15 weeks.....	64

Figure 2-9, A and B time course of effects of 100 mg/kg CPA treatment on hepatic DNA synthesis in female F-344/NHds rats aged 14-15 weeks.....	65
Figure 3-1 Optimisation of Hoechst dye staining: Paraffin sections were harvested from the liver of a F-344 rat aged 7-8 weeks.	71
Figure 3-2 Optimisation of concentration of PBS washing solution for staining procedures	72
Figure 3-3 Assessment of BrdU immunohistochemistry protocol:	73
Figure 3-4 Assessment of use of different doses of EdU to evaluate hepatic DNA synthesis:	75
Figure 3-5 Assessment of EdU staining in BrdU control treated tissue	76
Figure 3-6; Liver weight to body weight ratio (%) resulting from treatment with three different EdU concentrations.	78
Figure 3-7 Assessing the effect of using Hoechst alongside haematoxylin stain:	80
Figure 3-8 Assessing the effect of a dehydration protocol on use of Hoechst alongside haematoxylin staining	81
Figure 3-9 Body weight of rats during laboratory adaption period. Three groups of male F-344 rats, aged 14-15 weeks were used for the time course protocol of effects of 50 mg/kg/day Ciprofibrate.....	83
Figure 3-10 Time course of effects of ciprofibrate in F-344/NHsd rats. Groups of male rats aged 14-15 weeks were dosed with either 50 mg/kg/day ciprofibrate or corn oil (vehicle).	86
Figure 3-11 Micrographs illustrating the use of the base analogue stains EdU in immunohistochemical staining.....	88
Figure 3-12 Micrographs illustrating the use of the base analogue BrdU in immunohistochemical staining.....	89
Figure 3-13: Labelling index of hepatocytes of male F-344/NHsd rats treated with 50 mg/kg/day ciprofibrate or control (corn oil) and then injected i.p. with EdU.	91

Figure 3-14: Labelling index of hepatocytes of male F-344 rats treated with 50 mg/kg/day ciprofibrate or control (corn oil) and then injected i.p. BrdU.....	92
Figure 3-15: Effect of ciprofibrate or corn oil control on labelling indices of hepatocytes in F-344/NHsd rats, comparing groups treated with EdU and BrdU.....	93
Figure 3-16 Immunohistochemical staining with BrdU.....	94
Figure 3-17 Histochemical staining with EdU.....	96
Figure 3-18 Use of EdU and BrdU staining (example 1) to investigate whether the two peaks of DNA replication at 24 hr and 48 hr (arising from treatment with ciprofibrate) occur in related or different hepatocyte cells.....	98
Figure 3-19 Use of EdU and BrdU staining (example 2) to investigate whether the two peaks of DNA replication at 24 hr and 48 hr (arising from control treatment involving gavage with corn oil) occur in related or different cells.....	99
Figure 3-20 Use of EdU and BrdU staining (example 3) to investigate whether the two peaks of DNA replication at 24 hr and 48 hr (arising from treatment with ciprofibrate at 0 hr and then at 24 hr) occur in related or different cells, images taken at 200 x magnification.....	100
Figure 3-21 Use of EdU and BrdU staining (example 4) to investigate whether the two peaks of DNA replication at 24 hr and 48 hr (arising from treatment with corn oil control at 0 hr and then at 24 hr) occur in related or different cells, images taken at 200 x magnification.....	101
Figure 3-22 Percentage of labelled hepatocytes of F-344 liver rats following induction with 50% ciprofibrate.....	102
Figure 3-23 Effects of CPA on hepatic DNA synthesis in female F-344 NHsd rats as detected by BrdU staining.....	105
Figure 3-24 Effects of CPA on hepatic DNA synthesis in female F-344 NHsd rats as determined by labelling index of BrdU staining.....	106
Figure 3-25 Effects of CPA or corn oil control on liver growth in female F-344NHsd rats CAP after 3 hr.....	108

Figure 3-26 Standard curve to determine the RT-PCR efficiency. The efficiency is based on the r^2 value, with the regression correlation coefficient value r^2 determined as shown above.	111
Figure 3-27 Effect of CPA or corn oil control treatment on <i>CYP3A1</i> mRNA expression in liver cells of female and male F-344 rats.....	112
Figure 3-28 Effect of CPA or corn oil control treatment on <i>Scd1</i> mRNA expression in liver cells of female and male F-344 rats.....	113
Figure 3-29 Effect of CPA or corn oil control treatment on <i>Ccnd1</i> mRNA expression in liver cells of female and male F-344 rats.....	114
Figure 3-30 Effect of CPA or corn oil control treatment on <i>G0s2</i> mRNA expression in liver cells of female and male F-344 rats.....	115
Figure 6-1 Diagram shows the components of the central and peripheral nervous system.....	133
Figure 6-2 Diagram of the brain structure, illustrating differences in neuroanatomy between mice and humans.	135
Figure 6-3 Scheme of hippocampal with dentate gyrus layers in rodents.	136
Figure 6-4 Classification of glial cells and how they differ.....	138
Figure 6-5 Illustration of the glia cells.....	140
Figure 6-6 Diagram summarizes the most important functions of astrocytes	141
Figure 6-7 Schematic drawing illustrating astrogliosis (astrocyte proliferation).....	143
Figure 6-8 Diagram of the 26S proteasome structure.	148
Figure 7-1 Diagram shows conditional deletion of <i>Psmc1</i> in mouse, specifically with the <i>CaMKIIα</i> promotor (calcium/calmodulin-dependent protein kinaseII α).....	153
Figure 7-2 Method of box-dividing a brain into 1mm sections.	158
Figure 7-3 Diagram of organotypic slices system materials and method.	160
Figure 7-4 A diagram to illustrate the DAB reaction and how a labelled secondary antibody reacts with a primary antibody bound to a tissue antigen.	165

Figure 7-5 Using Image-J program for calculating the number of astrocytes in cortex region.....	168
Figure 7-6 Using Image-J program for calculating the number of astrocytes in hippocampus region.	169
Figure 7-7 Schematic diagram indicates the time courses of treating the organotypic slice culture with PPAR- γ agonist & antagonist, DMSO vehicle and free drug medium.....	171
Figure 8-1 Rat brain paraffin section stained with GFAP (Thermo scientific).....	173
Figure 8-2 Verification of the negative control staining in the presence and absence of primary antibody in rat brain paraffin section stained for GFAP (Thermo scientific).....	174
Figure 8-3 Rat brain paraffin embedded sections, illustrating astrocytes stained for GFAP from either Thermo scientific or Abcam.	176
Figure 8-4 Examining the impact of gasket thickness on clarity of image resolution.	178
Figure 8-5 Comparing astrocyte detection by using fluorescence and DAB stains in the CA1 layer of hippocampus.....	180
Figure 8-6 Comparison of astrocytes detection by using fluorescence or DAB stains in three different regions.	181
Figure 8-7 Representative image of Psmc1 and Cre genotyping, following agarose electrophoresis.	182
Figure 8-8 Maintenance of slice integrity remains unaffected for up to 2 weeks...	183
Figure 8-9 Detection of astrocytes using immunohistochemistry in slices cultured for 2 weeks.....	185
Figure 8-10 Immunohistochemical detection of GFAP after amended permeabilization and blocking stages.	186
Figure 8-11 Organotypic slice cultures of mutant and wild-type mice at 2 weeks of age.	188

Figure 8-12 Organotypic slice cultures of mutant and wild-type mice at 3 weeks of age.	189
Figure 8-13 Organotypic slice cultures of brains from mutant and wild-type mice at 4 weeks of age.....	190
Figure 8-14 Organotypic slice cultures of brains from mutant and wild-type mice at 5 weeks of age.....	191
Figure 8-15 Organotypic slice cultures of brain from mutant and wild-type mice at 6 weeks of age.....	192
Figure 8-16 Cryostat and paraffin sections of brains created from organotypic brain slice cultures from mutant and wild-type mice at ages 2 and 3 weeks.	194
Figure 8-17 Cryostat sections of mice brains were created from organotypic slice cultures at 4, 5 and 6 wks.	195
Figure 8-18 Paraffin sections of mutant and wild-type mouse brains created from organotypic slice cultures at 2 weeks of culture.	196
Figure 8-19 Coronal heamatoxylin and eosin stained section through the cortex (CTX) and hippocampus.	198
Figure 8-20; Detection of astrogliosis in mouse brain using GFAP ⁺ cells in the cortex.....	200
Figure 8-21 Number of astrocytes in wild-type and mutant mice between 2 and 6 weeks of ages in the dentate gyrus.....	201
Figure 8-22; Detection of astrogliosis via GFAP ⁺ cells in the CA1 area of the hippocampus, in mouse brain.....	202
Figure 8-23 Number of astrocytes in wild-type and mutant mice between 2 weeks and 6 weeks of age in the CA1 area of the hippocampus.	203
Figure 8-24; Using GFAP ⁺ cells to detect astrogliosis in the dentate gyrus of the mouse brain.	204
Figure 8-25 Number of GFAP ⁺ cells in wild-type and mutant mice between 2 weeks and 6 weeks of age in dentate gyrus area.....	205

Figure 8-26; Comparison of the number of GFAP+ cells in the cortex, CA1 and dentate gyrus, in wild type and mutant mice up to 6 weeks of age.....	206
Figure 8-27 Cell viability of 3T3 cells treated with rosiglitazone (PPAR γ agonist) for 24h.....	208
Figure 8-28 Bar chart shows the results obtained when reading the plates after 2 and 24 hours (24 hours post-seeding).....	208
Figure 8-29 Bar chart shows the results obtained after reading the plates after 2 and 4 hr, (72 hours post-seeding).....	209
Figure 8-30 Bar chart shows the results of the survival of the cells after seeding for 72 hours.....	209
Figure 8-31 Investigation of the effect of the PPAR- γ agonist; rosiglitazone on astrocyte numbers in thje cortex region, using wild-type organotypic slice cultures.	211
Figure 8-32 Investigation of the effect of the PPAR- γ agonist; rosiglitazone on astrocyte numbers in the cortex region of cultures from mutant mice.....	212
Figure 8-33 Immunohistochemical staining of GFAP through the cortical region of a brain slice from a wild-type mouse, treated with 50 and 100 μ M rosiglitazone...	213
Figure 8-34 Immunohistochemical staining of GFAP through the cortical region of brain slices from a mutant mouse treated with 50 and 100 μ M rosiglitazone.	214
Figure 8-35 Percentages change of GFAP ⁺ cells in the cortex of wild type and mutant mouse brain slices after treatment with 50 μ M and 100 μ M of rosiglitazone.....	215
Figure 8-36 Investigating the effect of the PPAR- γ agonist; rosiglitazone on astrocyte numbers in the hippocampal region of wild-type mice.....	216
Figure 8-37 Investigating the effect of the PPAR- γ agonist; rosiglitazone on astrocyte numbers in hippocampal region of mutant mice slices.....	217
Figure 8-38 Immunohistochemical staining of GFAP in the hippocampal region of slices from wild-type mouse brain treated with 50 and 100 μ M rosiglitazone.....	218
Figure 8-39 Immunohistochemistry staining of GFAP in the hippocampal region of mutant mouse brain slices treated with 50 and 100 μ M rosiglitazone.....	219

Figure 8-40 The number of GFAP ⁺ cells expressed in the hippocampal region of wild-type and mutant mice brains after treatment with 50 μM or 100μM rosiglitazone, expressed as a percentage of control.	220
Figure 8-41 Bar chart representing the effects of 50 μM and 100 μM rosiglitazone treatment in control mouse slices, compared with controls and combined agonist/antagonist treatment.....	222
Figure 8-42 Bar chart represents the effects of 50 μM and 100 μM rosiglitazone treatment in mutant mouse slices, compared with controls and combined agonist/antagonist treatment.....	223
Figure 8-43 Comparison of astrocyte number in the cortex of paraffin sections created from control and mutant mouse organotypic slice cultures.....	224
Figure 8-44 Comparison of astrocyte number in the cortex of paraffin sections created from treated organotypic slice cultures from wild type and mutant mouse brain.....	225
Figure 8-45 The change in the number of GFAP ⁺ cells in 50 μM and 100 μM rosiglitazone treated mutant and wild-type mouse brain slices, compared to controls.	227
Figure 8-46 The change in the number of GFAP ⁺ cells in 50 μM and 100 μM rosiglitazone treated wild-type and mutant mouse brain slices.	227
Figure 8-47 Effect of two different concentrations of rosiglitazone on the expression of astrocytes in the cortex and hippocampus in the brains of wild-type mice.	228
Figure 8-48 Effect of two different concentrations of rosiglitazone on the expression of astrocytes in the cortex and hippocampus in the brains of mutant mice.	229

List of Tables

Table 2-1 Quantification of RNA from Fisher rats.....	55
Table 2-2 The maximum recommended volumes of chemical substances for rats dosage.....	60
Table 2-3 Real time-PCR components.....	68
Table 2-4 : Real-time PCR cycle	68
Table 2-5: Primer and Probe sequences for qRT-PCR	69
Table 7-1 Structure of Rosiglitazone and T0070907 PPAR- γ antagonist	156
Table 7-2 Thermal cycle to release the DNA.....	162
Table 7-3 primers and nucleotides of the Cre and S ₄ genes preparation	163
Table 7-4 PCR temperature cycle for genotype detection.....	163
Table 8-1 Number of astrocytes in cortex region.....	201

Abbreviations

β -actin	Beta actin
BBB	Blood-brain barrier
Bd Wt	Body weight
BrdU	5-Bromo-2-Deoxyuridine
BSA	Bovine serum albumin
C57 black 6	Modified mice for use as models of human disease.
CaMKII α	Calcium/calmodulin-dependent protein kinaseII α
CAR	Constitutive androstane receptor
Ccnd1	Cyclin D1 a cell cycle
cDNA	Complementary DNA
CIP	Ciprofibrate
Click-iT EdU	Click-iT EdU Alexa Fluor 594 High-Through put Imaging
CNS	Central nervous system
CoA	Coenzyme-A
CPA	Cyproterone Acetate
Cre	Cre-lox recombination
CYP3A1	Cytochrome P450, family 3 subfamily A, polypeptide 1
DAB	3, 3'Diaminobenzidine Tetrahydrochoride
DAPI	4'6- diamidino-2-phenlindole
DMEM	Dulbecco's modified Eagle medium
DMSO	Dimethyl sulphoxide

DNA	Deoxyribonucleic acid
EDTA	Ethylene diaminetetraacetic acid
EDU	5-Ethynyl-2'-deoxyuridine
FAO	Fatty acid oxidation
F-344	Fisher-344
FCS	Fetal calf serum
FPBs	Paraformaldehyde in PBs
G0	Gap 0 phase
G1	Gap 1 phase
G2	Gap2 phase
GI R1	Group I rat NO 1
GII R1	Group II rat NO 1
GFAP	Glial Fibrillary Acidic Protein
H	Hepatocytes
HBSM	Hanks' balanced solution modified
HC	Histochemistry
HCL	Hydrochloric acid (hydrogen chloride in water)
HGF	Hepatocyte growth factor
H ₂ O ₂	Hydrogen peroxide
HIER	Heat induced epitope retrieval
HREs	Hormone response elements
HRP	Conjugated rabbit polyclonal antibody

HSC	Haematopoietic stem cell
HD	Hoechst dye
IHC	Immunohistochemistry
IF	Intermediate filament
I.P.	Intraperitoneal
IUPAC	International union of pure and applied chemistry
LBW	Liver-to-body weight
LI	Labelling index
MN	Micronuclei
M.O.M	Mouse on mouse
M-phase	Mitotic phase
M	Molarity
NGS	Normal goat serum
NHRs	Nuclear hormone receptors
P	Probe
PBS	Phosphate buffer saline
PCR	Polymerase chain reaction
PFA	Paraformaldehyde
FPBS	Formaldehyde in phosphate buffer saline
PPAR α	Peroxisome Proliferators Activated Receptor
PPRE	Peroxisome proliferators response element
PPs	Peroxisome Proliferators

PXR	Pregame X receptor
RAR	Retinoic acid receptor
RBW	Relative body weight
RT-PCR	Real time polymerase chain reaction
RXR	Retinoid X receptor
S/N	Signal-to-noise
S-phase	Synthesis phase
Scd1	Sterol-coenzyme A desaturase 1
SD	Standard deviation
TAE	Tris-acetate buffer and EDTA
TBS	Tris buffered saline
TdR	[³ H]thymidine
TGF α	Transforming growth factor
THR	Thyroid hormone receptor
TNF	Tumor necrosis factor
Tween-20	Polyoxyethylene sorbitane monolaureate
Ub	Ubiquitin
WT mouse	Wild type mouse
(WY14,643)	4-Chloro-6-(2,3-Xylidino)-2-Pyrimidinylthio (WY14,643)
	acetic acid

THE THESIS

GENERAL INTRODUCTION

PART I

CHAPTERS

- - 1 Introduction: Review of Literature
- - 2 Materials and Methods
- - 3 Results
- - 4 Discussion
- - 5 Conclusion

PART II

CHAPTERS

- - 6 Introduction: Review of Literature
- -7 Materials and Methods
- - 8 Results
- - 9 Discussion & Conclusion

PART III

CHAPTERS

- - 10 General Discussion
- -11 Future work

12 REFERENCES

13 APPENDICES

General Introduction

Peroxisome proliferators (PPs) are non-genotoxic carcinogens known for their ability to cause hepatocarcinogenesis in laboratory rodents. These chemicals act through nuclear receptors known as peroxisome proliferator-activated receptors (PPARs) (Gill, James et al. 1998). The mechanism by which non-genotoxic peroxisome proliferators induce hepatic tumours is not fully understood.

Three isoforms of peroxisome proliferator-activated receptors (PPARs) have been identified; α , γ , and β . All the PPARs isoforms heterodimerise with the retinoid X receptor (RXR) and bind to specific regions on the DNA of target genes called peroxisome proliferator hormone response elements (PPREs) (Ijpenberg, Jeannin et al. 1997, Mandard, Müller et al. 2004). These receptors have a strong binding affinity for both saturated and unsaturated fatty acids.

Humans are exposed to peroxisome proliferators including hypolipidemic agents, herbicides, plasticizers, industrial solvents and natural products. Some studies have reported that long-term administration of peroxisome proliferators results in liver cells being subjected to persistent oxidative stress resulting from marked proliferation of peroxisomes and a consequent differential increase in the levels of H_2O_2 (over a 20-fold increase) and increased activity of certain degradative enzymes (a two-fold increase) (Dhaunsi, Singh et al. 1994, O'Brien, Spear et al. 2005).

This study follows on from a previous study at Nottingham (Amer 2011) on the mechanism of action of liver growth by peroxisome proliferators. It also addresses the role of these peroxisome proliferators in nervous system degeneration.

The study aims to investigate the role of PP and PPARs in two systems; the liver and the brain. On this basis the thesis has been divided into two main parts investigating the role of peroxisome proliferators: firstly a part focusing on liver growth, and secondly a part focuses on neurodegenerative disorders.

The first part is devoted to the non-genotoxic carcinogenic peroxisome proliferator 'ciprofibrate' and the steroidal genotoxic carcinogen cyproterone acetate (CPA) in a liver system. This follows on from previous studies by Amer (2011) where many

genes were identified which were upregulated at early time points of acute response to ciprofibrate or CPA. Some interesting genes were chosen for follow up work in this study because microarray analysis and the RNA sequences work suggested that some genes were jointly highly expressed in response to dosing with ciprofibrate. This allowed a comparison of expression to be made between ciprofibrate and CPA in the present study using the real time PCR technique. In particular, investigations were made to gain insights into whether these whether these chosen genes might be part of a shared pathway(s), and if so to consider the implications for shared or different mechanisms of action of CPA and ciprofibrate. Also the previous CPA study was conducted using male rats, whereas the present study used female rats, since there was a suggestion from previous work (Amer 2011) that levels of DNA synthesis and genes induction were much higher in female rats but this had to be confirmed.

The second part of the study was dedicated to a study of the role of peroxisome proliferator-activated receptor γ (PPAR γ) in a neurodegenerative disorder. A mouse model of Parkinson's disease (PD) was used. Neurodegeneration refers to the pathological changes in the brain resulting from loss of neuron leading to deterioration of brain function. At a cellular level, neurodegeneration is seen as a gradual loss of structure or function of neurons which predominantly leads to neuronal death.

Peroxisome proliferator-activated receptor γ (PPAR γ) is expressed by macrophages, endothelial cells, and vascular smooth muscle cells. It regulates gene expression of proteins involved in lipid metabolism, vascular inflammation, and proliferation contributing to atherogenesis and post-angioplasty restenosis (Nagy, Tontonoz et al. 1998, Chinetti, Fruchart et al. 2000). The discovery of synthetic ligands for PPAR γ has led to significant enhancement of understanding of the mechanism of their ligand-dependent activation and subsequent biological effects, particularly with respect to the role of PPAR γ in neuroprotective activity by PPAR γ agonist.

Peroxisome proliferator activated-receptor gamma (PPAR- γ) has been implicated in neurodegeneration in a mouse model. It has been reported that peroxisome proliferators may be considered as potential therapeutic agents against

neurodegenerative disorders (Hirsch, Breidert et al. 2003, Aggarwal and Harikumar 2009). They were found to reduce memory impairment in a transgenic mouse model of AD significantly. Understanding the role of PPAR- γ may help elucidate this receptor's influence in the reduction of neuronal cell death in the CNS. This nuclear receptor may convey its neuroprotective effects via inhibition of astrocytes proliferation.

It was reported in the literature that the peroxisome proliferator-activated receptor gamma (PPAR- γ) has been shown to be involved in immune differentiation and playing a key role in the immune response during the inhibition of the inflammatory response. Current evidence has focused on attempts to elucidate the role of PPAR- γ agonist in an *in vivo* and *in vitro* model of neurodegenerative disease.

Recent evidence suggests neuroglia-mediated inflammatory mechanisms may stimulate disorders in the mouse brain. From this standpoint, astrocytes were used as a tool to monitor neurodegenerative disorder using an organotypic slice culture system of PD mouse model.

In this study, rosiglitazone, a PPAR- γ agonist, was used (at three different concentrations) since previous results indicated a positive effect of this drug on neurodegenerative processes through PPs activity. For example Sun Hong and colleagues (2012) studied the impact of a PPAR- γ agonist on cognitive impairment in epilepsy, revealing its inhibitory effect on astrocytic activity as a measure of brain inflammation.

Therefore, this thesis brings together two aspects of the activity of peroxisome proliferators namely (a) as effector molecules, and (b) their receptor function.

Part 1

The role of peroxisome proliferators in liver growth

1. Introduction - Review of Literature

1.1 The Liver

The liver is a large mass of glandular tissue located in the upper right of the abdomen, and most of its mass is found in the right lobe. It comprises about 4% of the body weight in rats and 2% in humans (Kamath, Wiesner et al. 2003). The liver has the ability to regulate its growth in animals and is the main detoxifying organ of the body and therefore may be injured by ingested toxins. When the liver is exposed to chemical injury, it triggers a mechanism by which hepatocytes begin to divide (Sherlock and Dooley 2002). This is mediated via activation of several genes. Given their medical importance the present study aims to identify some of the genes involved with the control and replication of hepatocyte cells.

1.1.1 Liver cells

The two main cells in liver are parenchymal and non- parenchymal. The parenchymal cells (hepatocytes) represent about 90% of the liver whilst non-parenchymal cells comprising mostly sinusoidal lining cells as well as hemopoietic, bile duct and blood vessels wall cells (Figure 1-1), account for the other 10%. The parenchymal cells are the largest cells in the liver which can vary in size but on average have a diameter of 25 μm . Moreover, they have a high concentration of deoxyribonucleic acid. The hepatocytes have many functions such as bile secretion, phosphorylation, haem synthesis, protein synthesis and beta oxidation (Krishnamurthy and Krishnamurthy 2009).

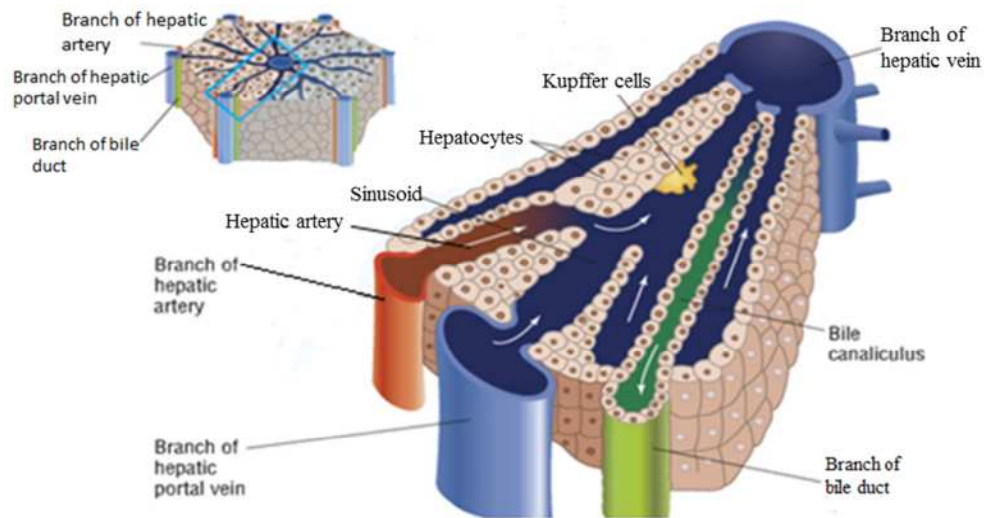


Figure 1-1 Illustration of the arrangement of liver cells in a lobule:

The figure shows hepatocyte cells (in light brown) present on the surface, the central vein (light blue), the bile canaliculus (a thin tube that merges and forms bile ductules), sinusoids (dark blue), and Kupffer cells (yellow; also known as stellate macrophages).

<http://www.thestudentroom.co.uk/showthread.php?t=1059551&page=210>

1.1.2 The liver cell cycle

As with many other eukaryotic cell types, the cycle of proliferating liver cells can be divided into four stages: G1, S, G2, and M phase (Figure 1-2). The S phase is characterised by a period of DNA synthesis leading to a doubling in the amount of DNA in the cell. At the end of the S-phase, the number of chromosomes has been replicated to $4n$ in diploid organisms. Hepatocytes are in general in the G0 phase, or quiescent phase, of the cell cycle (Seidman, Hogan et al. 2001). However, when induced to regenerate, hepatocytes are able to enter G1 phase and continue through the cell cycle (G1-S-G2-M), and at the end of M phase cell division occurs (Yoshida, Arii et al. 1992). Generally, hepatocytes may have one or two nuclei which contain $2n$, $4n$, $8n$ and even greater DNA amounts. In rat liver, the rate of DNA synthesis in hepatocytes increases after about 12 hr and peaks around 24 hr. This contrasts with non-parenchymal cells such as biliary epithelial cells or Kupffer cells, in which synthesis is slower - beginning around 48 hours and approximately 96 hr in endothelial cells. DNA synthesis starts in rat hepatocytes around the portal zone of the liver lobule and then proceeds towards the central vein. This contrasts with mice, in which DNA synthesis occurs around the central vein first and then extends to the portal zone (Al Kholaiifi, Amer et al. 2008).

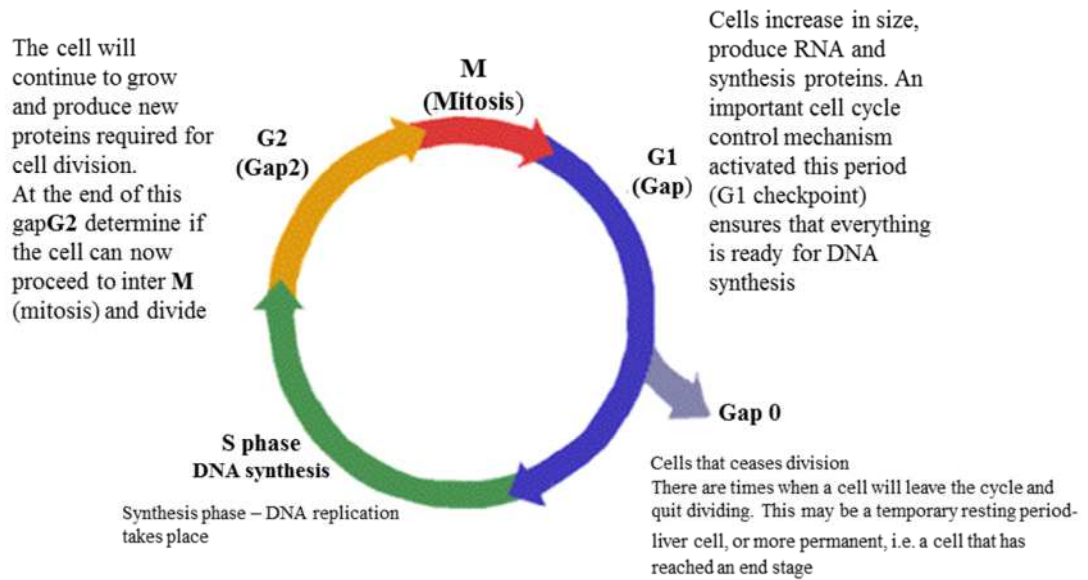


Figure 1-2 Cartoon illustration of cell cycle:

The cycle of proliferating cells is divided into four stages G1, S, G2, and M phase. The hepatocytes enter G1 phase and then DNA synthesis starts at S phase stage. Cell division occurs at the end of M phase. <http://www.biologymad.com>

1.1.3 Liver growth and its regeneration

Liver cells (hepatocytes) have a natural ability to proliferate by replication of the DNA during cell division. Given this regenerative ability, hepatocytes have a major role to play in reacting to damage to the liver. Biologically, in normal circumstances hepatocytes of adult rats seldom divide and proliferate. However, in instances of partial hepatectomy or tissue injury, hepatocytes can undergo DNA replication followed by cell division, with histological studies in rats revealing a high capacity to regain damaged liver cells (Grisham 1962, Fausto 2000). It has been reported that DNA synthesis in rat hepatocytes starts at 14 hr and reaches a peak at 24 hr. At 36 hr the liver may have doubled in size, and within a week the normal liver mass is fully restored (Widmann and Fahimi 1975). A full review of liver growth is beyond the scope of the present study.

1.1.4 Control of liver growth

The liver is the main detoxifying organ in the body and plays a major role in metabolism. It also has several other functions in the body including plasma protein synthesis, glycogen storage, decomposition of red blood cells, and hormone production (Taub 2004). Liver cell numbers may decrease as a result of chemical injury or viral infection. This can trigger a mechanism by which hepatocytes start to divide. The genes *c-fos*, *c-jun* and *c-myc* are known to be involved with activation of cell division and inhibition by other factors such as TGF β (Fausto and Webber 1993). Hepatocytes are relatively long lived and generally do not divide unless exposed to toxic injury or infection. As a result of liver injury some new hepatocytes are required to restore liver function, showing that hepatocytes have replicative capacity (Taub 2004).

1.2 Peroxisome proliferation

1.2.1 Peroxisomes

Peroxisomes are cytoplasmic sub-cellular organelles found in all eukaryotic cells, and comprise around 2% of the total cytoplasm and cellular protein content. They are characterized by a single membrane and have a metabolic role involved with lipid breakdown (Tabak, Murk et al. 2003). In 1954 Rhodin identified the peroxisomes naming them *microbodies*, because their function was at that point unknown (Singh 1997). It has been suggested that peroxisomes are not discrete organelles but actually exist in continuum with the endoplasmic reticulum (Matheson, Hanton et al. 2006). In the liver they are usually round and measure about 0.5-1.0 μm diameter. In rodents they contain a prominent central crystalloid part, but this may be absent in newly formed rodent peroxisomes as well as in human peroxisomes. Originally it was thought that rat liver peroxisomes contain hydrogen peroxide which generated oxidase enzymes and catalases. However, it was later revealed that they contain a complete fatty acid β -oxidation cycle (Fahl, Lalwani et al. 1984). Peroxisomes have a main metabolic role in the breakdown of long-chain fatty acids, thereby complementing mitochondrial fatty-acid metabolism.

1.2.2 Peroxisome proliferators

Many chemicals are known to increase the numbers of peroxisomes in rat and mouse hepatocytes. This phenomenon of ‘peroxisome proliferation’ coincides with replicative DNA synthesis and liver cancer in rodents (Holden and Tugwood 1999). Many of these peroxisome proliferator (PP) chemicals can modulate fatty acid metabolism (Heuvel 1999) and some xenobiotic and anabolic pathways such as cholesterol synthesis and dolichol synthesis (Latruffe, Pacot et al. 1995). The PP group of chemicals is especially significant to human health because they are potent carcinogens able to induce, for example, 100% multifocal liver cancer in rodents up to 1 year after exposure (Cattley, Marsman et al. 1991). However, they also have potential beneficial properties such as cellular receptor for a class of drugs used in

the treatment of dyslipidemia, also considered a treatment of non-alcoholic fatty liver disease.

Peroxisome proliferators are a diverse group of chemicals which differ slightly in structure but all induce characteristic effects in the liver of treated rats and mice (Mannaerts and Van Veldhoven 1993). Peroxisome proliferators include several chemicals which are unrelated structurally such as hypolipidemic drugs, plasticizers and organic solvents (which are used in the chemical industry and in herbicides), all of which cause liver carcinogenesis in laboratory rodents by a non-genotoxic mechanism (Ashby, Brady et al. 1994, Passilly, Schohn et al. 1999).

PPs have an effect both on lipid metabolism and carcinogenesis through binding to peroxisome proliferator activated receptors (PPARs). These receptors are found intracellularly on the nuclear envelope and can detach from here and themselves function as transcription factors regulating the expression of genes (Lee, Pineau et al. 1995). The peroxisome proliferator response has gained considerable interest due to its association with metastatic hepatocellular carcinomas in laboratory rodents.

Peroxisome proliferators are non-genotoxic hepatocarcinogens that cause cell proliferation and ultimately liver enlargement (Roberts, James et al. 2001). The mechanism of action by which peroxisome proliferators cause cancer is not understood (Cattley 2003). Some scientists have suggested that PPs promote liver growth by an increase in cellular oxidative stress via H₂O₂ production, leading to increased peroxisomal fatty acyl CoA (Kobliakov 2010). Peroxisome proliferators are considered "non-genotoxic" (i.e. not involving direct damage to DNA itself) and are classified as a novel class of epigenetic chemical carcinogens. It is believed that a major contributing factor to cancer formation by non-genotoxic carcinogens, including peroxisome proliferators, is altered gene expression.

The peroxisome proliferator-activated receptor alpha (PPAR α) is an essential factor in peroxisome proliferation in rodent hepatocytes. PPAR α serves as a receptor for diverse compounds, of particular interest are the family of fibrate chemicals due to their wide range of effects, which include induction of hepatic peroxisome proliferation, hepatomegaly, hepatocarcinogenesis, and activation of expression of

several enzymes such as CYP4A in rodents. In the present study efforts will be focussed on the PP ‘ciprofibrate’ (Figure-1.3) (see later, section 1.2.4). PPAR α has an influence on fatty acid metabolism and it is thought that this results in regulation of cell cycle control and apoptosis (Issemann and Green 1990, Koves, Ussher et al. 2008). PPAR α forms a heterodimer with a separate protein ‘retinoid X receptor’ (RXR) with activation by peroxisome proliferators leading to PPAR α binding to DNA regions termed peroxisome proliferator hormone response elements (PPREs). Human PPAR α s share many functional characteristics with the rodent receptors. However, humans appear to be refractory to the adverse effects to peroxisome proliferation (Roberts 1999).

1.2.3 Cyproterone acetate

Other classes of chemicals (i.e. independent of PPs) are also able to cause enlargement of the liver, but in contrast can act as genotoxic carcinogens (i.e. causing damage to DNA). One example is cyproterone acetate (CPA) (Figure 1.3), which is a steroidal anti-androgen (Siddique, Ara et al. 2008). It suppresses the action of testosterone and its metabolite dihydrotestosterone. It acts by blocking androgen receptors, thereby preventing androgens from binding to them which in turn reduces testosterone levels (Dehm and Tindall 2005). Cyproterone acetate has been used in animal experimentation to investigate the actions of androgens in fetal sexual differentiation.

It is worth mentioning that initial stages of CPA action have a completely different mechanism to the PP ciprofibrate mentioned above (Hasmall and Roberts 1999). Cyproterone acetate can be used as a drug as a gestagen and anti-androgen, and is a potent inducer of drug-metabolizing enzymes in female rat liver. CPA has the ability to stimulate liver enlargement in rats and laboratory mice. Administration of high doses of CPA over a long-term period may lead to liver tumour formation. It is hoped that a better understanding of how cell enlargement and division occurs in induced liver cells, as a result of CPA treatment, will help to better understand the relationship between induction of liver growth and hepatoma formation.

The initiating activity of CPA *in vivo* in the rat liver shows that it not only promotes but may be sufficient to induce complete carcinogenesis in rat liver. A key aspect of the initial stages of CPA action is that it binds to and activates the receptor protein Pregnane X Receptor (PXR), increasing reporter levels more than 7-fold. PXR serves as a regulator of CYP3A expression (Deml, Schwarz et al. 1993). Similar to PPAR, PXR is located in the nucleus and plays a major role in regulating lipid homeostasis as well as hepatic detoxification (Handschin and Meyer 2005).

In previous studies, the effect on liver growth following treatment with CPA was observed in Wistar rats. Effects were less pronounced in male Wistar compared to female Wistar rats. Administration with 5-10 mg/ CPA for 3 days showed a peak in DNA synthesis after 18-24 hr (Schulte-Hermann, Hoffman et al. 1980).

Systematic *IUPAC Name	3D** Structure	Structure
Ciprofibrate 2-[4-(2,2-dichlorocyclopropyl) phenoxy] 2-methylpropanoic acid		
Cyproterone acetate (CPA) Chloro-6-hydroxy-17 alpha methylene-1 alpha, 2 alpha pregnadiene-4,6 dione-3, 20 acetate		

*IUPAC (International Union of Pure and Applied Chemistry).

**Blue= oxygen, Red= carbon, Pink= hydrogen, Green= chlorine

Figure 1-3 Chemical formula and structure of cyproterone acetate.

<http://www.google.co.uk/search?newwindow=1&hl=en&tbm=isch&q=Cyproterone+acetate+CPA+3D+and+chemical+structure&spell=1&sa=X&ei=IkgJUpefHsru0gWnp0D4Bw&ved=0CFEQvwUoAA&biw=1366&bih=632>

As mentioned above, PXR is a nuclear hormone receptor which is linked to the induction and regulation of expression of cytochrome P450 3A monooxygenase (CYP3A) genes. PXR is initially expressed in the liver and intestine, and binds to a variety of drugs and xenobiotics, together with the retinoid X receptor (RXR) to form a heterodimer. This then binds to certain xenobiotic response elements that have been identified in CYP3A gene promoters to induce CYP3A gene transcription (Kliwer, Goodwin et al. 2002). PXR stimulates expression of several genes involved in metabolic elimination of unusual compounds and toxic endogenous substances (Guzelian, Barwick et al. 2006).

1.2.4 Ciprofibrate (peroxisome proliferators) compared to Cyproterone acetate (CPA)

Ciprofibrate is a potent PP that has tumour promoting activity in rodent liver (Klaunig, Babich et al. 2003). Ciprofibrate binds to and activates PPAR α (Bünger, Hooiveld et al. 2007). PPAR α forms a heterodimer with the retinoid X receptor (RXR), before then binding to specific regions of DNA called PPREs.

By contrast, cyproterone acetate (CPA) binds to and activates PXR. It has been reported that CPA induces cell proliferation and apoptosis and then ultimately causes liver cancer. CPA is a tumour promoting agent and a genotoxic carcinogenic chemical, in contrast to ciprofibrate which is considered a non-genotoxic carcinogen (Rotroff, Beam et al. 2010).

Thus a comparison can be made between the chemical classes to be studied in the present thesis. PPs are non genotoxic carcinogens (i.e. are non-mutagenic) (Roberts 1996), whereas the steroidal CPA is a genotoxic carcinogenic chemical.

The mechanism of action of non genotoxic carcinogenic may cause damage to the DNA structure indirectly. During carcinogenesis, PPs promote liver tumours by increasing oxidative stress in liver as a result of the creation of H₂O₂, whilst genotoxic chemicals such as CPA can stimulate the DNA directly to cause changes in the genome (Cavalieri, Frenkel et al. 2000).

However, there are also some similarities in PP and CPA activity in that both have a role in mediating the induction of hepatic CYP450, and both involve binding with the RXR family of proteins (Figure 1.4) (see section 1.2.6).

1.2.5 Induction of hepatic DNA synthesis by cyproterone acetate

It has reported that the treatment to rats with cyproterone acetate (CPA) or peroxisome proliferators (e.g. nafenopin) can cause DNA synthesis at 18 to 24 hr post treatment (Menegazzi, Carcereri-De Prati et al. 1997). Previous work at Nottingham by Amer (2011) had studied the effects of CPA on the induction of DNA synthesis at four different time points 1, 3, 5 and 24 hr as will be described below, (section 1.3).

1.2.6 Inducing the expression of hepatic Cytochrome P₄₅₀

The cytochrome P₄₅₀ (CYP₄₅₀) superfamily of proteins includes a broad range of enzymes (Thomas 2007). These enzymes generally stimulate the oxidation of organic substances. Evidence has increasingly indicated that orphan nuclear receptors such as PPARs, PXR and CAR have a role in mediating the induction of hepatic CYP₄₅₀ (see Figure; 1-5) (Waxman and Booth 2003, Finn, Henderson et al. 2009). It is important to understand the mechanisms through which xenochemicals induce the expression of hepatic P450 enzymes. It is known that both the constitutive androstane receptor (CAR) and PXR category of receptors are present within the cytoplasm of cells and both have the ability to bind different chemicals, which might enter the body either through ingestion of food or being produced as the products of metabolism e.g. by incorporation of one hydroxyl group into substrates in metabolic pathways (Lehmann, McKee et al. 1998, Kodama, Koike et al. 2004, Kapitulnik, Pelkonen et al. 2009). It is critical to mention that oxidative metabolism of several endogenous xenobiotics, including numerous toxins and carcinogens, might lead to production of ligands binding to such receptors (Brown, Reisfeld et al. 2008).

In the case of the receptor PXR, this is activated by a wide group of steroids and diversity of xenobiotics. PXR then binds with a separate protein RXR α to form a heterodimer. This can then bind to the regulatory regions of CYP3A and induce the Cyp3A family genes which in mice are called Cyp3A1 (compared to Cyp3A4 in humans) (Wan, An et al. 2000, Goodwin, Redinbo et al. 2002). It is worthwhile noting that most studies of CYP3A regulation have been carried out using rabbit and rats, while less studies have been performed in human both *vivo* and *in vitro* (Jones, Moore et al. 2000). Indeed, induction by CPA has shown differences in induction of CYP3A gene expression between species. The mouse and human pregnane X receptors (PXR) were shown to be consistently activated by compounds that induced CYP3A expression, consistent with a role of PXR in CYP3A regulation. However, human and rabbit PXR show a stronger transcriptional response than that seen in mouse and rats. The pregnane 16 α -carbonitrile is one of the potent stimuli that are usually used in the rat PXR than the human receptor. It has been demonstrated that many of the compounds that induce CYP3A expression bind directly to human PXR (Bulera, Eddy et al. 2001). It is also noteworthy that metabolic pathways in the liver mediated by RXR heterodimerization with PXR is compromised in the absence of RXR. The ligand activated nuclear receptors CAR, PXR and PPAR bind to their cognate DNA elements as heterodimers with RXR (Figure 1.4) (Jacobs, Dickins et al. 2003).

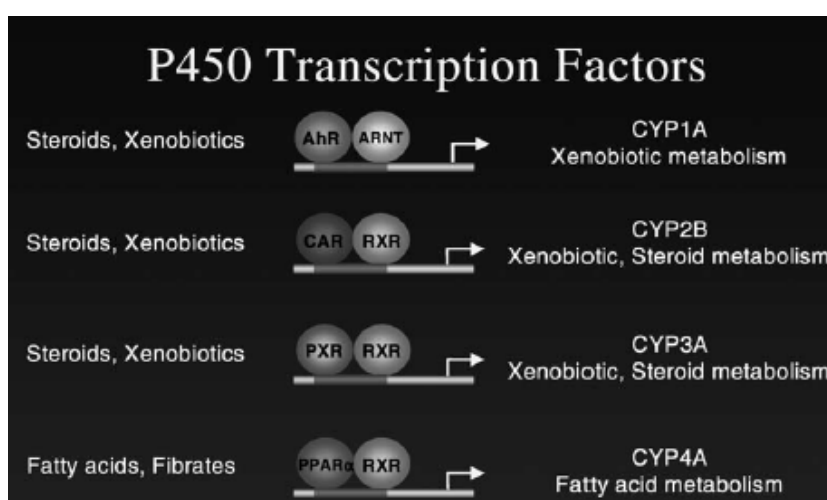


Figure 1-4; Diagram showing the mechanism of action of various P450 transcription factors (Jacobs 2004).

1.2.7 Effect of CPA (PXR) ligands on hepatic DNA synthesis

It is hoped that an improved understanding of the mechanisms of liver cell division and growth will pave the way to providing insights into the mystery of the basis of liver cancer. Using different chemicals such as ciprofibrate as a non-genotoxic carcinogen or CPA, as a genotoxic carcinogen, which both cause liver growth is anticipated to provide some clues as to how cell division and liver growth occur. However, CPA has a completely different mechanism from ciprofibrate (Crunkhorn, Plant et al. 2004). Like PPAR α , the PXR is a nuclear receptor that requires heterodimerization with retinoid X receptors (RXRs) (Figure 1.5). CAP (PXR) binds with RXR α whilst PPAR α binds with RXR α . There are three isoforms of the retinoid X receptor (RXR), RXR α , β and γ . It is believed that RXR α is the most abundant in liver of adult mammals (Cullingford, Bhakoo et al. 1998).

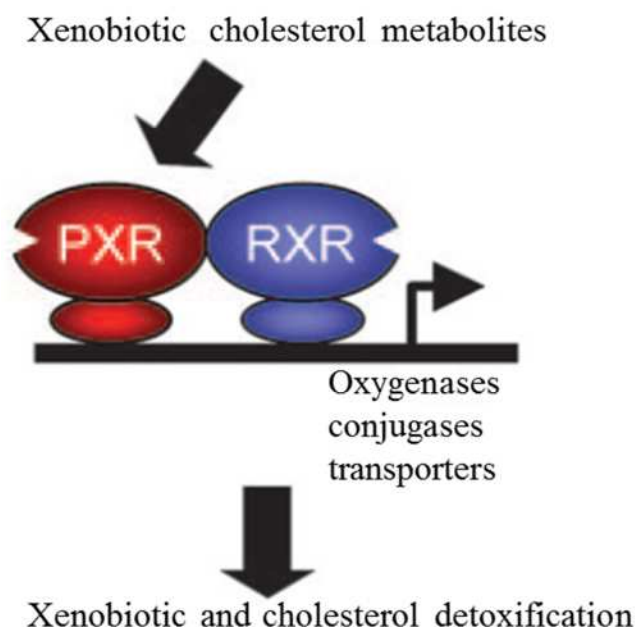


Figure 1-5 Schematic diagram of PXR binding to DNA as a heterodimer with RXR:

The diagram shows an example of PXR-induced detoxification of xenobiotics. PXR is an orphan nuclear receptor known to mediate the effects of xenobiotics. PXR requires heterodimerization with RXR for DNA binding. The downstream processes are mediated by CYPs belonging to the CYP1A, CYP2B, and CYP3A families. Their gene expression is affected by chemical inducers and stimulates the transcription of genes encoding CYP450. The super-gene family of cytochrome P450 is expressed mainly in the liver and is able to identify a tremendous diversity of xenobiotics, and catalyse the metabolic conversion of these xeno-chemicals to polar derivatives that are then eliminated from the body. Thus, PXR functions to regulate expression of several genes, with CYP3A being the most responsive (Goodwin, Redinbo et al. 2002, Yano, Hsu et al. 2005)

1.2.8 Hepatic CYP450 gene expression by Peroxisome proliferators and cyproterone acetate

Both PP and PXR inducers have the ability to stimulate transcription of an enormous number of genes. However, there is some commonality in that both can induce expression of hepatic CYP450 genes. PPs in particular can induce the transcription of CYP4A1 gene. For example, the effect of PPs on early gene expression has been studied *in vivo* in rats, revealing a significant induction of CYP4A1 after 6 hr (Woodyatt, Lambe et al. 1999).

By contrast, pregnane X receptors (PXR) play a key role in the regulation of CYP3A genes. Related to this, PXR regulates a large number of genes involved in xenobiotic metabolism, including oxidative processes (Kliwer, Goodwin et al. 2002). PXR binds to and activates transcription from specific response elements found in the CYP3A gene promoter from multiple species including human and rodents (LeCluyse 2001).

Considering the specific chemicals to be investigated in the present study, ciprofibrate and CPA are believed to induce an almost completely different set of genes by and large. However, this study follows on from a previous study carried out by Amer (2011) at Nottingham which identified several genes that interestingly appeared to be jointly induced by either PPs or CPA. This work will be explained in more detail in the following section.

1.3 Previous Work Leading to the Present Study

Despite their medical importance the mechanism by which PPs induce hepatocyte hypertrophy and hyperplasia is not currently well understood. Understanding the mechanism by which liver growth is induced by PPs in rodents will hopefully provide insights into how natural liver growth occurs and have medical benefits for human health if the mechanism of PP toxicity can be understood and remediated. Knowledge gained from the mechanism of PP activation might also then be applied to other chemical carcinogens.

Given their medical importance the PP group of chemicals have been the subject of ongoing research at Nottingham. Previous work, leading up to the present study, was undertaken by Amer (2011) who investigated aspects of the mode of action of the PP chemical ciprofibrate. Both histochemical and molecular biology studies were made. Firstly, histochemical studies found that treating rats during a time course with two separate doses of ciprofibrate (50 mg/kg body weight) at 0 and 24hr resulted in a subsequent biphasic pattern of DNA synthesis of cell division, with increased DNA labelling evident at 24 hr and at 48 hr following treatment (Figure 1.6). However, it was not clear if the same or different groups of cells were responding to the treatment. This is a significant question as it might suggest that certain liver cells might be particularly sensitive to PP induction. Identifying particular cells, and the genes activated in these cells, might provide valuable insights into the basis of PP induction. Secondly, microarray, real-time PCR and RNA seq work was undertaken to identify genes that were up-regulated following treatment with ciprofibrate. This led to the identification of a series of at least 1000 genes that were up-regulated at early time points (1, 3 and 5 hr) after treatment in male rats (Amer 2011). Of particular interest genes were identified that were related to the cell cycle (e.g. *Gos2*, *Ccnd1* and *Scd1*).

Meanwhile, previous parallel work at Nottingham studied the effects of CPA activation of liver cell growth and division (Amer 2011). The fact that other chemical factors such as CPA also lead to cell division and carcinogenicity in liver cells

suggests that some common genetic mechanisms regulating DNA replication and cell division might be activated by both PPs, such as ciprofibrate, and chemicals such as CPA. It is therefore of great fundamental and medical interest to try to identify any such common genetic pathways. Again, both histochemical and molecular biology studies were made of the mode of action of CPA. Firstly, histochemical studies were made to investigate the effects of CPA on the induction of DNA synthesis at four different time points 1, 3, 5 and 24 hr. Male and female Fisher rats were used to study the induction of DNA synthesis at a dose of 100 mg/kg CPA. A labelling index involving staining of cells with the histochemical BrdU was used to assess DNA synthesis. It was found that male rats yielded low labelling index values of approximately only 6 % (as a percentage of all cells) at 24 hr compared to female rats which showed much higher labelling, with values of approximately 50% detected (Amer 2011). This was a very interesting finding, suggesting that female rats exhibited much higher peaks in the DNA synthesis than males, under CPA treatment, under the same conditions (age and dose) i.e. the genes involved in signalling were most likely induced much more in female than male rats. These finding will be investigated further in the present study, using two time points at 3 and 24 hr and also using real-time PCR methodology rather than the microarray technique used in the previous study (see section 1.4). Secondly, preliminary microarray and real-time PCR work was undertaken to identify genes that were up-regulated following treatment with CPA. This led to the identification of a series of a 1377 genes that were up-regulated at early time points (1, 3 and 5 hr) after treatment in male rats. For example the *Ccnd1* gene showed a 2.9 fold change, *Scd1* showed a 13.2 fold change and *Scd4* showed a 15.6 fold change at 3 hr. (Amer 2011).

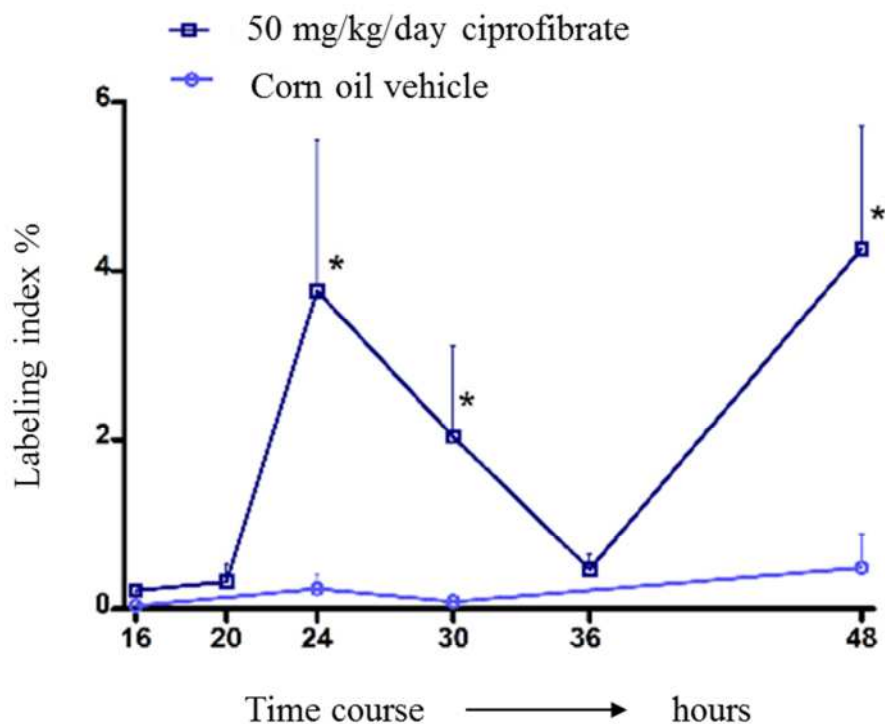


Figure 1-6 Time course showing change in labelling index following treatment with 50 mg/kg/day ciprofibrate compared to labelling index of control corn oil treatment.

Graph shows the induction of hepatic DNA synthesis, as judged by a DNA labelling index, in male F-344/NHsd rats aged 14-15 weeks. A biphasic pattern of DNA synthesis was evident, one peak of labelling being observed at 24 hr and the other at 48 hr following ciprofibrate treatment. The rats were gavaged with either corn oil or with ciprofibrate at time 0 and at 24 hr. The animals injected i.p with BrdU were then killed, and visualization of BrdU-stained hepatocyte nuclei undertaken. The same procedure was performed at 30, 36 and 48 hr (n=6). The data showed significant differences in the percentage of cells labelled between the test and the control treated for 24 hr and 48 hr ($P < 0.0001$) (Amer, 2011).

1.4 The hypotheses and aims of the first part of the current project: liver cell growth

Work undertaken in the first part of current thesis focussed on gaining an understanding of the effects of non-genotoxic and genotoxic carcinogens on liver DNA synthesis and cell division. Non-genotoxic and carcinogenic drugs have been shown to have some beneficial properties, being able to improve the outcome of specific medical conditions, related to their ability to signal through transcriptional factors. However, they can also have detrimental affects on the liver, for example they might cause cancer through mechanisms that do not involve direct DNA damage.

Ciprofibrate and cyproterone acetate (CPA) were used in the present study as examples of non-genotoxic and genotoxic carcinogens, respectively. Insights into their mode of action have come from prior research by Amer (2011) who demonstrated firstly that two rounds of ciprofibrate treatment resulted in a subsequent biphasic pattern of liver DNA synthesis in rodents, Secondly, these earlier studies suggested that a gender difference, in terms of degree of response of DNA synthesis, occurred in male and female rodents treated with CPA. Finally, the earlier work had identified a series of genes which showed altered expression as a result of ciprofibrate treatment.

The hypotheses

- I. That there are two distinct hepatocyte cell populations that respond to ciprofibrate treatment in a time dependent fashion, rather than a particular subset of cells that are the only cells responding to treatment.
- II. That there is gender differences, in terms of resulting gene expression and level of DNA synthesis, in rodents treated with cyproterone acetate (CPA).
- III. That the mechanism of action of CPA and ciprofibrate are completely different and they do not share common pathways of action.

The aims

1. To characterise DNA synthesis in rodents following two rounds of ciprofibrate treatment in order to determine whether the hepatocytes responding over time are the same or distinct cell populations. To do this it will first be determined if two base-pair analogues, namely EdU and BrdU, can be used to stain nuclei undergoing DNA replication at the two rounds of liver cell replication at 24 hr and 48 hr.
2. To examine the effect of cyproterone acetate (CPA) on hepatic growth in female F-344/NHsd rats, to find out if differences in response occur between rats of different genders. This will be achieved by determining labelling indices at 24 hr after induction and comparing results to previous data from male rats.
3. To determine levels of mRNA expression of the *G0s2*, *Ccnd1*, and *Scd1* genes following CPA treatment by real-time PCR methodology. These genes, which are associated with DNA synthesis, had previously been identified as being upregulated in response to ciprofibrate and/or CPA treatment. It was therefore of relevance to use RT-PCR to confirm if the same genes showed a response to CPA treatment., as this would give insights into whether the chemicals have similar or different pathways of action.

2. Materials and methods

2.1 Materials

2.1.1 Animals

Male and female Fisher (F-344/NHsd) rats were purchased from Harlan UK limited (Bicester, UK). Two groups of rats were purchased, one group aged 8-9 weeks and other aged 14-15 weeks, which were all housed 6 rats per cage. The experiments were performed in accordance with protocols from Scientific Procedures (Act 1986). All animals were given human care handling and husbandry. They were housed in plastic cages in biologically clean rooms with filtered air. Temperature and relative humidity were held at 22 ± 2 °C and $50 \pm 5\%$ respectively and were maintained on a 12-hr light/dark cycle. Rats were maintained on a standard lab diet and purified water with addition of libitum. For CPA experiments female F-344/NHsd (Fisher) rats at 13-14 weeks of age (187.0 ± 18 g) were used. The animals were housed 4 rats per cage to the group of 3 hr at killing (to study effects of CPA treatment) and 6 rats per cage for 24 hr at killing (for labelling index experiments). Treated animals were given 100 mg/kg CPA at time Ø and BrdU 2 hr prior of sacrifice. The animals were treated, anaesthetised and killed according to a Schedule 1 method, at the designated establishment (BMSU, QMC at the University of Nottingham) recognized by project and personal licenses.

2.1.2 Chemicals

2.1.2.1 Immunohistochemistry materials

All chemicals were obtained at highest grade possible. Ultrapure Tris Base was obtained from Melford. Acetic acid (glacial), xylene, ethanol, methanol, sodium phosphate and haematoxylin stain were purchased from BDH (UK). 3,3'-diaminobenzidine tetrahydrochloride (Adabi Mohazab, Javadi-Paydar et al.), polyoxyethylene sorbitane monolaureate (Tween-20), bovine serum albumin (BSA) and formalin solution, 10% formalin (approx. 4% formaldehyde) were obtained from Sigma (UK). Hydrochloric acid and 30% hydrogen peroxide (H₂O₂) and cobaltous

chloride were obtained from Fischer scientific (UK), ammonium hydroxide from Aldrich (UK). Hoechst dye 33258, which binds specifically to DNA (nuclei), and poly-L-lysine-coated slides (Polysine™) were obtained from Fischer UK), whilst pure paraffin wax (MP 56deg c) were obtained from Lottbrige Drove (Eastbourne, UK). Pure water was produced in the Nottingham laboratory. BrdU (5-bromo-2'-deoxyuridine), and cell proliferation kits were purchased from Amersham TM (UK). Anti-BrdU (Bromodeoxyuridine) antibody, used as the primary antibody, and Goat Anti-mouse HRP conjugate, used as the secondary antibody, were obtained from Bio-Rad laboratories (UK)

The immunohistochemistry technique of BrdU was optimised to gain efficient results. Hepatic cell which have been labelled with BrdU antibody can be used as evidence that a cell has divided (Figure 2-1) (Boenisch 2001).

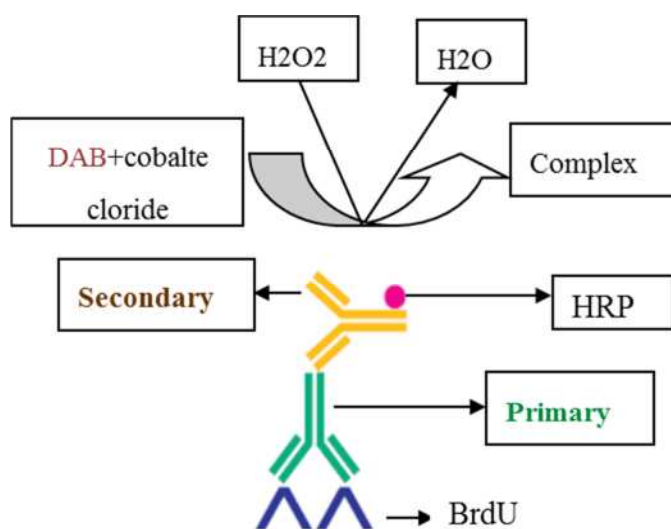


Figure 2-1 Enzyme-labelled secondary antibody reaction with primary antibody bound to tissue antigen.

BrdU (shown in blue) that is given to the animal i.p should bind to replicating DNA. The primary antibody in green (anti-BrdU mouse monoclonal antibody) then binds to the BrdU. A peroxidase anti-mouse IgG secondary antibody (in orange) is next directed against the primary antibody, followed by the (HRP) Horse Radish Peroxidase enzyme (in pink). Details of immunochemical staining methods as described by (Boenisch, Farmilo et al. 2001).

2.1.3 EdU chemistry materials

Phosphate buffered saline (PBS), 3% Bovine serum albumin (BSA) in PBS (3% BSA in PBS) were prepared using pH 7.4, deionised water from the Nottingham laboratory. An EdU (5-ethynyl-2'-deoxyuridine) Cell Proliferation Assay (Click-iT® EdU Alexa Fluor® 594 Imaging) kit with 50 coverslips (cat#10084) was obtained from Invitrogen TM. The latter contains 12 reagents named component A to L. Components A, B, C, D, F, G and H are required. Component A, EdU; B, Alexa Fluor® 594 azide; C, DMSO solvent solution; D, EdU reaction buffer (1X); F, EdU reaction buffer (10X); G, reaction buffer; H, copper sulphate. 5-ethynyl-2'-deoxyuridine (EdU) incorporation into DNA was detected using this kit, and all the reaction steps were performed at room temperature to keep the samples moist. In the EdU reaction a thymidine analogue, in which a terminal group replaces the methyl group, is incorporated into cellular DNA during DNA synthesis. The terminal alkyne group is then detected via its reaction with fluorescent azides, in a Cu (I)-catalyzed covalent reaction between an azide and an alkyne. The EdU contains the alkyne and the Alexa Fluor dye contains the azide (Figure 2.2).

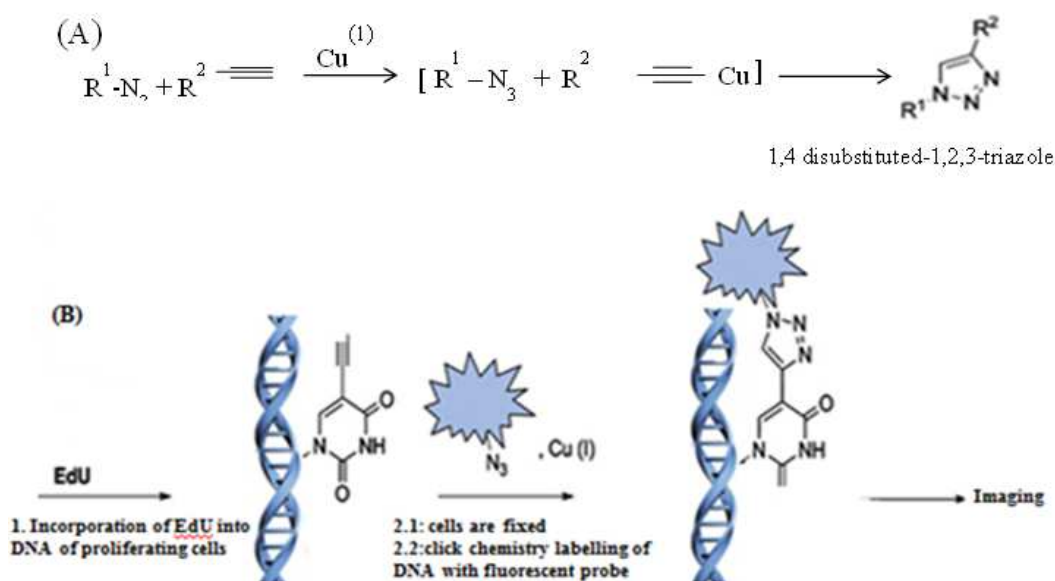


Figure 2-2 Schematic of the click reaction for detecting EdU incorporated into cellular DNA.

(A) The Cu (I) catalysed 1,3-dipolar cycloaddition reaction of organic azides (R^1-N_3) with terminal acetylenes ($R^2-\equiv$). (B) 1: Use of 5-ethynyl-2'-deoxyuridine (EdU), a thymidine analogue that carries a terminal alkyne group to label DNA in cells as a result of incorporation into cellular DNA during DNA replication. A copper catalyzed covalent reaction subsequently occurs between an azide and an alkyne. EdU, a thymidine analogue in which a terminal alkyne group replace the methyl group, with a suitable fluorescent probe (Salic and Mitchison 2008).

2.1.4 Total RNA isolation

1 ml of Tri reagent solution from Sigma (UK) was used to isolate total RNA from samples that had been treated with CPA at 3 hr, according to manufacturer's instructions. Frozen liver tissue (80-90 mg) from each animal was placed in a 1.5 ml Eppendorf tube and RNA extracted using the Tris reagent. 200 μ l (1-bromo-3-chloro-propane) from Sigma (B9673)- 600 μ l of isopropanol- 75% ice cold ethanol were used for washing the RNA pellet which was re-suspended in DEPC water (diethyl pyro carbonate) and the RNA stored at -80°C until use. Concentrations of RNA were determined as in section 2.1.4.1. and using 2% agarose gels See appendix page 274.

2.1.4.1 Quantifying the RNA

Two methods were used to check if the samples were pure without significant amount of contaminants such as proteins, phenol, agarose or other nucleic acids. These were as follows.

1-Spectrophotometer determination of amount of RNA or DNA. For quantifying the amount of DNA or RNA reads were taken at wavelengths of 260 nm and 280 nm.

2-Thermo-scientific Nanodrop 1000 spectrophotometer: a nanodrop machine was used and the quantity of RNA was determined according to the manufacturer's schedule (Table 2.1).

Table 2-1 Quantification of RNA from Fisher rats.

	RNA sample	Measure ng/ml
Control Group	GI R1	077.2
	GI R2	159.9
	GI R3	121.1
	GI R4	116.2
Treated Group	GII R1	106.4
	GII R2	097.6
	GII R3	044.2
	GII R4	122.4

2.1.5 Other chemicals and instruments

The peroxisome proliferator -2-[4-(2, 2-dichlorocyclopropyl) phenoxy]-2-methylpropanoic acid (ciprofibrate) was obtained from Hangzhou BM Chemical (China). Chloro-1 β , 2 β -dihydro-17-hydroxy-3'H-cyclopropa [1, 2] pregna-4, 6-diene-3, 20-Dione (cyproterone acetate: CPA) was obtained from Sigma (UK). These chemicals were dissolved in corn oil before use. Polysine slides have an advantage that they are not affected by chemicals, enzyme predigestion or heating, making them ideal for immunohistochemical or tissue sections. Slides were purchased from Thermo Scientific (UK). LucaEM Camera DL-604mtvp was used to capture the images of tissues which were detected by using DAPI and mCherry filters and white light. The camera was purchased from ANDOR Technology (UK), which was attached to a Leitz WetzlarTM light microscope.

2.2 Methods

2.2.1 Experimental Design

Animal experiments were designed to reduce the number of animals as much as possible, whilst bearing in mind that the number of animals in each group must be at least 6 to produce meaningful statistical analysis. The least stressful procedures possible were employed to reduce suffering, distress and lasting harm to the animals in accordance with Home Office (UK) regulations. The animals were housed on the basis of body weight into appropriate number of groups to minimise random variation and allow suitable statistical analyses. The animals age 7-8 weeks were used for the optimisation experiments. The animals age 14-15 weeks were used to perform time courses assays.

2.2.1.1 Initial optimisation of staining techniques

Before main experiments were performed to study the effects of PP action, it was first necessary to perform control experiments to ensure that satisfactory staining could be achieved with the base analogues EdU and BrdU, and also that Hoescht dye could be used to identify nuclei of the rat liver cells under study. The concept behind this work was that Hoescht staining could be used to identify all cell nuclei in the field of scoring, and then EdU and BrdU staining could be used to identify those cell nuclei undergoing division, which could be expressed as a cell labelling percentage index value. Previous studies had already determined an optimum concentration for BrdU usage (Amer 2011) but optimum concentrations for EdU had not been determined. Therefore, in initial work the effects of staining using three different concentrations of EdU were investigated. Eight male F-344/NHsd rats aged 7-8 weeks were grouped into 4 groups of two rats. Each group was injected intraperitoneal (i.p) as follows (Figure 2-3): 2 rats were injected i.p with 100 mg/kg BrdU in 10 ml/kg PBS 2 hrs before the killing of the animals. 2 rats were injected i.p with 2mg/kg EdU in 5ml/kg in PBS, 2 rats were injected i.p with 5mg/kg EdU in

5ml/kg PBS and 2 rats were injected i.p with 25mg/kg EdU in 5ml/kg PBS. The injections were conducted 2 hr before the killing of the animals.



Figure 2-3 Schematic showing different injection treatments, either BrdU or EdU, and relative time of killing of animals.

The animals were anaesthetised and killed by a schedule 1 method at the designated establishment (BMSU, QMC, University of Nottingham) recognised by the project and personal license. Three different concentrations of EdU were investigated.

2.2.2 Time course protocol of effects of 50 mg/kg/day ciprofibrate

After initial optimisation of the staining protocols, main experimental work was then performed to determine the effects of ciprofibrate treatment, together with control experiments to allow gavage and animal exposure to the experimental procedures. Experiments were designed to serve several objectives. After determining the optimal concentration of EdU, the design was devised taking into account the legal obligation to reduce the number of animals according to Home Office regulations. This study follows a previous study which has been performed by Amer (2011). This research found two peaks of labelling index at 24 hr and 48 hr when rats were treated with 50 mg/kg/day ciprofibrate. This study will focus on those two peaks. The same conditions that were used in the previous study with regard to age, concentration of ciprofibrate, number and time of dosage (Figures 2-4 to 2-7). Six animals were used in each of the three control and treated groups. As recommended by the Home Office regarding the administration of substances to laboratory animals, each animal received an amount of 2.0-2.4 ml for gavaging (Table 2.2). The treated animals were anaesthetised and killed according to a schedule 1 method at the designated establishment (BMSU, QMC at the University of Nottingham).

Two complementary time course protocols were undertaken. First, the effects of staining with BrdU or EdU alone after 22 hr were determined in animals (sacrificed at 24 hr) that were either treated with ciprofibrate or corn oil (control) at time zero (Figures 2-4 A, B; Figure 2-6 A,B). This served as a control to confirm the staining protocol and provide background labelling index data. Second, animals were stained with EdU after 22 hr and then with BrdU after 46 hr (before being sacrificed at 48 hr), with animals either treated with ciprofibrate or corn oil (control) at both zero and 24 hr stages (Figures 2-5 and 2-7). The latter experiment was especially significant for assessing the possible dual labelling of cells (section 2.2.3).

Table 2-2 The maximum recommended volumes of chemical substances for rats dosage

NO.	Method	Dosing volume
1.	Oral	20 ml/kg
2.	Subcutaneous	5 ml/kg
3.	Intramuscular	0.1 ml (total)
4.	Intravenous	5 ml/kg
5.	Intraperitoneal	10 ml/kg

2.2.2.1 The control vehicle groups

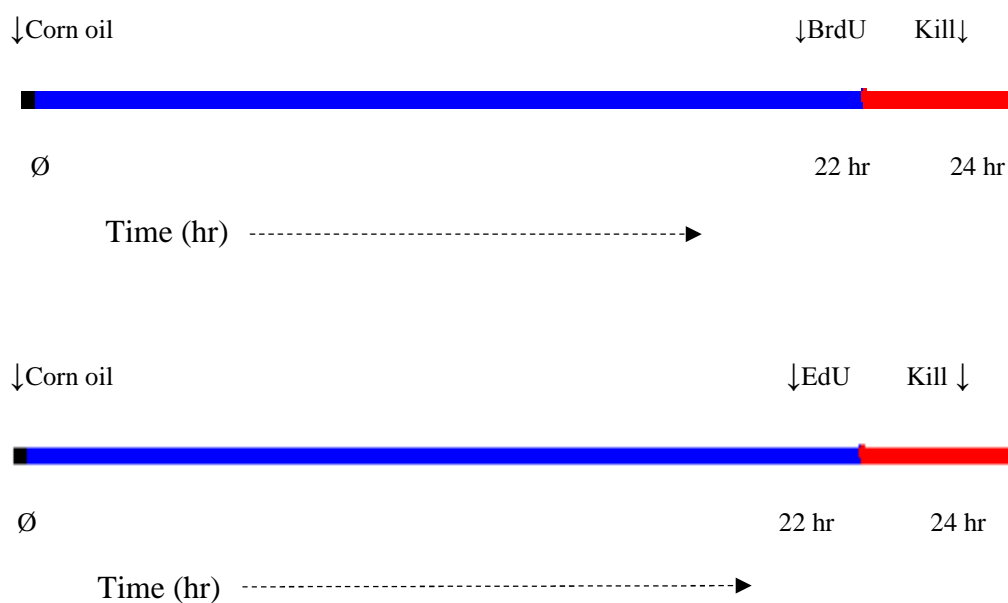


Figure 2-4 Time course of the effects of control corn oil treatment on hepatic DNA synthesis in male F-344/NHsd rats aged 14-15 weeks.

Two groups containing six male F-344/NHsd rats each were gavaged with 20ml/kg corn oil at time \emptyset and then injected i.p after 22hr with either 100 mg/kg BrdU in 10 ml/kg PBS or 2 mg/kg EdU in 5 ml/kg PBS. The animals were then killed at 24hr.

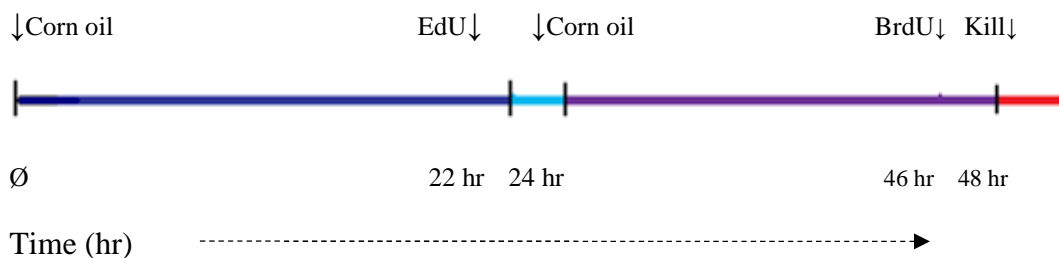


Figure 2-5 Time course of procedures for treatment of rats in control vehicle group 3

Six male F-344/NHsd rats aged 14-15 weeks were gavaged with 20 ml/kg corn oil at time \emptyset and then injected i.p with 2 mg/kg EdU in 5 ml/kg PBS at 22 hr, and were then gavaged again with 20 ml/kg corn oil at 24 hr. At 46 hr the animals were injected with 100 mg/kg BrdU in 10ml/kg prior to killing at 48 hr. The body weight was taken before every gavaging and injection treatment.

2.2.2.2 The treated groups

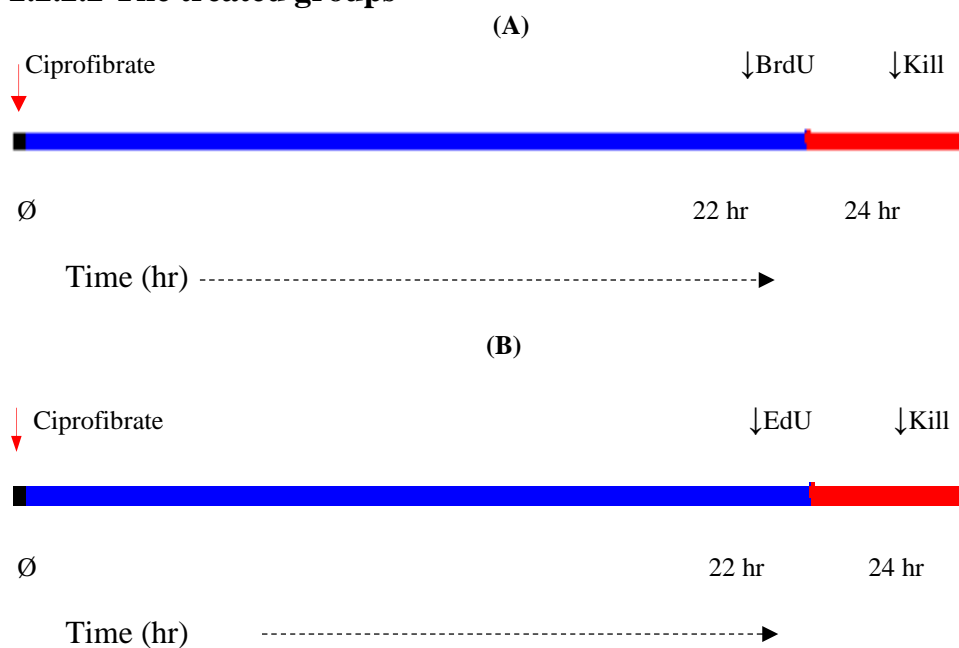


Figure 2-6, A and B: Time course of effects of treatment with 50 mg/kg ciprofibrate on hepatic DNA synthesis in male F-344/NHsd rats aged 14-15 weeks.

Two groups of six male F-344/NHsd rats each were gavaged with 50 mg/kg ciprofibrate dissolved in 20 ml/kg corn oil at time \emptyset and then injected i.p with either 100mg/kg BrdU (group A) in 10 ml/kg PBS after 22 hs or with with 2 mg/kg EdU (group B) in 5 ml/kg PBS after 22 hr . The animals were weighted before injection with BrdU or EdU. The animals were then killed at 24 hr with Dolethal (pentobarbital) intraperitoneal in 10 ml/kg.

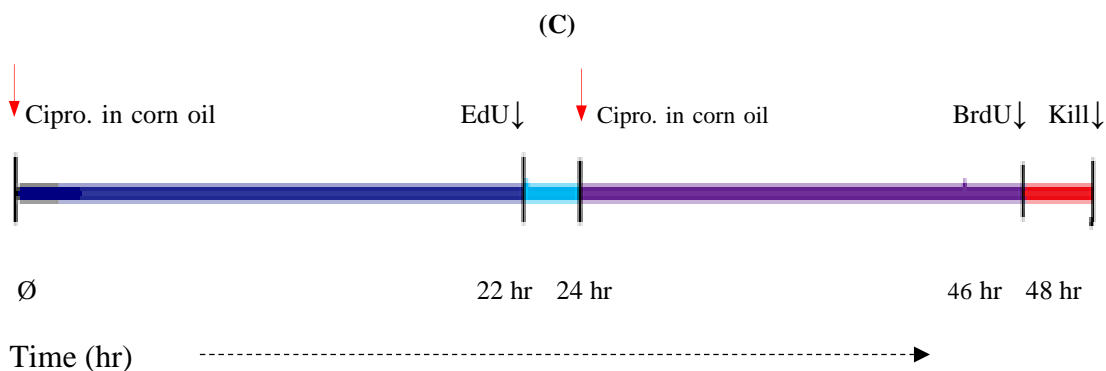


Figure 2-7 C: Time course of effects of treatment with 50 mg/kg ciprofibrate on hepatic DNA synthesis in male F-344/NHsd rats aged 14-15 weeks in treatment group 3.

Six male F-344/NHsd rats were each gavaged with 50 mg/kg/day ciprofibrate dissolved in 20ml/kg corn oil at time \emptyset and then injected i.p with 2 mg/kg EdU in 5 ml/kg PBS at 22 hr and then gavaged again with 50 mg/kg/day ciprofibrate dissolved in 20 ml/kg corn oil at 24 hr. At 46 hr the animals were injected with 100mg/kg BrdU in 10ml/kg prior to killing at 48 hr. The body weight was taken before every gavaging and injection treatment.

2.2.3 Measuring dual labelling of liver hepatocytes

It has been reported that the DNA synthesis begins in rat liver cells between 12 and 18 hr after exposure to a xenobiotic and then rapidly peaks between 20 and 24 hr *in vivo* (Grisham 1962). Peroxisome proliferators also show high level of induction of DNA synthesis *in vitro* 24 hr after dosing (Lindroos, Zarnegar et al. 1991). Peroxisome proliferators have in addition been shown to induce high levels of DNA synthesis in both *in vivo* and *in vitro*, with 3% and 29% respectively of cells being found at s-phase (Plant, Horley et al. 1998). The main objective of the present study was to determine whether the two peaks of cell division at 24 and 48 hr are related (i.e. whether the same or different cells were involved) using the double labelling technique with the base analogue stains EdU and BrdU. Therefore it was necessary to check the number of dual-labelled cells arising from use of the two analogues. The benefit of measuring the number of dual labelled hepatocytes is to find out the proportion of liver cells that have undergone DNA synthesis and compare the results with the number of normal liver cells that undergo DNA synthesis.

2.2.4 Time course protocol of effects 100 mg/kg CPA

To compare previous results, which were based on male rats, female Fisher rats were induced with 100mg/kg CPA. 20 female F-344/NHsd rats aged 14-15 weeks were used. These were split into 4 groups: 2×6 rats for 24 hr kill experiment (treated and control) and 2×4 rats for 3 hr kill experiment (treated and control) (Figure 2.8 and 2.9). The animals were treated, anaesthetised and killed by a schedule 1 method at the designated establishment (BMSU, QMC at the University of Nottingham). Experiments were designed in such a way that RNA could be extracted after 3 hr for analysis of RNA induction by RT-PCR, whilst those killed 24 hr after treatment could be used to determine the labelling index to compare to previous results with male rats (Amer 2011).

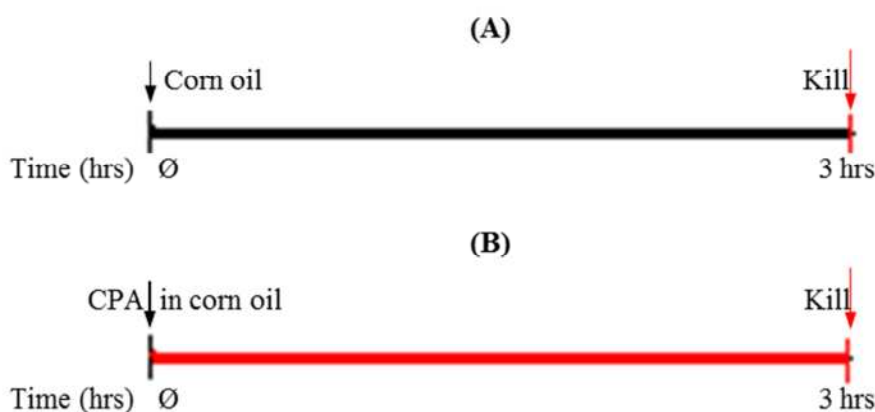


Figure 2-8; A and B Time course of effects of 100 mg/kg CPA treatment on hepatic DNA synthesis in female F-344/NHds rats aged 14-15 weeks.

Four female rats were gavaged either with 20ml/kg corn oil at time 0 (control vehicle group) or with 100 mg/kg CPA dissolved in 20mg/kg corn oil at time 0 (treated group). 3 hr later both groups were killed with Dolethal (pentobarbital) intraperitoneal in 10 ml/kg (samples were taken at this point for RT-PCR analysis of RNA induction of genes of interest).

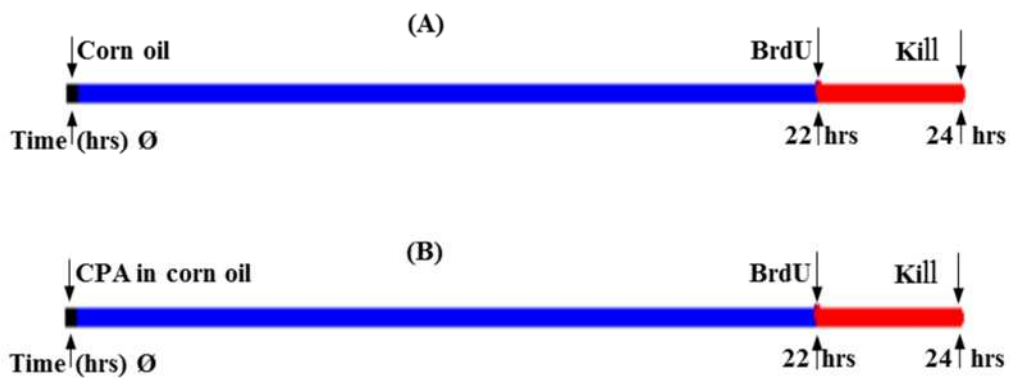


Figure 2-9, A and B time course of effects of 100 mg/kg CPA treatment on hepatic DNA synthesis in female F-344/NHds rats aged 14-15 weeks.

Each of the six female rats were gavaged at time 0 with either 100mg/kg CPA, dissolved in 20 ml/kg corn oil, or a corn oil control. At 22 hr the animals were injected i.p 10 ml/kg BrdU. 2 hr later they were killed with Dolethal (pentobarbital) intraperitoneal in 10 ml/kg.

2.2.5 Tissue processing

The animals were killed by terminal anaesthesia (pentobarbital). Immediately after confirming death, the heart was emptied of blood by using cardiac puncture. It was necessary to remove the remaining blood in liver because this would otherwise interfere with the fixation process. The whole liver was taken from each animal and weighed for comparison of body weight to liver weight ratio. A section of left lobe of the liver and parts of colon intestinal tissue were fixed in 10% formalin. The colon section was used as positive control for the EdU and BrdU staining procedures. Small parts from left lobe of the liver were taken and stored directly in liquid nitrogen and then kept at -80°C until use. Fixed tissues were dehydrated and placed in a Shandon Citadel 2000 Automated Tissue Processor. The tissues underwent processing in this machine for 15.5 hr with the following stages: 70 % ethanol for 6.5 hr then 80 %, 90 %, 95 % ethanol 1 hr for each. Then 3 hr in 100% ethanol; (an hour in each container of ethanol). The tissues were passed through 3 containers of 100% xylene, 1 hr each. The last stage was paraffin wax used for 2 hr which was automatically changed to a different container after 1 hr. Tissue was removed and embedded with paraffin and kept overnight at room temperature. The paraffin blocks were embedded in ice for 48 hr before sectioning. The tissues were sliced at thickness of $4.5\ \mu\text{m}$ and collected on polysineTM slides and dried at 37°C overnight. All subsequent staining steps were performed in a moisture chamber.

2.2.6 Detecting DNA synthesis and cell cycle population

Observation using a Leitz WetzlarTM light microscope was used to detect hepatocyte DNA synthesis that stained with BrdU. A DAPI filter was used to determine the nuclei, and mCherry filter was used to detect replicative cells which stained with click-iT EdU. All micrographs were taken using a Luca^{EM} Camera DL-604mtvp. The photos were taken using an exposure time of 100 ms and a medium setting was used for binning. At least 2,000 nuclei were systematically observed in random fields to calculate labelling indices between both staining groups of EdU and BrdU. A magnification of 400X was used during identification and a counting while a magnification of 200X was used to display cell population of EdU and BrdU groups.

2.2.7 Statistics

Statistical analysis of data was performed using Prism (GraphPad Prism 5, GraphPad Software, 2007). All values are expressed as mean \pm standard deviation. The calculated values were analyzed by student's t-test. The T-test was used for comparison of control and treated EdU and BrdU groups and to compare EdU with BrdU groups. The differences were considered significant among groups if $p < 0.05$.

2.2.8 Real – time PCR materials

2.2.8.1 Probes and primers

Real time PCR primers and probe design were obtained using the PRIMER 3 software (Rosen and Skaletsky, 2000) at: <http://frodo.wi.mit.edu/primer3/>. Real-time PCR measures DNA amplification as it occurs. This technique enables one to determine the starting concentration of nucleic acid. The primers and probes were amplified with an endogenous control gene which has been chosen on the ground that the gene expression would be expected to be consistent in both the control and CPA treated samples. Quantitative real-time PCR TagMan[®] gene master mix was used (from ThermoScientific) which provides a fluorescence reading of mRNA expression during each cycle of the PCR. The amount of master mix used was 19 μ l in 45 μ l of DECP water, and the primers concentrations were 10 pmol/ μ l and 5 pmol/ μ l of the probes.

2.2.8.2 Preparing the RT-PCR reaction

A high capacity RNA-to-cDNA kit was used to prepare the RT reaction mix (AbGene) (per 20- μ l reaction). The total amount of RNA was 2 μ g per 20- μ l reaction as shown in Tables 2.3 – 2.5.

Table 2-3 Real time-PCR components.

Component	Volume/reaction (μ l)	
	+RT	-RT
2X RT Buffer	10.0	10.0
20X RT Enzyme Mix	1.0	-
Nuclease-free H ₂ O	Q.S. \neq to 20 μ l	Q.S. to 20 μ l
Sample	Up to 9 μ l	Up to 9 μ l
Total Reaction per	20.0	20.0

Table 2-4 : Real-time PCR cycle

Cycles	Temperature	Time
1	50 ^o C	2 min
1	95 ^o C	10 min
40	95 ^o C	20 sec
40	60 ^o C	1 min

Table 2-5: Primer and probe sequences for qRT-PCR

Target RNA (Rat gene)	Probe / *Primer	Sequence	Report dye
β -actin	P F R	CAA GAT CAT TGC TCC TGA GCG CTG ACA GGA TGC AGA AGG AG GAT AGA GCC ACC AAT CCA CA	Cy5-BHQ2
AhR	P F R	TAT CAG TTT ATC CAC GCC GCT GAC ATG GCA GCT TAT TCTGGG CTA CA CAT GCC ACT TTC TCC AGT CTT A	Joe
CYP3A1	P F R	TAG AGC CTT GCT GTC ACC CA AGT GGG GAT TAT GGG GAA AG CAG GTT TGC CTT TCT CTT GC	FAM-BHQ1
Scd1	P F R	TCA TGC TGG GGC GAA ACT TT TCC TGC TCA TGT GCT TCA TC GGA TGT TCT CCC GAG ATT GA	Joe
Ccnd1	P F R	CTG GAT GCT AGA GGT CTG CGA GCG TAC CCT GAC ACC AAT CT GGC TCC AGA GAC AAG AAA CG	Joe
GOs2	P F R	CAG GCC CTG ATA GCA GAA GG GGT GTG GTG CTC GGT CTA GT ACA AAG TCG CCT CCT GTG TC	Cy5-BHQ2

*P, probe; F, forward primer; R,

3. Results

3.1 Validation of Methodology

3.1.1 Detection of EdU and BrdU

For the main histochemical work, either Hoechst or haematoxylin stains were used to visualise all cell nuclei within the field of vision depending on the gene analogues to be used. In the case of BrdU, this was always used in conjunction with haematoxylin, whilst EdU was always used in conjunction with Hoechst dye. Standard protocols were available for the use of haematoxylin (Schutte, Reynders et al. 1987) , so the use of this dye did not require optimisation. However, initial work was required to optimise the use of the Hoechst stain as follows.

3.1.1.1 Optimisation of Hoechst dye concentration

The aim of this experiment was to determine the best concentration of Hoechst dye to use to identify cell nuclei whilst reducing the background to gain a high signal-to-noise ratio. A range of concentrations of Hoechst dye were used, namely 50 μ g/ml, 10 μ g/ml, 5 μ g/ml, 1.0 μ g/ml and 0.1 μ g/ml. It was found that a concentration of 1.0 μ g/ml dye was the most appropriate (see Figure 3.1), as background fluorescence was reduced whilst still allowing detection of nuclei. Micrograph Figure 3-1E shows that the liver cell nuclei are clear and larger in comparison to the gut section in micrograph Figure 3-1F, where the nuclei are smaller and irregular and reticulated [viewed under the same magnification (200 X)]. The nucleolus decreases in size from 7 to 1 μ m² between these cell types (Altmann and Leblond 1982).

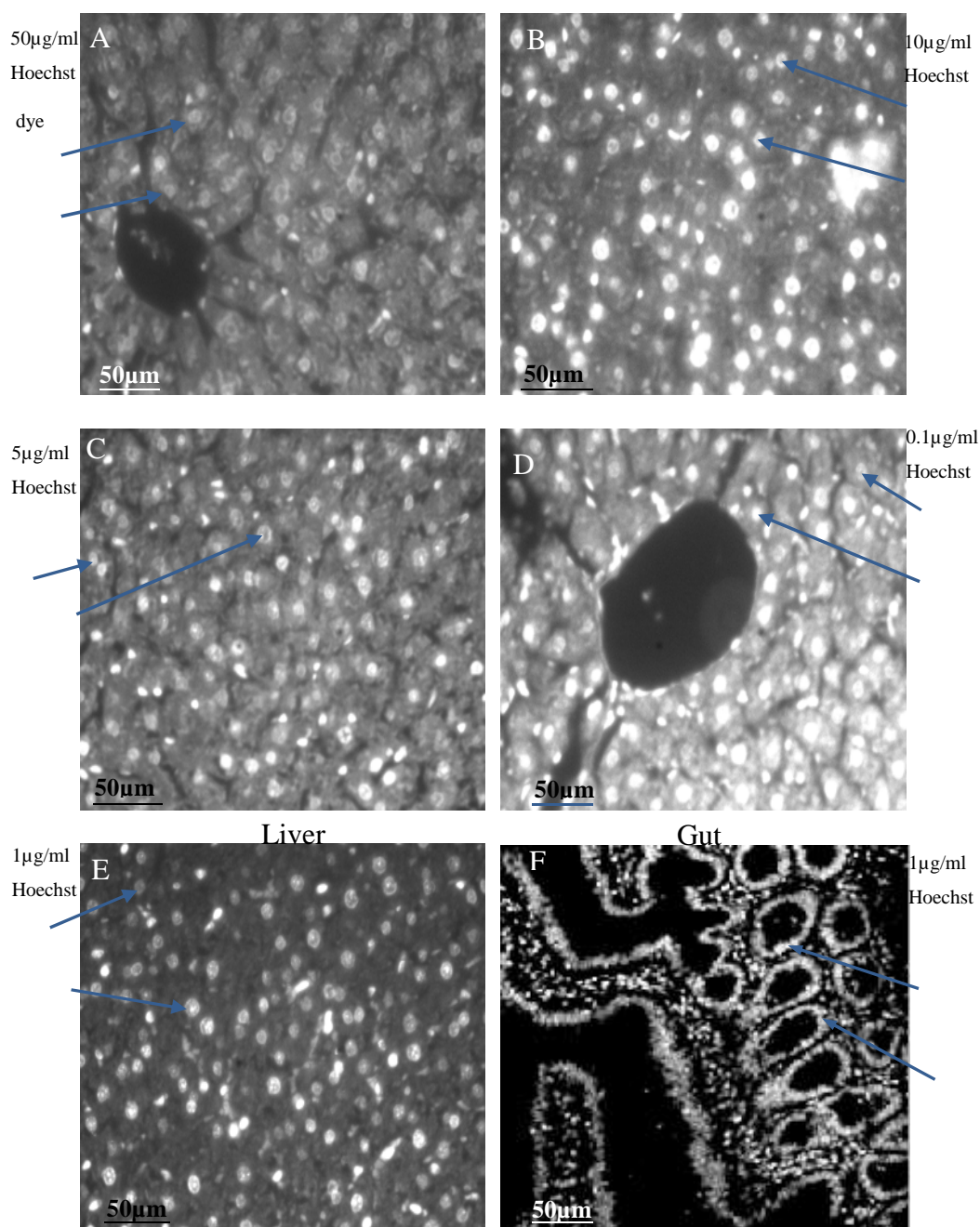


Figure 3-1 Optimisation of Hoechst dye staining: Paraffin sections were harvested from the liver of a F-344 rat aged 7-8 weeks.

The rat was injected i.p with 100 mg/kg BrdU. Slides of liver sections were stained with five different concentrations of Hoechst dye; (A) 50 µg/ml, (B) 10 µg/ml, (C) 5 µg/ml, (D) 0.1 µg/ml and (E) 1 µg/ml. Nuclei are visible after staining as indicated by the arrows. (F) Section of colon stained with 1 µg/ml Hoechst dye as a positive control. Hoechst dye was diluted in PBS solution and histochemistry techniques were performed as described in Table 1 in the appendix section. All slides had an exposure time = 100ms, binning level = 2, magnification = 400X.

3.1.1.2 Optimisation of washing solution (PBS).

To improve the background to noise ratio, the concentration of washing solution was optimised. The phosphate buffer solution (PBS) was modified into two different concentrations of NaCl. Three slides were prepared for each of the washing solutions. The slides were washed using either 0.2 M or 1 M of PBS. The results showed that the effect of varying the NaCl concentration of the PBS gave varying background to noise ratio when staining with Hoechst dye. Using a concentration of 0.2 M PBS was better than 1 M (Figure 3-2).

The duration of washing was also modified. 8 slides were prepared from the same section and each 2 slides underwent one of these washing times: (5 min X2, 10 min X2, 15 min X2 and 20 min X2). Results from these washing procedures showed that the best time was 2X 5 min.

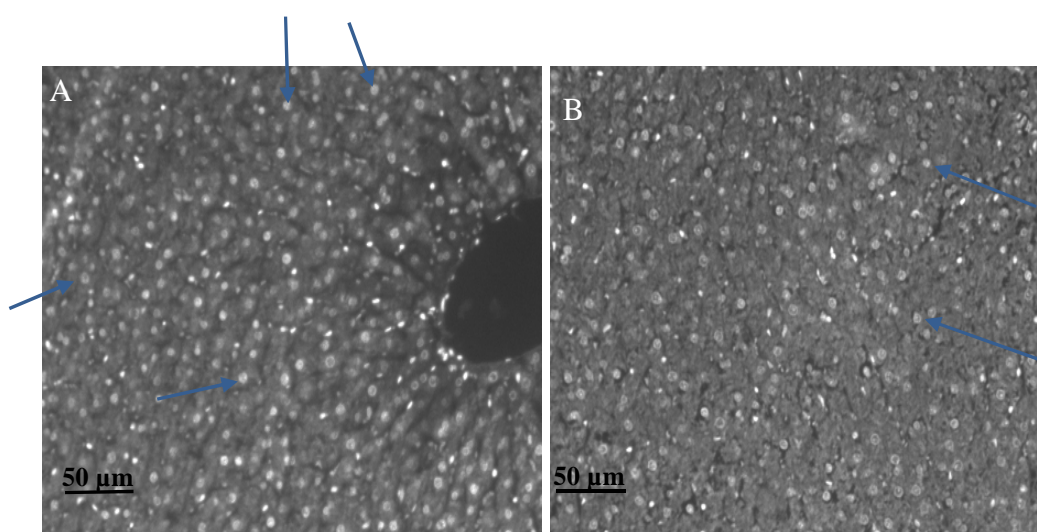


Figure 3-2 Optimisation of concentration of PBS washing solution for staining procedures

Liver sections were harvested from a rat aged 7-8 weeks. Two slides were prepared from the same tissue and then stained with 1 $\mu\text{g/ml}$ Hoechst dye. Slide (A) was washed in 0.2 M PBS whilst (B) was washed in 1 M PBS. The washing time used was 2X 5 min for each section. Blue arrows indicate liver cells. Magnification 400 X.

3.1.1 3 Assessment of immunohistochemistry protocol:

BrdU is a synthetic thymidine analogue that is incorporated into DNA during the S phase of the cell cycle. The BrdU immunohistochemistry technique has widespread use (Muskhelishvili, Latendresse et al. 2003). However, it was still necessary to check that the protocol worked properly. Two male F-344/NHsd rats aged 7-8 weeks were injected i.p with 100 mg/kg BrdU 2 hr before killing. Immunohistochemistry for the BrdU paraffin section technique (see Table 1 in Appendix) was used to stain the liver and colon sections as follows: stain with 1:1000 μ l, 1:750 μ l and 1:500 μ l of primary anti-BrdU body with the diluent buffer. The same concentration of secondary antibody (1:50 μ l) was used for all the different concentrations of primary antibodies. The results showed that using 1:750 μ l of primary antibody with 1:50 μ l of secondary antibody gave the best labelling index (Figure 3.3). The protocol was able to restrict incorporated BrdU to the cell nuclei with a good signal-to-noise ratio.

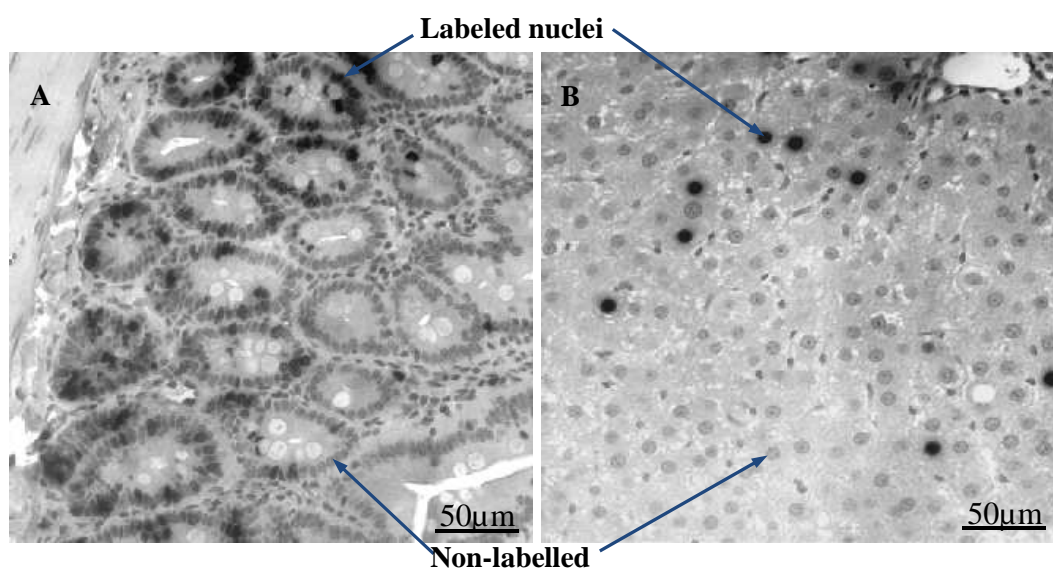
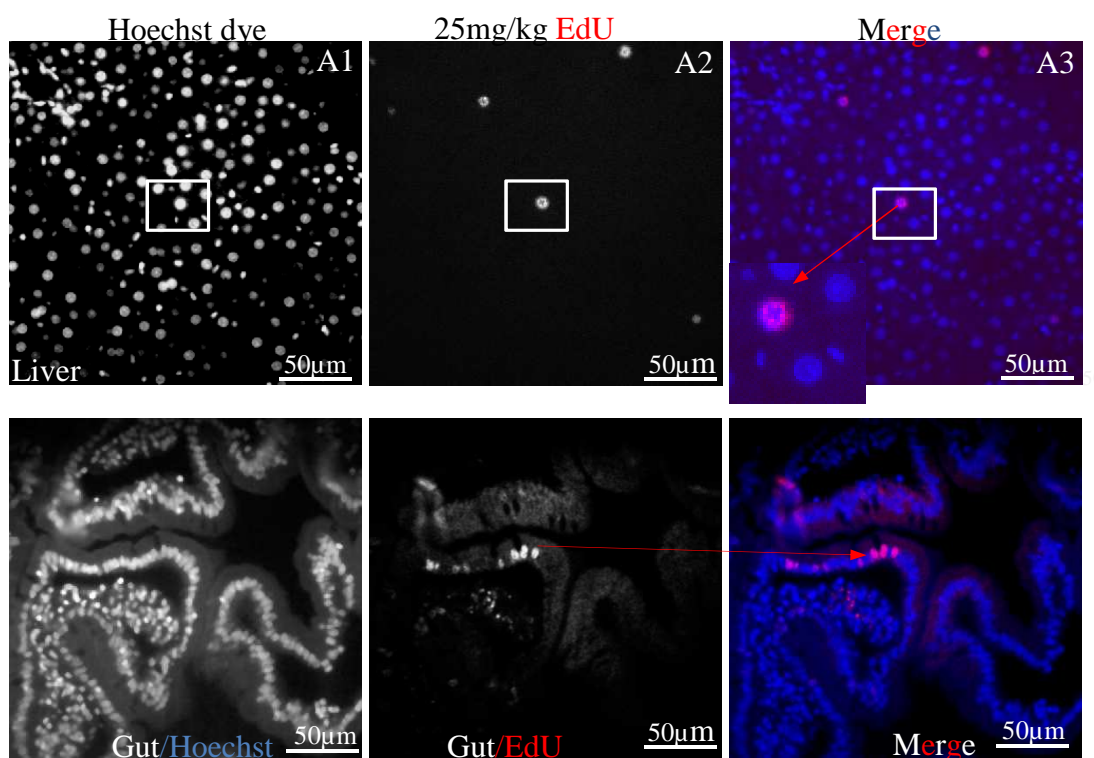


Figure 3-3 Assessment of BrdU immunohistochemistry protocol:

A; colon section and B; liver section. BrdU labelling was achieved with an immunohistochemistry protocol utilising primary and secondary anti-BrdU antibodies (Bio-Rad) and an Amersham cell proliferation kit. Liver and colon sections were harvested from an animal which was injected i.p with 100 mg/kg BrdU. The concentration of primary anti-BrdU was 1:750, and the concentration of secondary anti-BrdU was 1:50. The slides were examined under light microscope at 400X magnification. Micrographs were taken with a LucaEM DL-604 camera. Scale bar = 50 μ m.

3.1.2 Optimisation of the dose of EdU to monitor hepatic DNA synthesis

In order to determine the optimal dose of EdU for staining of DNA synthesis in hepatic cells, three different concentrations were assessed. Three groups of male F-344 rats aged 7-8 weeks were injected i.p with 2, 5 or 25 mg/kg of EdU. The colon sections were used as a positive control alongside the liver sections. A fourth group was injected with 100 mg/kg BrdU which was used as a negative control Figure 3-4. As shown in Figure 3-6 below, the hepatic cells responded well with the three concentrations of the click-iT EdU used. The EdU succeeded in identifying the replicative DNA synthesis. All the EdU concentrations yielded acceptable results and therefore the lowest concentration (2 mg/kg) was used in the further studies.



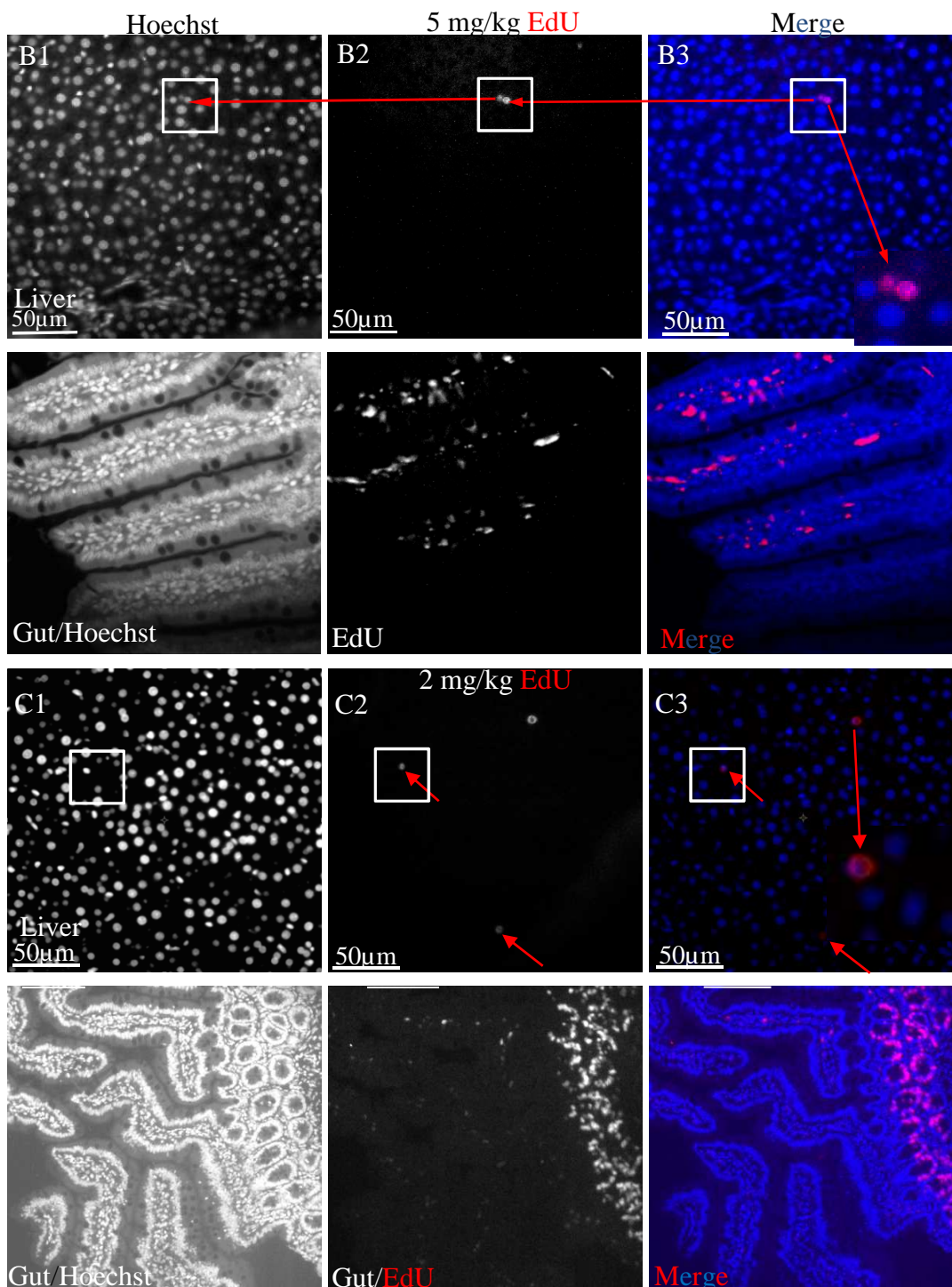


Figure 3-4 Assessment of use of different doses of EdU to evaluate hepatic DNA synthesis:

Micrographs of liver and gut were taken by a Luca^{EM} DL-604 Camera at 400X magnification. Micrograph A2; represents liver section of rat injected with 25 mg/kg EdU, B2; liver section of rat injected with 5 mg/kg EdU; and C2, liver section of rat injected with 2 mg/kg EdU. The liver and gut tissues were sliced to 4.5 µm thickness and mounted on polysine slides. All sections (liver and colon) were stained by EdU or Hoechst histochemical techniques as described in the appendix (table 2). Micrographs A1, B1 and C2 were stained with Hoechst, whilst A3, B3 and C3 are micrographs 1 and 2 merged using Photoshop. Gut sections were used as a control and are shown below each row of liver sections. Arrows are used to highlight representative stained nuclei.

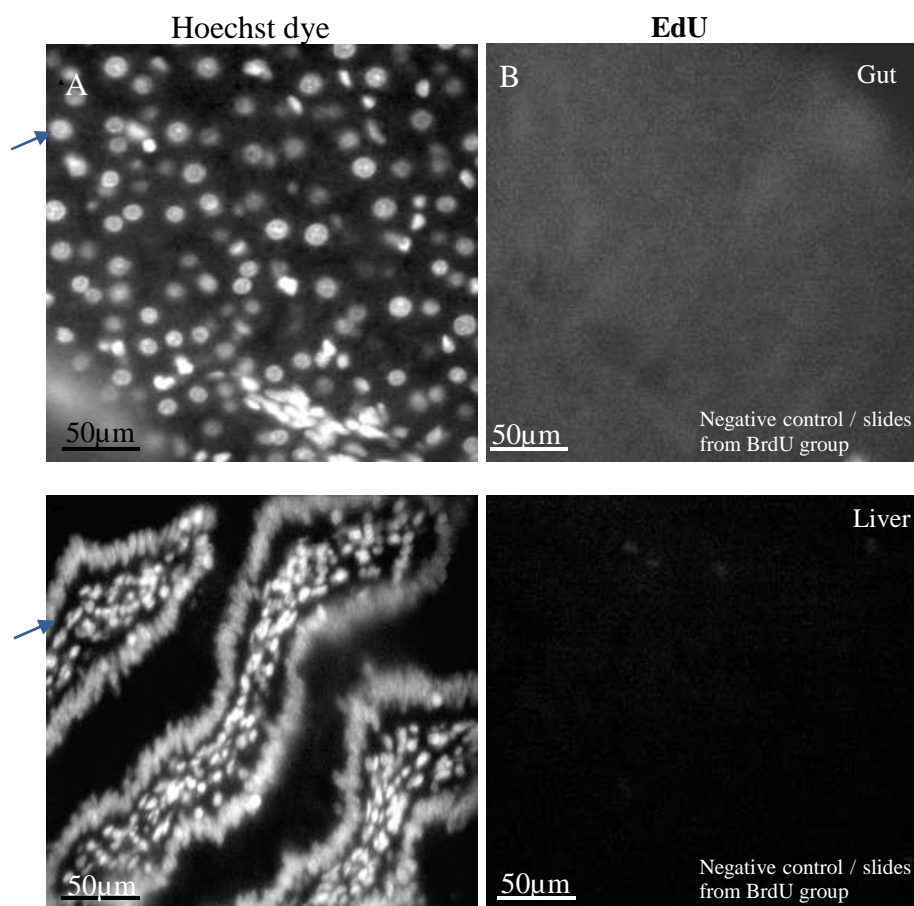


Figure 3-5 Assessment of EdU staining in BrdU control treated tissue

Micrographs of liver and gut were taken by a Luca^{EM} DL-604 camera at 400X magnification. Micrograph (A) liver section taken from a rat injected with 100mg/kg BrdU and (B) gut section as a control. Both sections were used as a negative control for the EdU stain. The liver and gut tissues were sliced to 4.5 µm in thickness and mounted on polysine slides. All sections (liver and colon) were stained with Click iT EdU histochemical technique. The gut section was used as a positive control for Hoechst staining. Arrows indicate cells labelled with the Hoechst dye in liver and gut.

3.1.3 Investigation of EdU doses to monitor hepatic DNA synthesis

The aim of this experiment was to choose between three different concentrations of EdU, based on its ability to detect hepatic DNA synthesis, with the aim of determining the lowest dose to reduce the severity of impact on rat cells. Eight male F-344 rats at age 7-8 weeks were brought from Harlan. The rats were divided into 4 groups and each two of them were injected intraperitoneal (i.p) with 100 mg/kg BrdU in PBS or 2, 5 or 25 mg/kg EdU in PBS, respectively, 2 hr prior to kill. The rats were sacrificed 2 hr after injection and animals body weight (data not shown), and the percentage liver weight to body weight ratio was determined (Figure 3-6). Liver tissues were put in formaldehyde fixative with a part of colon included as a positive control for immunohistochemistry. The results showed that all three concentrations of EdU yielded acceptable results, with a significantly higher liver weight to body weight ratio detected only when using the highest concentration of 25 mg/kg EdU (Figure 3-6). The average liver weight to body weight ratio (%) in the rats dosed with BrdU was 4.30 ± 0.04 and the average of the three dosing EdU concentrations were 4.27 ± 0.06 , 4.3 ± 0.12 and 4.65 ± 0.3 , respectively.

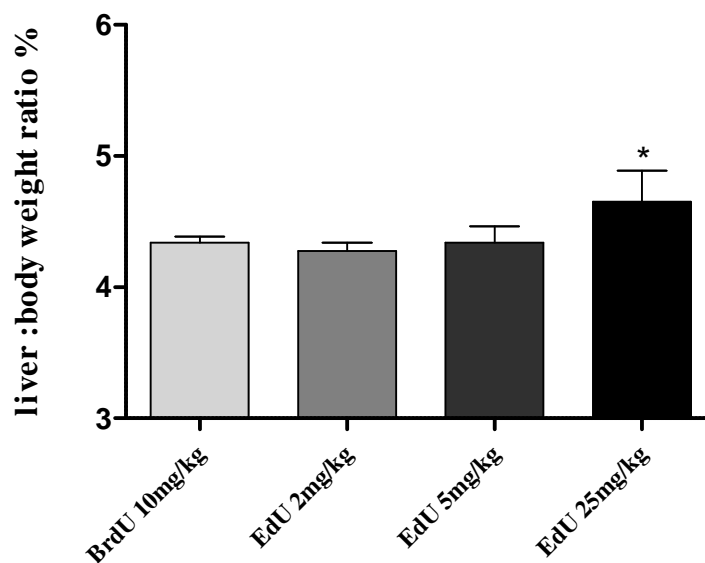


Figure 3-6; Liver weight to body weight ratio (%) resulting from treatment with three different EdU concentrations.

Male F-344NHsd rats aged 7-8 weeks, were injected with either BrdU or EdU and killed after 2 hr. All data are expressed as mean \pm SD. There were no statistically significant differences between BrdU and EdU groups. (n=2), except for the EdU 25mg/kg concentration which exhibited a significantly different liver weight to body weight ratio (starred) compared with all other concentrations of EdU and BrdU, according to a one way ANOVA test using Tukey's multiple comparisons test ($P < 0.05$). ($P < 0.05$).

3.1.4 Preliminary work for dual labelling of treated cells

Initially it was aimed to sequentially stain the same liver sections, first with EdU and then with BrdU (or vice versa). Thus it was hoped to see whether the same, or different groups of cells, were dividing (in response to ciprofibrate treatment) by analysis of the same individual slide. However, despite extensive experimental work and assaying of many different conditions and sequential use of the various dyes [e.g. Hoechst followed by haematoxylin stain (Figure 3-7) use of different dehydration protocols (Figure 3-8) etc.] unsatisfactory results were obtained, with no reliable staining protocol found (full data not shown). It is important to note that such sequential use of both dyes on the same tissue sample has not, to our knowledge, been previously reported.

Therefore in subsequent work closely aligned tissue sections were used for the dual labelling experimental work as explained in section 2.2.3.

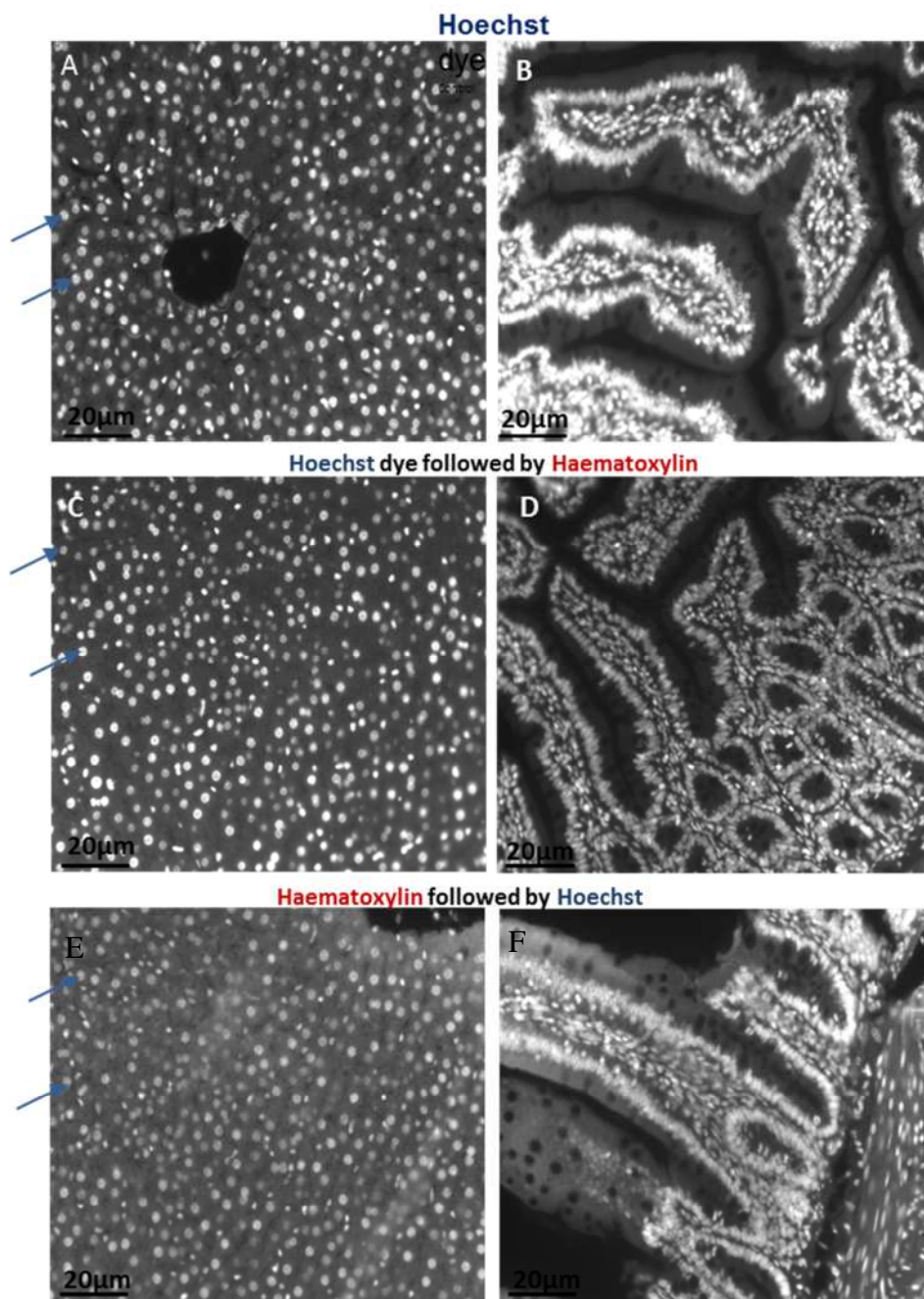


Figure 3-7 Assessing the effect of using Hoechst alongside haematoxylin stain:

Liver and colon sections were harvested from male F-344 rats aged 7-8 weeks which had been injected i.p with 2 mg/kg EdU 2 hr before killing. A and B, liver and colon sections were stained with Hoechst dye alone as a positive control for the Hoechst dye. C and D; liver and colon sections were stained with Hoechst dye followed by Haematoxylin. E and F; liver and colon sections were stained with Haematoxylin followed by Hoechst. Colon sections were used as positive control. The slides were examined using light microscope with a DAPI filter. Arrows indicate nuclei. The micrographs were taken with a Luca^{EM} DL-604 camera at 200X magnification.

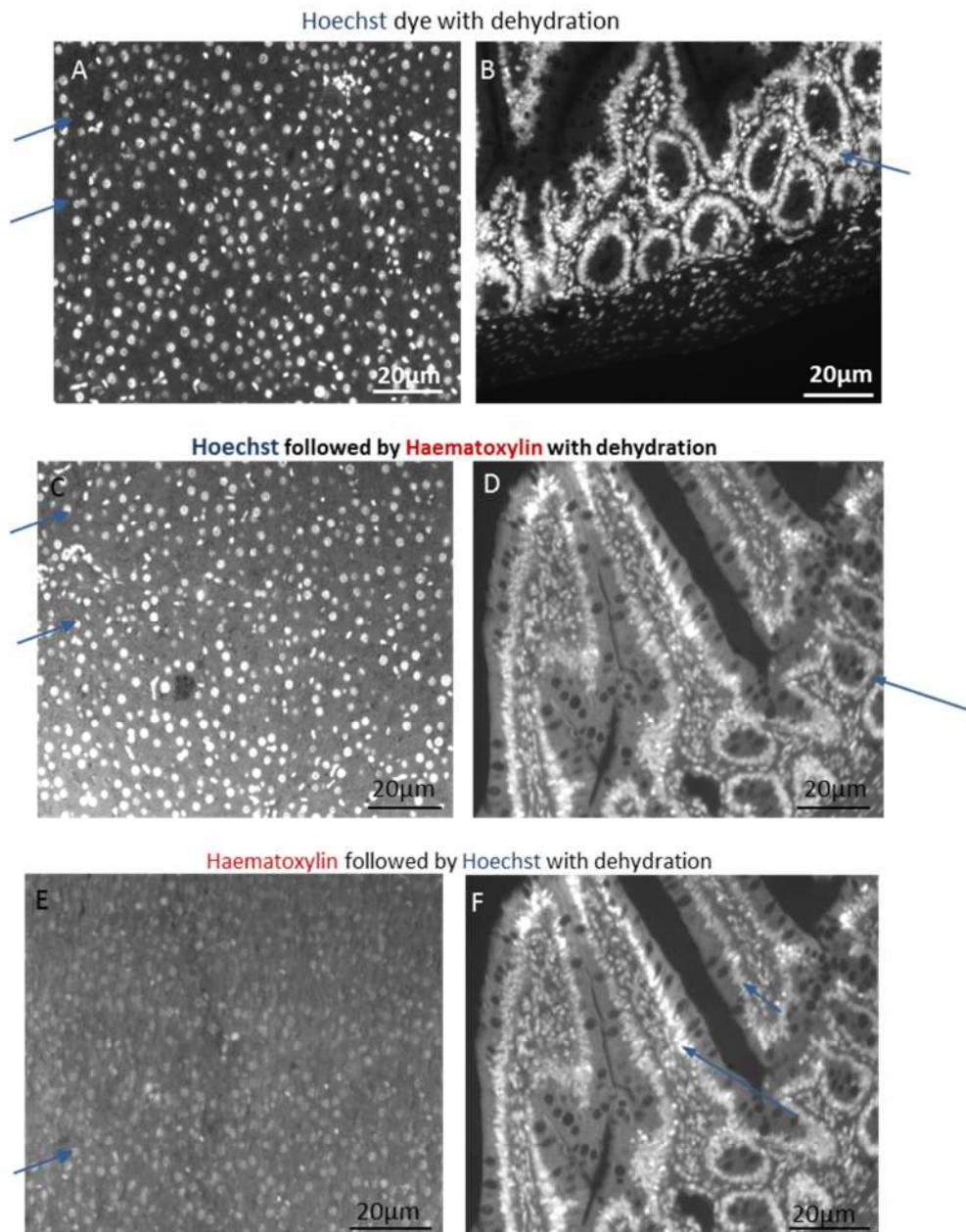


Figure 3-8 Assessing the effect of a dehydration protocol on use of Hoechst alongside haematoxylin staining

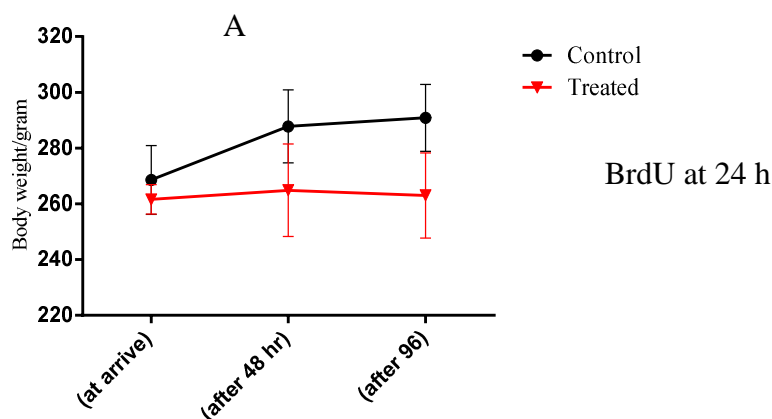
Liver and colon sections were harvested from male F-344 rats aged 7-8 weeks which had been injected i.p 100 mg/kg BrdU 2 hrs before killing. A and B, liver and colon sections were stained with Hoechst dye alone as a positive control for the Hoechst dye. C and D; liver and colon sections were stained with Hoechst dye followed by Haematoxylin. E and F; liver and colon sections were stained with Haematoxylin followed by Hoechst. Colon sections were used as positive control. The slides were examined using light microscope with a DAPI filter. Arrows indicate nuclei. The micrographs were taken with a Luca^{EM} DL-604 camera at 200X magnification.

3.1.4 Induction of hepatic DNA synthesis by ciprofibrate in male F-344/NHsd rats

The aim of this experiment was to test the hypothesis that ciprofibrate will induce hepatic, replicative DNA synthesis during the process of augmentative growth in male F-344/NHsd rats aged 14-15 weeks. 36 rats were used which were housed randomly. These were split into three independent subset groups of 12 rats, which were then split into 6 treated and 6 control rats i.e. a total of 6 rats \times 6 groups with three independent groupings. The three sets of 12 rats were later used either to investigate the effects of BrdU injection, EdU injection effects or in the dual labelling 48 hr experiment. The animals were monitored by their body weight daily before and during the experiment [Appendix: Table 5 displays the gavage procedure of ciprofibrate, injection of EdU and BrdU, body weight and liver weight].

3.1.4.1 Time course protocol of effects of 50 mg/kg/day ciprofibrate

Before starting the experiment, it was necessary to monitor the animal's health. Figures 3-9 A-C shows the body weight of the six groups of rats used in the time course protocol of effects of 50 mg/kg/day Ciprofibrate experiment as described in method section 3.1.3. The body weights of the rats were measured periodically, and results indicated that they were in a healthy state suitable for experimentation. Figure 3-9 A shows the body weight of the rats used for the experiment when BrdU was injected.



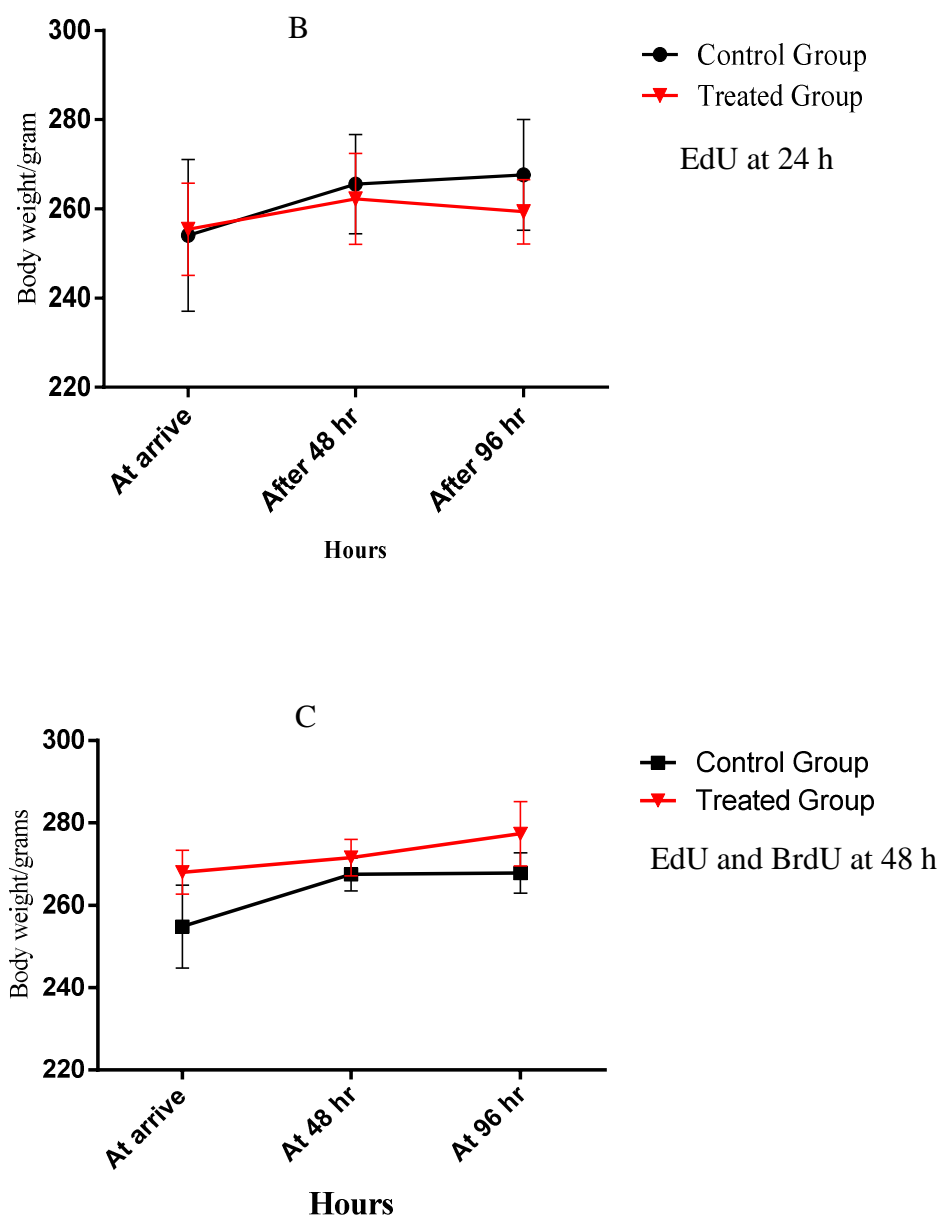
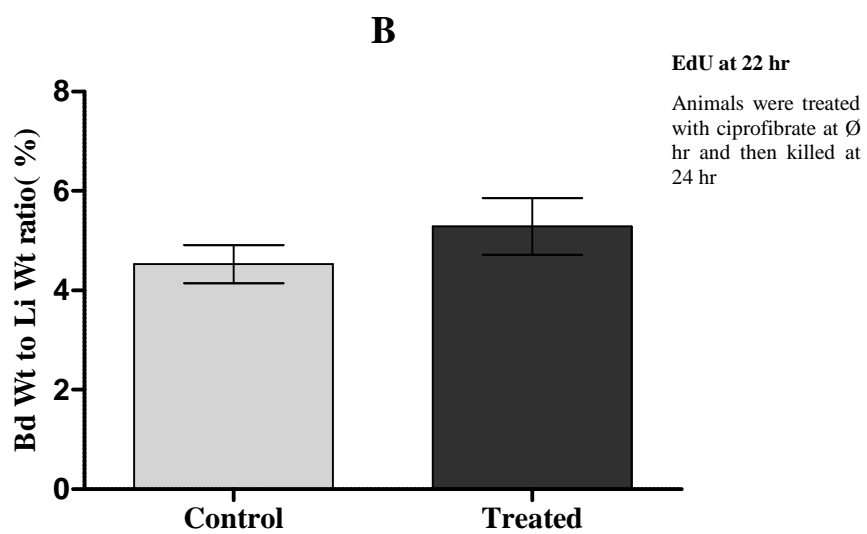
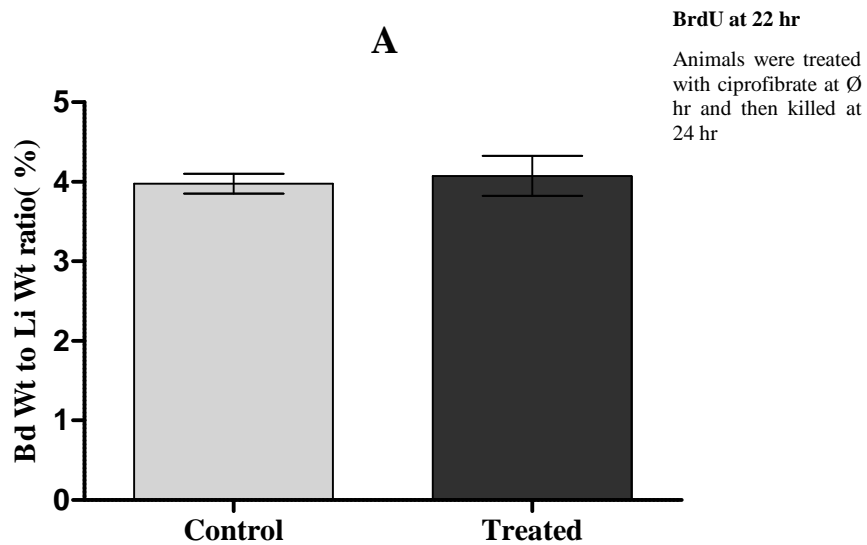


Figure 3-9 Body weight of rats during laboratory adaption period. Three groups of male F-344 rats, aged 14-15 weeks were used for the time course protocol of effects of 50 mg/kg/day Ciprofibrate.

To ensure that rats were in a suitable state of health for experimental work they were weighed regularly both before and during the experimental work. There was no significant difference in body weight amongst the rats. A; all rats will be used for the effects of BrdU injection. B; will be used for EdU injection effects. C; will be used in 48 hr experiments. The animals were provided with good conditions in terms of the temperature and relative humidity, being held at 22 ± 2 °C and 40 ± 5 %, respectively. The animals were fed a standard lab diet with tap water ad libitum. Data shown are mean \pm SD (n=6). Statistically there were no significant differences from the control group in the body weight over 96 hr in groups (A, B and C).

3.1.4.2 Time course effects on relative liver weight to body weight of male F-344 rats aged 14-15 weeks treated with 50mg/k ciprofibrate

Six groups of male F-344 rats were used in the time course experiment to look at the effects of 50 mg/kg/day ciprofibrate on liver weight to body weight ratio (as described in methods section 2.2.2 above). Statistically a t-test was performed to compare control and treated groups in each of the following injection treatments. Figure 3-10 A: represents rats gavaged with either corn oil or 50 mg/kg ciprofibrate at time \emptyset and injected i.p with 100 mg/kg BrdU after 22 hrs then killed at 24 hr. In this case the mean liver weight: body weight ratio (%) was 3.97 ± 0.12 in control and 4.07 ± 0.25 in treated rats. Figure 3-10 B; rats were gavaged at time \emptyset with either corn oil or 50 mg/kg ciprofibrate. At time 22 hr they were injected i.p with 2mg/kg EdU, and then at 24 hr the animals were killed. The mean was 4.5 ± 0.38 in control group and 5.2 ± 0.57 in treated group. Figure 3-10 C; rats were gavaged at time \emptyset with either corn oil or 50 mg/kg ciprofibrate. At 22 hr they were injected i.p with 2mg/kg EdU, and then gavaged again with 50 mg/kg ciprofibrate. At 46 hr the rats were injected i.p with 100 mg/kg BrdU, and then 2 hr later the animals were killed. The mean was 3.53 ± 0.22 and 5.44 ± 0.27 control and treated rats respectively.



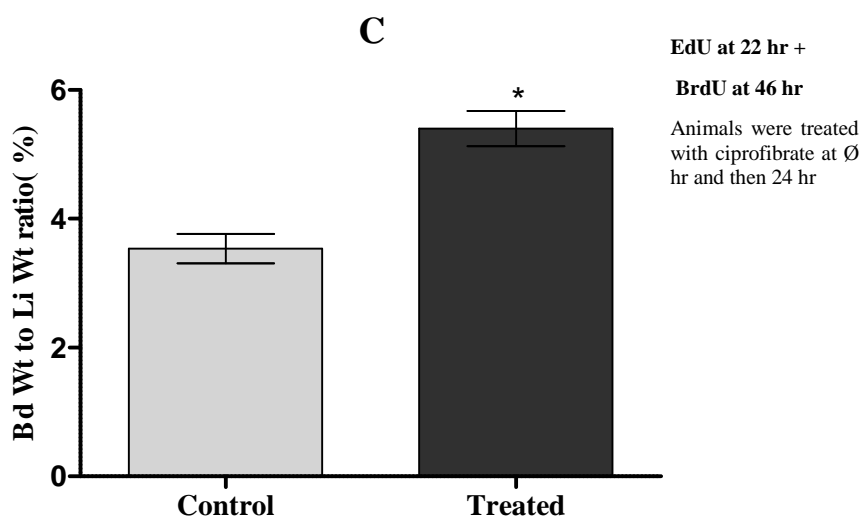
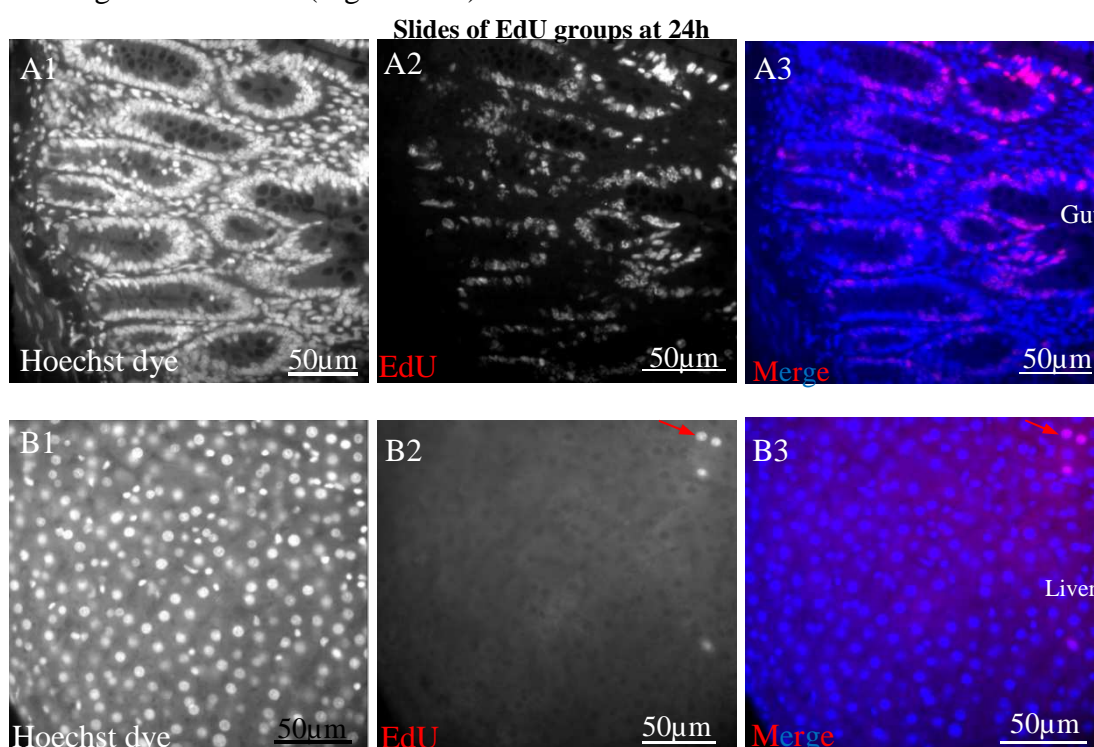


Figure 3-10 Time course of effects of ciprofibrate in F-344/NHsd rats. Groups of male rats aged 14-15 weeks were dosed with either 50 mg/kg/day ciprofibrate or corn oil (vehicle).

Figures represent three groups of rats which were injected 2 hr prior to kill with either EdU or BrdU or both. A shows liver weight to body weight ratio for the group injected i.p with BrdU 2 hr prior to kill. B shows liver weight to body weight ratio for the group injected i.p with EdU 2 hr prior to kill. C shows liver weight to body weight ratio for the group injected i.p with EdU at 22 hr and BrdU at 46 hr and then killed at 48 hr. There were no statistically significant differences between control and treated groups in groups A and B, while there was a significant difference between control and treated in group C according to a student's t-test ($P < 0.05$). All data are expressed as mean \pm SD ($n = 6$). Statistically significant differences between the control and treated rats as indicated by an asterisk.

3.1.5 Using base analogue stains EdU and BrdU

To test the hypothesis that ciprofibrate will induce hepatic, replicative DNA synthesis during the process of augmentative growth in F-344 rats, two different analogue stains (EdU and BrdU) were used. After optimisation of the EdU staining technique, it was essential to test the EdU stain with both control and treated groups of animals. As a negative control BrdU groups were used to ensure that the results were not artefacts and vice versa of EdU. Figure 3-11 shows that the click-iT EdU stain gave reliable staining, with nuclei undergoing DNA replication clearly visible in both control (Fig 3-11 A and B) and treatment (Fig 3-11 C and D) groups, whereas not in where BrdU control staining was used without the primary monoclonal anti-BrdU antibody, (Fig 3-11 E and F). Meanwhile, the complete BrdU immunohistochemistry protocol also gave clear and reliable results with darkly staining nuclei evident (Figure 3-12).



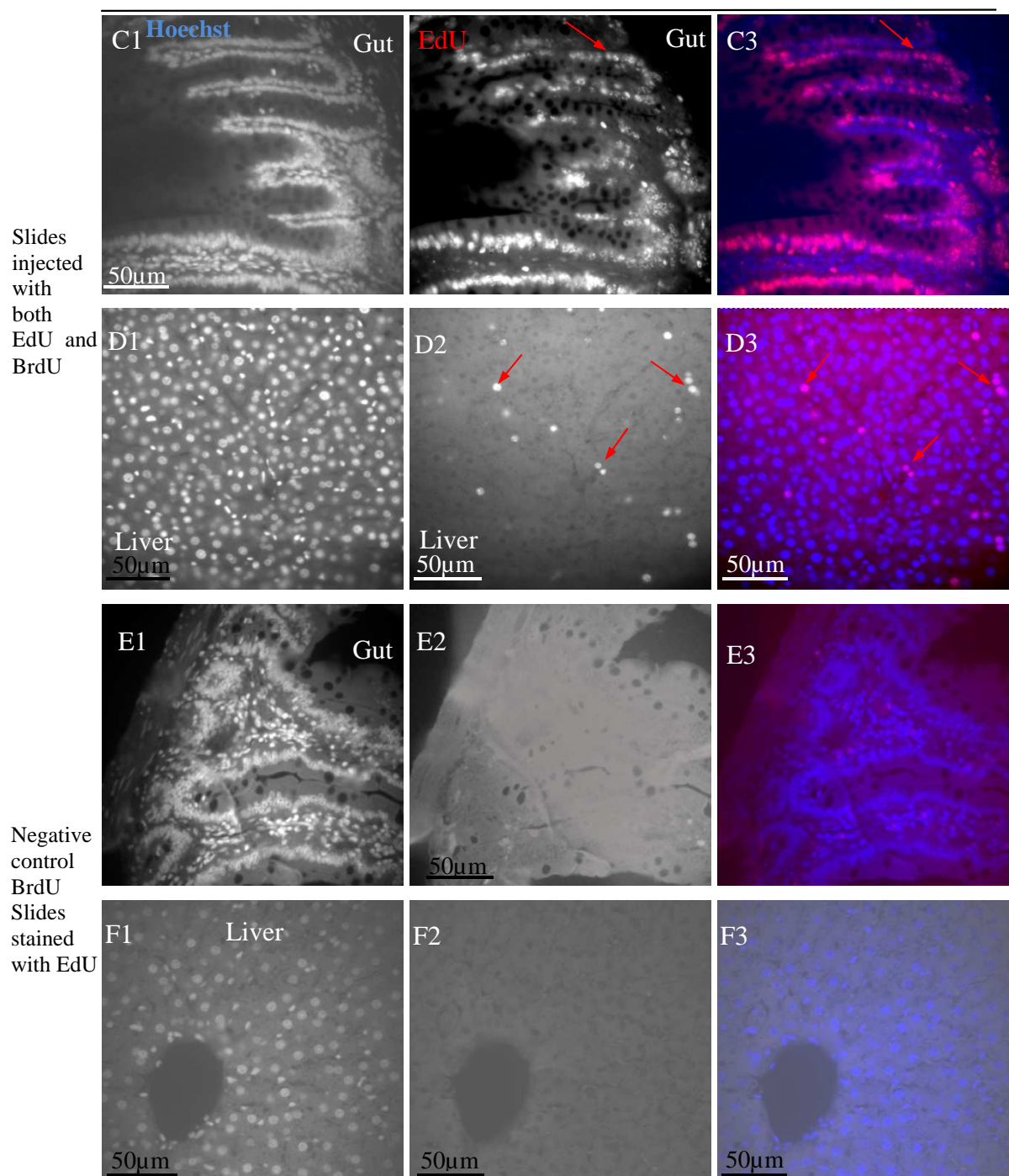


Figure 3-11 Micrographs illustrating the use of the base analogue stains EdU in immunohistochemical staining.

The figure shows a series of slides prepared from male F-344/NHsd rats aged 14-15 weeks. (A and B) Gut and liver sections, respectively, from rat gavaged with corn oil (control group) then injected i.p with 2 mg/kg EdU. (C and D) Gut and liver sections, respectively, taken from rats treated with ciprofibrate then injected i.p with 2 mg/kg EdU. (E and F) Gut and liver sections, respectively, taken from a rat gavaged with ciprofibrate then injected i.p with 100 mg/kg BrdU. Micrographs numbered (1) were stained with Hoechst stain alone, those numbered (2) were stained with EdU, those numbered (3) are coloured merged images produced using Photoshop. The **red arrows** indicate replicative DNA synthesis. The micrographs were taken with Luca^{EM} DL-604 camera using an exposure time of 100ms and a medium setting (2) for binning at 400X magnification.

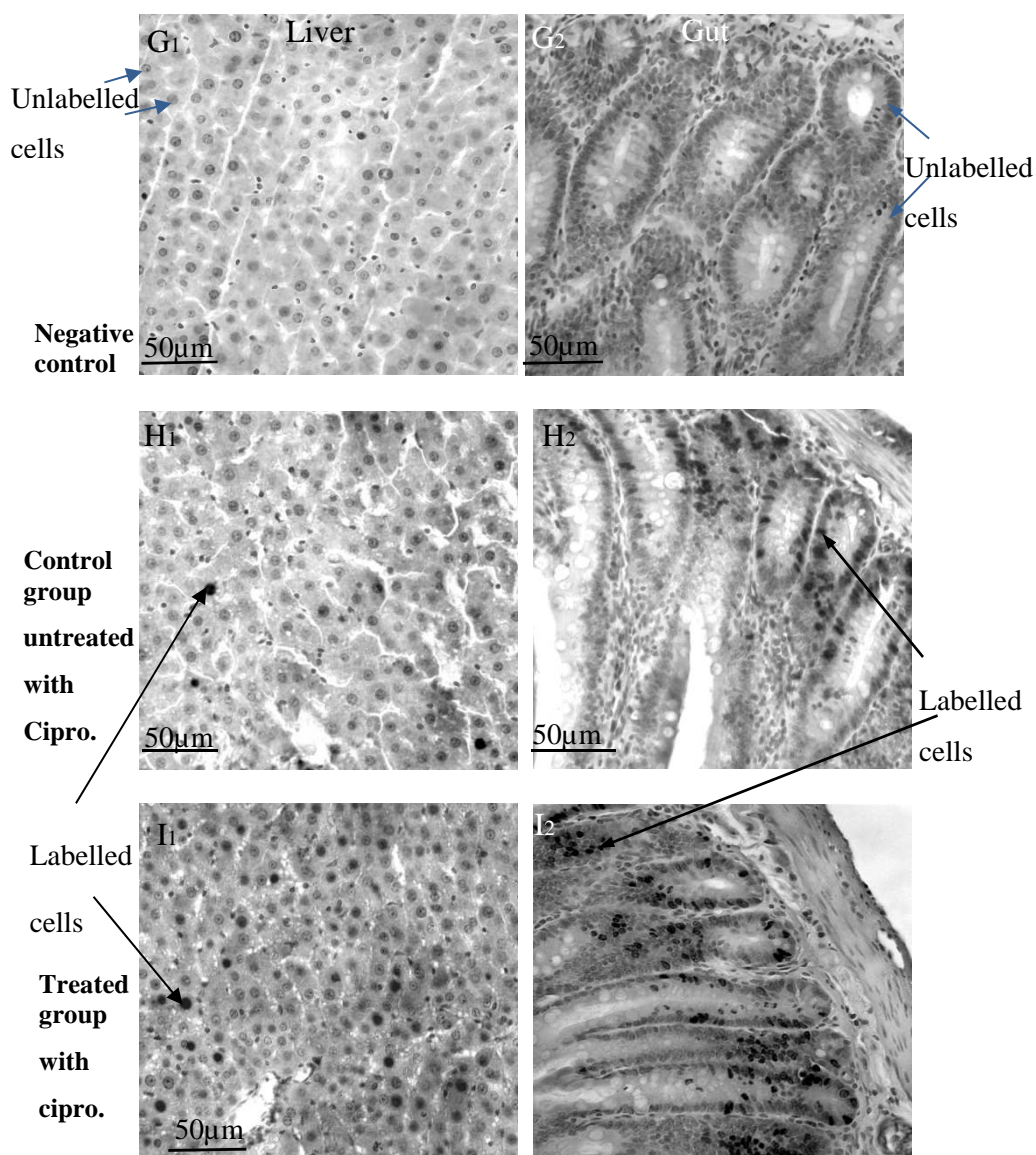


Figure 3-12 Micrographs illustrating the use of the base analogue BrdU in immunohistochemical staining.

The figure shows slides prepared from male F-344/NHsd rats, aged 14-15 weeks. (G1 and G2) shows liver and gut sections, respectively, taken from a rat treated with ciprofibrate then injected i.p with 100 mg/kg BrdU. These tissues were stained without the primary anti-BrdU antibody. (H1 and H2) shows liver and gut sections, respectively, taken from a rat gavaged with corn oil (control vehicle) then injected i.p with 100 mg/kg BrdU, these tissues were stained in the presence of both primary and secondary anti-BrdU antibodies. (I1 and I2), shows liver and gut sections, respectively, taken from a rat gavaged with ciprofibrate then injected i.p with 100 mg/kg BrdU, these tissues were stained in the presence of both primary and secondary anti-BrdU anti-bodies. The micrographs were taken with a Luca^{EM} DL-604 camera using an exposure time of 100 ms and setting (1) for binning at 400X magnification.

3.1.6 Comparison of induction of DNA synthesis by EdU and BrdU staining

An experiment was first performed to determine whether there was any effect on the animal resulting from staining, through calculating the liver weight to body weight ratio and comparing the results with control group. The results obtained showed that both histochemical markers alone had no significant effect on rats (Figure 3-13 A, B).

It was then necessary to confirm that both EdU and BrdU staining identified a similar number of cells undergoing DNA replication, to ensure that both stains could be used to reliably detect any such cells to obtain reliable results. Male F-344 rats, aged 14-15 weeks, were used. Two groups of six rats each (control and treated) were injected i.p with 2 mg/kg EdU at 22hr. Two groups of six rats each (control and treated) were injected i.p with 100 mg/kg BrdU at 22hr (method section 2.2.1). 2,000 nuclei were counted for each liver tissue slide to determine the hepatic DNA labelling index. Nuclei were labelled with click-iT EdU which gave a bright red colour (e.g. Figure 3-17 note that nuclei appear white in these images due to use of a high resolution black and white detection camera) indicating that the cells underwent DNA division. By contrast, nuclei labelled with BrdU gave a black/brown colour (e.g. Figure 3-16; note that nuclei appear black in these images due to use of a high resolution black and white detection camera). Also, non-labelled nuclei were counted. The percentage of the labelled nuclei was then calculated. Both EdU and BrdU were shown to give reliable results when randomly choosing an area of the tissue under a microscope, the nuclei were systematically counted until 2,000 nuclei were reached. This was done for both staining groups, BrdU and EdU (control and treated). Comparison of results of the induction of DNA synthesis by BrdU & EdU showed that there was no significant difference between EdU and BrdU stains as shown in Figures 3-13, 3-14 and 3-15 below.

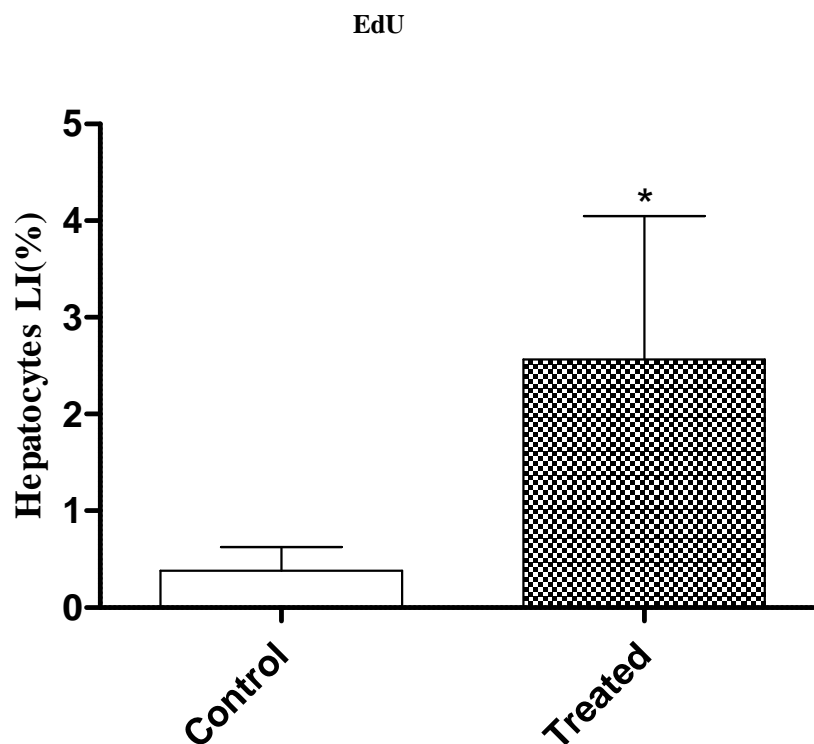


Figure 3-13: Labelling index of hepatocytes of male F-344/NHsd rats treated with 50 mg/kg/day ciprofibrate or control (corn oil) and then injected i.p. with EdU.

Time course showing the effects of ciprofibrate treatment on groups of male rats aged 14-15 weeks which were dosed with 50 mg/kg/day ciprofibrate or corn oil control (vehicle) at time \emptyset , and then injected with EdU 2mg/kg i.p 2 hr prior to sacrifice at 24 hr. Values represent mean \pm S.D, (n=6).

*Control and treated groups were statistically different from each other according to a student's t-test at $P < 0.05$.

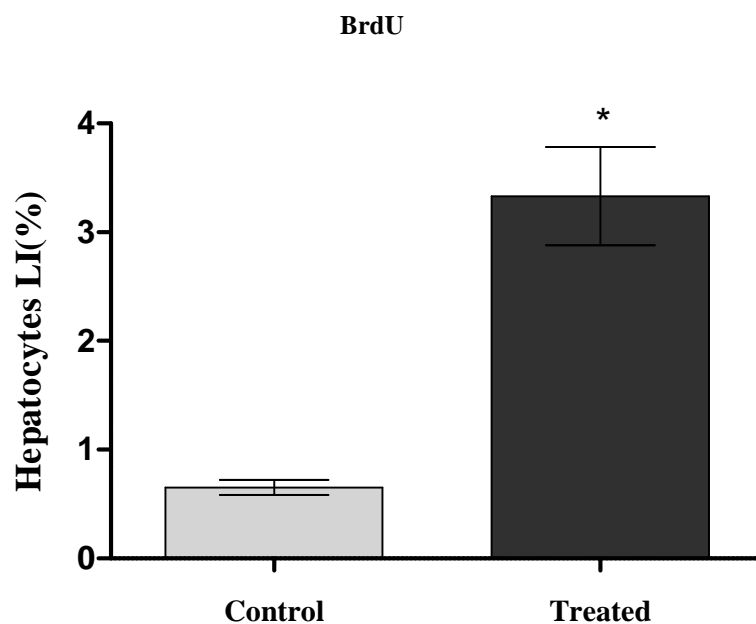


Figure 3-14: Labelling index of hepatocytes of male F-344 rats treated with 50 mg/kg/day ciprofibrate or control (corn oil) and then injected i.p. BrdU.

Time course showing the effects of ciprofibrate treatment on groups of male rats aged 14-15 weeks which were dosed with 50 mg/kg/day ciprofibrate or corn oil control (vehicle) at time 0, and then injected with BrdU 100mg/kg i.p 2 hr prior to sacrifice at 24 hr. Values represent mean ± SD (n=6).

*Control and treated groups were statistically different from each other according to a student's t-test at $P < 0.05$.

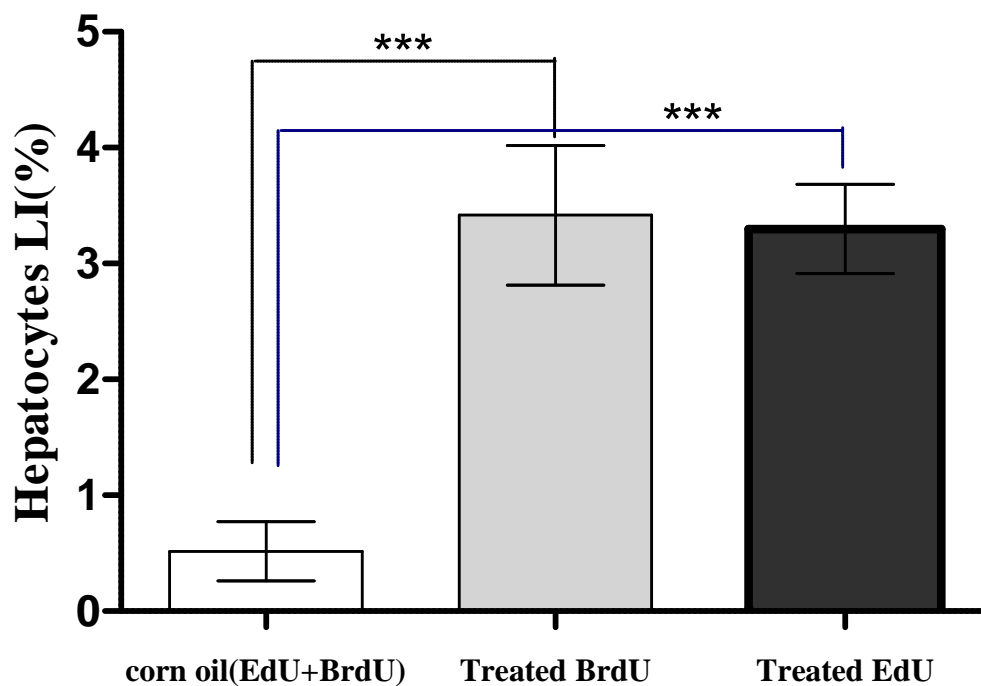


Figure 3-15: Effect of ciprofibrate or corn oil control on labelling indices of hepatocytes in F-344/NHsd rats, comparing groups treated with EdU and BrdU.

The diagram shows the comparison of labelling indices of groups which were injected with EdU or BrdU against a corn oil control. Groups of six male F-344 rats aged 14-15 weeks were dosed with 50 mg/kg/day ciprofibrate or control corn oil (vehicle) at time \emptyset and then injected at 22 hr i.p with either 100 mg/kg BrdU or 2 mg/kg EdU prior to kill at 24 hr. Values are expressed as mean \pm SD, (n=6). Control and treated groups were statistically different from each other according to a one way ANOVA *** Significant difference between control and both treated groups, $P < 0.05$.

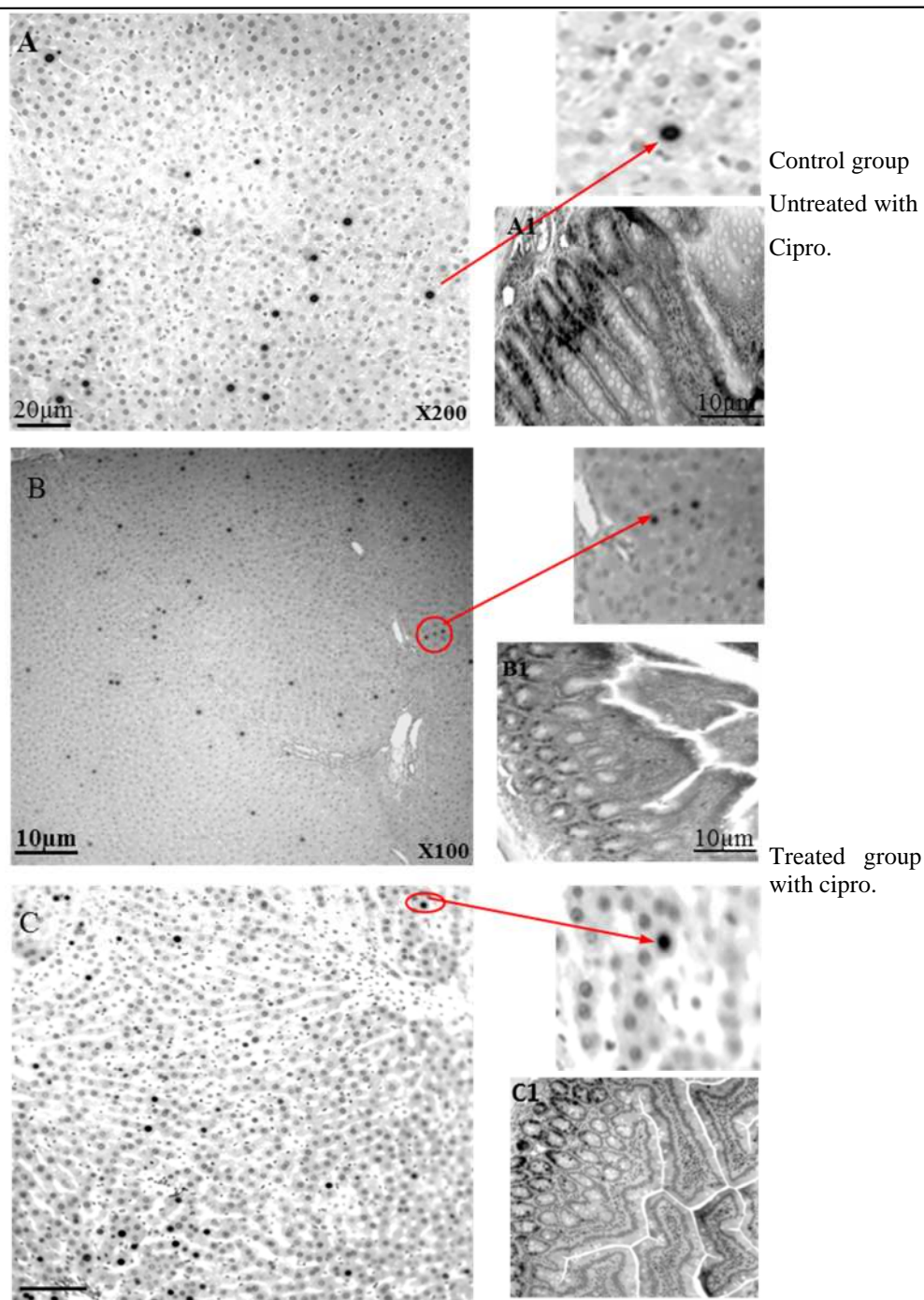
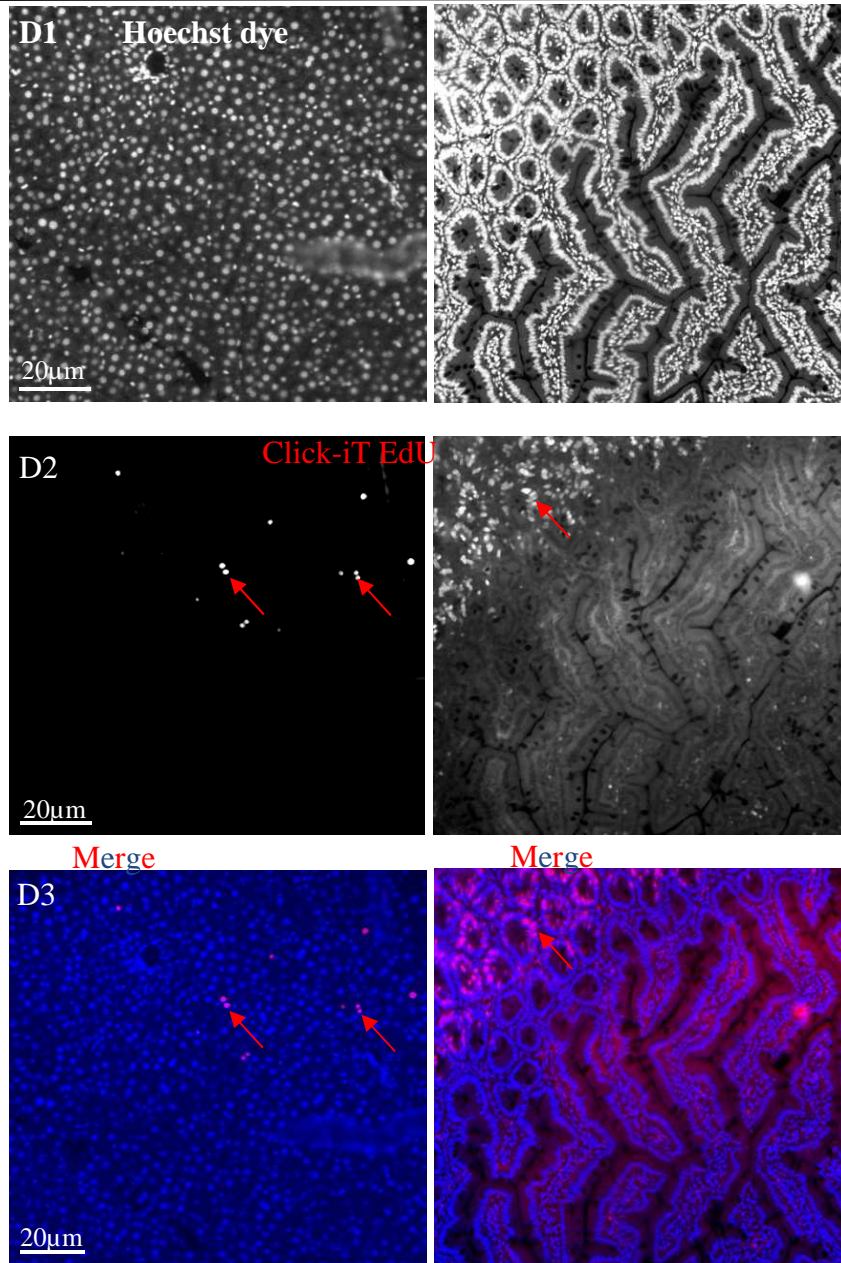


Figure 3-16 Immunohistochemical staining with BrdU.

The figures show slides prepared from male F-344/NHsd rats, aged 14-15 weeks. Liver and gut sections were taken from rats either treated with ciprofibrate or from corn oil treated control groups. They were injected i.p with 100 mg/kg BrdU. The tissues were stained by an immunohistochemistry technique. (A and A1) shows liver and gut sections, respectively, taken from a rat gavaged with corn oil (control vehicle group) then injected i.p with 100 mg/kg BrdU. (B and B1) and (C and C1) shows liver and gut sections, respectively, taken from rats gavaged with ciprofibrate then injected i.p with 100 mg/kg BrdU. The slides were examined with a light microscope. The micrographs were taken with a Luca^{EM} DL-604 camera using an exposure time of 100 ms and setting (1) for binning at either 100X or 200 X magnifications. Red arrows indicate replicative DNA synthesis, with inserts showing magnified images from originals of A, B and C.



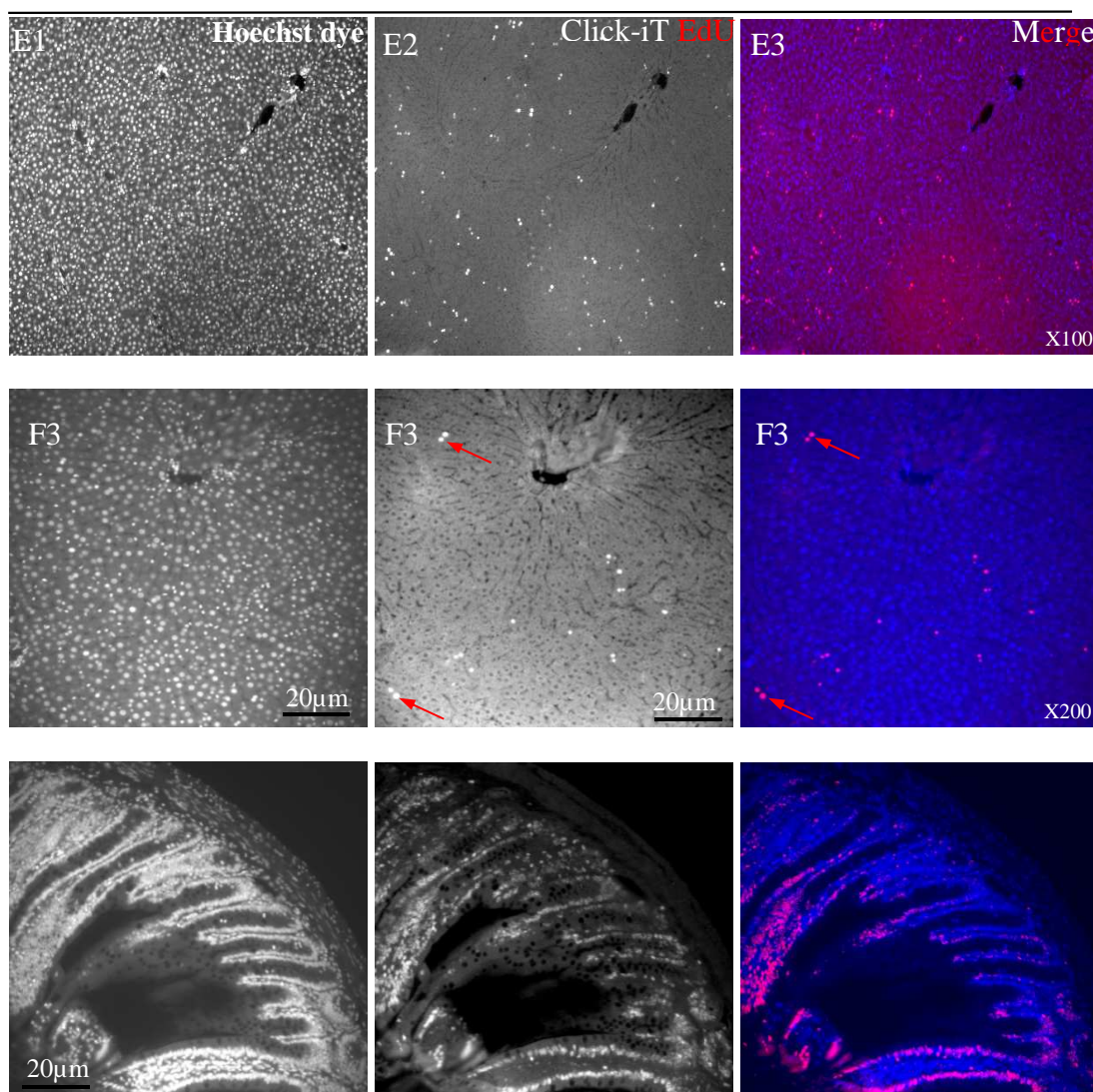


Figure 3-17 Histochemical staining with EdU.

The figure shows slides prepared from male F-344/NHsd rats aged 14-15 weeks. The figure displays nuclei detected with Hoechst dye compared to replicative DNA synthesis detected with the click-iT EdU protocol. (D1-3) show liver and gut sections (right and left hand sides, respectively) taken from a rat gavaged with corn oil (control group) then injected i.p with 2 mg/kg EdU. The animal was killed 24 hr after treatment. Image D1 was stained with Hoechst, D2 with Click-iT Edu, and D3 shows a merged colour image produced using Photoshop. (E and F) show two separate examples of liver sections taken from a rat treated with ciprofibrate then injected i.p with 2 mg/kg EdU at 200X magnification. Images E1 and F1 were stained with Hoechst, E2 and F2 with Click-iT Edu, and E3 show merged colour images produced using Photoshop. Finally, images G1-G3 show staining of gut sections as a positive control, G1 was stained with Hoechst, G2 with Click-iT Edu, and G3 shows a merged colour image produced using Photoshop. Replicative DNA synthesis shown in Click-iT stained images as white spots, as indicated by red arrows. The micrographs were taken with a Luca^{EM} DL-604 camera using an exposure time of 100 ms and a medium setting (2) for binning at either 100X or 200 X magnifications.

3.1.7 Use of both EdU and BrdU to distinguish if the two peaks of cell division are related

A key aim of the present project was to try and find out if ciprofibrate causes the same cells to divide repetitively, or whether different cells divide at different treatment times. To investigate these questions, two groups of six male -344/NHsd rats were used as described of section 2.1.1. The animals were gavaged with either corn oil (control vehicle group) or ciprofibrate (treated group) at time 0. Both groups were then injected i.p with 2 mg/kg EdU at 22 hr. At 24 hr the animals were gavaged again with either corn oil or ciprofibrate. At 46 hr the animals were injected i.p with 100 mg/kg BrdU. At 48 hr the animals were killed. After fixation the samples underwent tissue processing, where sections were sliced to a thickness of 4.5µm. Then successive tissue slices were stained i.e. these were slices directly in contact with each other, and were expected to pass through the same hepatocytes. The first of these slices was stained with click-iT EdU and second one was stained with BrdU. Staining was performed separately to allow for the different staining chemical procedures, which meant that double staining of the same tissue slice was not feasible (results not shown). The two micrographs were then superimposed together using the program Photoshop CS4 (Adobe). This experiment was performed with liver sections taken from both control and treated rats. Gut sections were used as a positive control.

The results revealed the key observation that the cells which divide at 24 hr are different from those which divide at 48 hr in both control and treated liver rat tissues (Figures 3-18, 3-19, 3-20 and 3-21). This result was consistently obtained in at least three independent experimental groups of animals (Figures 3.18, 3.20 and 3.21).

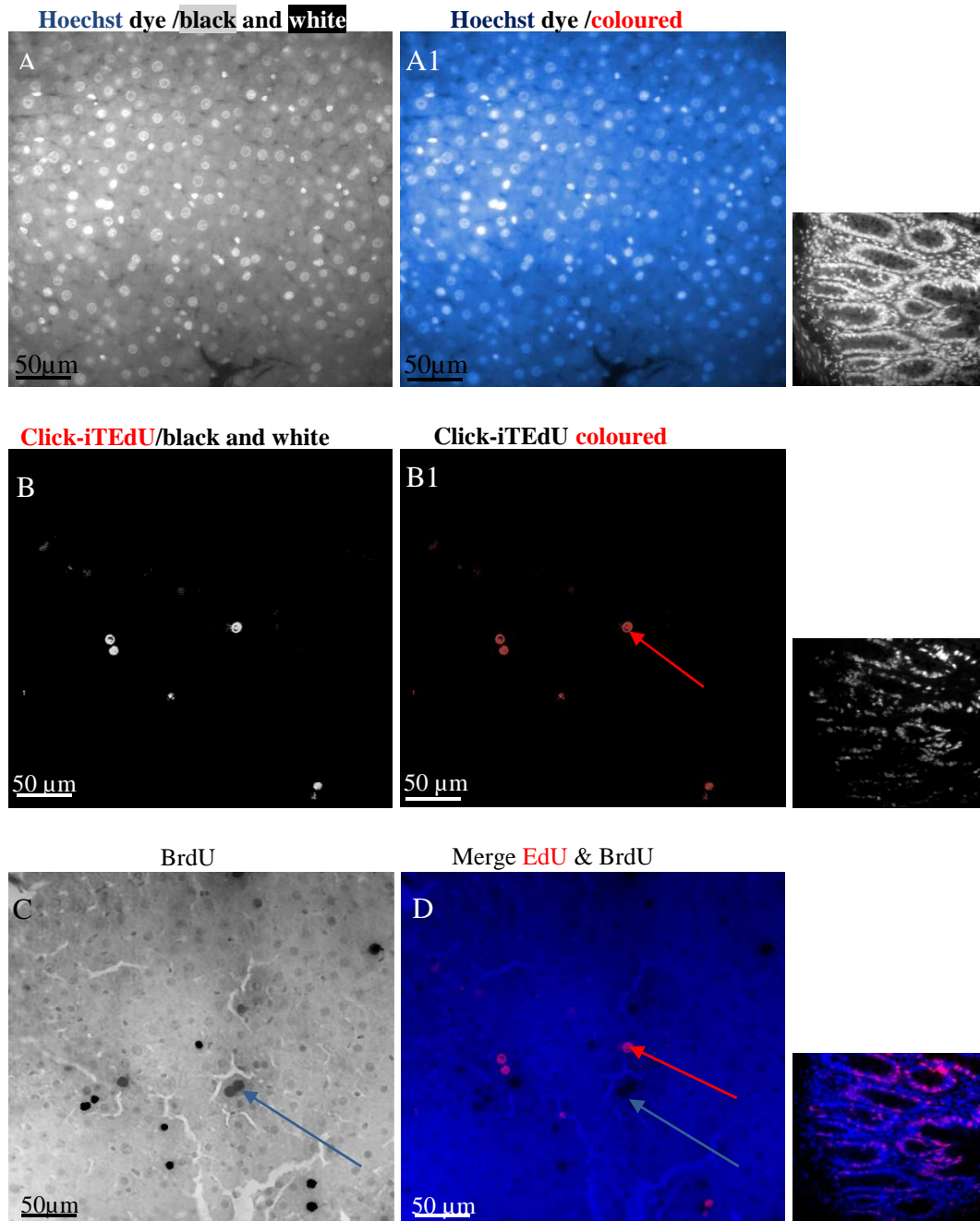


Figure 3-18 Use of EdU and BrdU staining (example 1) to investigate whether the two peaks of DNA replication at 24 hr and 48 hr (arising from treatment with ciprofibrate) occur in related or different hepatocyte cells.

The figure shows slides prepared from male F-344/NHsd rats aged 14-15 weeks. (A) displays nuclei detected with Hoechst dye and (A1) the same micrograph after colouration with Photoshop. (B) shows replicative cells detected with the click-iT EdU protocol and (B1) the same micrograph after colouration with Photoshop. (C) shows replicative cells detected with the BrdU stain. (D) Shows results of EdU and BrdU staining merged together with Photoshop. The replicative cells detected with the BrdU staining appear as black spots, whereas replicative cells detected with the click-iT EdU protocol appear as red spots. The animal was killed at 48 hr. The micrographs were taken with a LucaEM DL-604 camera using an exposure time of 100 ms and a medium setting (2) for binning at 400X magnification. Red arrows indicate replicative DNA synthesis detected by the EdU marker, blue arrows indicate replicative DNA synthesis detected with the BrdU marker. Images to right hand side show gut (colon) section controls.

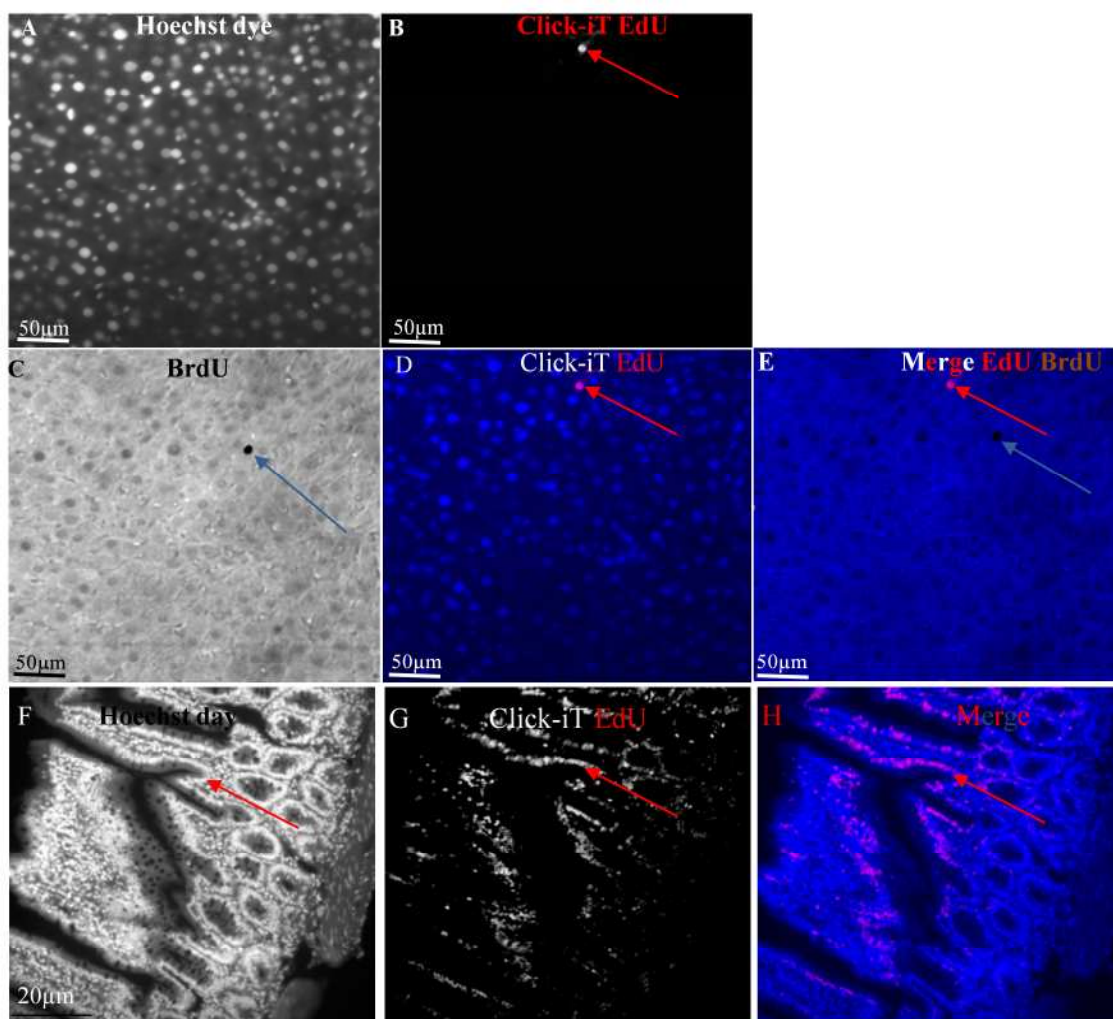


Figure 3-19 Use of EdU and BrdU staining (example 2) to investigate whether the two peaks of DNA replication at 24 hr and 48 hr (arising from control treatment involving gavage with corn oil) occur in related or different cells.

The figure shows slides prepared from male F-344/NHsd rats aged 14-15 weeks. (A) Displays nuclei detected with Hoechst. (B) Shows replicative cells detected with click-iT EdU, as indicated by red arrow pointing to white spot. (C) Shows replicative cells detected with the BrdU stain, the replicative cells appearing as black spots (arrowed). (D) Shows replicative cells detected with the click-iT EdU protocol after colouration with Photoshop, replicative cells shown as red spots. (E) Shows results of EdU and BrdU staining merged with Photoshop. The animal was killed at 48 hr after treatment with EdU and BrdU. The micrographs were taken with a Luca^{EM} DL-604 camera using an exposure time of 100 ms and a medium setting (2) for binning at 400X magnification. Images F, G, H at bottom are gut (colon) section controls.

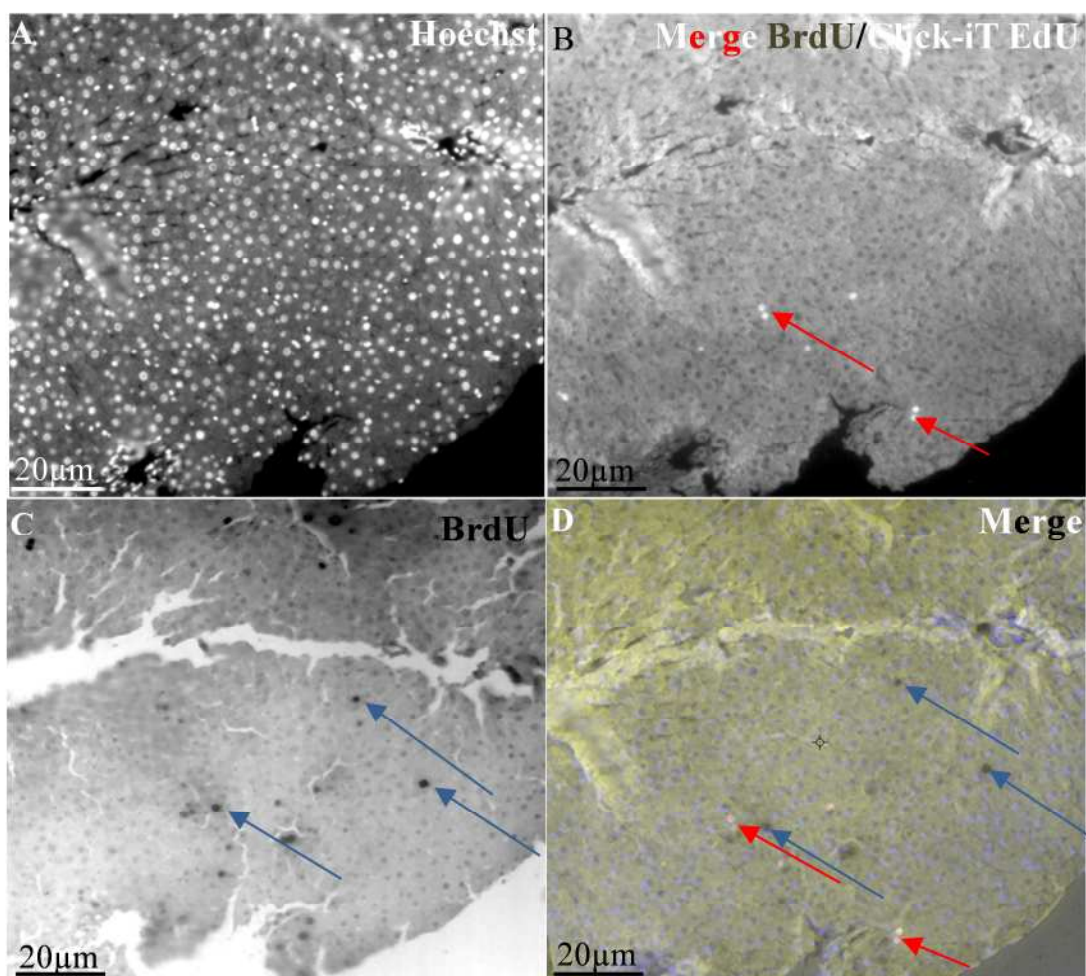


Figure 3-20 Use of EdU and BrdU staining (example 3) to investigate whether the two peaks of DNA replication at 24 hr and 48 hr (arising from treatment with ciprofibrate at 0 hr and then at 24 hr) occur in related or different cells, images taken at 200 x magnification.

The figure shows slides prepared from male F-344/NHsd rats aged 14-15 weeks. The animals were killed at 48 hr after being gavaged with ciprofibrate at 0 hr and then at 24 hr. The animals were injected with EdU at 22 hr and then with BrdU at 46 hr. (A) Displays nuclei detected with Hoechst dye. (B) Shows replicative cells detected with click-iT EdU, as indicated by **red arrow** pointing to **white** spot. (C) Shows replicative cells detected with the BrdU stain, as indicated by **blue arrows** pointing to black spots. (D) Shows results of EdU and BrdU staining merged with Photoshop. The animal was killed at 48 hr. The micrographs were taken with a Luca^{EM} DL-604 camera using an exposure time of 100 ms and a medium setting (2) for binning at 200X magnification.

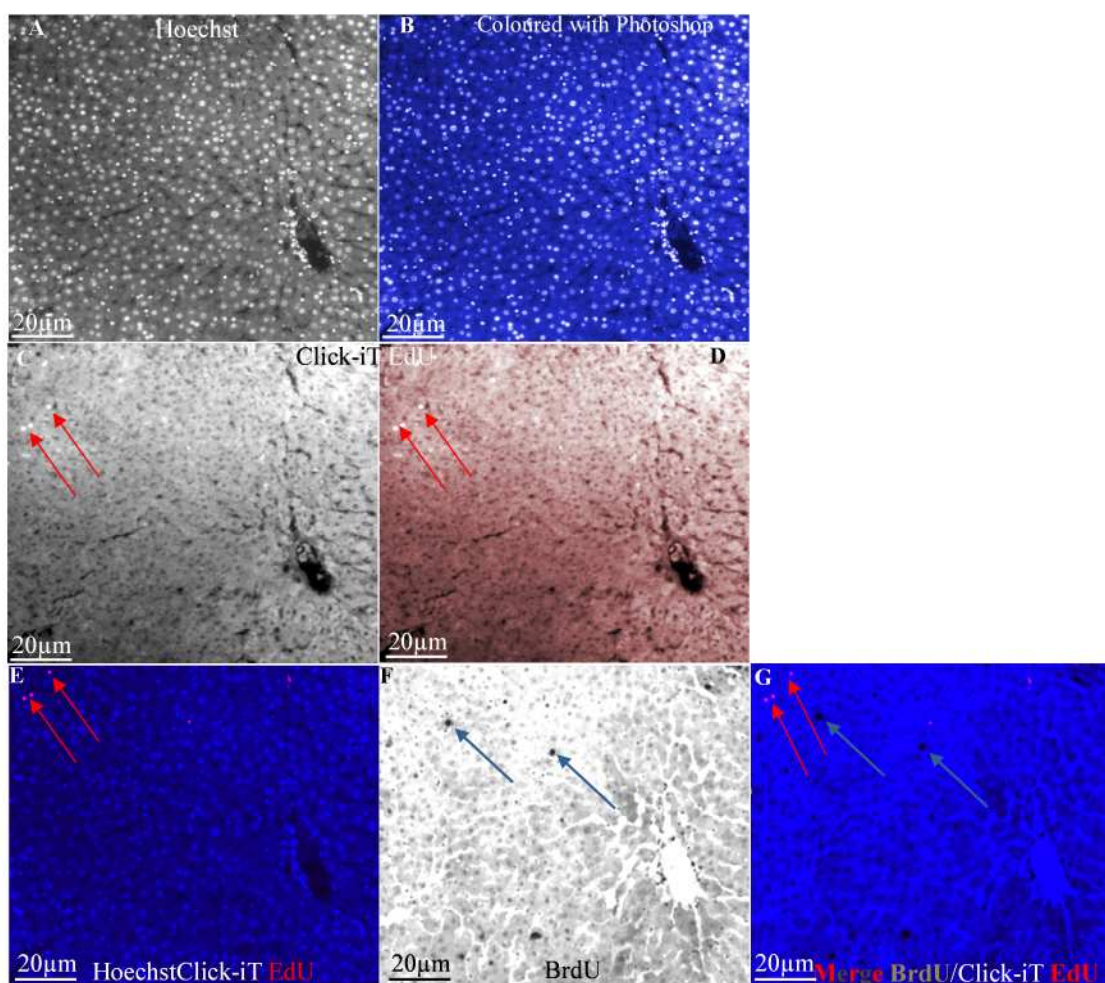


Figure 3-21 Use of EdU and BrdU staining (example 4) to investigate whether the two peaks of DNA replication at 24 hr and 48 hr (arising from treatment with corn oil control at 0 hr and then at 24 hr) occur in related or different cells, images taken at 200 x magnification.

The figure shows slides prepared from male F-344/NHsd rats aged 14-15 weeks. (A) displays nuclei detected with Hoechst dye and (B) the same micrograph after colouration with Photoshop. (C and D) shows replicative cells detected with the click-iT EdU protocol and (E) the same micrograph after colouration with Photoshop. (F) shows replicative cells detected with the BrdU stain. (G) Shows results of EdU and BrdU staining merged together with Photoshop. The replicative cells detected with BrdU staining appear as **black spots** (blue arrows), whereas replicative cells detected with the click-iT EdU protocol appear as **white** or **red spots** (red arrows). The animal was killed at 48 hr. The micrographs were taken with a LucaEM DL-604 camera using an exposure time of 100 ms and a medium setting (2) for binning at 400X magnification. Red arrows indicate replicative DNA synthesis detected by the EdU marker, blue arrows indicate replicative DNA synthesis detected with the BrdU marker).

3.1.8 Percentage of hepatocytes labelled with EdU and BrdU after induction with 50 mg/kg ciprofibrate

To be confident that the results obtained were reliable (showing that different groups of cells were undergoing division at the 22 and 46 hr points of ciprofibrate treatment), it was important to find out if the number of cells being labelled is above or below the average number of normal liver cells undergoing staining which is 3.5% (± 0.5). 500 labelled nuclei were counted in samples that were labelled with either EdU or BrdU to find the average. Figure 3-22 shows that the average percentage of cells labelled with EdU and BrdU was 3.4 ± 0.7 and 3.6 ± 0.1 , respectively, and the average of the total labelled cells with both markers was $5.5\% \pm 1.1$, which was in line with the expected value of 3.5% as mentioned above.

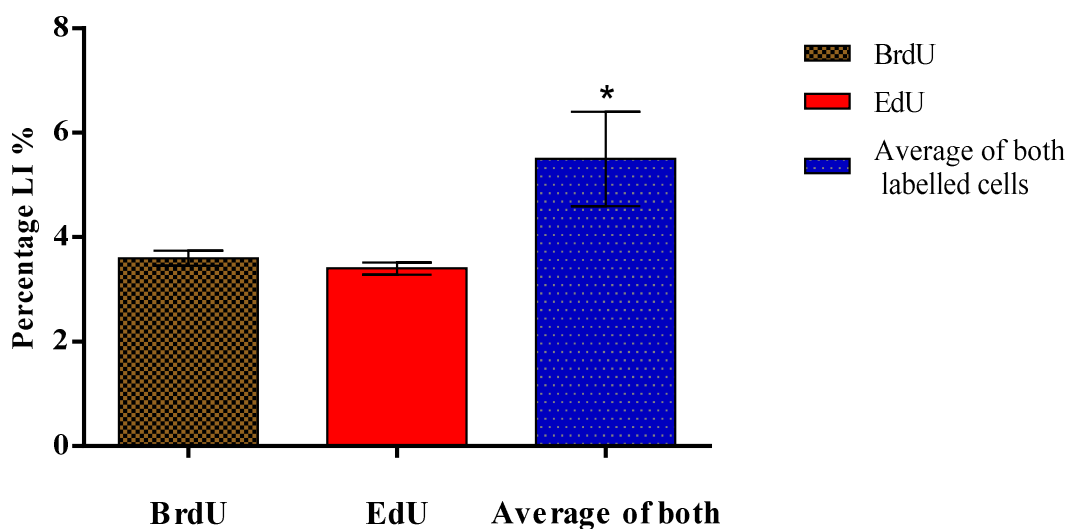


Figure 3-22 Percentage of labelled hepatocytes of F-344 liver rats following induction with 50% ciprofibrate.

Three groups of animals were gavaged with ciprofibrate and then injected either BrdU or EdU, or with both EdU and BrdU (dual-labelled) at 24 and 48 hr. Paraffin liver section were prepared after 48 hr ($n=6$). There was no statistically significant difference between individual EdU with BrdU staining. However, there was a statistically significant greater number of dual labelled cells according to a one-way analysis of variance, $P<0.05$. Error bars indicate mean \pm SD ($n=6$).

3.2 Induction of DNA synthesis induced by CPA (PRX)

It has been hypothesised that liver growth of rats resulting from treatment with non-genotoxic carcinogens could involve some common early gene and protein expression changes that could ultimately be used to predict chemical hepatocarcinogenesis (Plant 2008). There are other chemicals besides PP family toxins which might cause liver growth. Krebs (1998) reported evidence that CPA showed genotoxic activity linked to mutagenesis and promotion of specific DNA adducts and in rat liver cells (Krebs, Schäfer et al. 1998).

In the previous study of Amer (2011) it was found that dosing male F-344/NHsd rats with 100 mg/kg CPA resulted in upregulation of at least 21 genes and down regulation of at least 10 genes during the early hours of treatment at 1, 3 and 5 hr according to analysis by microarray technology. However, despite the widespread use of microarray technology, the use of microarray data has been challenged regarding its reliability and reproducibility (Baker, Harries et al. 2004). Not to mention the expensive cost for the microarray technology.

The present study had two main aims, following on from work by Amer (2011). A first aim was to verify the observation that differences in response are evident between male and female rats. A second aim was to make a preliminary study using real time PCR to investigate whether genes known to show altered expression as a result of ciprofibrate treatment were also altered in expression by CPA treatment. Female F-344/NHsd rats aged 14-15 weeks were dosed with 100 mg/kg CPA to confirm induction of hepatic DNA synthesis, or with corn oil (vehicle) as a control. The experiment was performed on two different occasions as described in section 2.2.2 (Figures 2-8 and 2-9). The first time point was 3 hr; as the mice were gavaged at time \emptyset and then killed, in order to extract RNA for RT-PCR work. The second time point was 24 hr, with rats being injected intraperitoneally (i.p) with 100 mg/kg BrdU 2 hr before killing in order to confirm induction of DNA synthesis by histochemical means. Liver samples extracted 3 hr after initial treatment were kept at -80°C until use for RNA induction analysis with real time PCR to compare changes in gene expression with livers from earlier time points of male Fisher rats, by dosing F-344 rats with CPA and comparing the labelling index between male and female rats at 24hr.

3.2.1 Effect of CPA (PXR) ligands on hepatic DNA synthesis in female Fischer rats

CPA had been used as a positive control to ciprofibrate in previous work at Nottingham (Bell pers comm). During such work it was inadvertently found that dosing male F-344 rats with 100 mg/kg CPA gave only a 6% labeling index, whilst CPA gave a 50% labeling indices in female rats at 24hr (Amer 2011). This suggested that female rats could be used as a better model system to study gene induction.

In order to confirm the high level of induction of DNA synthesis in hepatocytes, 12 female F-344/NHsd rats aged 14-15 weeks were bought a week before use, so they could acclimatize to their environment before giving them more stress of dosing and handling. The rats were grouped into 2 X 6 and gavaged with 100 mg / kg CPA at time 0 hour, which was dissolved in corn oil, and injected with BrdU i.p 2 hr prior to killing, as described in section 2.2.2 (Figure 2-9). The rats were weighed every other day (before and after the dosage) to ensure that they were healthy. Anti-primary and secondary BrdU antibodies were applied to detect hepatocytes proliferation after 24 hr. The aim of this experiment was to investigate the effects of CPA activation of liver growth and cell division. Labeling indices of BrdU detection in female rats were compared with that obtained from male rats at 24hr by Amer (2011) under the same conditions.

Data obtained showed that the liver weight to body weight ratio was significantly different between the control and treated groups (Figure 3-24, A and B). The control value was $3.6 \pm 0.07\%$ compared to the treated group $4.2 \pm 0.09\%$ at 24hr. The results indicated that the labeling index of treated female rats showed a very high level of $38.8 \pm 7.9\%$ in comparison with the control group where the value was $1.2 \pm 0.3\%$ (Figure 3-23). In summary the immunohistochemistry results using BrdU labelling showed that hepatocytes proliferation is markedly higher in treated than in control female rats, and that labelling in female rats (labeling index of DNA synthesis of $38.8\% \pm 7.9\%$) was markedly higher than in previous studies by Amer (2011) involving male rats (only $5.0\% \pm 1.0$).

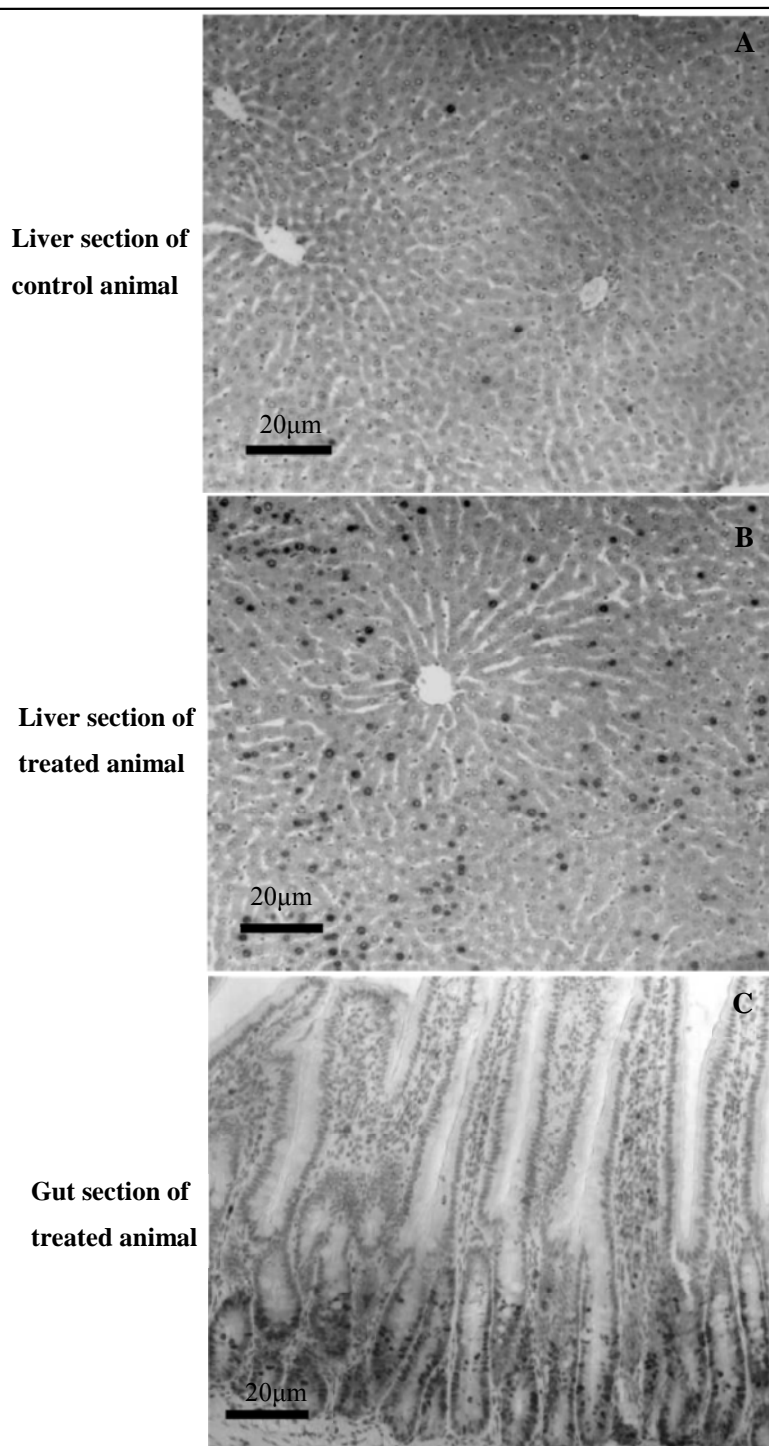


Figure 3-23 Effects of CPA on hepatic DNA synthesis in female F-344 NHsd rats as detected by BrdU staining.

Groups of female rats were gavaged with 100 mg/kg CPA and DNA replication detected by BrdU staining at 24 hr. (A) Liver tissue of control animal. (B) Liver tissue of CPA treated animal. Sections were labelled with an anti-BrdU antibody (DNA replication indicated by dark black nuclei) and counterstained with haematoxylin. (C) Gut section of treated animal, used as a positive control for BrdU staining. The micrographs were taken with a Luca^{EM} DL-604 camera at 200X magnification.

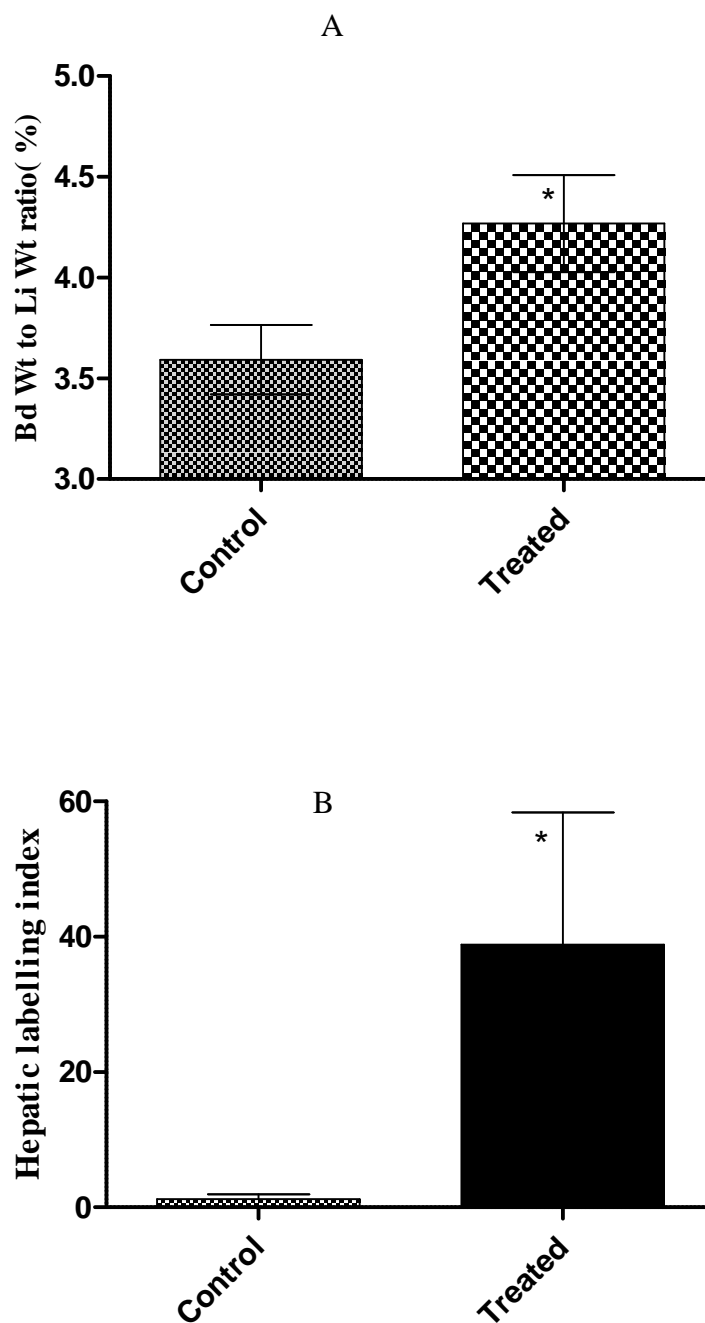


Figure 3-24 Effects of CPA on hepatic DNA synthesis in female F-344 NHsd rats as determined by labelling index of BrdU staining.

Group of female F-344 rats aged 14-15 weeks were dosed at time 0 hr, with either corn oil (control vehicle) or 100mg/kg CPA. At 22 hr they were dosed intraperitoneally (i.p) with BrdU and killed at 24 hr. (A) shows liver weight to body weight ratios of different treatments. (B) shows BrdU labelling index at 24 hr of different treatments. All data expressed as mean \pm SD (n=6). There were statistically significant differences between control and treated groups according to a student t-test ($P < 0.05$), as indicated by an asterisk.

3.2.2 Early induction of DNA synthesis by CPA in female F-344 /NHsd rats

It has reported that cyproterone acetate (CPA) can induce liver tumours in rats, with a higher incidence in female than males (Lake, Renwick et al. 1998, Otteneder and Lutz 1999, Brambilla and Martelli 2002). However, it is noteworthy that in order to induce liver tumours in female rats higher dosage levels had to be used. Meanwhile, CPA treatment very rarely gives rise to liver cancer in human patients (Kasper 2001).

As previously mentioned (section 1.3.10), it has suggested that some common genetic mechanisms regulating DNA replication and cell division might be activated by both PPs (e.g. ciprofibrate) and other chemicals such CPA (Wallenius, Wallenius et al. 2000). It is therefore of great fundamental and medical interest to try to identify any common genetic pathways. Work has previously been undertaken by Amer (2011) to identify genes induced by both ciprofibrate and CPA, using microarray technology. The results concerning ciprofibrate treatment were followed up by RNA seq analysis, but not the results of the CPA analysis. It was apparent that genes related to DNA synthesis in male rats were induced to a much higher level in female rats following CPA treatment. This result was confirmed by the present study where a labeling index of DNA synthesis of $38.8\% \pm 7.9\%$ was found for female rats compared to only $5\% \pm 1$ found previously in male rats (Amer 2011) (section 3.2.1). Work in the present study therefore focussed on genes induced in female rats.

Group of female F-344/NHsd rats at age 14-15 weeks were gavaged with either corn oil (control vehicle) or 100 mg/kg CPA dissolved in corn oil at time 0 hr. The animals were anaesthetized and killed 3 hr later by schedule 1 method. The animals were weighed and after killing the livers were removed and weighed. Analysis of results with student's t-test showed no significant difference between liver to body weight ratio for control ($3.2 \pm 0.04\%$) and treated group ($3.0 \pm 0.08\%$) (Figure 3-25).

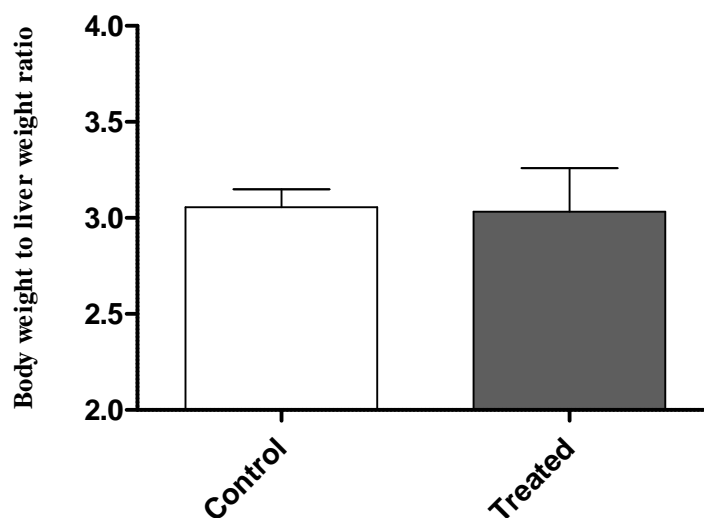


Figure 3-25 Effects of CPA or corn oil control on liver growth in female F-344NHsd rats CAP after 3 hr.

Graph shows liver weight to body weight ratio of female F-344 rats aged 13-14 weeks which were dosed with either 100mg/kg CPA or corn oil (vehicle) at time 0 and killed after 3 hr. All data expressed as mean \pm SD (n=4). There was no statistically significant difference between control and treated groups according to a student's t-test ($P < 0.05$).

3.2.3 Real time PCR results of CPA induction

Previous microarray studies had identified a series of genes related to early stages of cell division which were induced by ciprofibrate treatment. It was therefore of great interest to investigate whether any of these genes were also induced by cyproterone acetate (CPA) as this might indicate shared pathways relating to cell division and carcinogenesis and it is of major medical interest to identify such genes. Unlike previous work, the real time PCR method rather than microarray was used.

Both previous and work from the current study had shown that gene expression responsible for induction of liver cell response is much higher in female rats than in male rats. Therefore studies were undertaken with female rats. Samples from female F-344 rats treated with 100 mg/kg CPA and control vehicle corn oil for 3 hr was analysed with this technique as shown in section 2.2.2. Primers and probes were designed for selected genes on grounds of the previous study to allow comparison between them at the same time point with two different techniques. In this preliminary study target genes were chosen on the basis that they were involved in the cell cycle, so had possible links to carcinogenesis, and were found to show highly altered gene expression (e.g. be highly induced) by RNA seq. analysis for samples dosed with ciprofibrate (Amer 2011).

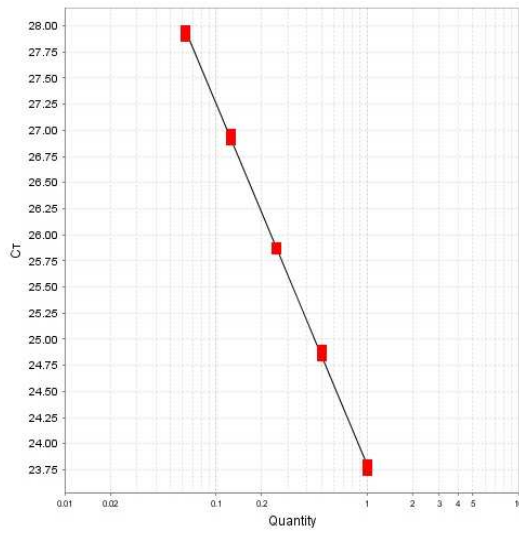
The genes chosen were *CYP3A1*, *Scd1*, *Ccnd1*, and *G0s2* together with two genes *AhR* and β -*actin* which were used for normalization. Amer (2011) found that *G0s2*, *Ccnd1* and *Scd1* were up-regulated when male rats were treated with ciprofibrate at 1 and 3 hr after dosing, but not at 24 hr. The *G0s2* and *Ccnd1* genes are involved in the cell cycle pathway, whilst *Scd1* is involved in PPAR signalling pathway (Zandbergen, Mandard et al. 2005).

In this study real time PCR was used to compare and confirm the results in both studies at one time point, namely 3 hr. The mRNA of male rats for all experiments was obtained from my colleague Abeer Amer to compare the induction between genders. Real time PCR was performed for male and female samples during the same RT-PCR experimental run.

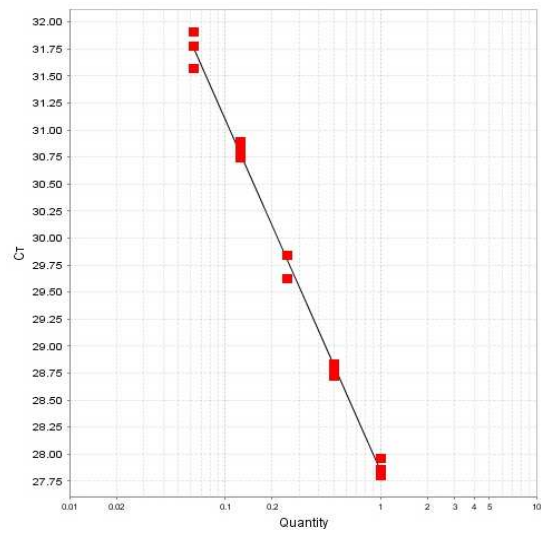
3.2.3.1 Standard curves for genes of interest

A relative standard curve method was utilized to study expression levels of genes of interest whereby standard cDNA (complementary DNA) dilutions are required in order to quantify relative concentrations of the target and reference gene in the samples. The standard curves represent the amplification efficiency and regression coefficient for the genes, *CYP3A1*, *Ccnd1*, *Scd1*, *G0s2*, *AhR* and β -actin. The amplification efficiency for real-time PCR reaction should be $100\% \pm 10\%$ and the regression coefficient (r^2) should be so close to 1 (Fraenkel, Wallen et al. 1993, Bustin, Benes et al. 2009).

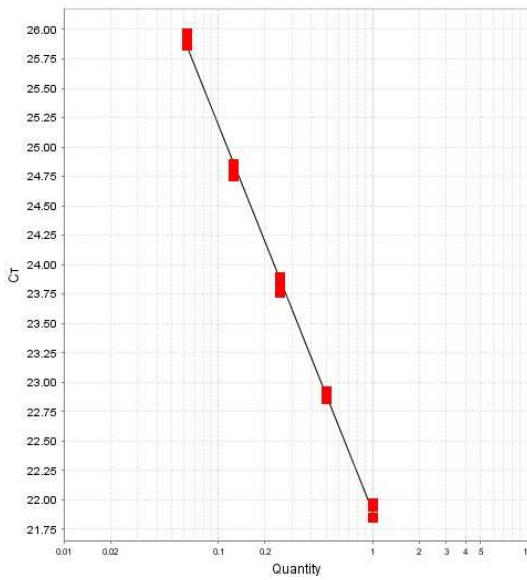
All genes studied showed efficient amplification, with the results of the regression coefficient (r^2) values being close to 1, meaning that all target genes are within ~ 9% of 100% and 0.99 ± 0.007 of the r^2 . The regression and efficiencies were as follows: the *CYP3A1* ($r^2 = 0.99$ & 101.2% of the efficiency), the *Scd1* ($r^2 = 0.99$ & 11.3% efficient), the *Ccnd1* ($r^2 = 0.99$ & 101.1% efficient), the *G0s2* ($r^2 = 0.99$ & 101.3 % efficient), the *AhR* ($r^2 = 0.99$ & 101.1 % efficient) and the β -actin ($r^2 = 0.99$ & 98.9% efficient). Figure 3-26 shows the standard curves of these genes.



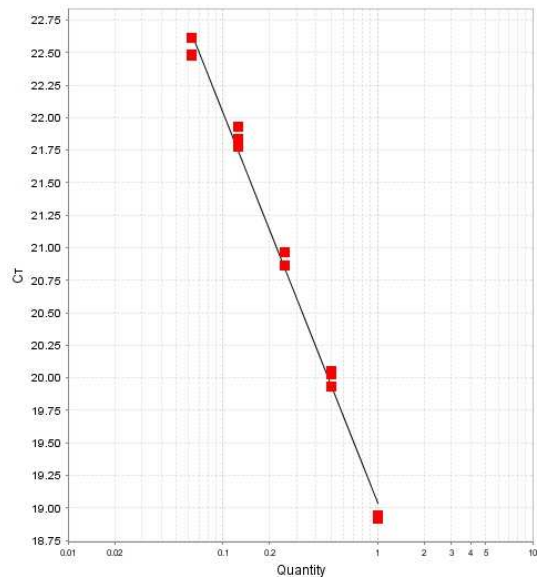
AhR, $r^2 = 0.99$ Eff% = 101.119.



Ccd1 $r^2 = 0.995$ Eff% = 103.056



GOs2, $r^2 = 0.993$ Eff% = 101.393



Scd1, $r^2 = 0.993$ Eff% = 115.339

Figure 3-26 Standard curve to determine the RT-PCR efficiency. The efficiency is based on the r^2 value, with the regression correlation coefficient value r^2 determined as shown above.

3.2.4 Effects of CPA on *CYP3A1* gene expression

This experiment was conducted to investigate the possible induction of *CYP3A1* mRNA in male and female rats which were treated with 100mg/kg CPA at time 0 hr and were then killed 3 hr later.

The results for the treated samples with CPA showed a statistically significant induction of *CYP3A1* expression both in treated female rats compared to the control group, and also between male and female treated rats at this relatively early induction of DNA synthesis (Figure 3-27). It is noted that a literature review revealed that the PXR agonist (pregnenalone-16 α -carbonitrile) can also highly induce *CYP3A1* expression (Mikamo, Harada et al. 2003, Bailey, Gibson et al. 2011).

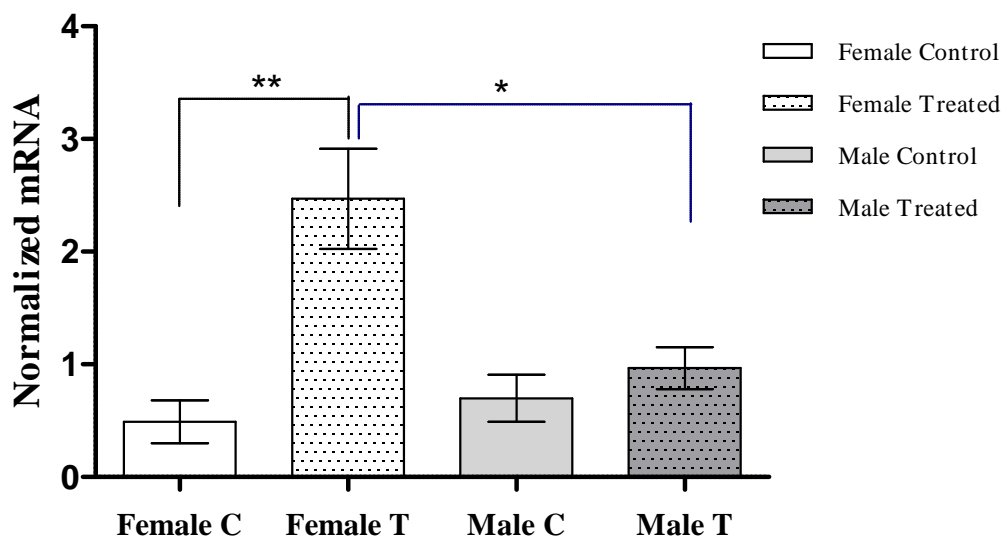


Figure 3-27 Effect of CPA or corn oil control treatment on *CYP3A1* mRNA expression in liver cells of female and male F-344 rats.

Figure shows the effects of treatment of either 100 mg /kg CPA or a corn oil control vehicle on *CYP3A1* mRNA expression, for both female and male rats treated at 0 hr and assayed at 3 hr. Expression was assessed using real-time PCR. Statistically significant differences were evident between the control and treatment groups, and male and female groups, as indicated by an asterisk. All data expressed as mean \pm SD (n=3). Statistical analysis according to a one-way analysis of variance (Tukey's multiple comparison test), $P < 0.05$.

3.2.5 Effects of CPA on sterol-coenzyme A - desaturase 1 (*Scd1*) gene expression

This experiment was performed to investigate the induction levels of *Scd1* gene expression in both male and female samples following CPA treatment. The aim was to find out the level of induction between control and treated rats and compare the results with female rats to those of previous male samples.

Although the treated females showed an increase in *Scd1* mRNA compared to the control rats, the difference was not significantly different at this early 3 hr stage of induction of DNA synthesis (Figure 3-28). Interestingly, the difference between treated female and treated male rats was statistically significant, and there was a significant difference between control male and treated female rats (Figure 3-28).

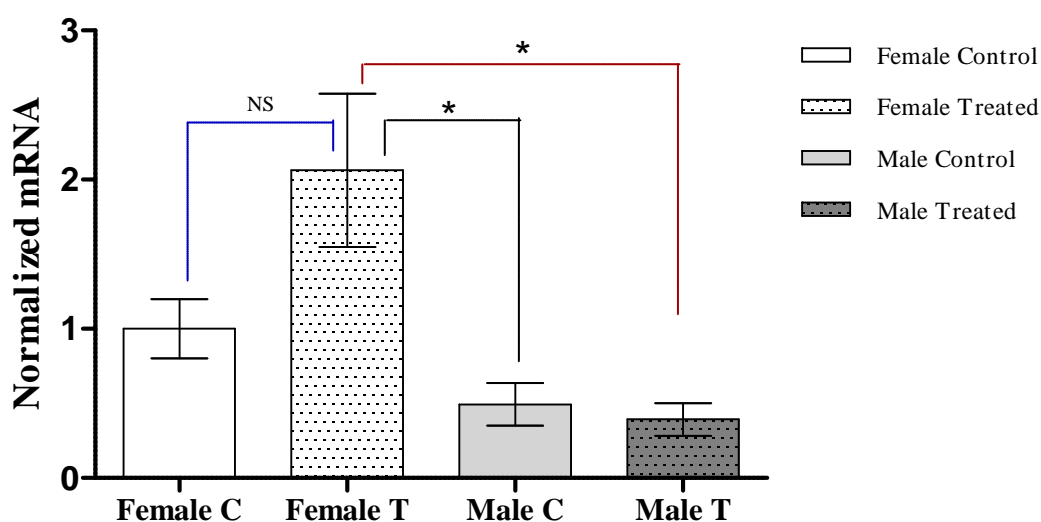


Figure 3-28 Effect of CPA or corn oil control treatment on *Scd1* mRNA expression in liver cells of female and male F-344 rats.

Figure shows the effects of treatment of either 100 mg /kg CPA or a corn oil control vehicle on *Scd1* mRNA expression, for both female and male rats treated at 0 hr and assayed at 3 hr. Expression was assessed using real-time PCR. Statistically significant differences were evident between male and female groups, as indicated by an asterisk, but there were no statistically significant differences between control and treated female and male rats. All data expressed as mean \pm SD (n=3). Statistical analysis according to a one-way analysis of variance (Tukey's multiple comparison test), $P < 0.05$.

3.2.6 Effects of CPA on cyclin D1 (*Ccnd1*) gene expression

This experiment was carried out to test the effects of CPA on the induction levels of *Ccnd1* mRNA at 3 hr after treatment, a gene known to be involved with control of the cell cycle.

The expression of *Ccnd1* at this early time point was extremely high in treated female rat compared to both the female control and treated male rats (Figure 3-29). The results for the treated female showed a statistically significant induction of *Ccnd1* after 3 hr treatment; with a > 2.6 fold change and > 5 fold change comparison to male treated (Figure 3-29).

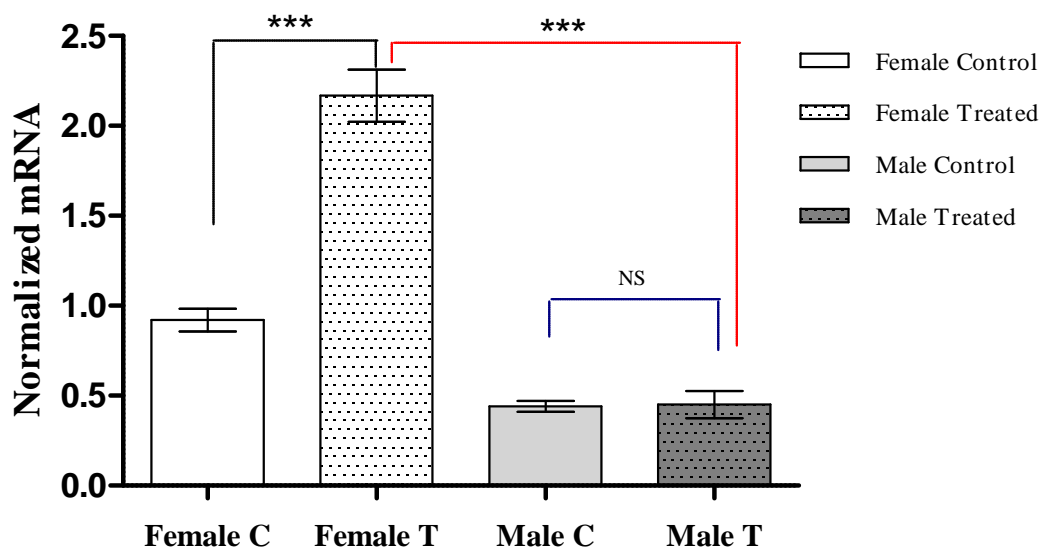


Figure 3-29 Effect of CPA or corn oil control treatment on *Ccnd1* mRNA expression in liver cells of female and male F-344 rats.

Figure shows the effects of treatment of either 100 mg /kg CPA or a corn oil control vehicle on *Ccnd1* mRNA expression, for both female and male rats treated at 0 hr and assayed at 3 hr. Expression was assessed using real-time PCR. Statistically significant differences were evident between the control and treated groups in female rats, and between female and male rat groups according to a one-way analysis of variance (Tukey's multiple comparison test), $P < 0.05$. All data expressed as mean \pm SD (n=3).

3.2.7 Effects of CPA on expression of *G0s2* gene involved with G0/G1 switching

This experiment was conducted to investigate the effects of CPA on induction levels of the *G0s2* gene (involved in G0/G1 switching) compared to a corn oil control in female F-344 rats at a 3 hr time point after treatment. Results were then compared with similar gene expression data for male rats.

The induction of *G0s2* in female treated with CPA showed no significant difference from the control, and there were also no significant differences between control and treated male rats (Figure 3-30).

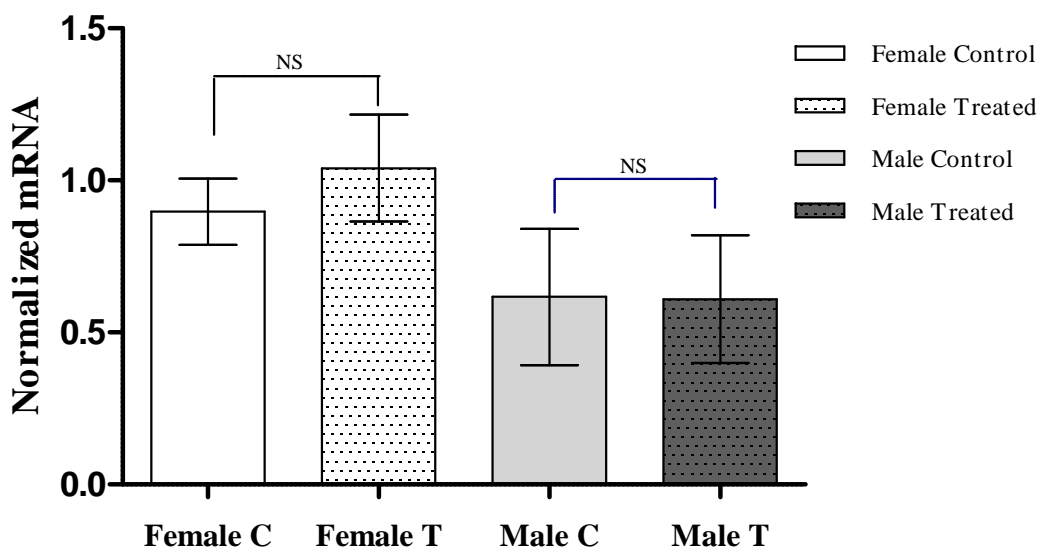


Figure 3-30 Effect of CPA or corn oil control treatment on *G0s2* mRNA expression in liver cells of female and male F-344 rats.

Figure shows the effects of treatment of either 100 mg /kg CPA or a corn oil control vehicle on *G0s2* mRNA expression, for both female and male rats treated at 0 hr and assayed at 3 hr. Expression was assessed using real-time PCR. There were no statistically significant differences between the control and treated groups of rats groups according to a one-way analysis of variance (Tukey's multiple comparison test). All data expressed as mean \pm SD (n=3).

4. Discussion

The present study had two main objectives. Firstly, to determine whether particular liver cell populations respond to repeated treatment by the peroxisome proliferator (ciprofibrate), or whether independent cell populations respond to treatment. Secondly, to undertake preliminary studies to determine whether similar sets of genes are induced in female rat liver cells by the genotoxic carcinogen cyproterone acetate (CPA) as are induced by ciprofibrate. In order to achieve these objectives various experimental works was undertaken as discussed below.

4.2 Rationale and method validation

4.1.1 Optimisation of Hoechst dye concentration

A histochemical approach was utilised in order to determine whether the two peaks of cell division observed by Amer (2011) following repeated ciprofibrate treatment (one at 24 hr and the other at 48 hr, following treatment at \emptyset and 24 hr) were related. The two histochemical and immunohistochemical stains used were EdU and BrdU, which are both base-pair analogues that stain nuclei undergoing DNA replication as a result of incorporation into DNA during novel DNA synthesis (Cappella, Gasparri et al. 2008). It was hypothesized that if EdU was administered to animals at 24hr which had been pretreated with ciprofibrate at \emptyset hr, then this stain would be incorporated into nuclei of dividing hepatocyte cells at 24hr. If animals were then treated with a second dose of ciprofibrate and then allowed to live for a further day, then administration of BrdU at 48 hr would be expected to lead to incorporation of the latter stain into nuclei of dividing hepatocyte cells at that stage. Thus, if the same cells are responding to ciprofibrate treatment then cells would be co-stained by both dyes, whereas if different cells were responding then there would be little or no double staining of hepatocyte cells.

In order to achieve a good background to noise ratio staining by Hoechst dye was optimised before being used to reveal the total number of nuclei. Meanwhile EdU

was used to detect specifically cell nuclei undergoing replicative DNA synthesis. Many studies have investigated the relative fluorescence intensity of Hoechst dye, e.g. Lalande and Miller (1979) examined concentrations from 1µg to 20µg/ml. A reduction of Hoechst 33258 dye (Bisbenzimidazole) concentration to below 1µg/ml has been linked to decreased background fluorescence (McGowan, Kurtis et al. 2002).

Hoechst dye at a concentration of 2µg/ml was found to accurately and clearly detect nuclei in liver cells prepared from adult rats (Lamas, Chassoux et al. 2003).

In this study, 5 different concentrations were examined, from 0.1µg/ml to 50µg/ml, to reveal the effect of these concentrations on fluorescent signal. A Hoechst dye stock of 5µg/ml was prepared using distilled water then PBS was used to make the five concentrations. Stock solution was stored at 4 °C and protected from light. The experiments show that using 1.0 µg/ml dye concentration gave the best results as background fluorescence was reduced. In order to obtain good background to noise ratio, the washing solution (PBS) was optimised as well. The results show that a concentration of 0.2M NaCl was better than 1M NaCl. In addition, the time of washing was optimised concluding that 2 X 5 min gave the best results. It was also found that Hoechst dye gave much better results in the presence of moisture so a small chamber was designed to meet this condition (Figure 3.7).

4.1.2 Assessment of immunohistochemistry protocol

BrdU and IHC techniques are widely used as an experimental procedure to label DNA synthesis within replicative nuclei and have been used in a variety of studies of cell biology including investigations of cell proliferation of liver growth *in vitro* and *vivo* (McGinley, Knott et al. 2000, Ueda, Saito et al. 2005). BrdU is incorporated into DNA during DNA synthesis of cell proliferation during the S-phase of the cell cycle. In this study BrdU Immunohistochemistry for the BrdU paraffin section technique was used to stain liver and colon sections, the latter included as these undergo much cell division so provide a suitable control for cell and nuclei staining. Primary anti-BrdU antibodies purchased from Amersham and Sigma were assessed

at three concentrations 1:1000 μ l, 1:750 μ l and 1:500 μ l. The same concentration of secondary antibody 1:50 μ l was used for all the different concentrations of primary antibodies. Primary anti-BrdU antibodies were applied to positive sections and incubated for 45 min. Negative control section were held in 0.2M PBS during the primary incubation. The secondary antibody (Bio-Rad laboratories) was applied to all sections (positive and negative) and incubated for 30 min. Using 1:750 μ l of primary antibody with 1:50 μ l of secondary antibody gave the best labeling index as shown in Figure 3-12. These optimisations were concordant to several former studies, where in most of them the secondary antibody used was the same as the above concentration, but different results with the primary antibody were obtained depending on the source of purchase (Connolly and Bogdanffy 1993, Constan, Sprankle et al. 1999, Ezaki, Yoshida et al. 2009, Ross, Plummer et al. 2010).

4.1.3 Optimisation of the dose of the EdU

EdU was used as stain to detect DNA synthesis in proliferating cells during cell division. EdU is incorporated into DNA of nuclei of proliferating cells and can be subsequently detected by fluorescence resulting from an antibody bound copper azide (Salic and Mitchison 2008). In particular, the click-iT EdU reaction relies on incorporation during DNA replication – with the terminal alkyne group of EdU containing a thymidine analogue which replaces methyl groups in DNA. Then the terminal alkyne group can be detected via reaction with a fluorescent copper azide. EdU staining has been utilised in a variety of different eukaryotic cells and has been incorporated strongly into the DNA of proliferating mammalian cells. For example, Salic *et al* (2007) injected EdU into an adult mouse i.p with 100 μ g of EdU in PBS. This resulted in staining of cells of the small intestine, with red nuclei observed of cells that had been in S-phase (Salic and Mitchison 2008). In this project three concentrations of EdU were tested to establish an optimal dose of EdU. A group of six animals was injected with 2, 5, and 25 mg/kg EdU (n=2 per dose). As shown in Figure (3-6) all of the EdU concentrations gave acceptable staining, therefore the

lowest concentration 2 mg/kg was used. Indeed, using the this small amount lowest concentration of EdU showed no signs of EdU toxicity, which confirms results of Cappella in his *vivo* study in adult mice (Warren, Puskarczyk et al. 2009).

4.1.4 Using base analogue stains EdU and BrdU

It was necessary to make sure that the hepatic DNA synthesis which was detected by both EdU and BrdU with immunohistochemistry was at the same level i.e. to ensure that these stains detected the same cells, and same number of cells, rather than providing artifactual results. Comparisons of BrdU and EdU histochemistry showed no statistically significant differences. Thus, click-iT EdU incorporated into DNA synthesis of cells in the same manner as BrdU, revealing that all cells showed similar labelling indices with both stains (Nwe and Brechbiel 2009). The EdU showed high efficient fluorescence without the need for denaturation, unlike BrdU which required all slides to be denaturated (Warren, Puskarczyk et al. 2009). A study by Cappella showed that labelling with EdU gave slightly increased staining compared to BrdU (Cappella, Gasparri et al. 2008). The finding is in disagreement with this project, because there were no statistically significant differences between EdU and BrdU stains. Indeed, on the contrary, the labelling with BrdU showed a slightly increased as displayed in Figure 3-15 although this was not statistically significant.

4.1.5 Use of both EdU and BrdU to distinguish if the two peaks of DNA replication and cell division are related

This project was initiated to test the underlying hypothesis that certain hepatocytes might have an increased ability to divide, due for instance to increased expression of specific genes, which might therefore make these hepatocytes, more susceptible to carcinogens. If so these cells would be more likely to undergo division at two different times following toxin treatment. To determine whether ciprofibrate causes the same cells to divide repetitively, or whether different cells divide at different times, two different stains were used. Liver and gut tissues of 4.5 μm thickness were

prepared. The first and second slices of tissue were taken, the first slice was stained with click-iT EdU and second one was stained with BrdU separately. The two micrographs were then superimposed together using the programme Photoshop. This experiment was performed with liver sections taken from both control and treated rats. The results revealed the key observation that the cells which divide at 24 hr are different from those which divide at 48 hr in both control and treated liver rat tissues as displayed in Figures 18 and 19. In other words, ciprofibrate does not cause the same cells to divide repetitively but instead different cells divided at different times. This suggests that there is no specific type of hepatocytes which have a particular physiological character, such as increased expression of certain genes, that makes them more likely to divide at the different times and be susceptible to carcinogens. This finding is consistent with that of Gournay, 2002 who suggested that only mature hepatocytes have the ability divide. (Gournay, Auvigne et al. 2002).

4.1.6 Percentage of labelled hepatocytes in liver

It is known that approximately 3.5% of liver cells normally undergo DNA synthesis (Lucier, Tritscher et al. 1991), which was similar to the average number of replicative DNA synthesis found by BrdU & EdU labeling in the present study. 500 labelled nuclei were counted in both samples that were labelled either EdU or BrdU to find average. Single labelled cells with EdU and BrdU were calculated and results showed that the average of dual labelled is $(5.5\% \pm 1.1)$. EdU and BrdU alone have shown 3.4 ± 0.7 and 3.6 ± 0.1 respectively.

4.2.1 Effect of PXR ligands on hepatic DNA synthesis in female rats dosed with CPA:

In the second part of this study work was undertaken to determine whether similar sets of genes are induced in female rat liver cells by the genotoxic carcinogen cyproterone acetate (CPA) as are induced by ciprofibrate. This followed previous work was done by Amer (2011). The latter studies investigated the induction of DNA

synthesis by peroxisome proliferators (PP) alongside CPA to make a preliminary analysis of whether subsets of the genes induced by PPAR α and CPA were the same. This could be of medical importance as traditionally PPAR α has a non-genotoxic mode of carcinogenesis, whereas genotoxic carcinogens can bind intracellular receptors that bind DNA at specific DNA recognition sites.

The experiment was conducted under the same conditions implemented by Amer (2011), such as animal age, dose and BrdU concentration. However, studies were conducted using female rats as these were more likely to show increased changes in gene expression. Two groups of female F-344/NHsd rats were dosed with 100 mg/kg CPA or corn oil (vehicle). The rats were then injected intraperitoneally with 100 mg/kg BrdU 2 hr prior to killing either at 3 or 24 hr after initial treatment (Schulte-Hermann, Hoffman et al. 1980, Martelli, Campart et al. 1996). The dose of the CPA used was chosen on the basis of following the biological conditions used in the previous experiment (Amer 2011) and which had additionally been used elsewhere in the literature (Coleman and Best 2005, Guzelian, Barwick et al. 2006).

4.2.2 Induction of hepatic DNA synthesis by CPA (PXR)

There has been growing interest over the current decade in the role of xenobiotics that are characteristic non-genotoxic carcinogens. There is growing concern based on evidence implicating some xenobiotics in liver growth (Sueyoshi and Negishi 2001, Zhang, Xie et al. 2008), the worry being whether these chemicals are safe or not? Studies were therefore taken to try to shed light on mechanisms of action of cell division and whether this is related to cancer. By understanding how liver growth works, it was hoped to gain insights into mechanisms of liver cancer on the grounds that, if it were known how these chemicals cause cell division, it would give clues as to how liver growth occurs. Two previous studies have been carried out by Al-Khulaifi (2008) and Amer (2011) focusing on the role of ciprofibrate (associated with PPAR α) in liver growth with several experiments conducted on the livers of mice and rats. In addition, Amer (2011) used CPA (associated with PXR) in male F-

344 rats as a positive control to study ciprofibrate gene induction. Amer (2011) examined effects of CPA on hepatic DNA synthesis in male F-344NHsd rats at 4 time points; 1, 3, 5 and 24 hr of dosing. CPA is thought to have a completely different mechanism compared with ciprofibrate.

In the present study, female F-344NHsd rats rather than males were used to investigate effects of CPA on hepatic DNA synthesis at 3 and 24 hr of dosing. The former work of Amer (2011) was performed using microarray technique while real time PCR was utilized here to confirm the former and current results. In male F-344 rats 6% induction of DNA synthesis in liver was observed, whereas this was ~ 39.0 % in average of hepatocyte labeled were in female F-344NHsd rats at 24 hr in the present study. This finding was concordant with the study of Amer (2011) in which the labeling index was approximately 50% in female rats (Amer 2011). It is also consistent with a previous study carried out by Martelli (1996) who found that the dosing of CPA 100 mg/kg led to a higher induction of gene expression in female rather than male rats after 3 days treatment (Martelli, Campart et al. 1996).

4.2.3 Effect of PXR ligands on hepatic DNA synthesis in female Fisher rats

The pregnane X receptor (PXR) is a nuclear receptor that works as a sensor to the presence of foreign toxic elements or xenobiotics, and responds by up regulating the expression of proteins implicated in the detoxification of such chemicals. PXR is activated by several endogenous and exogenous chemicals including steroids, antibiotic and many other compounds (Quattrochi and Guzelian 2001). It has been reported that the PXR has a central role in the regulation of the *CYP3A4* gene and others involved in drug metabolism and bile acid synthesis (Goodwin, Redinbo et al. 2002, Shukla, Sakamuru et al. 2011). It was of interest in the present study to assess whether there might be some shared mechanisms, activated by both PPs (e.g. ciprofibrate) and CPA (linked to PXR), that regulate DNA replication and cell division (Wallenius, Wallenius et al. 2000, El-Sankary, Gibson et al. 2001).

Therefore studies were undertaken using real-time PCR methodology to assess whether any down or up-regulation was evident in response to CPA treatment in 3 genes previously found to be down or up-regulated by ciprofibrate according to findings from microarray analysis (Amer 2011). Also included in studies as a control for gene expression was an examination of expression of the *CYP3A1* gene, for which increased expression had previously been shown in response to CPA treatment. Overall it was found that some genes (e.g. *Ccnd1*) appear to be specifically induced by either CPA or ciprofibrate with no mutual overlap, whereas some other genes might be a common target for the hepatic DNA synthesis (e.g. *Scd1* and *G0s2*) as follows.

4.2.4 Effect of CPA on *CYP3A1* gene expression

CPA has been shown to be a potent inducer of *CYP3A1* expression in rat and mouse, triggering binding of the PXR receptor to its cognate DNA elements as heterodimer with RXR and activation of transcription of genes such as *CYP3A1* (Figure 3.3.1)(Moore, Parks *et al.* 2000, Sueyoshi and Negishi 2001, Pascussi, Gerbal-Chaloin *et al.* 2003). Other studies have shown that prolonged exposure to CPA caused liver carcinogenesis in rats, but that the liver could return to a normal weight when the administration was stopped (Pichard and Ferry 2005). In the present study, short-term administration with CPA confirmed that *CYP3A1* gene expression was significantly induced (2.5 fold difference) in female treated compared to female control (and from female treated to male treated) at 3 hrs following treatment with CPA. This finding was consistent with studies of *in vitro* induction of *CYP3A1*-mRNA in rat liver slices treated with testosterone hydroxylation, which in turn displayed that *CYP3A1* induction was more sensitive in liver from female rats than male liver (Glöckner, Wagener *et al.* 2003, Hartley, Dai *et al.* 2004). This first finding of increased *CYP3A1* expression provided a valuable control for the real-time PCR work as it confirmed that a gene previously known to be up regulated by CPA treatment was indeed confirmed to be up-regulated in the present study.

4.2.5 Effect of CPA on *Scd1*

The stearoyl-CoA desaturase-1 (*Scd1*) gene encodes an iron-containing enzyme which stimulates a rate limiting step in the synthesis of unsaturated fatty acids. Moreover, *Scd1* plays a key role in an increase of triglyceride as a result of accumulation of carbohydrate in the body. This in turn acts to increase *Scd1* gene expression in liver via a sterol response element binding protein (Ntambi 1995, Hashimoto, Ishida *et al.* 2013).

In previous studies Amer (2011) found that the expression of the *Scd1* gene was induced by ciprofibrate after 3, 5 and 24 hr. It was significantly induced by PPAR α (ciprofibrate) after 3 hr induction (13.2 fold change). Meanwhile, microarray analysis of male rats treated with CPA found a 2.2 fold change. Interestingly, the induction with CPA in male rats showed that *Scnd1* expression was slightly lower than the control samples at all the time points.

In the present study by contrast, real time PCR analysis of *Scd1* showed a slight up-regulation (1 fold change) with CPA in treated compared to control female samples after 3 hr, although no difference was found between control and treated male rats. This result is not consistent with the findings of the Amer (2011) and does not support a common pathway for hepatic DNA synthesis between CPA or PPAR α .

4.2.6 Effect of CPA on *Ccnd1*

The *Ccnd1* gene encodes a protein involved in cell division. Cyclin D1, a cell cycle protein involved in regulation of cell proliferation, is associated with several cancers and other diseases. Previously, it was found that the expression of the *Ccnd1* gene was significantly induced by PPAR α (ciprofibrate) after 3 hr (1.8 fold change), but was then down-regulated at 5 hr time point compared in treated to control male rats (Amer 2011). Meanwhile, microarray analysis of male rats treated with ciprofibrate revealed up-regulated expression on *Ccd1* (2.9 fold change) at 3 hr.

It seems that this data for this gene is controversial because treatment with CPA of male F-344 rats at 1, 3 and 24 hr had shown no significant difference when compared with control rats, which showed significant high induction (> 2.3 fold change) at 5 hr.

In the present study in contrast, real time PCR analysis of *Ccnd1* showed up-regulation (1.5 fold changes) following CPA treatment compared to control female samples at 3 hr. Also there was ~1.5 fold change from treated female to treated male at 3 hr time point. *Ccnd1* might be a common target for hepatic DNA synthesis, i.e. it is possible that *Ccnd1* is not specific for PPs nor the CPA. This is consistent with Pribiri, 2001 (Severino) who found that the induction with thyroid hormone showed high induction of *Ccnd1* at early time of DNA synthesis and induced cell division in the rat (Severino, Locker *et al.* 2011). Therefore *Ccnd1* may be considered a gene that is expressed in common by both ciprofibrate and CPA treatment.

4.2.7 Effect of CPA on *G0s2*

The effects of CPA on the induction levels of *G0s2* mRNA, involved with G0/G1 switching at 3 hr showed no significant difference between the control and treated female Fisher rats; in addition there was no significant difference between control and treated male rats. These results are consistent with those of Amer (2011) who found that the induction of *G0s2* in male F-344 rats showed no significant difference in all samples treated with CPA at time points 1, 3 and 5 hr, while the induction with ciprofibrate showed that the expression of *G0s2* was significantly higher (> 5 fold change) (Amer 2011), which suggested that *G0s2* might be a target for increased DNA synthesis (Sueyoshi, Mitsumata *et al.* 2010). This finding supports a previous finding by Amer, where the *G0s2* is considered specific to ciprofibrate (PPAR α).

5. CONCLUSION

Peroxisome proliferators are a class of chemicals that have diverse effects in rats and mice including increased DNA synthesis and peroxisome proliferation. These chemicals act through ligand activation of nuclear membrane receptors termed 'peroxisome-proliferator-activated receptors' (PPARs), which themselves act as nuclear transcription factors (Heuvel, Thompson *et al.* 2006, Fiskerstrand, H'Mida-Ben Brahim *et al.*) (Hosoe, Nakahama *et al.* 2005) (Yuan, Chen *et al.* 2010).

PPs induce a cellular process characterised by a dramatic increase in the size and number of peroxisomes correlated with both hepatocyte hypertrophy (i.e. an increase in the size of liver cells) and hyperplasia (i.e. an increase in the number of liver cells during replicative DNA synthesis and cell division). Peroxisome proliferators include herbicides, plasticisers, hypolipidemic drugs and synthetic fatty acids. However, the mechanism of action of increased hepatocyte growth is not currently understood. It was hoped that gaining understanding relating to the mechanism by which increased liver growth is induced by PPs in rodents would hopefully provide insights into how natural liver growth occurs and have medical benefits for human health if the mechanism of PP toxicity can be overcome. Knowledge gained from the mechanism of PP activation might also then be applied to other chemical carcinogens.

In the present study, firstly the mode of action of the peroxisome proliferators (ciprofibrate) was investigated. Previous work had indicated that two successive doses of ciprofibrate treatment separated by 24hr led to two rounds of liver cell replication, but it was not clear whether the same or different hepatocyte cells were involved in this growth response. To study this phenomenon, histochemical experimental work was undertaken to assess whether the same or different hepatocyte cells were stained during the two rounds of cell division following ciprofibrate treatment. The two histochemical stains used were EdU and BrdU, which are both base-pair analogues that stain nuclei undergoing DNA replication. It was hypothesized that if EdU was used to stain cells at 24 hr and then BrdU at 48 hr, that if the same cells were responding to ciprofibrate treatment then cells would be

co-stained by both dyes, whereas if different cells were responding then there would be little or no double staining of hepatocyte cells – instead different cells would be stained. F-344/NHsd rats, aged 7-8 weeks, were injected with three different concentrations of EdU to determine the amount of the EdU required to allow measurement of the labelling index of hepatocytes. 2 mg/kg EdU was found to be an efficient amount for detecting replicative DNA synthesis. Finally, optimised protocols for BrdU staining were then established. Primary anti-BrdU antibodies were purchased from two sources, Sigma and Amersham. The primary antibody purchased from Amersham provided clear and reliable results at a concentration of 1:750 μ l. The concentration of secondary anti-BrdU antibody (1:50 μ l) used was the same as in previous work.

Experimental work undertaken to determine if the same, of different hepatocyte cells, were induced to divide during the two rounds of cell division following ciprofibrate treatment revealed a key result that the cells undergoing division at 24 hr were not related to those that undergo division at 48 hr. This is of medical significance as it suggests that there are not hepatic cells that are especially sensitive to repeated PP treatment, but that different cells can respond and therefore there is a more general risk of increased cell division and carcinogenesis from such non-genotoxic carcinogenic compounds.

In related studies, previous work had investigated the effects of the genotoxic carcinogen cyproterone acetate (CPA) on hepatocyte growth of male rats treated with 100 mg/kg CPA. In the present study female rats were treated with CPA, to firstly evaluate whether differences in labelling indices were present compared to male rats, as indicated by Amer (2011). Female F-344/NHsd rats, aged 14-15 weeks, were treated at time 0 with CPA and then injected i.p with BrdU at 22 hr, and rats were killed 2 hr later. Results showed that the female rats were found to indeed have a considerably higher labelling index (50%) compared to male rats (6%), confirming the results of Amer (2011). This finding suggested that upregulation of gene expression in female rats should be much higher as well, which might provide an exciting opportunity to identify sets of genes involved in carcinogenic response, with

overlap to those involved in PP response. To investigate this phenomenon further another experiment was designed where the rats were gavaged at time 0 with 100 mg /kg CPA and then killed 3 hr later. In this study, the focus was on early DNA synthesis of genes stimulation whose expression had been shown to be up- or down-regulated in a previous study by Amer (2011) at the same 3 hr time point. This study was conducted on female rats, compared with males in the previous study, given the potential to detect greater differences in gene expression.

An analysis was made by real time PCR of four genes of interest as a preliminary pilot study (*Scd1*, *Ccnd1*, and *G0s2*). This showed some statistically significant differences between the control and CPA treated group, and also some significant differences between male and female treated rats e.g. the induction of *Ccnd1* in female fisher rats with CPA was significantly higher than in control and male fisher rats at 3 hr. However, the expression of *G0s2* in CPA – treated female rats showed no significant difference from the control and male treated rats and results with *Scd1* expression were also inconsistent with those of Amer (2011). Thus overall there was little evidence of shared pathways between CPA and ciprofibrate activity and therefore different mechanism of cell toxicity are likely to be present, albeit with some potential overlap as shown by the *Ccnd1* gene, whose expression was upregulated in response to exposure to both chemicals.

.

.

Part 2

The role of peroxisome proliferators in a model of a neurodegenerative disorder

6. Introduction - Review of Literature

6.1 Introduction to part two

An improved understanding of the mechanisms causing and affecting pathogenicity, has resulted in an advance in treatment development are increasing to understanding the reasons and mechanisms of the pathogenicity and development ways of treatment. Proliferation of a specific cell type is a response to acute brain injury or infection that involves activation and an increased recruitment of astrocytes and microglia. As a result there is, increased production of cytokines, (chemokines) (Bartholdi and Schwab 2006). Understanding the causes of neurodegenerative diseases is necessary, given that in many cases, the inflammatory response remains unclear. Researchers have begun to address some of the problems that may the cause nervous system degeneration, such as oxidative stress or dysfunction of the proteasome system (Emerit, Edeas et al. 2004, Halliwell 2006).

This study aims to shed some light on the process of astrocyte proliferation in such diseases as Parkinson's or Alzheimer. The activation of astrocytes has been tracked in order to understand the mechanisms and speed of development of neurodegenerative disorders. For example, Lewy body Dementia is a neurodegenerative disorder affecting the motor system. Lewy bodies are the abnormal accumulation of protein inside nerve cells resulting in PD (Goedert, Clavaguera et al. 2010). A number of studies have investigated the causes of neurodegenerative disorders, some of which have focused on the role of the ubiquitin system (Di Napoli and McLaughlin 2005). Thus, one of the important steps in the emergence of neurodegeneration is the dysfunction of the ubiquitin proteasome system (Hara, Nakamura et al. 2006). Currently, inhibiting the proteasome system is one of methods used in the preparation of neurodegeneration models. Therefore, a 26S proteasome of mouse cortical brain tissue has been inhibited to represent 26S proteasomal dysfunction of neurodegenerative disease (Petrucci and Dawson 2004, Bedford, Hay et al. 2008). This mouse neurodegeneration model ($Psmc1^{fl/fl}$; $CaMKII\alpha$ -Cre) has been used alongside models of wild-type pups ($Psmc1^{fl/fl}$; $CaMKII\alpha$ -Wt). The main focus of the project is to explain the specific role of

astrocytes in the inflammatory response as well as to attempt to reverse any detrimental changes. Currently, there is growing interest in the importance of peroxisome proliferators in the treatment of brain inflammation (Bernardo and Minghetti 2006, Klegeris, McGeer et al. 2007, Saavedra, Sánchez-Lemus et al. 2011). There is growing evidence that peroxisome proliferator-activated receptors may be useful as a therapeutic target for neurologic disease and CNS injury as their activation affects pathologic mechanisms. Therefore, PPAR activation has beneficial effects in many pre-clinical models of neurodegenerative diseases and CNS injury (Mandrekar-Colucci, Sauerbeck *et al.* 2013).

The peroxisome proliferator activated gamma receptor (PPAR- γ) has been shown to be involved in immune differentiation as well as playing a key role in the immune response during the inhibition of the inflammatory response. New evidence has indicated that the presence of PPAR- γ agonists, either via food or drugs are most likely beneficial to human health by acting as anti-inflammatory molecules (Martin 2009). This study highlights the importance of PPAR- γ agonists in reducing activated gliosis using rosiglitazone (PPAR- γ agonists) to inhibit astrocyte proliferation in a mouse model representing the neurodegenerative disorder.

To study astrocyte proliferation, organotypic slice culture systems have been utilized *in vitro*. Organotypic cultures have the advantage that they are open to a variety of experimental manipulations. To ensure comparability of the *in vitro* model with animals, *in vivo* paraffin sections were used alongside for identification of astrocyte populations. Confocal and light microscopy were used to observe the astrocytes in the organotypic brain culture, cryostat and paraffin sections.

6.1.1 The nervous system

The nervous system is divided into two main sections, the central nervous system and the peripheral nervous system (Dahlstrand, Lardelli *et al.* 1995, Nieuwenhuys, Voogd *et al.* 2007). The central part consists of the brain and spinal cord, and the peripheral of sensory neurons, ganglia which are neurons providing connections between different neurological structures of the nervous systems, and nerves. Neurons and glial cells make up both the peripheral and central nervous systems, the

neurons being the main building unit of the nervous system (Pakkenberg and Gundersen 2011). Glia is a Greek word meaning ‘glue’ or ‘sticky’. Glial cells are important in preserving homeostasis, and myelin integrity, as well as providing support and protection for neurons in the brain. However, glial cells do not participate directly in the transfer of the neuronal signals. Glial cells outnumber neurons by about 10:1 depending on the brain region (Hilgetag and Barbas 2009). As well as supporting neurons, glial cells act as insulation for electric charges between neurons and neurotransmitters (Oligodendrocytes in the CNS and Schwann cells in the PNS, and supply neurons with vital nutrients. They also aid disposal of dead and damaged cells, and secrete factors for the growth of neurons (Jessen and Mirsky 2005).

This study focused on glial cells, especially astrocytes, which are the biggest glial cells in size. The following diagram summarizes the structure of the nervous system (figure 6-1).

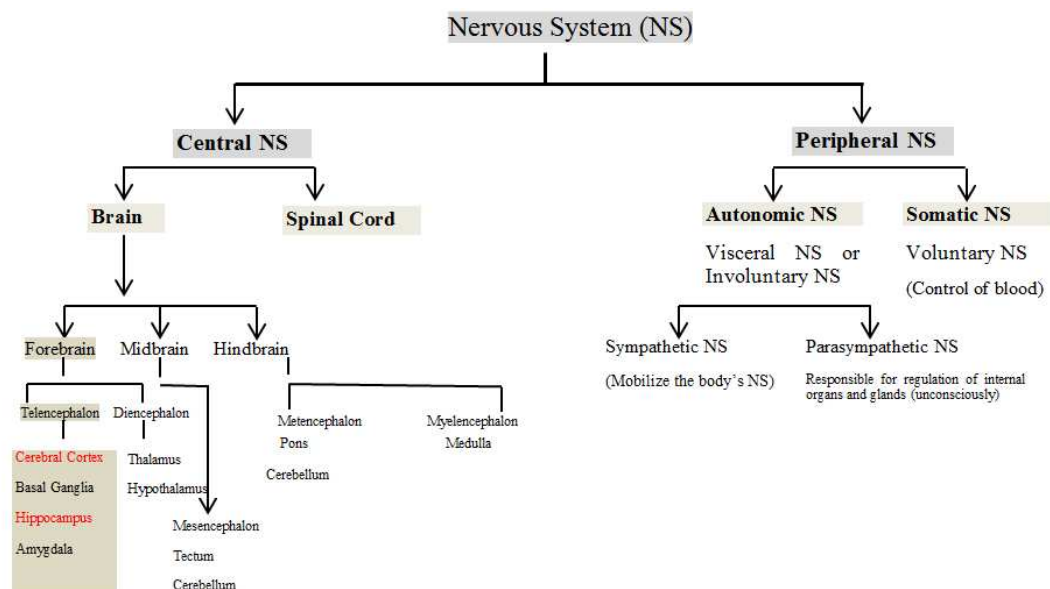


Figure 6-1 Diagram shows the components of the central and peripheral nervous system

6.1.1.1 The cortex

The cerebral cortex is neural tissue that surrounds the brain, representing the grey area of brain. The cerebral cortex is divided into left and right hemispheres, and is responsible for higher brain functions where information processing occurs (Smith, Fries *et al.* 2009). This region plays a key role in memory, attention, and integration of ideas in addition to language development, perception and awareness (Del Cul, Dehaene *et al.* 2009). It is a layered structure consisting of either three or six layers. The three layered areas, such as the olfactory cortex and hippocampus, represent phylogenetically older parts of the brain (Archicortex) while the neocortex the most recently developed part consists of six layers, each of which has a different structure in terms of neurons and connectivity. The human cerebral cortex has a much larger surface area than other primates and ranges in thickness between 2–4 mm (Fischl and Dale 2000).

The cortical layers are called grey matter due to the fact that the brains in preserved material tend to be grey in colour, and consist of neurons and their unmyelinated fibers. Below this layer is the white matter, which is made up of myelinated axons. These connect neurons in the cerebral cortex with each other, as well as to nerve cells in other parts of the central nervous system.

The surface of the cerebral cortex is characterized by extensive folds. These folds or gyri are separated by grooves, called "sulci". The cortex can be split into several layers called phylogenetically, the neo-cortex (called iso-cortex), is distinguished into six horizontal layers. The hippocampus is one of the oldest parts of the cortex (also called archi-cortex), it has three cellular layers, and is divided into subfields. Neurons in various layers connect vertically to form small microcircuits, called columns. Different neocortical architectonic fields are distinguished by variations in the thickness of these layers, their predominant cell type and other factors such as neurochemical markers, Figure 6-2 shows the hippocampus and cerebral cortex in both human and mouse (Abeles 1991, Semendeferi, Armstrong *et al.* 2001).

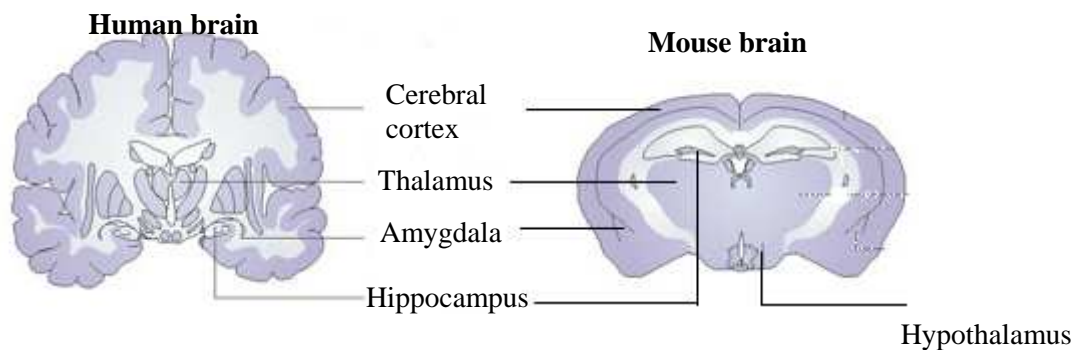


Figure 6-2 Diagram of the brain structure, illustrating differences in neuroanatomy between mice and humans.

Figure Shows hippocampus and cerebral cortex in both human and mouse. www.nature.com/nrd/journal/v4/n9/fig_tab/nrd1825_F2.html

6.1.1.2 The biology of the hippocampus:

The hippocampus is a major component of vertebrates and human brains, in particular. The term was derived from its curved shape in coronal sections of the brain, where the term contains two Greek words; (hippos) meaning ‘horse’ and (kampi) meaning ‘curve’. It plays an important role in linking information from short-term memory to long-term memory. It has extensive links with the cerebral cortex (Bliss and Collingridge 1993, Piekema, Kessels *et al.* 2006). Moreover, it is a fore brain structure, located under the cerebral cortex in mammals. In primates, the hippocampus is located in the medial temporal lobe, below the cortical surface. It contains two main interlocking parts; Ammon's horn and the dentate gyrus. In the dentate gyrus (DG), CA1 and CA3 fields are often referred to as the hippocampus proper. Both hippocampus and the dentate gyrus are representing the main parts of forebrain (Figure 6-3). Based on previous research, it is evident that the hippocampus is part of the brain system responsible for spatial memory and navigation (Gluck, Meeter *et al.* 2003, Kullmann 2011). Therefore, the hippocampus is a major target for research to find explanations for diseases of the central nervous system and neurodegeneration in particular.

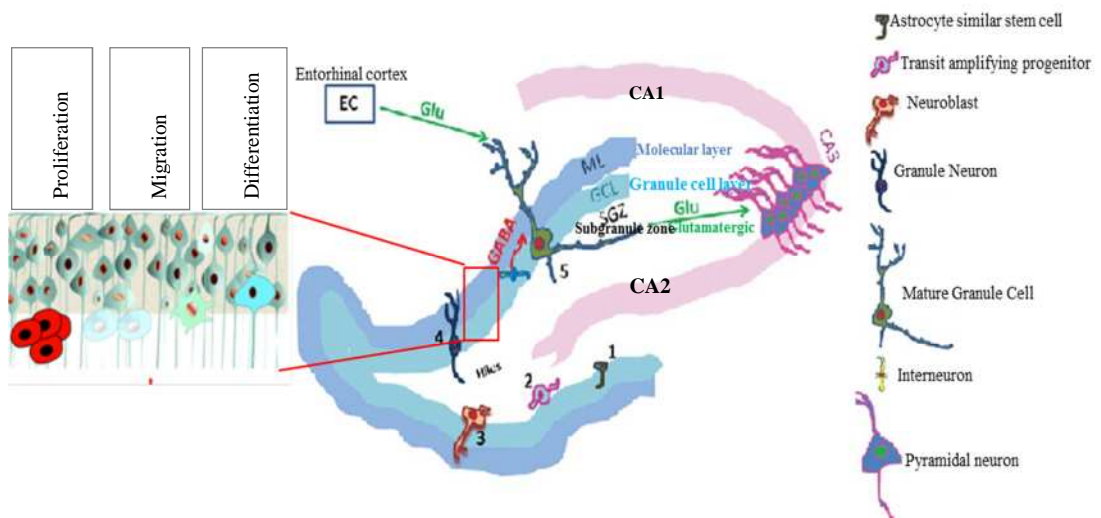


Figure 6-3 Scheme of hippocampal with dentate gyrus layers in rodents.

Schematic illustration of the three layers of dentate gyrus area. The sub-granular zone of the dentate gyrus houses transit amplifying progenitor cells. These cells mature into neuroblasts, which migrate into the granule cell layer (GCL) and differentiate into granule neurons (Mature Granule Cell). The newly generated granule neurons allow interconnections by extending axonal projections along the mossy fiber towards the CA3, and into the molecular layer. Mature cells receive glutamatergic inputs from the entorhinal cortex; GABAergic inputs from the interneurons and provide glutamatergic inputs to the CA3 neurons. The diagram adapted from from (Abrous, Koehl *et al.* 2005, McCaffery, Zhang *et al.* 2006).

6.1.1.3 Dentate gyrus

The large number of small blood vessels that lie within the dentate gyrus give it a toothed appearance, thus called the dentate gyrus (DG) (Van Praag, Shubert et al. 2005). The dentate gyrus is part of the hippocampus, which is believed to be responsible for forming new memories (Neves, Cooke et al. 2008). It is characterized by its granular layer and it has three layers; molecular layer, granular layer (which gives granular shape to the DG and polymorphic layer. The CA3 pyramidal cells operate as a single auto-association network to store new episodic information. The dentate gyrus is important, mainly during learning, to help to produce a new pattern in the CA3 cells. Namely, the zone from the DG to CA3 is essential for the process of learning (Gilbert, Kesner *et al.* 2001). Therefore, some studies have been conducted to determine the ability of hippocampus to store new information as well as how quickly the CA3 auto-association system is operating during recall using modified synapses in pathways from the hippocampus to the cerebral cortex (Kesner 2007).

6.2.1 Neuroglia (glial cells)

Historical accounts indicate that neuroglia were described for the first time in 1856 by the German pathologist Rudolf Virchow (Norman, Ulrich et al. 1958). His first drawings of glia were unlike the modern image of an astrocyte, but similar to an activated microglial cell. Virchow was the first to introduce the concept of neuroglia. Pio del Rio-Hortega (1882–1945) is also one of the first who described glial cells (Kettenmann, Hanisch et al. 2011). Neuroglia are glial cells that have great capacity to protect neurons in the brain. Neuroglia, contain two types of cells (microglia and macroglia) and both have diverse functions (Figure 6-4). Microglia have essential developmental and phagocytic roles in the brain, and are embryologically derived from the mesoderm. Macroglia are large cells comprising of oligodendrocytes and astrocytes. Astrocytes provide important structural, metabolic and trophic support to neurons. Neuroglial cells comprise about half the total volume of the cells that make up the brain and spinal cord. Their ratio differs from one part of the brain to another. For example, in the cerebral cortex most of the glia are oligodendrocytes (75.6%); astrocytes account for 17.3% and microglia (6.5%). Humans are known to have the most abundant and largest astrocytes of any animal. Moreover, the amount of brain tissue that is made up of glial cells in human brain contains 90%, compared to 65% in a mouse. (Bartus and Dean III 2009).

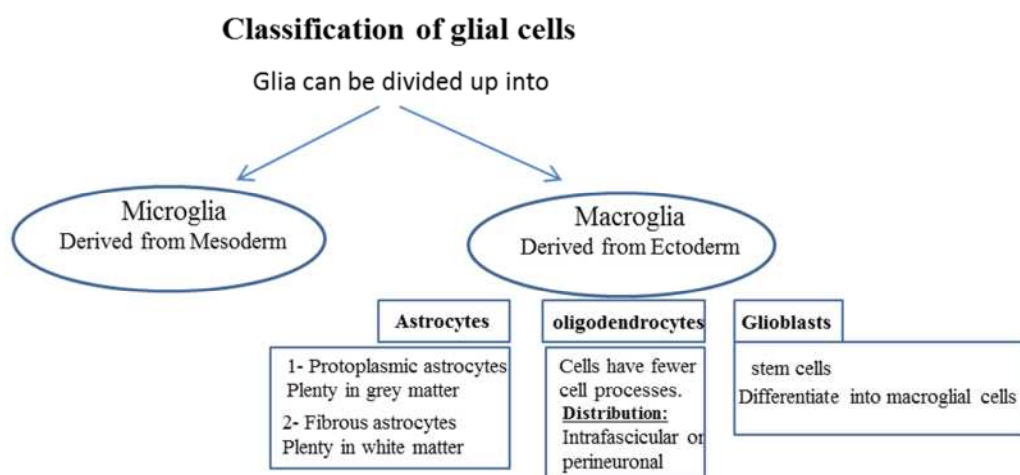


Figure 6-4 Classification of glial cells and how they differ.

www.mananatomy.com/basic-anatomy/glial-cells-neuroglia

6.2.1.1 Microglia

Microglia represent the first line of immune defense in the central nervous system. They account for 20% of the total glial population, and are the macrophages of the brain and spinal cord (Olson, Zamvil *et al.* 2003, Hauwel, Furon *et al.* 2005). Microglia recognizes foreign bodies, engulf them, and are extremely sensitive to small pathological changes in the CNS (Yang, Han *et al.* 2010). Microglia are activated in the spinal cord after acute injury and in chronic disease and it is suggested that these cells have an innate immune memory of tissue injury and degeneration. Namely that inflammation is associated with a decline in function of microglia leading to neurodegenerative disease (Hanisch and Kettenmann 2007).

6.2.1.2 Astrocytes

Astrocytes differ from neurons in terms of form and functions in the brain. Astrocytes can be divided into two kinds based on their location and morphology. Protoplasmic astrocytes are most abundant in the grey matter and have branched processes. The second type, called fibrous astrocytes have long and fibre-like processes and are located in the white matter (Nedergaard, Ransom *et al.* 2003, Sofroniew and Vinters 2010). As there are significantly more astrocytes in the brain than neurons (Figure 6-5) they are vital for normal neurotransmission to occur (Volterra and Meldolesi 2005). Astrocytes also have a key role in stabilizing, and modulating synaptic activity. Moreover, they are implicated in the pathological states of reactive gliosis and glial scar formation that accompany injury, and may be associated with brain tumour development, including glioblastomas. Functions of astrocytes include physical and metabolic support for neurons, detoxification, and guidance during migration, regulation of energy metabolism, electrical insulation, transport of blood-borne material to the neuron, control of fluid movements between the intracellular and extracellular space and reaction to injury. In addition, astrocytes are predominantly important in determining the tissue response to ischemia and CNS trauma. They are responsible for reducing excitotoxicity, whereby nerve cells

become damaged and die as a result of excessive stimulation from neurotransmitters e.g. glutamate. (Volterra, Bezzi *et al.* 2006).

This study focused on the presence of astrocytes in the two main regions, cortex and hippocampus, where it has been reported that on average, astrocytes make up about 18% of the total neuroglial cell population. Astrocytes perform many functions in the cortex such as regulating blood flow and influencing neuronal responses (Peters, Leahu *et al.* 1994). Glial cells can be identified by their expression of the main intermediate filament, glial fibrillary acidic protein (GFAP).

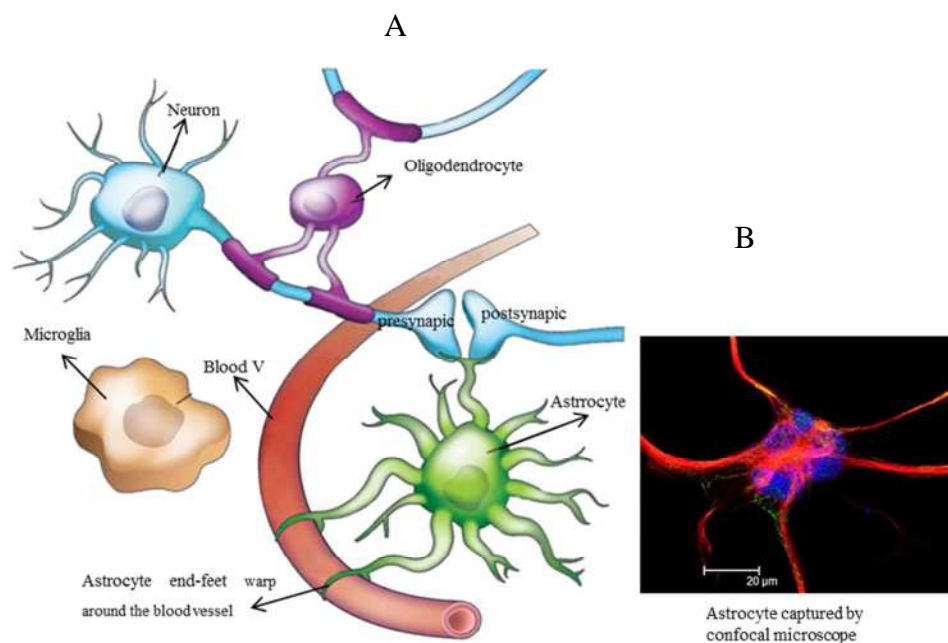


Figure 6-5 Illustration of the glia cells.

A; Astrocyte (in green colour) processes make contact with the neuronal synapses and the blood vessel. B; Astrocyte under confocal microscope. Astrocytes are in contact with both neurons and the small blood vessels. Astrocytes serve to alter blood flow in response to neuronal activity. (Allen and Barres 2009, Egolf 2012).

6.2.2 Fundamental functions of astrocytes

Some anatomical studies suggest that astrocytes in mice are about 2.5 times smaller than in humans (Kimelberg and Nedergaard 2010). Studies have indicated several vital functions of the astrocytes which can be summarized into eight points that allow neurons in the brain to function optimally (Figure 6-6).

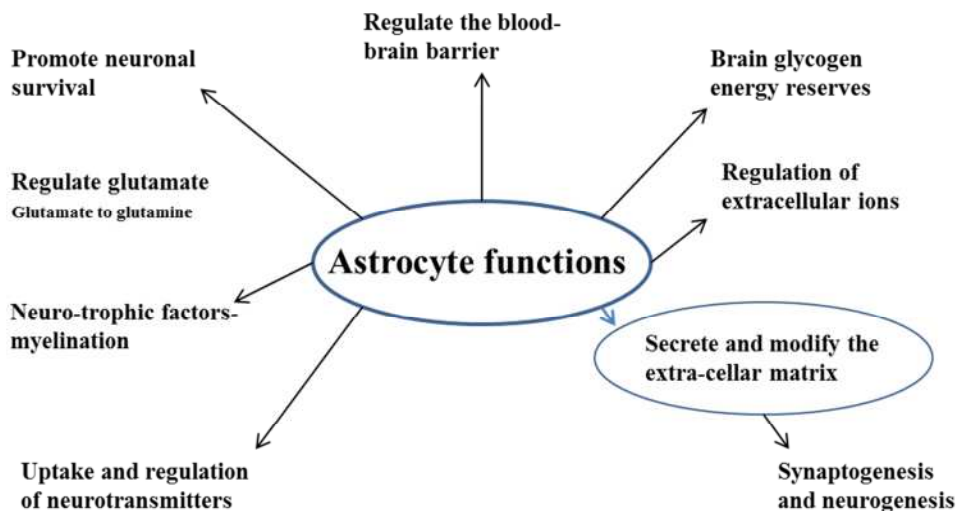


Figure 6-6 Diagram summarizes the most important functions of astrocytes

Astrocytes maintain and regulate glycogen as energy reserves, as well as serving several other functions. They support neurons through the availability of glucose, and play a vital role in the regulation of K^+ and H^+ ions and water transport (via astrocytic end feet). Glutamate uptake by astrocytes prevents an *excitotoxic glutamate rise in the extracellular space. Astrocytes can also produce neuro-trophic factors, and are involved in the metabolism of neurotransmitters.

http://missinglink.ucsf.edu/lm/introductionneuropathology/Response%20to_Injury/Astrocytes.htm

6.2.3 Gliosis

Gliosis is an accumulation of astrocytes in damaged regions of the CNS. This proliferation of astrocytes occurs as a result of two processes, hypertrophy and hyperplasia. The activation of astrocytes is an indication of damage to the nervous system due to stroke, trauma, growth of a tumor, or neurodegenerative disease, which is one of the most common of sources of damage e (Pekny and Nilsson 2005). Gliosis is a reactive cellular process leading to scar formation in the central nervous system, as a result of injury. This action creates a dense fibrous network of neuroglia in areas of damage. Glia scar formation identifies a reactive cellular process including astrogliosis that follows the brain injury, which usually leads to death and disappearance of the neurons, known as gliosis (Djebaili, Guo *et al.* 2005, Bignami and DAHL 2008).

6.2.4 Mechanism of action of gliosis (proliferation of astrocytes)

Gliosis can be defined as proliferation of astrocytes resulting in an increase of astroglia in the damaged areas of the central nervous system (Logan, Berry *et al.* 2006). It is believed that astrocytes help to retain the structure of cells in addition to the main function of holding neurons together in a 3-D matrix. They also serve many other functions such as maintenance of the extra cellular environment and stabilization of cell–cell communications in the CNS (Bear, Connors *et al.* 2006). Astrocytes become active and start proliferating in response to injury such as trauma, tumor brain growth or neurodegenerative disorders (Buffo, Rolando *et al.* 2010). Due to brain injuries, astrocytes undergo physiological changes which lead to increased synthesis of glial fibrillary acidic protein (GFAP), which astrocytes express. The expression of GFAP occurs in astrocytes. GFAP is an important intermediate filament (IF) protein that allows the astrocytes to initiate synthesis of more cytoskeletal supportive structures (Franke, Krügel *et al.* 2003) .

Astrocytosis; (astrogliosis) is defined as an increase in the number of astrocytes due to the damage of adjacent neurons (Barbeito, Pehar *et al.* 2004). Due to an injury,

astrocytes become activated, which results in trigger molecules produced at site drive of further brain injury. This process is called astrogliosis (cell hypertrophy) and is followed by up-regulation of intermediate filaments (IF) and increased cell proliferation. At this stage; the astrocytes migrate towards the injured area to create the glial scar (Figure 6-7 E), and release factors mediating the tissue inflammatory response (Blackburn, Sargsyan *et al.* 2009). It has been reported that the reactive astrocytes can repopulate stem cell numbers after damage. The reactive process of astrocytosis is followed by hypertrophy as mentioned earlier, and then up-regulation of the intermediate filament (IF) protein, whereas the stem cells contain Nestin a member of the intermediate filament (IF) protein family that is especially abundant in neuroepithelial stem cells. There is also expression of vimentin, and GFAP. The cells enter the stage of cell proliferation, while astrocytes can continue to divide and migrate to form the glial scar, and release factors mediating the tissue inflammatory response. The next schematic (Figure 6-7) illustrates the active mechanisms of astrogliosis (glial scar formation).

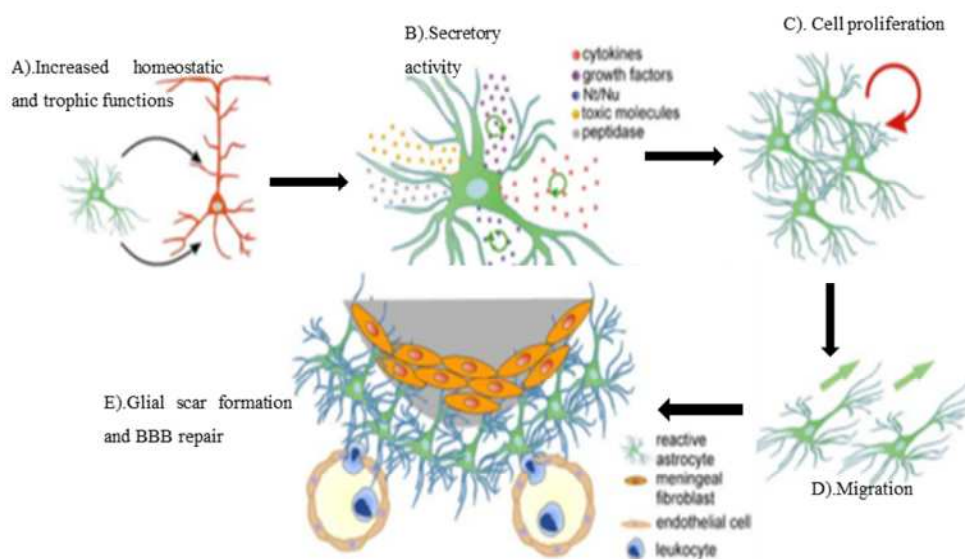


Figure 6-7 Schematic drawing illustrating astrogliosis (astrocyte proliferation).

A: Production of growth factors step (cytokines) and release of nucleotides and toxic compounds. B); Astrogliosis; (cell proliferation). C): Migration towards the lesion. D). Reactive astrocytes contribute in glial scar formation. (Buffo, Rolando *et al.* 2010).

6.2.5 Role of astrocyte in promotes neuronal survival

Many studies indicate that astrocytes are the supporting cells for neurons in the nervous system (Zhang, Li *et al.* 2009). Astrocytes provide structural support for neurons. In addition, they are responsible for maintaining the homeostasis of the brain tissues. However, a high activation of astrocytes and microglia is an indication of uncontrolled inflammation, predominantly resulting in neuronal cell death. Thus, astrocytes are stimulated to trigger cell proliferation, as a reaction to the destruction of adjacent neurons because of CNS trauma (Song, Stevens *et al.* 2002, Luna-Medina, Cortes-Canteli *et al.* 2005).

6.2.6 Reactivation of astrocytes during CNS injury

Reactive gliosis is distinguished by cellular hypertrophy and proliferation of astrocytes. Proliferating microglia form a bordering glial scar around the damaged area. Reactive gliosis is a natural reaction that occurs during brain injury, and the formation of the glial scar protects the brain, despite also causing inhibition of neuronal regeneration. The brain is exposed to varying intensities of injury, both moderate and high grade. Moderate astrogliosis occurs after mild trauma, whereby the combination of molecular changes and impact on functional activity leads to cellular hypertrophy. In severe astrogliosis, scar formation generally occurs and continues along cellular borders, causing tissue damage and/or inflammation. Glial scars tend to persist for long periods of time and act as barriers to inflammatory cells. This in turn protects intact tissue from nearby accumulations of inflammatory cells (Buffo, Rolando *et al.* 2010, Allaman, Bélanger *et al.* 2011).

6.3 Neurodegenerative diseases

‘Neurodegenerative’ refers to the pathological changes in the brain, resulting from loss of neurons, ultimately leading to deterioration of brain function. At a cellular level, neurodegeneration is seen as a gradual loss of structure or function of neurons leading to neuronal death. Many neurodegenerative diseases including Parkinson’s, Alzheimer’s, multiple sclerosis, ALS lateral sclerosis and Huntington’s disease occur as a result of neurodegenerative disorders (Minagar, Shapshak et al. 2002, Pryce, Ahmed *et al.* 2003, Romero and Rodríguez Luque 2011). The hallmark of many neurodegenerative diseases is the accumulation of intracellular or extracellular protein. Some studies *in vitro* and *in vivo* have provided new visions into neurodegeneration disorders, furthering understanding of the mechanisms regulating protein processing, specifically neurodegenerative disease proteins. The understanding of such disorders facilitates the development of therapies, that may prevent occurrence of severe memory loss, communication problems or the aforementioned diseases (Zecca, Youdim *et al.* 2004). These types of diseases belong to the category of dementias which result in cognitive deficits (loss of cognitive ability as a result of a brain injury (Dementia and MCI , Robinson 1998, Schneider, Wilson *et al.* 2003).

6.3.1 Anti-Inflammatory role of PPARs in neurodegenerative disorders

Recent studies point towards the role of peroxisome proliferator activated receptors in protecting against inflammation, particularly in the central nervous system. New evidence has shown a beneficial effect of targeting peroxisome proliferators activated receptor gamma PPAR- γ , to improve the outcomes of neurodegenerative disease. Several recent studies have shown that PPAR- γ agonists inhibit neuronal degeneration. For example; oral treatment with potent PPAR- γ agonists such as telmisartan, provides neuro-protection against cell death and neuro-inflammation (Shoelson, Lee *et al.* 2006, Akaike, Takada-Takatori *et al.* 2010).

6.3.2 Neuro-inflammation in parkinsons' disease (PD), Alzheimer (AD) and Sclerosis

Most of the studies performed on the PPAR- γ receptor have been in relation to the microglia, to understand its role during inflammation. Studies on astrocytes are less abundant (Carta and Pisanu 2012). The present study focuses on the role of astrocytes, and understanding how they are activated to proliferate, ultimately resulting in neurodegenerative disorders.

6.3.2.1 Alzheimer disease and microglial phagocytic role

Studies suggest that Alzheimer's disease (AD) is associated with age, gender and varies between brain regions. The cause and progression of Alzheimer's disease is not well understood. Alzheimer's disease involves glial inflammation associated with amyloid plaques in the grey matter of the brain. This would lead to abundance of microglia, and astrocytes, leading to progressive neuronal degeneration and ultimately death (Lipton 2005). The role of the microglial cells in the AD brain is controversial, as it remains unclear whether the microglia form the amyloid plaques or react to them in a macrophage-phagocytic role. Some evidence has shown the role of phagocytosis by microglia in the brain, although there is also evidence that microglia show differential selection to specific types of amyloid plaque in the AD brain. This may explain why microglia are sensitive to the presence of foreign bodies (McGeer, Itagaki *et al.* 1988, Wyss-Coray and Mucke 2002).

6.3.2.2 Parkinson's disease

Parkinson's disease is a degenerative disorder in the central nervous system characterised by loss of dopaminergic neurons in the extrapyramidal motor system. The pathology of the disease is characterized by the gathering of a protein called α -synuclein into Lewy bodies in neurons. The α -synuclein gene was identified as the main element of Lewy bodies. Lewy bodies (LBs) cause gradual degeneration of

neurons progressing to full Parkinson's disease. The ubiquitin proteasome system (UPS) became the most important way to verify the mechanism of PD. The UPS is a highly regulated and controlled system, thereby avoiding protein degradation in the brain (Olanow, Kiebertz *et al.* 2008).

6.3.2.3 Ubiquitin Proteasome System

Proteasomes are very large protein complexes, found inside all eukaryotes and archaea, and in some bacteria. In eukaryotes, they are located in the nucleus and the cytoplasm. The cells of organisms work hard to maintain the healthy balance of proteins. The main function of the proteasome is to degrade unwanted or damaged proteins by proteolysis, a chemical reaction that breaks peptide bonds. Enzymes that carry out such reactions are called proteases. Their important regulatory role is carried out by the ubiquitin proteasome system (UPS). Proteasomes are part of a major mechanism by which cells regulate the concentration of particular proteins and degrade misfolded proteins. The degradation process yields peptides of about seven to eight amino acids long, which can then be further degraded into amino acids, to be used in synthesizing new proteins. In a sense, the UPS is responsible for detecting destroyed or faulty proteins. Proteins are tagged for degradation with a small protein called ubiquitin, (Figure 6-8). The tagging reaction is catalyzed by enzymes called ubiquitin ligases.

Ubiquitin is a small regulatory protein that has been found in almost all tissues of eukaryotic organisms. Among other functions, it directs protein recycling. Ubiquitin binds to proteins and labels them for destruction. The ubiquitin tag directs proteins to the proteasome, which is a large protein complex in the cell that degrades and recycles unwanted proteins. Once a protein is tagged with a single ubiquitin molecule (monoubiquitination) or many (polyubiquitination), this is a signal to other ligases to attach additional ubiquitin molecules. The result is a poly-ubiquitin chain that is bound by the proteasome, allowing it to degrade the tagged protein (Rogers, Paine *et al.* 2010).

Therefore, the UPS can be over-active, whereby useful proteins are destroyed, or underactive, causing harmful proteins to build up to toxic levels. Homeostasis requires the right amount a specific protein at the right time (Kimura and Tanaka 2010). Failure of the ubiquitin proteasome system can result in diseases such as; Alzheimer’s disease, infectious diseases, some cancers and inflammatory diseases such as Rheumatoid (Oddo 2008, Moreau, Luo *et al.* 2010).

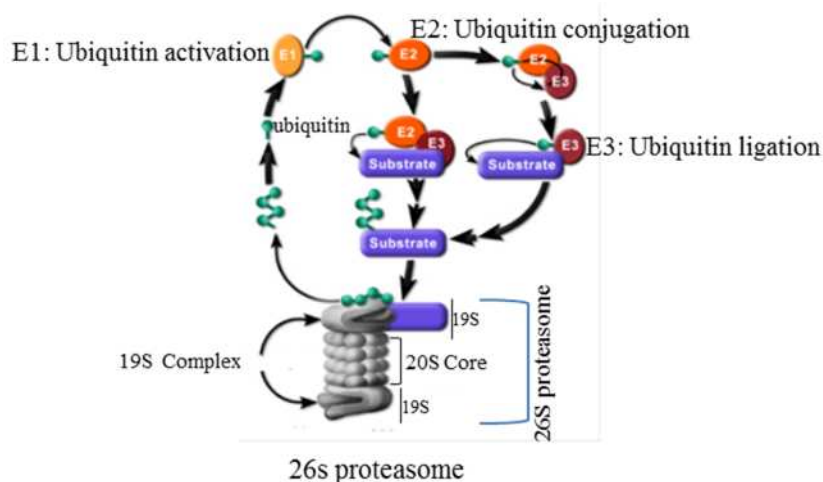


Figure 6-8 Diagram of the 26S proteasome structure.

The 26S proteasome system composes of two sub-complexes: a 20S core particle that carries the catalytic activity, and a regulatory 19S regulatory particle. Ubiquitination and degradation processes undergoing three steps to degrade misfolded proteins. (E1) activates and binds to ubiquitin. The activated ubiquitin is transferred to a cysteine group, an ubiquitin-conjugating enzyme (E2). Then, the ubiquitin is transferred to the substrate by the action of an ubiquitin ligase enzyme (E3). Depletion of 26S proteasomes in mouse brain neurons shows 26S proteasomal dysfunction caused neurodegeneration (Ciechanover 2005).

6.4 Peroxisome proliferator-activated receptors (PPARs) in the brain

As referred to in Chapter one, peroxisomes are organelles found in almost all eukaryotic cells. In 1978, Arnold describes the peroxisome proliferators in both neurons and glia (Cristiano, Bernardo *et al.* 2001). It became known that astrocytes contain high levels of peroxisomes (Moreno, Farioli-Vecchioli *et al.* 2004). Peroxisome proliferator-activated receptors are ligand-activated transcription factors, as part of the steroid/thyroid hormone category, in the superfamily of nuclear receptors. Other studies showed that PPAR transcription factors are pharmaceutical drug targets in inflammatory degenerative diseases (Stuchbury and Münch 2005). The transcription factors include three isoforms that have been identified: PPAR α (NR1C1), PPAR β (NR1C2) and PPAR γ (NR1C3), encoded by different genes. The latter includes two isoforms, namely PPAR γ 1 & PPAR γ 2 (Yu, Matsusue *et al.* 2003, Aleshin, Grabeklis *et al.* 2009). PPARs heterodimerize with RXR receptors and bind to specific DNA sequences, termed peroxisome proliferator response elements (PPREs).

PPARs are found in the nervous system during rodent embryogenesis. PPAR β represents the most abundant of the three isoforms, while PPAR α and PPAR γ decrease in the postnatal brain. The three isoforms were detected in the hippocampal area, with high concentrations of PPAR β found in the dentate gyrus and CA1 region, compared to PPAR γ , which is more concentrated to the CA3 region (Luna-Medina, Cortes-Canteli *et al.* 2007, Yi, Park *et al.* 2007). Moreover, PPAR- γ is shown highly expressed in most other brain areas, especially cortex.

6.4.1 Rosiglitazone; PPAR- γ agonist

PPAR- γ isoform is a subfamily of the nuclear hormone receptor, named peroxisome proliferator-activated receptor gamma. Thiazolidinediones (TZDs) belong to a group of PPAR- γ -agonists, and rosiglitazone is one of the TZDs used in the treatment of type 2 diabetes. The mechanism of the agonist involves binding to the PPAR receptors in fat cells (Malinowski and Bolesta 2000, Culman, Zhao *et al.* 2007).

The current evidence suggests that PPAR- γ may be involved in reducing brain cell inflammation and inhibiting glial cell proliferation (Bernardo and Minghetti 2006, Hirsch, Breidert *et al.* 2006, Schintu, Frau *et al.* 2009, Carta 2013). Moreover, other evidence has emerged, suggesting that PPAR- γ agonists, whether natural or synthetic, may regulate brain disorder by inhibiting several functions associated with glial cells and microglial activation (Bernardo and Minghetti 2006).

6.5 Aims of project part 2

The main aims of this project are to understand the role of astrocyte proliferation and its relation to neural insult this may contribute to fundamental understanding of how pathological changes come about in the CNS. Recent evidence suggests neuroglia-mediated inflammatory mechanisms may stimulate disorders in the mouse brain (Gavériaux-Ruff and Kieffer 2007). To test the hypothesis that the number of astrocytes increase in both cortex and hippocampus *in vivo*, the brains of mice aged 2-6 weeks were dissected and immunohistochemistry was performed. Pups aged 1-5 days, were used for brain culture purposes *in vitro*. L. Bedford's lab has created a mouse model ($Psmc1^{fl/fl}$; $CaMKII\alpha-Cre$), whereby the mice do not survive for longer than 3-4 months. The main goal is to follow the evolution of pathology through the ages from 2 weeks to 6 weeks of culturing, and then try to improve or reduce the disease using PPAR- γ agonist.

The hypotheses

1. Astrocyte proliferation contributes to the neuropathology seen in a mouse model of dementia ($Psmc1^{fl/fl}$).
2. Rodent organotypic slice cultures can be used to further understand neurodegenerative diseases.
1. Peroxisome proliferators such as rosiglitazone can be used to inhibit astrocyte proliferation in a mouse model

The aims

1. Characterize the temporal and spatial aspects of astrocyte proliferation in the $Psmc1^{fl/fl}$ mouse model and compare to age matched controls.
2. Evaluate the use of organotypic slice cultures system, to observe the progression of astrocyte proliferation and determine whether this progression is comparable *in vivo*.
3. Investigate the effects of a PPAR- γ agonist on astrocyte proliferation in dementia with a lewy body disease model.

7. Materials and method

7.1 Materials

7.1.1 Animals

A mouse model of neurodegeneration with 26S proteasome dysfunction was used. It pathologically represents dementia with Lewy bodies disease (Psmc^{1fl/fl};CaMKII-Cre) (Bedford, Hay *et al.* 2008). This mouse model depends on a system known as Cre-loxP recombination, which allows the DNA modifications to be targeted to a specific cell type (Kuhn and Torres 2002). Cre is a 38 kDa recombinase protein derived from bacteriophage P1, which has the ability to cut and recombine DNA between two similarly orientated loxP sites, reference to Figure 7-1.

It was reported that 26S proteasome function is essential for normal neurological function in mice. In a previous experiment in Bedford's lab, it was shown that these mice are more anxious in open-field analysis and displayed obvious spatial learning deficits in the Morris water maze task at 6 and 8 weeks, respectively. These animals have a short lifespan; they die when aged 3–4 months, as a result of lacking interest in locating food.

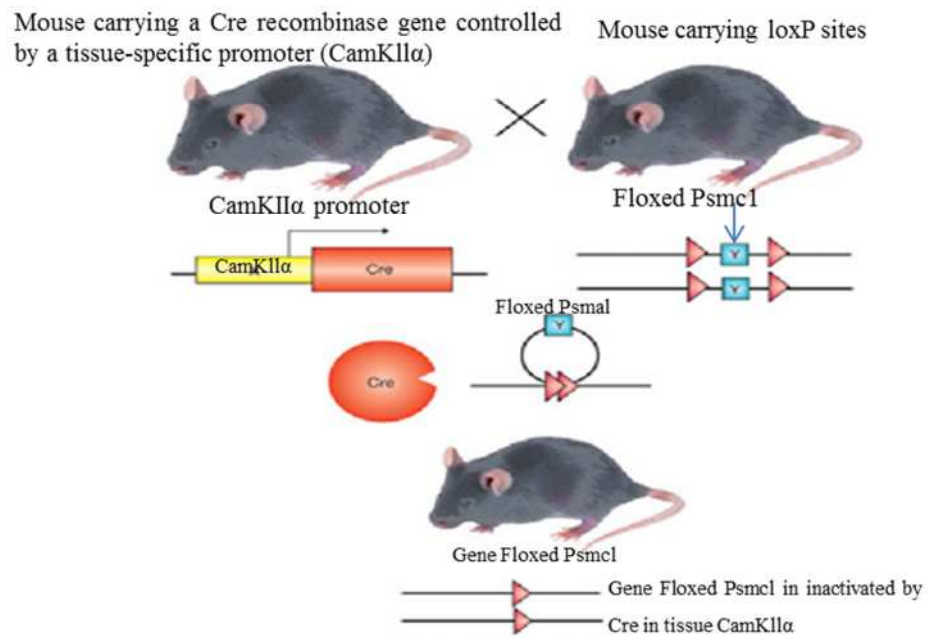


Figure 7-1 Diagram shows conditional deletion of *Psmc1* in mouse, specifically with the CaMKII α promoter (calcium/calmodulin-dependent protein kinaseII α).

Expressed cells have 26S proteasome dysfunction, and therefore Ub accumulation pathologically resembling neurodegeneration that occur in Parkinson's' disease and LBD.

7.1.2 Immunohistochemistry materials

Glial fibrillary acidic protein (GFAP) primary antibodies from thermo scientific were used to identify the astrocytes. GFAP is a common marker used to distinguish astrocytes via intermediate filament proteins (Takamiya, Kohsaka *et al.* 1988, Miguel-Hidalgo, Baucom *et al.* 2000).

7.1.3 Culture mediums

Hanks' Balanced Salt solution containing sodium bicarbonate, without phenol red, sterile-filtered, PH 7.1-7.5, glucose concentration 0.9 - 1.1 g/l from Sigma was used as a basic salt solution in all sterile procedures. Culture medium was Dulbecco's Modified Eagle Medium (D-MEM) - 1X, liquid (containing 4500 mg/L; D-glucose), sodium pyruvate, L-glutamine and 25 mM HEPES buffer, Sodium Bicarbonate (PH 7.2) but without sodium pyruvate or phenol red.

7.1.4 Chemicals and instruments

Normal goat serum was purchased from Vector, bovine serum albumin (BSA) from sigma. Three types of slide were used; cavity slides (depression slide) for organotypic slices, coated slides (APES) for paraffin embedded sections and chrome gelatinised slides for cryostat sections. The slide sizes were 1.0-1.2 mm; Slides were purchased from Fisher. Paraffin embedded sections were prepared using Microtome-LEICA RM2145. Cryostat sections were prepared on a Cryostat CM1900 and McILWAIN tissue chopper was used to produce the organotypic brain slices. Brains were processed in a Leica-TP 1020 tissue processor prior to paraffin embedded sections being prepared. The organotypic slices were incubated in Galaxy S Co2 Incubator. Axiovert 25 PCR machine was used for amplification of DNA from the brains isolated from the pups.

7.1.5 Inserts and slide types

TransWell® permeable supports 0.4 µm polyester membrane – 12 mm inserts, 12 well plates was used for organotypic brain slice cultures (Corning Incorporated-Corning, NY 14831 the USA). See section 7-2-3. Micro-plate 96 well purchased from IWAKI / EZ-BirdShut®.

Three types of slides were used in the study: cavity slide, APES (2% 3-aminopropyltriethoxysilane) and gelatin-coated (gelatinised) slides.

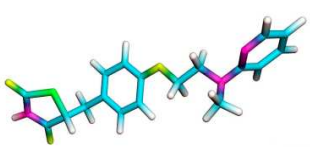
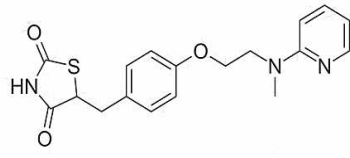
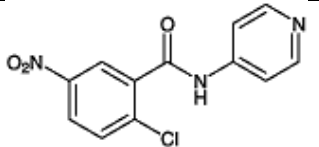
7.1.6 Mounting medium

To cover the slides, DABCO (1-4-Diazabicyclo-2-2-2-octane) in 90% glycerol in phosphate buffered saline (PBS) was used after mounting the fluorescent brain tissue. (100 mg of DABCO in 5 ml of PBS and then add 45 ml of glycerol and max well, and store at 4⁰C).

7.1.7 Peroxisome proliferator-activated receptor gamma (PPAR- γ) agonist and antagonist

Peroxisome proliferator activated receptor gamma agonists have been used to investigate the effect of reducing astrocyte activation on neurodegenerative disorders. Rosiglitazone (PPAR- γ agonist) and the antagonist (T0070909) were used in this study, both purchased from sigma.

Table 7-1 Structure of Rosiglitazone and T0070907 PPAR- γ antagonist

Systematic *IUPAC Name	3D Structure	structure
<p>Rosiglitazone (<i>RS</i>)-5-[4-(2-[methyl(pyridin-2-yl)amino]ethoxy)benzyl]thiazolidin e-2,4-dione</p>		
<p>T0070907(PPAR-γ antagonist) blocks PPAR-γ function</p>		

*IUPAC (International Union of Pure and Applied Chemistry).

7.1.8 Microscopes

The DMRB Fluorescence Microscope Leica^{EM} was used to capture fluorescent images of tissues. These were detected by using DAPI (wavelength 350/50 – 460/50), mCherry filters; (480/40 – 535/50) and Rhodamine RedTM (TRITC, 545/20 – 610/75). The Leica DM4000B light microscope fitted with MicroPublisher 3.3RTV camera was used for pictures. Images were captured on a Confocal Microscope (Leica TCS SP2) and analysed off line on a workstation equipped with Velocity software.

7.1.9 Statistics

One way and two-ways ANOVA, followed by a post hoc student t-test were performed for statistical analysis, where P values <0.05 were considered significant.

7.2 Methodology

7.2.1 Sample preparation

For whole brain fixation, mice were injected with Heparin, then anesthetized using isoflurane inhalation, and perfused transcardially. Perfusion was initiated by washing out the blood with 0.9 % saline solution at 37⁰C until the perfusate became clear. This was then followed by perfusion of 4% paraformaldehyde (Bustin, Benes et al.) in 0.1 M PBS, PH 7.4 at 4⁰C. The brains were dissected out and stored in Eppendorf tubes containing 4% PFA overnight for post-fixation.

In vitro, brains from postnatal pups aged 1-5 days were used to prepare organotypic slices at thickness 300 µm and cultured for periods of 2, 3, 4, 5 and 6 weeks. For fixation, slices were washed 4 times in PBS and then fixed for 20 minutes in 4% PFA. The inserts of the organotypic slices were embedded in paraffin prior to being sectioned. Slices were stored in 4⁰C until required for immunohistochemistry with either rhodamine red or DAB stains. The slices were labelled with fluorescent rhodamine red.

7.2.2 Determination of area of interest using a box dividing protocol

To determine the specific areas of interest (i.e. within the cortex and hippocampus) a box dividing slice technique was used for both mutant and control pups to match paraffin embedded sections with the organotypic slices.

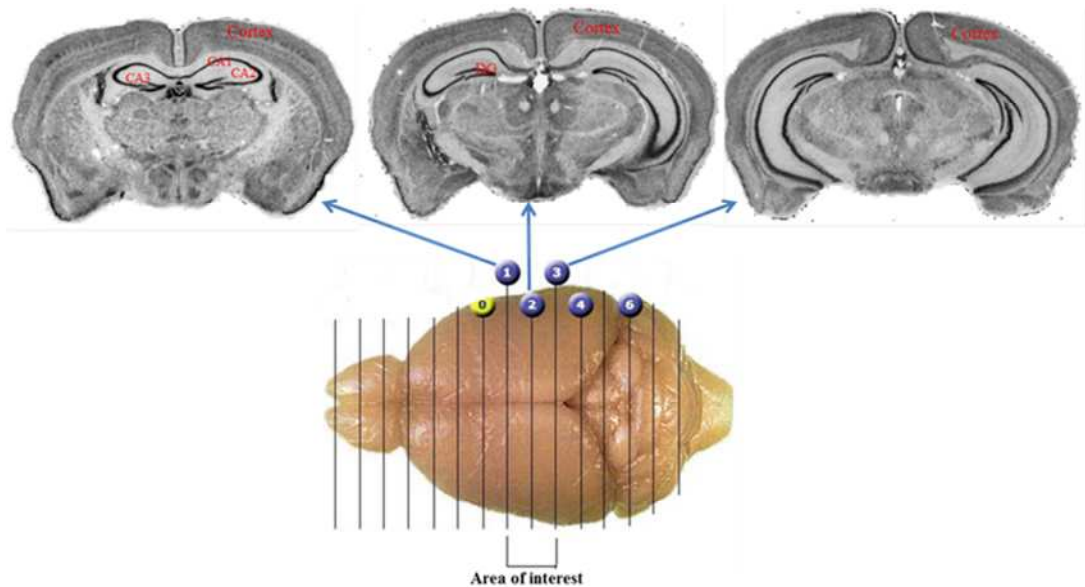


Figure 7-2 Method of box-dividing a brain into 1mm sections.

Brain is placed onto divider and the same section is taken to preparing the paraffin embedded brains to look at the same area of interest. after fixation overnight mouse brain dissected into 1 mm using box dividing of gel agarose.

www.mbl.org/atlas165/atlas165_frame.html

7.2.3 Organotypic Slice Culture

Postnatal slices can be maintained in culture from weeks to months, which is the reason for the use of new-born C57 black 6 modified (*Psmc1^{fl/fl}; CaMKII α -Cre*) and wild-type (*Psmc1^{fl/fl}; CaMKII α -Wt*) mice aged 1-5 days, in this study.(Gähwiler, Capogna et al. 1997).

The experiments were performed in accordance with protocols from the Scientific Procedures (Act 1986) and the Home Office recommendations with regards to killing by schedule 1 method, at the designated establishment (BMSU, QMC at the University of Nottingham). Mouse pups were decapitated, the brain removed and cut into 200, 300 and 325 μ m thick tissue slices using a Mcilwain Tissue Chopper. The various thicknesses were checked to select the best for long term survival in culture. Chosen slices were transferred to a sterile petri dish containing Hanks' Balanced Salt solution then dissected slices were detached from each other under the microscope using sterile needles and carefully transferred to the transwell membrane inserts.

Organotypic slice cultures were grown for periods of 2, 3, 4, 5 and 6 weeks in culture harvested from control and mutant pups. 1 or 2 brain slices were placed into each transwell insert with 500 μ l medium (Dulbecco's Modified Eagle Medium) in the base of a 12 multi-well plate. The tissues were strictly controlled in terms of sterilization, temperature and rate of carbon dioxide availability and the media was changed regularly. Therefore, the slices were incubated at 36-37⁰C in 5% CO₂ and the medium changed every second day. The culture medium contained the following components: 89 ml DMEM, 10 ml FCS and 1 ml glutamine. All procedures were carried out under strict sterile conditions.

The diagram below (7-3) illustrates how the brain slices were cultured *in vitro*.

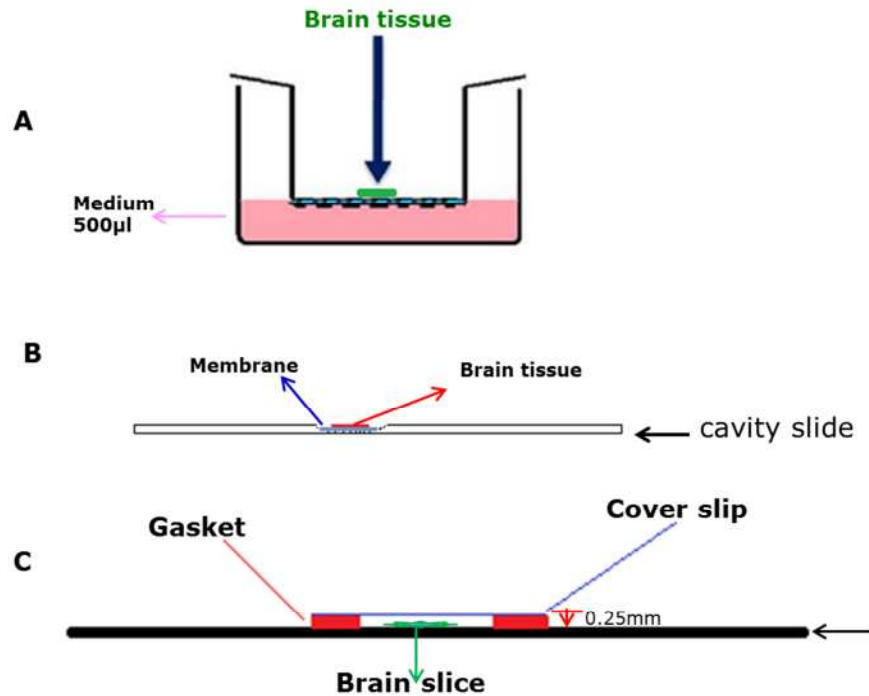


Figure 7-3 Diagram of organotypic slices system materials and method.

A; 0.4 µm transwell inserts were placed in each well of the 12 well plates. To avoid damaging of slices, two types of slide were used - cavity slide and normal slide, provided with frame. B; The brain tissue must be centrally placed on the membrane during the immunohistochemistry protocol. C Gaskets prevent any pressure on the brain slices when being coverslipped.

7.2.4 Tissue fixation of organotypic slices

The cultured slices were washed in PBS and fixed in 4% paraformaldehyde for 20 minutes. Organotypic slice cultures were grown for periods of 2, 3, 4, 5 and 6 weeks in culture, once harvested from control and mutant pups. Organotypic slices cultures were re-washed three times in PBS. The slices were immersed in PBS and stored at 4⁰C until required for use. Storage time was kept to a minimum to avoid loss of immunogenicity of the samples. Details of storage time for the slices are mentioned in results section.

7.2.5 H&E staining

The paraffin embedded sections were deparaffinised in xylene twice, for 10 minutes each. Slides were then washed in 100% ethanol For 10 minutes three times, followed by 90 % ethanol, 70%, and 50% respectively for 5 minutes each. Once washed in tap water for 5 minutes slides were submerged in freshly filtered haematoxylin for 5 minutes. After being washed in running tap water until it ran clear, they were dipped in 1% acid alcohol then rinsed again in water. After a minute wash in Scott's tap water, slides were immersed in eosin for 5 minutes. Subsequent dehydration involved washing in running tap water, 50%, 70%, 95% ethanol and 3 different containers of 100% ethanol, followed by xylene. Slides were coverslipped with DPX and left to dry. (See appendix). Positive staining showed cell nuclei as blue, and cytoplasm as pink.

7.2.6 Distinguishing between a mutant and control animals using DNAreasy technique to release gDNA

An ear or tail biopsy was taken from the mouse and placed in an Eppendorf tube. 20µl DNAreasyTM was added (Anachem) to cover the tissue then placed in the PCR machine. The samples were run on a PCR programme, entitled 'lysis 20' as shown below. This programme cycles the sample through various thermal conditions.

Primers were used for genotyping the DNA, which distinguished between control and mutant mice used in the study.

Table 7-2 Thermal cycle to release the DNA

NO	Temperature cycle	Time
1.	65 ⁰ C	15 mins
2.	96 ⁰ C	2 mins
3.	65 ⁰ C	4 mins
4.	96 ⁰ C	1 mins
5.	65 ⁰ C	1 mins
5.	96 ⁰ C	30 sec
6.	20 ⁰ C	hold

Note: DNAreasy- lysate can be used directly in PCR (DNA releasyTM can be made up to 40%) and stored at -20 °C for future use.

DNA was prepared from the animals after the genomic DNA has been extracted from the biopsy sample, where 2µl of DNA is needed for each sample. Positive and negative controls were included. The preparation will be for x + 2 samples to avoid any shortage.

7.2.6.1 Running the samples in PCR

The DNA samples were prepared to detect homozygote and heterozygote pups, mutant (*Psmc1^{fl/fl}*; *CaMKII α -Cre*) and wild-type pups (*Psmc1^{fl/fl}*; *CaMKII α -Wt*). The table below shows primers and nucleotides (dNIPs) of the Cre and S₄ genes.

Table 7-3 primers and nucleotides of the Cre and S₄ genes preparation

NO	S4 gene components	Cre gene components
1.	dNIPs 1 μ l x n = x μ l	dNIPs 1 μ l x n= x μ l
2.	10X 1 μ l x n = x μ l	10X 1 μ l x n= x μ l
3.	D130 0.5 μ l x n = x μ l	Cres 0.5 μ l x n= x μ l
4.	LB3 0.5 μ l x n = x μ l	Creas 0.5 μ l x n= x μ l
5.	X316 0.5 μ l x n = x μ l	Taq 0.05 X n= x μ l
6.	Taq 0.05 X n = x μ l	
7.	Total x ₁ μ l	Total x ₁ μ l
8.	DNA 2 μ l for each sample	DNA 2 μ l for each sample
10.	dH2O x ₂ μ l /x ₂ = 100- x ₁	dH2O x ₂ μ l /x ₂ = 100- x ₁

Table 7-4 PCR temperature cycle for genotype detection

NO	Temperature cycle	Time
1.	94.0 °C	3 mins
2.	94.0°C	15 sec
3.	64.0 °C	15 sec
4.	72.0 °C	30 sec
5.	Go to 2 REP 34	
6.	72.0 °C	3 mins
7.	T = 94.0 °C	3 mins
8.	Hold at 15.0 °C	Enter

Run 3% gel agarose and check the results.

7.2.7 Immunohistochemistry

Immunohistochemistry has been used with both fluorescence and DAB stains for whole brain sections, as well as sections from organotypic brain slices. Rhodamine red goat anti-mouse as a fluorescent secondary antibody was used in paraffin embedded, organotypic slice culture and cryostat sections. DAB stain was used *in vivo* and *in vitro* whereas organotypic slices were prepared for paraffin sectioning embedded for all target age groups.

7.2.7.1 Mouse on mouse (M.O.MTM) immuno-detection kit.

The Vector® M.O.M. TM immunodetection kit for mouse tissues has the advantage of very low background staining, which has been a problem in other studies (Chang 2009). Paraffin-embedded brain sections from mice aged 2-6 weeks were de-waxed through xylenes and rehydrated with different concentrations of ethanol 100 %, 95% and 70% respectively for 10 minutes each, then rinsed for 5 minutes in tap water. 10 mM sodium citrate buffer pH 6 was employed as antigen retrieval, which was necessary to uncover hidden antigen sites. For endogenous peroxide, slides were incubated in 3% H₂O₂ (hydrogen peroxide) for 5 minutes, then immersed in tap water for 5 minutes. Blocking reagent was applied (block endogenous peroxidase activity) to block non-specific binding. Sections were washed three times for 5 minutes in PBS, and then in working solution of M O MTM diluent. The sections were incubated with primary antibody raised against the antigen of interest. Labelled secondary antibody was added, which is biotinylated anti-mouse M O M IgG Reagent, for 30 minutes. To perform Avidin/Biotin blocking, the avidin of biotinylated enzyme complex (ABC) is then added, which binds to the biotinylated secondary antibody (Figure 7-4). The incubation with a substrate for the enzyme generates a brown color resulting from DAB breakdown. Table 1 in the appendix summarizes the immunohistochemical process used for the paraffin embedded sections.

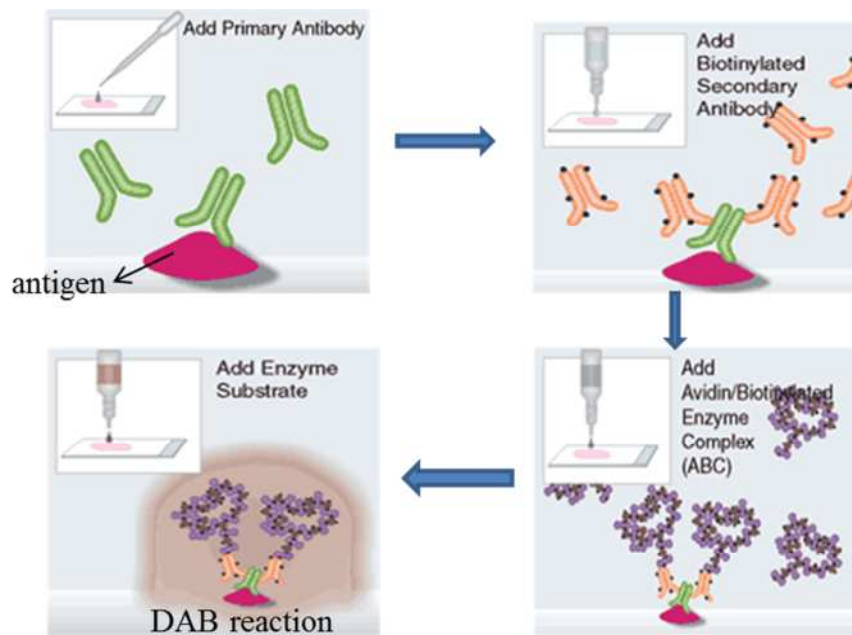


Figure 7-4 A diagram to illustrate the DAB reaction and how a labelled secondary antibody reacts with a primary antibody bound to a tissue antigen.

Immunohistochemical staining of paraffin sections (mouse on mouse kit – vector labs PK-2200). Incubation of brain tissue with primary antibody overnight at 4°C is followed with a secondary antibody conjugated with a peroxidase enzyme for 1 hour. The ABC complex was added to tissue sections followed by DAB which is oxidized; the generation of brown color can detect under the light microscope. Longer incubations may result in an increase in background staining.

The diagram is adapted from php.med.unsw.edu.au/cellbiology/index.php?title=Group_3_Project-Immunohistochemistry.

7.2.7.2 Immunohistochemistry technique for rhodamine-red fluorescent organotypic slice cultures

Organotypic slice cultures were fixed in 4% PFA for 20 minutes and then washed with PBS three times, for 5 minutes each. Slices were immersed in PBS and stored at 4⁰C until required, which was be within two weeks of fixation. Slices were rewashed with PBS, and permeabilized by incubation with 0.5% Triton X-100 in PBS, in a humidity chamber at room temperature. Non-specific protein binding was blocked with 10% bovine serum albumin (in 0.5% Triton X-100 in PBS) for 2 hours at RT, and then washed with PBS. Slices were incubated overnight at 4⁰C in primary antibody 1 µl:150 µl (anti-GFAP) in solution of 0.5% triton-X100 in PBS, then washed with PBS for 20 minutes. Rhodamine- conjugated secondary antibodies – (goat anti-mouse, 1 µl:400 µl) in 0.5% triton-X100 in PBS was applied and incubated for 3 hours at room temperature. The tissue was then washed with PBS four times for 20 minutes, and finally incubated with DAPI stain for 20 minutes at room temperature. After washing in PBS 4 more times for 20 minutes, mounting medium was added to the slide and then cover slipped and sealed with nail varnish.

7.2.7.3 Immunohistochemistry technique for paraffin sections and organotypic slice cultures

Immunofluorescent and immunohistochemical staining were performed on both whole brain sections and organotypic brain slices. Organotypic slice cultures were fixed with 4% paraformaldehyde in PBS for 20 min at room temperature and immuno-fluorescent staining was conducted. Tissues were permeabilized with 0.5% Triton-X-100 in PBS for 1 h at room temperature. Nonspecific binding sites were blocked with 10% bovine serum albumin (BSA, Sigma) with 0.5% Triton-X-100 in PBS. Organotypic slices were incubated with anti-GFAP antibody (1:150 µl) in solution of 10% normal goat serum with 0.5% Triton-X-100 in PBS overnight (16-18 hrs) at 4⁰C in a humidity chamber. Secondary antibody: Rhodamine red goat anti-mouse IgG (1:200 µl) in 10% normal goat serum with 0.5% Triton-X-100 in PBS was added to the slides and incubated for 3 hours in the humidity chamber at room temperature.

After washing with PBS, the slices were incubated with DAPI stain for 20 minutes at room temperature.

After dewaxing in xylene, the slides were immersed in three different concentrations of ethanol as follows: 100%, 95% and 70% and washed gently in running tap water. The sections were washed with PBS twice for 10 minutes in each container. The most important step is antigen retrieval, which involves steaming the sections for 40 minutes. This step was optimised several times to get the best result. The slides were left to cool for 20 minutes then blocked with 5% normal goat serum dissolved in 0.25% Triton X-100 in PBS for 2 hours in a humidity chamber at room temperature. The sections were then washed twice with PBS and incubated with primary antibody 1: 150 μ l GFAP with 5% normal goat serum in PBS overnight, at 4⁰C in a humidity chamber. The sections were again washed with PBS and incubated with rhodamine red- secondary antibody 1: 500 μ l with 5% normal goat serum in PBS for 1 hour in the humidity chamber at room temperature. The sections were washed several times with PBS and then incubated with DAPI nuclear stain for 20 minutes. After washing with PBS 4- 5 times, slices were finally mounted in DABCO and coverslipped and sealed with nail varnish.

7.3.1 Image-J program for calculating the number of astrocytes

To evaluate whether or not rosiglitazone (PPAR- γ agonist) has positive effects, by reducing brain disorders seen in the mutant mice, there was a requirement to accurately count the number of astrocytes. Unbiased stereological methods had been used since 1984 and recently, a more modern software, Image-J is commonly used (Lalancette-Hébert, Gowing et al. 2007, Sadeghi, D'Haene et al. 2008). Image-J has the ability to convert coloured cells to black and white, making it easier to calculate the number of labelled cells. All images were counted at the same magnification. An objective lens was used at 20 X with a unified frame for counting all slides. The counting frame size was 400X360 μ m. The standard was computed by counting the number of astrocytes in the region of tissue that appeared between the grids. Three sections per mouse were used for the analysis. All astrocytes shown in the cortex and hippocampal regions were counted (Figures 7-5 and 7-6). The data was averaged and

analysed by a two-tailed unpaired Student's t test and one way ANOVA; post-hoc tests included Dunnett's multiple comparison test. Data are expressed as mean \pm SD.

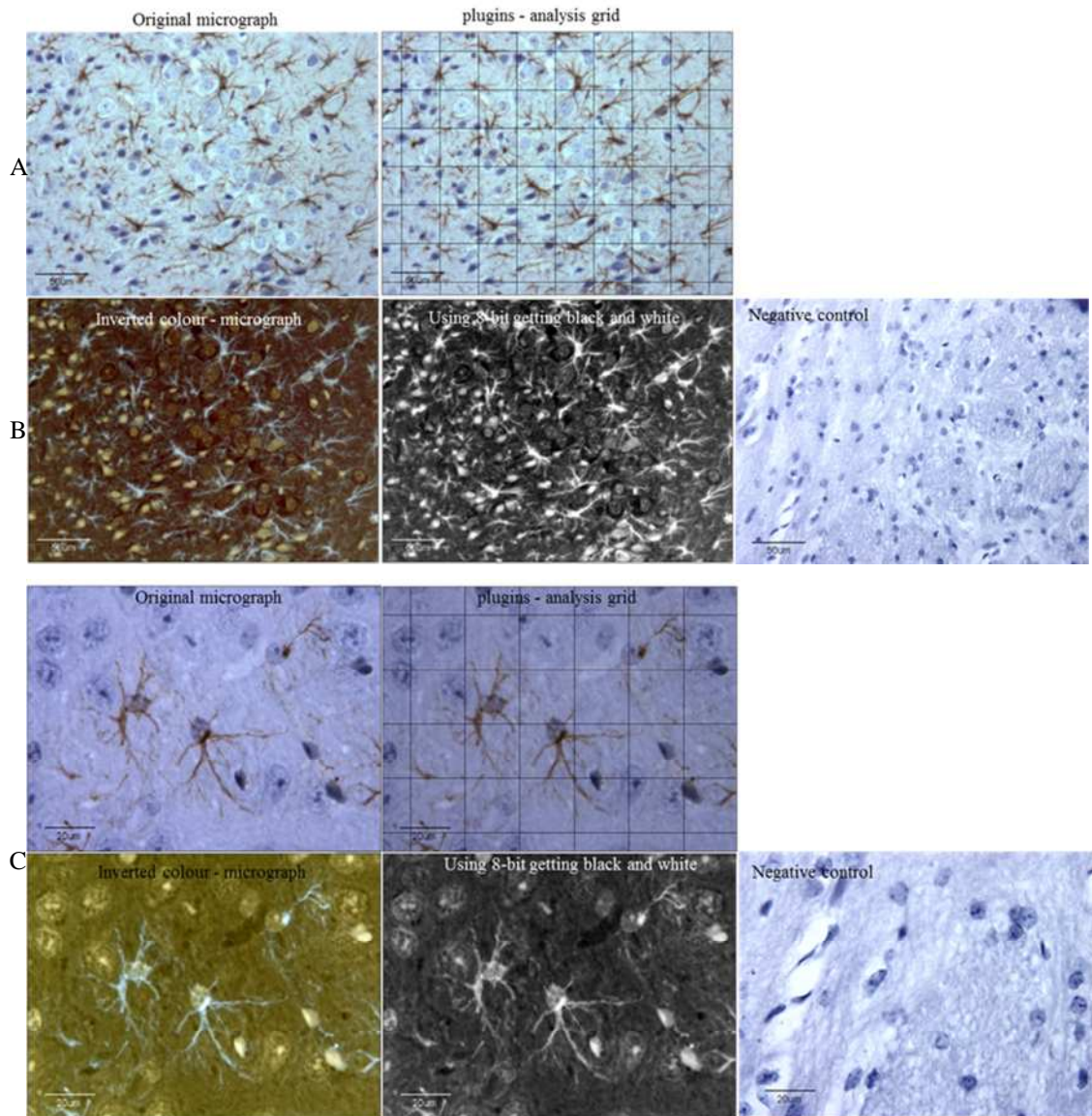


Figure 7-5 Using Image-J program for calculating the number of astrocytes in cortex region.

Images of the slices containing the cortex were captured at 20x and 40 x magnifications. A: illustrates the grid that the programme places over the image. B: Colour changes are applied to make the astrocytes more easily visible. C: At high magnifications and appropriate colour contrasts, the astrocytes in each grid were counted.

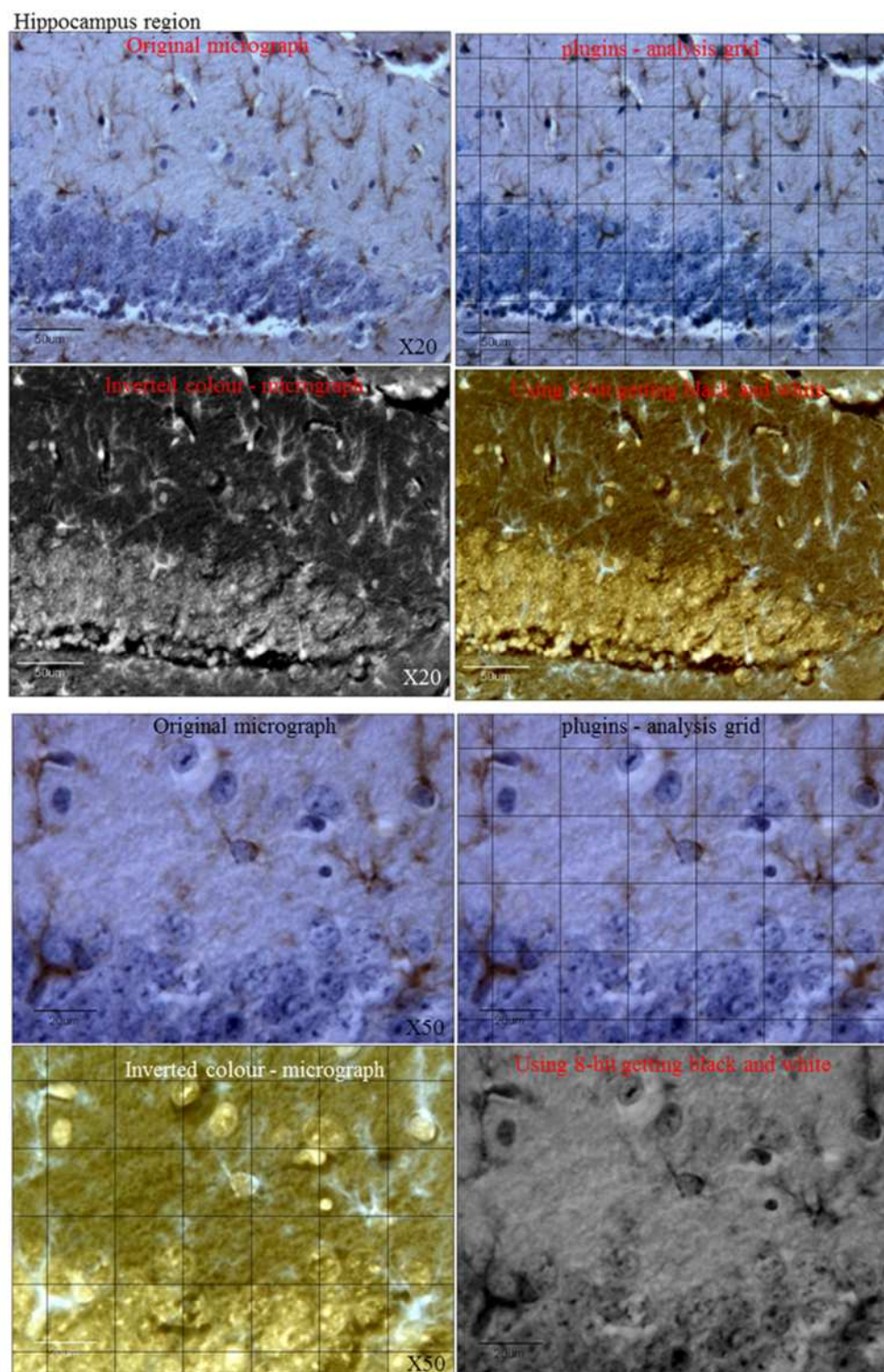


Figure 7-6 Using Image-J program for calculating the number of astrocytes in hippocampus region.

Brain tissue slices in the hippocampal region (CA1 zone) were captured at magnification X 20 and 40 X. Images A; the CA1 area before and after using Image-J to input a grid. B; same images undergo colour contrast changes to clarify astrocytes. C; same images at high magnification and different background to show astrocytes body.

7.4.1 Resazurin cell viability assay

Resazurin is a reagent that is not toxic to cells and is stable in culture medium. It is used to provide a quantitative measure of cell viability and allows the user to measure cell proliferation *in vitro*, via redox reaction that releases a fluorescent signal. Resazurin is a blue dye and non-fluorescent, also known as (AlamarBlue Reagent). The colour change from blue to red is characteristic of this assay and causes the cells to become fluorescent. This assay was conducted to investigate whether the PPAR- γ has toxic effects on brain tissue (Sarker, Nahar *et al.* 2007). The Fibroblast 3T3 cell line was used as the standard for toxicity testing, as they are fast growing cells, and are highly sensitive to toxic materials (Seiler, Visan *et al.* 2004). 3T3 cells were grown into two 96 well plates for 24 and 72 hours prior to addition of the fluorescent reagent. Resazurin (440 μ M) solution and phenol red-free HBSS (Ca²⁺ and Mg²⁺) were needed to prepare stock solution. The concentration was 12 mg of Resazurin dissolved in 100ml HBSS. A stock solution contains 10% of resazurin mixed with 90% of culture medium of use. After growing cells for 24 hours and 72 hours, the media was aspirated from the wells and replaced with resazurin working solution. Results were analysed for both plates and in a several time points 1, 2, 4, 6 and 24 hours of incubation. The results have been translated to graphical forms and can be found in the results section 8-6-3.

7.5.1 Effect of PPAR- γ agonist rosiglitazone on the reduction of astrocyte proliferation

Organotypic slices from the cortex and hippocampal areas were cultured separately. The concentrations of T0070907 PPAR- γ antagonist used were 25, 50 and 100 μ M. T0070907 PPAR- γ antagonist was used separately, and with an agonist as a negative control. In this assay 4 controls were used, which are DMSO vehicle, T0070907 alone, free drug medium, and agonist followed with antagonist. Organotypic slices were grown up to the fifth week. On the first day of the sixth week, experiments were conducted as outlined in the following diagram. The medium was changed every 2 days. Figure 7-5 shows time course of treating organotypic slice culture with PPAR- γ agonist & antagonist and vehicles.

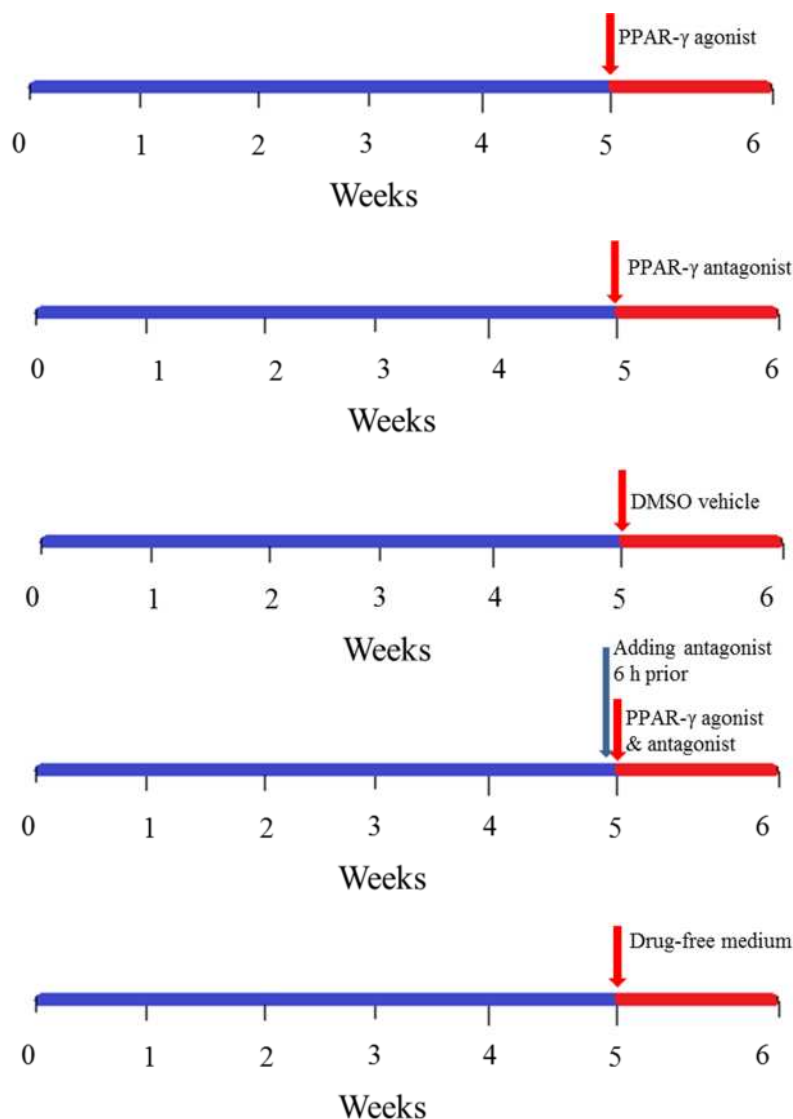


Figure 7-7 Schematic diagram indicates the time courses of treating the organotypic slice culture with PPAR- γ agonist & antagonist, DMSO vehicle and free drug medium.

The slices which were treated with agonist alongside antagonist were pre-treated with the antagonist alone, for 6 hours. The organotypic slices were allowed to grow for 5 weeks, and treatment started at the end of the fifth week for a week. The medium was changed every second day. Organotypic slices were prepared from the cortex and hippocampus of both the mutant and wild-type pups.

8. Results

This chapter is divided into two parts; validation of materials & methods and investigation of the role of PPAR- γ in preventing astrocyte activation. This study has provided further understanding of this receptor's influence in the reduction of neuronal cell death in the CNS.

8.1 Immunohistochemistry validation

8.1.1 Validation of GFAP marker to stain astrocytes of paraffin sections

The aim of this study was to detect astrocytes *in vitro*, using an organotypic slice culture. To achieve this, it was important to ensure that astrocytes are detected reliably *in vivo* and then *in vitro* using a Glial Fibrillary Acidic Protein (GFAP) marker. Paraffin-embedded brain tissues of mice and rats were prepared for this experiment. The rat brain sections have been employed as a positive control. A technical challenge was to improve the captured image, and to improve the access of the primary antibody into the cell, by varying the temperature to 25°C Celsius during this process. The underlying mechanism can be described as antigen retrieval, which facilitates the break of protein cross-links that have been formed by formalin during tissue fixation; thereby uncovering hidden antigenic sites. Result shows that GFAP is detectable with good signal-to-noise ratio in Figure 8-1.

Triplicate paraffin embedded sections were incubated at room temperature and compared to triplicates of paraffin embedded brain sections incubated at 4°C overnight. The results showed that this temperature difference had an impact on the detection of GFAP. There is increased intensity and clarity of astrocytes, as referred to (Figure 8-1, B) which represents incubation at 4°C overnight. This is in addition to a difference in the detection number of astrocytes which were more numerous, in favor of 4°C. To verify the integrity of the results, Figure 8-2 is showing a negative control staining in the presence and absence of primary antibody in rat brain paraffin section stained for GFAP (Thermo scientific).

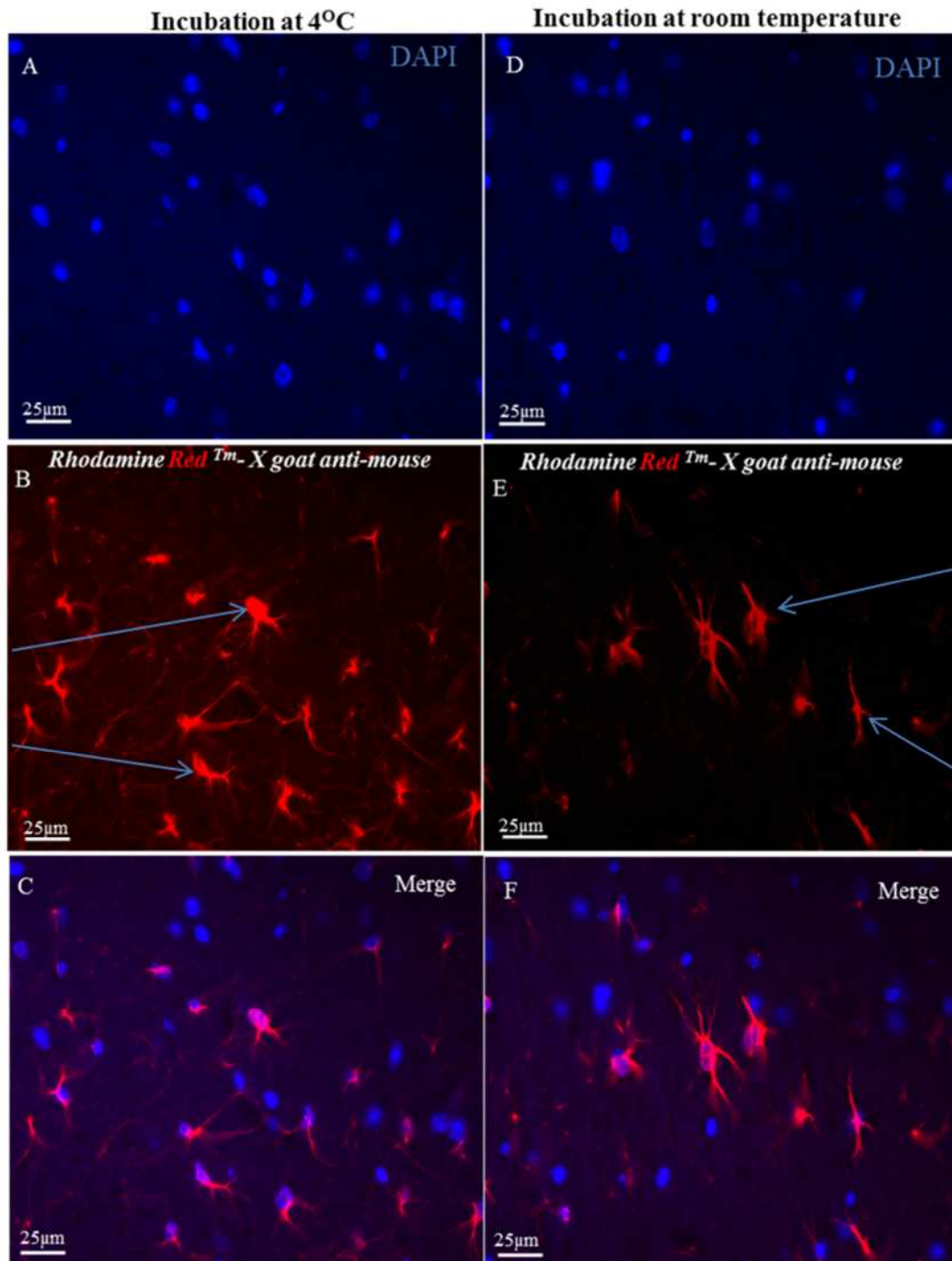


Figure 8-1 Rat brain paraffin section stained with GFAP (Thermo scientific).

A, B and C illustrate slices that were treated with a GFAP antibody and incubated over night at 4°C.; D and E: Slices were treated with a GFAP antibody and incubated over night at room temperature. The arrows refer to GFAP⁺ cells Magnification X63, scale bar 25 µm.

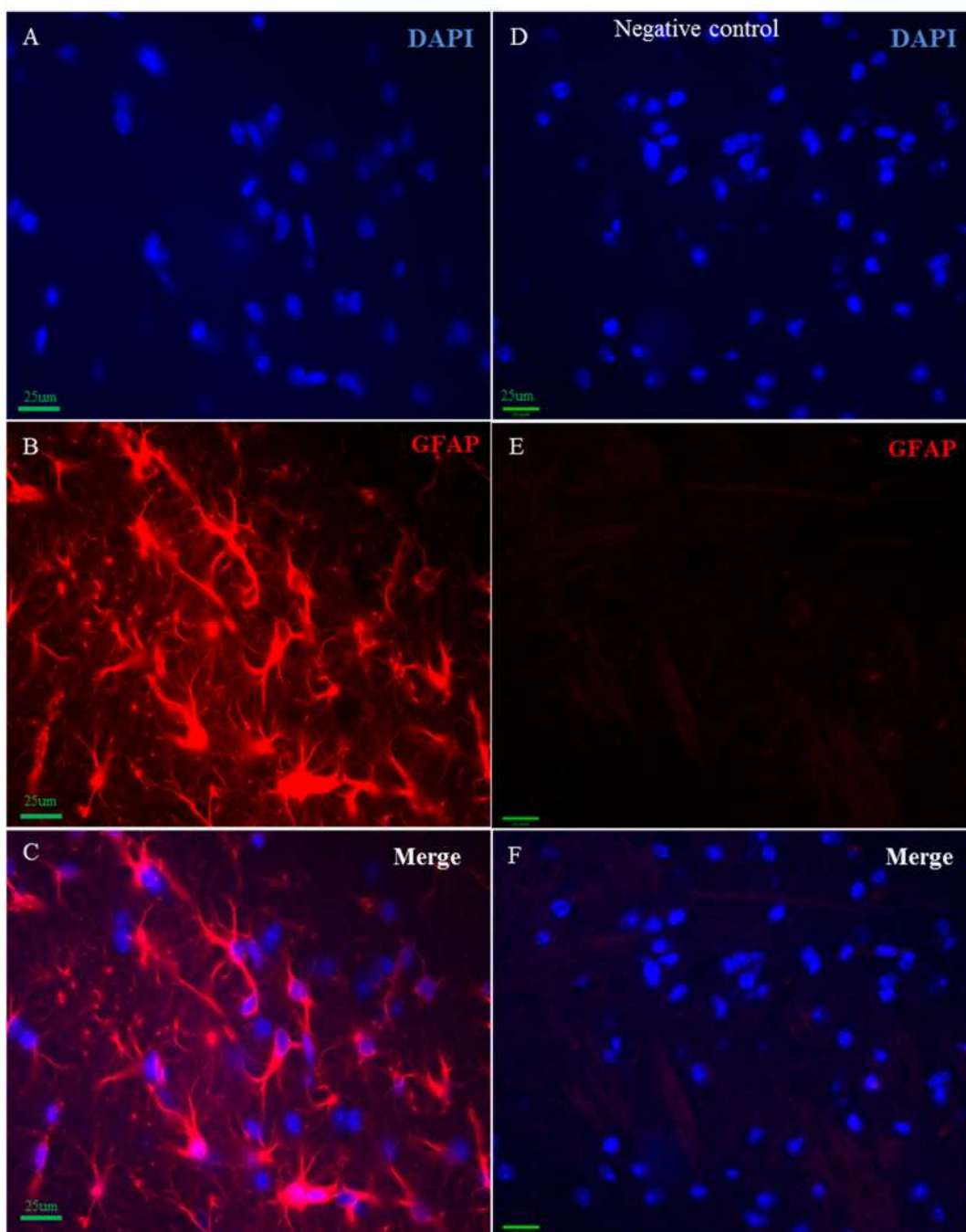


Figure 8-2 Verification of the negative control staining in the presence and absence of primary antibody in rat brain paraffin section stained for GFAP (Thermo scientific)..

The slides were incubated overnight with primary antibody at 4⁰C. A, B and C: slices were treated with a GFAP antibody and a fluorescent stain. D, E and F represent negative control of immunohistochemistry staining. Brain tissue stained without primary antibody show negative results Magnification X63, scale bar 25µm.

8.1.2 Optimising GFAP primary antibodies to stain astrocytes of rat and mouse paraffin sections

Previously, difficulties using immunohistochemistry in detecting astrocytes by using anti-GFAP have been experienced. Therefore, it was important to optimise the protocol by varying the source of primary antibodies to detect GFAP. The anti-GFAP reagents (GFAP - Astrocyte Marker from Abcam and GFAP antibody from Thermo Scientific) were purchased and checked. Three concentration ratios (1:100, 1:150 and 1:200) of the two reagents have been investigated. The incubation with the primary antibody was performed at 4°C, and the time of incubation with primary antibody was restricted to 18 hours. Paraffin embedded sections of rat brain tissues were used as a positive control. The anti-GFAP antibody from Thermo Scientific showed good results with a dilution ratio of 1:150 (Figure 8-3; A, B and C) whilst the antibody from Abcam required a 1:100 dilution to detect the astrocytes (Figure 8-3; D, E and F). However, using a dilution of 1:200, both antibodies gave rise to non-specific binding and false-positive results (data not shown). The primary antibody from Thermo Scientific gave a brighter fluorescent signal compared to the antibody from Abcam. This experiment also revealed that the antigen retrieval time must be not less than 40 -45 minutes.

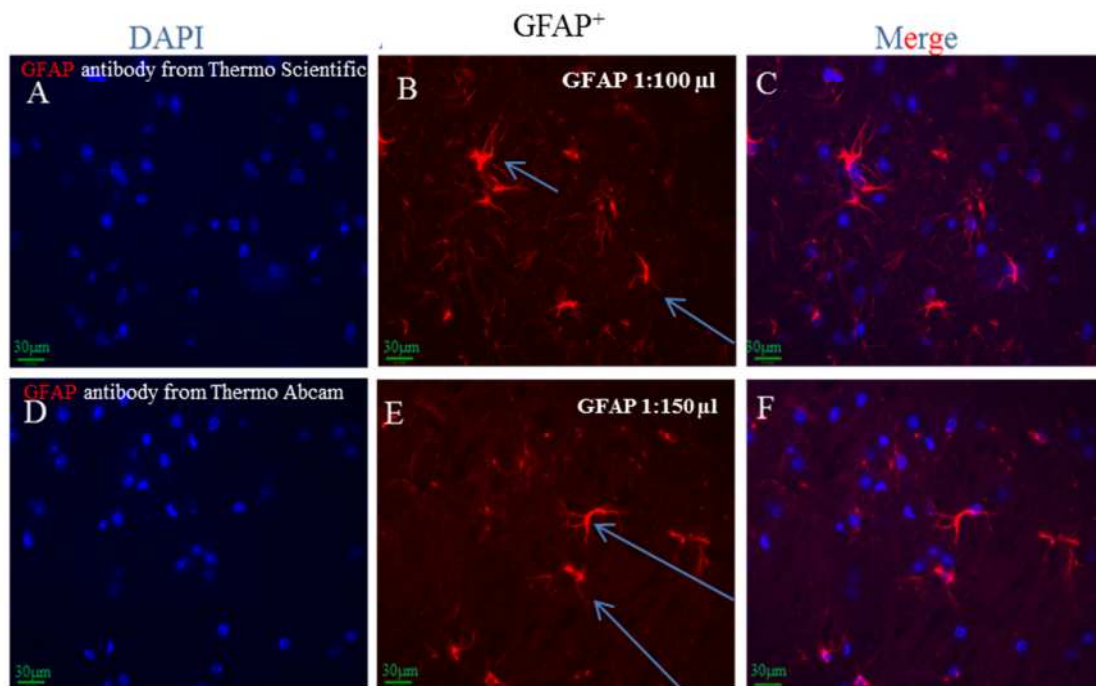


Figure 8-3 Rat brain paraffin embedded sections, illustrating astrocytes stained for GFAP from either Thermo scientific or Abcam.

The slides A, B and C represent astrocytes detection after overnight incubation (18 hr) at 4°C with primary antibody from (Thermo scientific). D, E and F show astrocytes detection after overnight incubation with primary antibody from (abcam). Arrows refer to differences in astrocytes brightness. The tissues were stained with GFAP antibody by fluorescent immunohistochemistry staining. Micrographs have been captured with DMRB microscope Magnification X63, scale bar = 100 pixels (1 pixel = 0.3 µm).

8.1.3 Examining the impact of gasket thickness on clarity of image resolution for organotypic slice cultures

To avoid coverslip pressure damage to the organotypic slice cultures during mounting for microscopy, it was necessary to use a gasket that serves as a bridge between the coverslip and the organotypic slice to protect it from damage. It was necessary to discover the exact gasket thickness that would provide protection and still retain a minimal working distance from the objective lens. Paraffin embedded brain sections were prepared with and without the gasket to investigate the effect of the gasket on micrograph clarity. As in Figure (8-4; B), immunohistochemistry protocols gave clear and reliable results without gaskets. With gaskets the astrocyte resolution was lower as you can see in Figure (8-4; A). However, to avoid any chance of altering the slice morphology by coverslip pressure it was decided to use gaskets of thickness 0.25 mm. A justification of this decision is that the slice thins down from 300 μm to approximately 150 μm after the culture period.

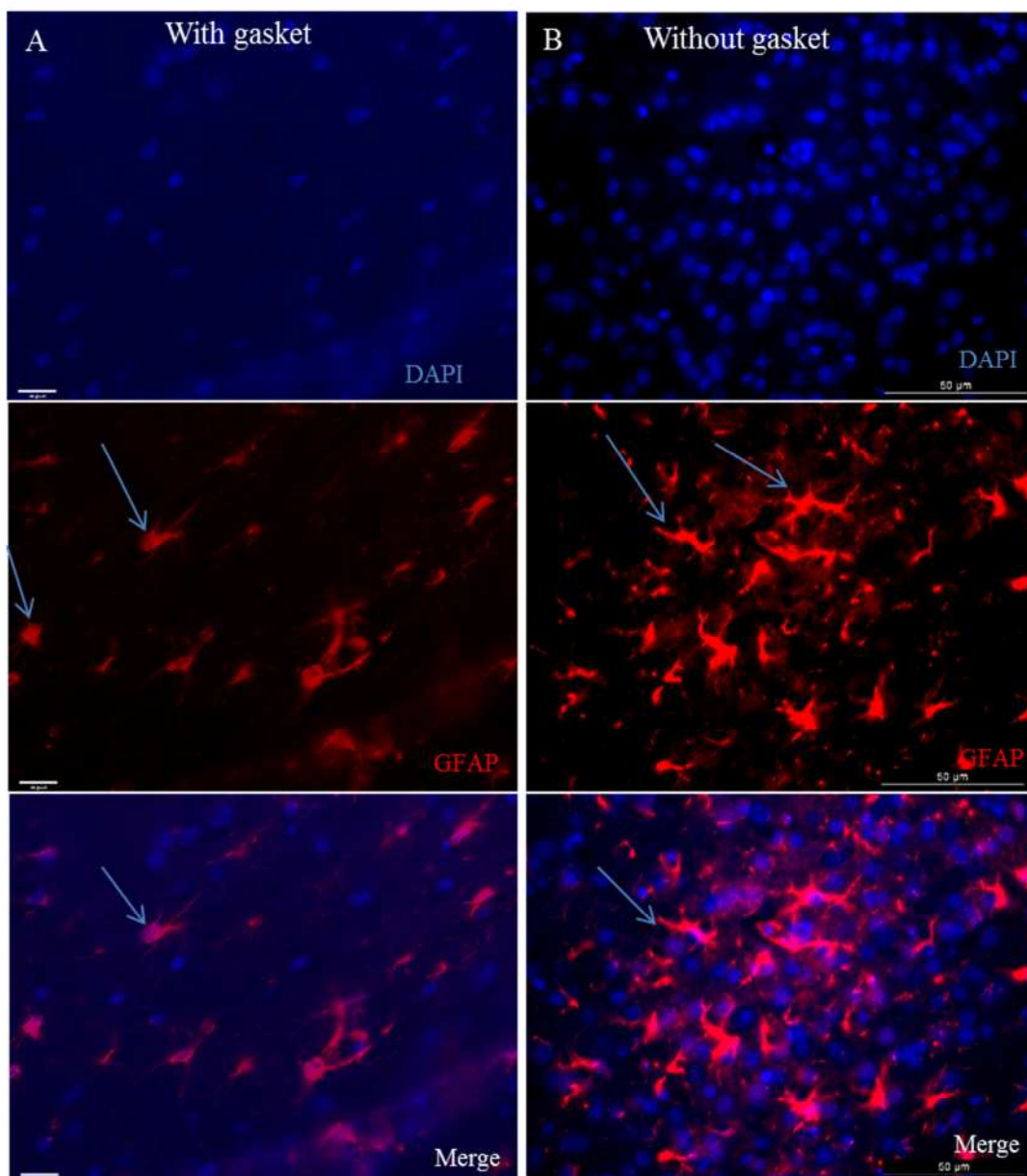


Figure 8-4 Examining the impact of gasket thickness on clarity of image resolution.

The figure shows slides prepared from male C57 black 6 mouse brain aged 1-2 days. The figure displays nuclei detected with DAPI and the astrocytes detected with Rhodamine™ red. The micrographs revealed a fluorescent image with and without use of the gasket. Column A shows astrocytes in the presence of the gasket; the cells can be seen, but with less clarity. Column B shows astrocytes without a gasket, and the cells can be seen in a good resolution, with more refined micrographs. Arrows refer to GFAP⁺ cells. The micrographs were taken with DMRB fluorescence HAMAMATUS digital Camera C4742-95, magnification X40.

8.2.1 The differences between the staining of astrocytes in the brains of mice between fluorescent with fluorescent Rhodamine and DAB markers

Preliminary results obtained when the astrocytes were stained with fluorescent Rhodamine red revealed the difficulty in counting the astrocytes, especially in the dentate gyrus of hippocampus. This is in addition to the already mentioned loss of clarity due to gasket thickness. Paraffin embedded sections of brain tissues were prepared from either wild-type or mutant 2 week old mice. The reason for using these age groups in particular, is that the astrocyte proliferation still low between wild-type and mutant pups, which might facilitate the comparison. The slides were stained either with M.O.MTM kit followed by DAB, or rhodamine red. After incubation the sections were incubated in primary antibody against GFAP, and then secondary antibody – a biotinylated anti-mouse IgG. The avidin of the biotinylated enzyme complex (ABC) was then added, which bound to the biotinylated secondary antibody. The incubation with a substrate for the enzyme generated a brown color, resulting from DAB breakdown (Figures 8-5; B & 8-6; B). For Rhodamine red, a fluorescent marker conjugated to a secondary antibody was applied after the primary GFAP antibody for 1 hour followed by washing several times with PBS to remove unbound antibodies. DAPI stain was added then washed with PBS then 5 μ l mounting medium was added, and the slide sealed with nail varnish (Figures 8-5; A & 8-6; A). Both protocols are more fully described in the appendices. The results revealed that both staining regimes are acceptable, but it was decided that the DAB stain was more appropriate, as it made it easier to identify astrocytes in the hippocampal area, particularly the dentate gyrus. The staining is also more stable after the procedure. Figure 8-6 displays the comparisons of the two stains in three different areas of interest. Astrocytes labeled with DAB are more clearly distinguishable in the cortical areas.

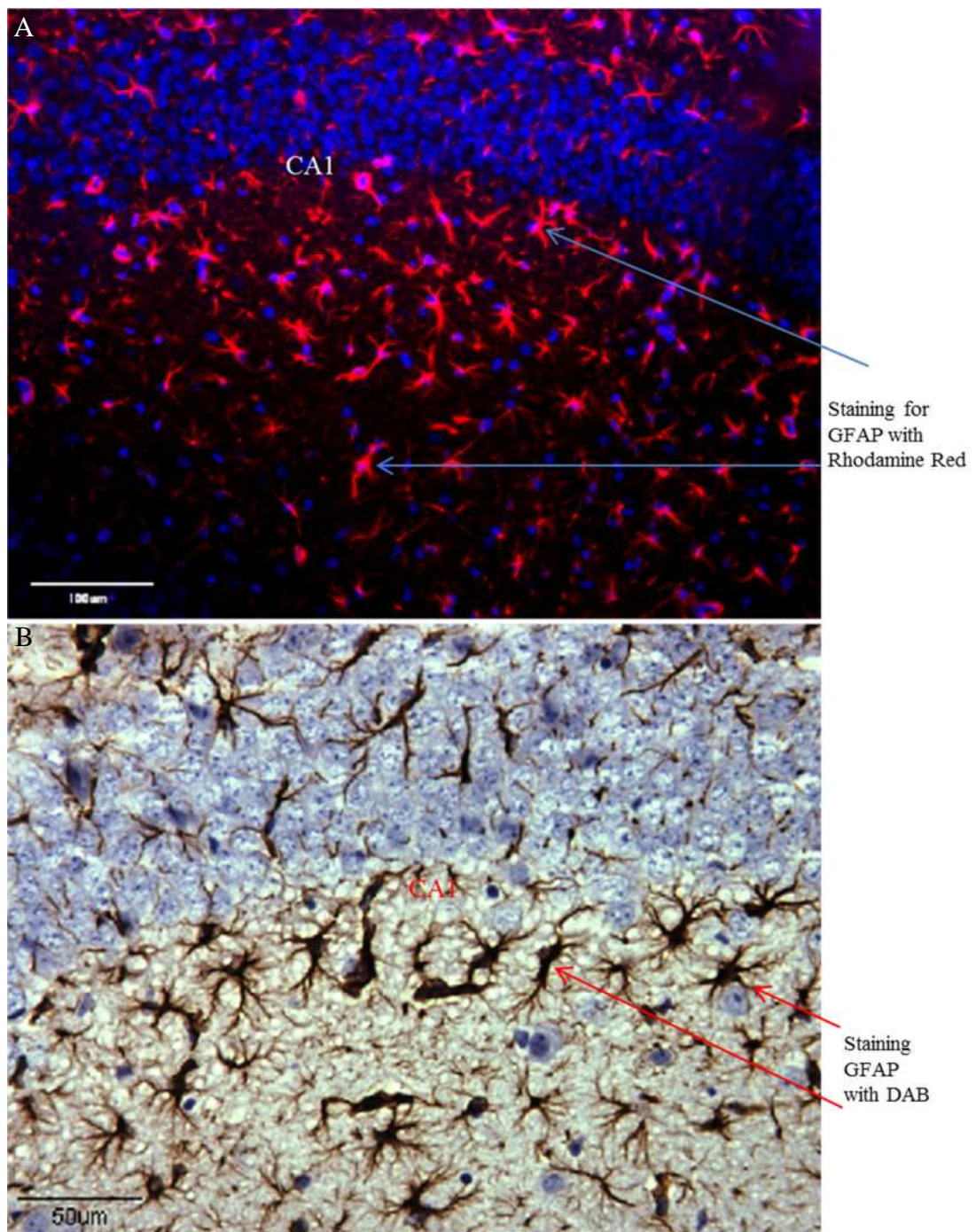


Figure 8-5 Comparing astrocyte detection by using fluorescence and DAB stains in the CA1 layer of hippocampus.

There is a less clearly defined border of astrocytes in micrograph A, while it is clearly defined in micrograph B. Both micrographs were captured at magnification X20.

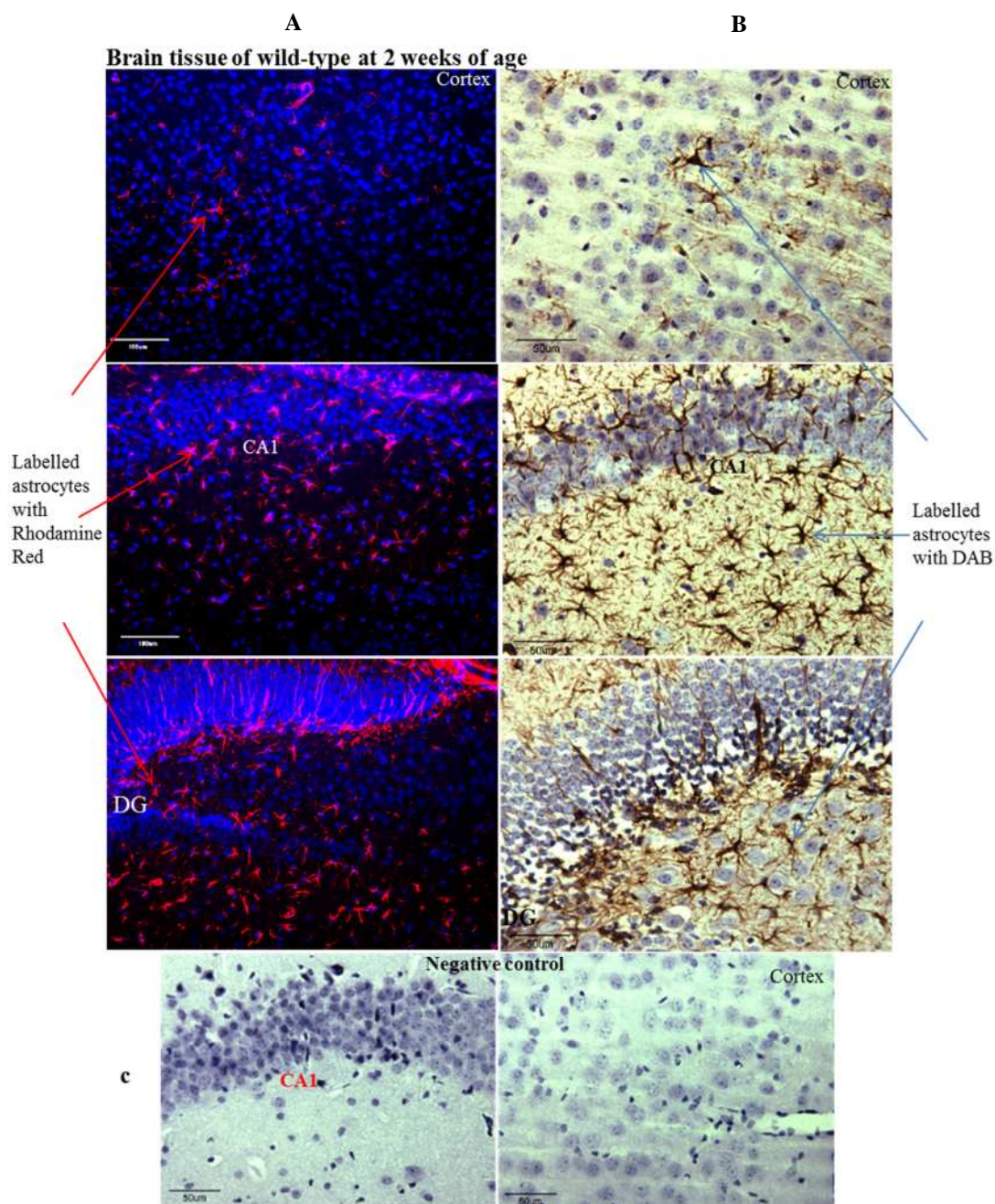


Figure 8-6 Comparison of astrocytes detection by using fluorescence or DAB stains in three different regions.

Paraffin embedded brain tissue sections were harvested from wild-type 2 week old mice that. 3 slides were used with each stain. The arrows point to labelled astrocytes with the two different stains. Micrograph C: slides underwent the immunohistochemistry protocol without primary antibody. Micrographs were captured with DMRI fluorescent microscope and light microscope. The magnification is X20

8.3.1 Determining the genotype of mouse pups

Before proceeding with culturing the organotypic slices, it was necessary to identify mutant and wild type pups, using PCR analysis. The genomic DNA from the tails of the mice was extracted using DNARELEASE™ and the lysis 20 PCR program. This was followed by PCR amplification (see materials and methods section 7-2-6). 9 µl of PCR product was taken from each sample and loaded onto 3% agarose gels, which were run at 145 V and 400 mA for 30 minutes. PCR bands for Cre recombinase and S4 proteasomal subunit genes were detected by using a UV trans-illuminator (Figure 8.7). The gels revealed a single band of both genes for the animals, indicating a floxed S4 gene, which could be targeted and inactivated by Cre recombinase in the forebrain region i.e. animals numbered 2, 6 and 7 are mutants, while the others are wild type and used as a controls.

Three control and mutant pups were used for organotypic slice cultures; they were scarified and their brains were dissected immediately.

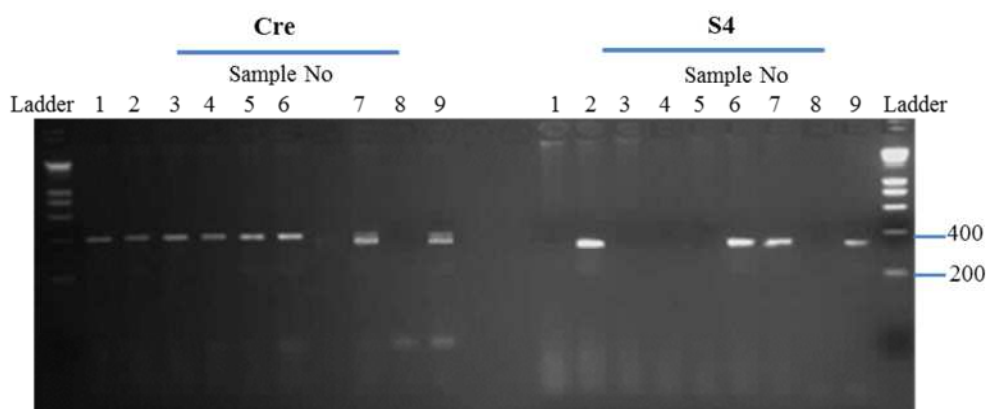


Figure 8-7 Representative image of Psmc1 and Cre genotyping, following agarose electrophoresis. Bands were detected using a UV trans-illuminator.

Tissue biopsies were obtained from the mouse tails for the DNA genotyping of 9 pups.

8.4.1 Astrocyte detection in organotypic slice cultures technique

The antibodies used against the GFAP antigen in the paraffin embedded sections were successful, allowing easy detection of the astrocytes. This was an important step before commencing immunohistochemistry *in vitro*. Organotypic slice cultures were prepared at either 300 or 400 μm , from new-born (postnatal) mice aged three to five days old. The brain tissue slices were cultured for two to six weeks, according to the protocol in Materials and Methods section 7-2-3. Slices were observed daily with the medium changed every 48 hours. Figure 8-8 shows that the maintenance of slice integrity remained unaffected. After 24 hours of culture, the cells were in healthy condition, which continued after two weeks of culture. The organotypic slices were derived from mutant and wild-type pups.



Figure 8-8 Maintenance of slice integrity remains unaffected for up to 2 weeks.

Organotypic slice cultures were harvested from postnatal wild-type and mutant pups. The slices were cultured for up to 6 weeks. A & B organotypic slice cultures after 24 hours of culturing. C & D: the slices were fixed at 2 weeks of age before immunohistochemistry was performed. The medium was changed every 48 hours, and the images show the organotypic slices in good health. The micrographs are captured with Olympus CKX41 camera. Magnification X 10.

The purpose of this experiment was to detect astrocytes and as a result, find the most suitable of the two thicknesses tested. After two weeks of culture, the slices of the first age group were fixed for 20 minutes in 4% PFA, followed by four gentle washings with PBS to avoid separation of brain tissue from the membrane. All following steps were performed in cavity slides as shown in section (7-2-3). The slices underwent permeabilisation and were then blocked in 5% BSA for 2 hours at room temperature, as described in the materials and methods (7-2-4). The cavity slide was changed for a normal slide at the last stage of the protocol, provided with gaskets (frames) of 0.25 mm thickness 0.25 mm. Frames were used as gaskets for protection of the organotypic slices against pressure of the coverslips. Results show that astrocytes are detectable at 300 μm thickness in both wild-type and mutant animals at two weeks of age, viewed in Figure 8-9. It is worthwhile to mention that after a few weeks in culture the slices thinned down to less than the gasket thickness of 250 μm . Although both thicknesses can be used to detect astrocytes, less thickness gives better clarity (data not shown). It is clear that astrocytes appear contracted in the wild-type slices (Figure 8-9; B), while astrocyte processes appear longer and more branched in the mutant brain slices (Figure 8-9; E).

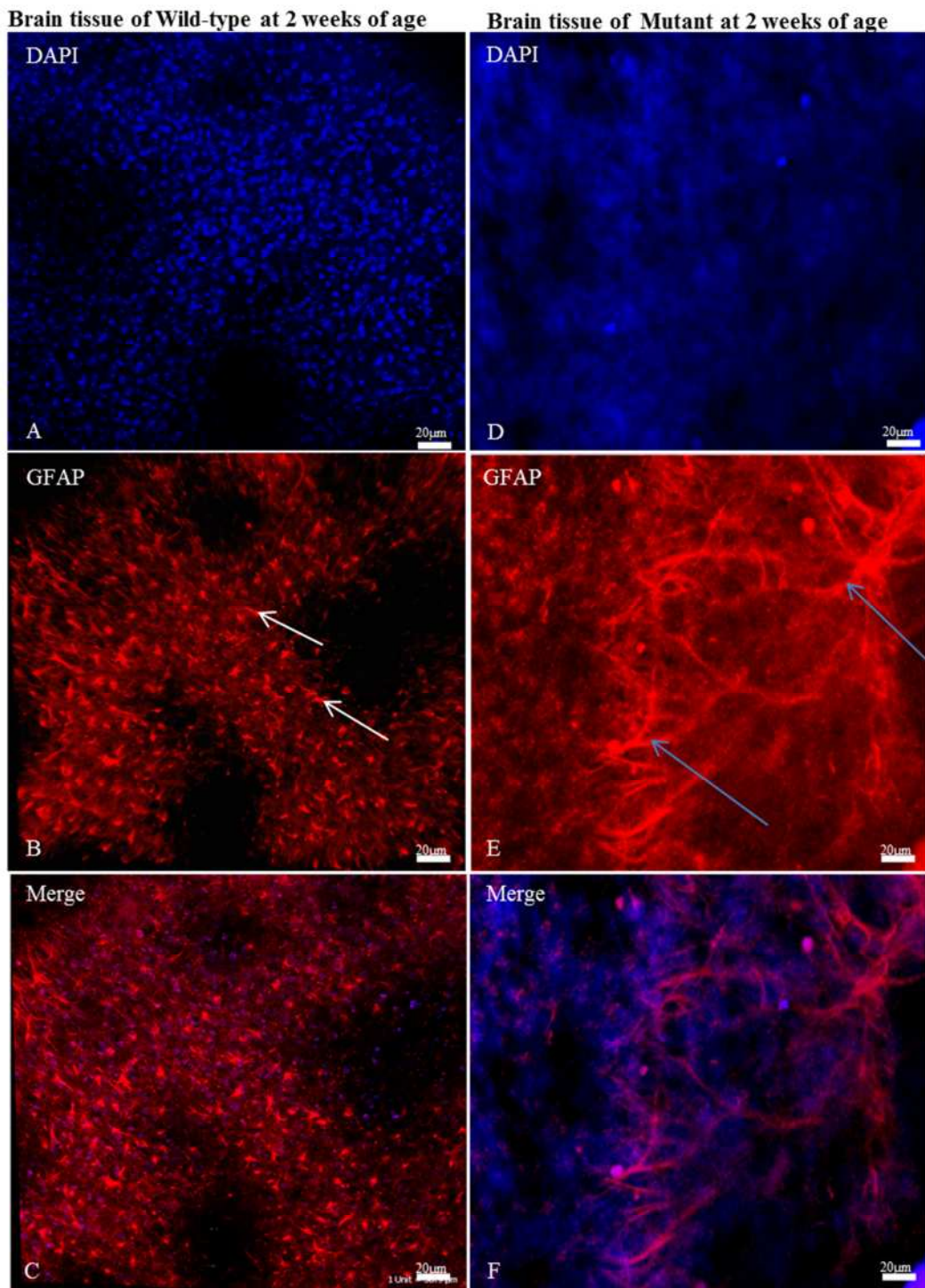


Figure 8-9 Detection of astrocytes using immunohistochemistry in slices cultured for 2 weeks. Confocal images of organotypic slice cultures were taken of both wild-type and mutant pups. B; White arrows indicate contracted astrocytes in brain tissue of wild-type animals. E; blue arrows referred to long processes of astrocytes in mutant animals. The micrographs were captured with confocal DMIRE microscope (Leica SP2). Magnification X 20.

8.4.2 Optimisations to improve immunohistochemical protocol

In order to enhance the morphological characteristics of organotypic slice cultures, several optimisations have been conducted. The stages of the optimisation can be summed up in three points: permeabilisation, blocking non-specific binding and the thickness of slices. To amend the permeabilisation step, the concentration of TritonX-100 was changed from 0.1% to 0.5%. In addition, the time of incubation was extended, from two hours to overnight. Originally, 5% bovine serum albumin with 0.1% TritonX-100 in PBS was used in the blocking procedure, which was changed to 10% of BSA with 0.5% Triton X-100 in PBS and incubated overnight, rather than for two hours. The optimal thickness of slice culture was 200- 250 μm . Following the above protocol precisely resulted in good quality images as seen in Figure 8-10. The result confirmed that the detection system works with good signal-to-noise ratio. The astrocyte and their nuclei are clear; however there is no difference in astrocytes number between control and mutant slices, which was expected in this early age.

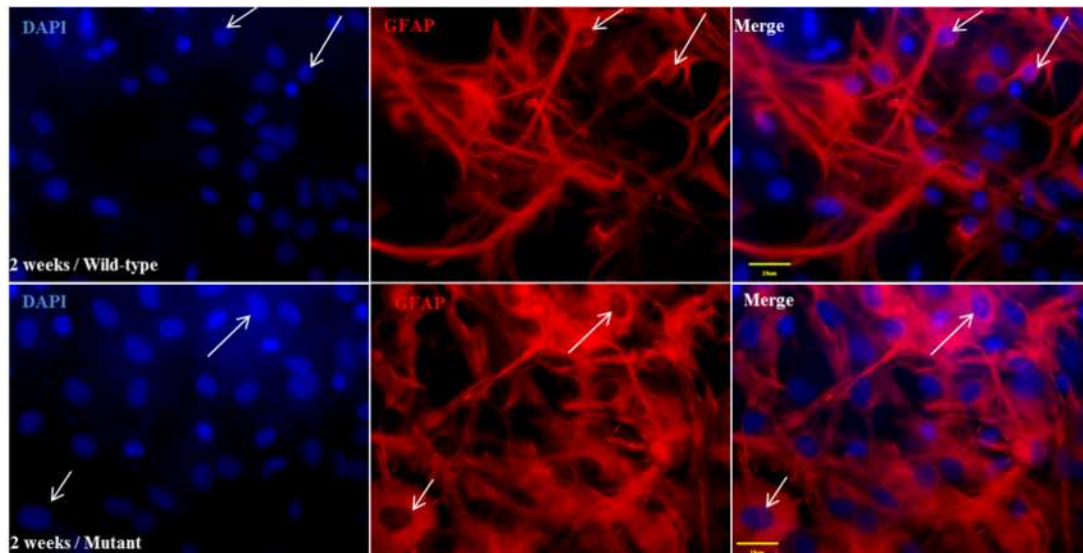


Figure 8-10 Immunohistochemical detection of GFAP after amended permeabilization and blocking stages.

Organotypic slice cultures of wild-type and mutant pups were prepared from animals at age 4-5 days and cultured for 2 weeks. The slices were fixed in 4% PFA, and then immunohistochemistry performed. Arrows indicate some nuclei of astrocytes, each one of them representing a single astrocyte body. Micrographs were captured with DMRB Fluorescence Microscope Luca^{EM}, magnification X63, scale bar 25 μm .

8.4.3 Validation of the use organotypic slice cultures to observe astrocytes, and detect proliferation.

To assess pathological injury in the brains of mice, and ultimately investigate whether the development of gliosis was comparable *in vitro* and *in vivo*, organotypic brain slices were cultured for 2, 3, 4, 5 and 6 weeks. The slices were harvested from brains of mutant and wild-type postnatal mice aged 3-4 days. Brain tissues were sliced at 250 μm thickness and cultured then fixed with 4% PFA for 20 minutes according to target ages. Immunohistochemistry was performed using anti-GFAP antibody and Rhodamine RedTM. The results showed that at all ages, gliosis was detectable under both ordinary fluorescent or confocal microscopy. Interestingly, it was observed that nuclei from the astrocytes in the mutant brains were different from those in the control animals. The astrocyte nuclei in the controls looked smaller in weeks 2, 3, and 4, but became identical during the fifth and sixth week. Additionally, they adopted an oval form in the mutants while remaining spherical in the wild-type slices (it can be seen in Figures 8-11 to.8-15).

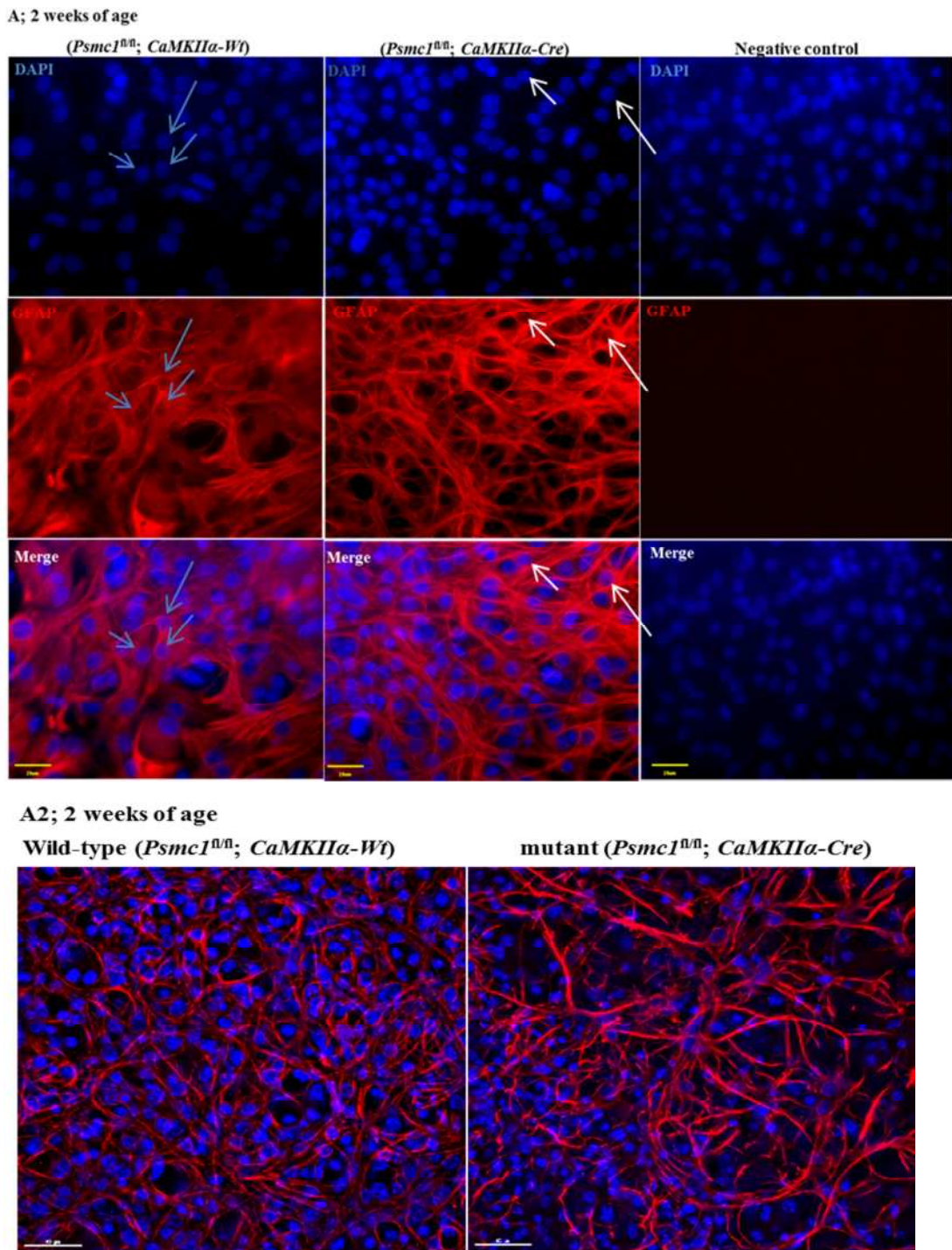


Figure 8-11 Organotypic slice cultures of mutant and wild-type mice at 2 weeks of age.

A1; Brain slices from mice at two weeks of age were grown in an organotypic slice culture system. Slices were fixed and left for 24 hours in PBS at 4°C, and immunohistochemistry performed using anti- **GFAP** antibody. Two different microscopes ordinary fluorescent (A) and confocal (A2) were used to see if there was any difference in the cells. Use of the ordinary microscope was suggested. A1; Micrographs were captured by ordinary fluorescent microscope. The blue arrows indicate examples of single body's of astrocytes and its nucleus in control animals, while white arrows represent the same cells in mutant slices (magnification 63X). A2 shows the same slices under examination using a confocal microscope, **GFAP** in red and **DAPI** in blue at magnification X40.

The following micrographs (Figure 8-12) show that after three weeks of culture, astrocytes are detectable. Note that the nuclei in wild-type brain slices are circular and appear almost twice size of those in the mutant brain slices (blue circle; Figure 8-12) which are small in size and are oval in shape (white circle; Figure 8-12).

B; 3 weeks of age

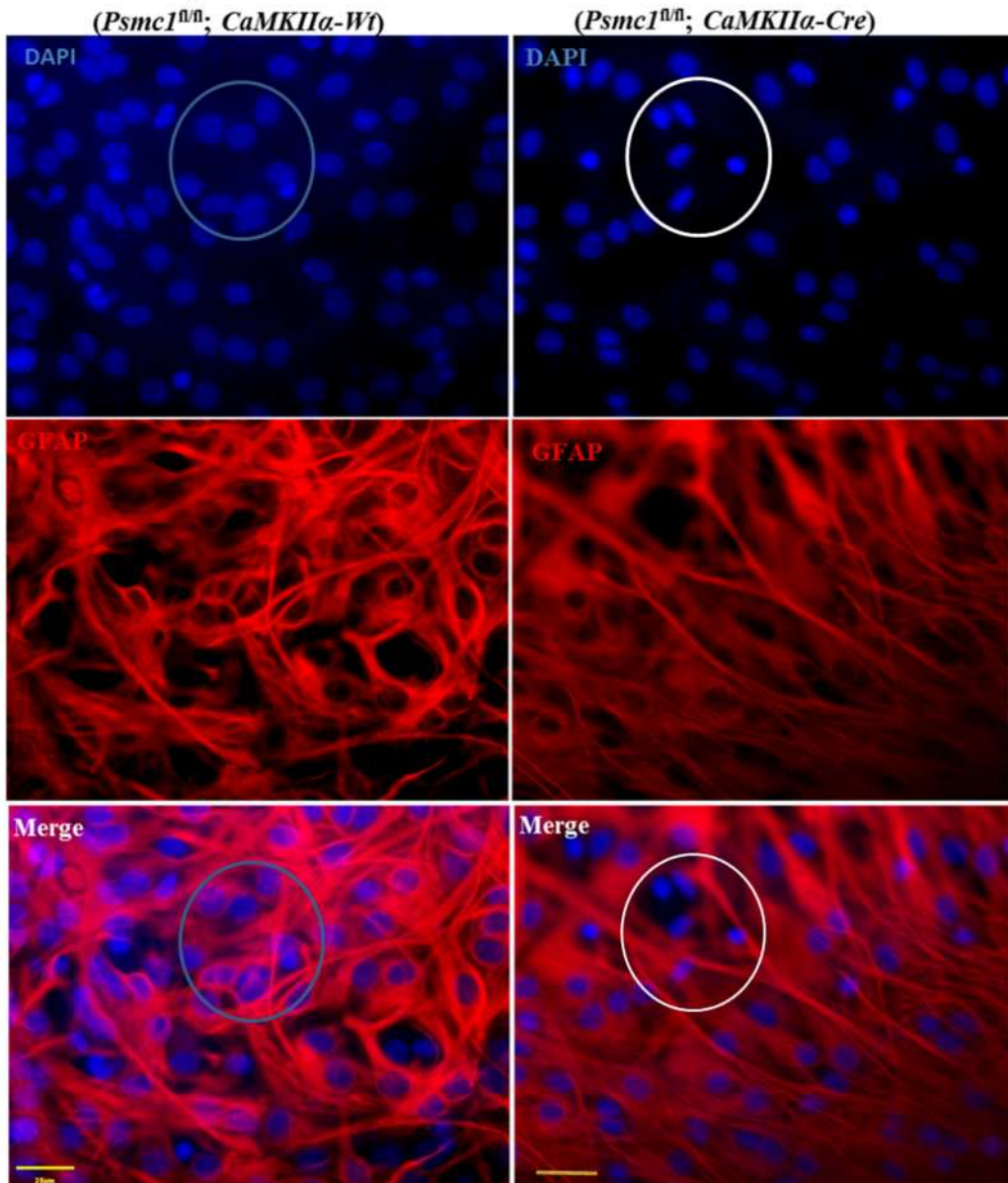


Figure 8-12 Organotypic slice cultures of mutant and wild-type mice at 3 weeks of age.

B; Mouse brain sections were grown in an organotypic slice culture system. Immunohistochemistry was performed using anti-GFAP and Rodamine Red marker. In the third week, it is difficult to note whether there is a difference in the number of astrocytes between mutant and control cultures. Micrographs were captured by ordinary fluorescent microscope at magnification 63X, scale bar 25μm.

Astrocytes were detectable after week four of culture. In wild-type slice cultures, nuclei were still round in shape and larger (see blue circle in Figure 8-13) than those in mutants slice cultures (see white circle in Figure 8-13). At this age of culture it suggests that the number of astrocytes is increasing in the mutant cultures.

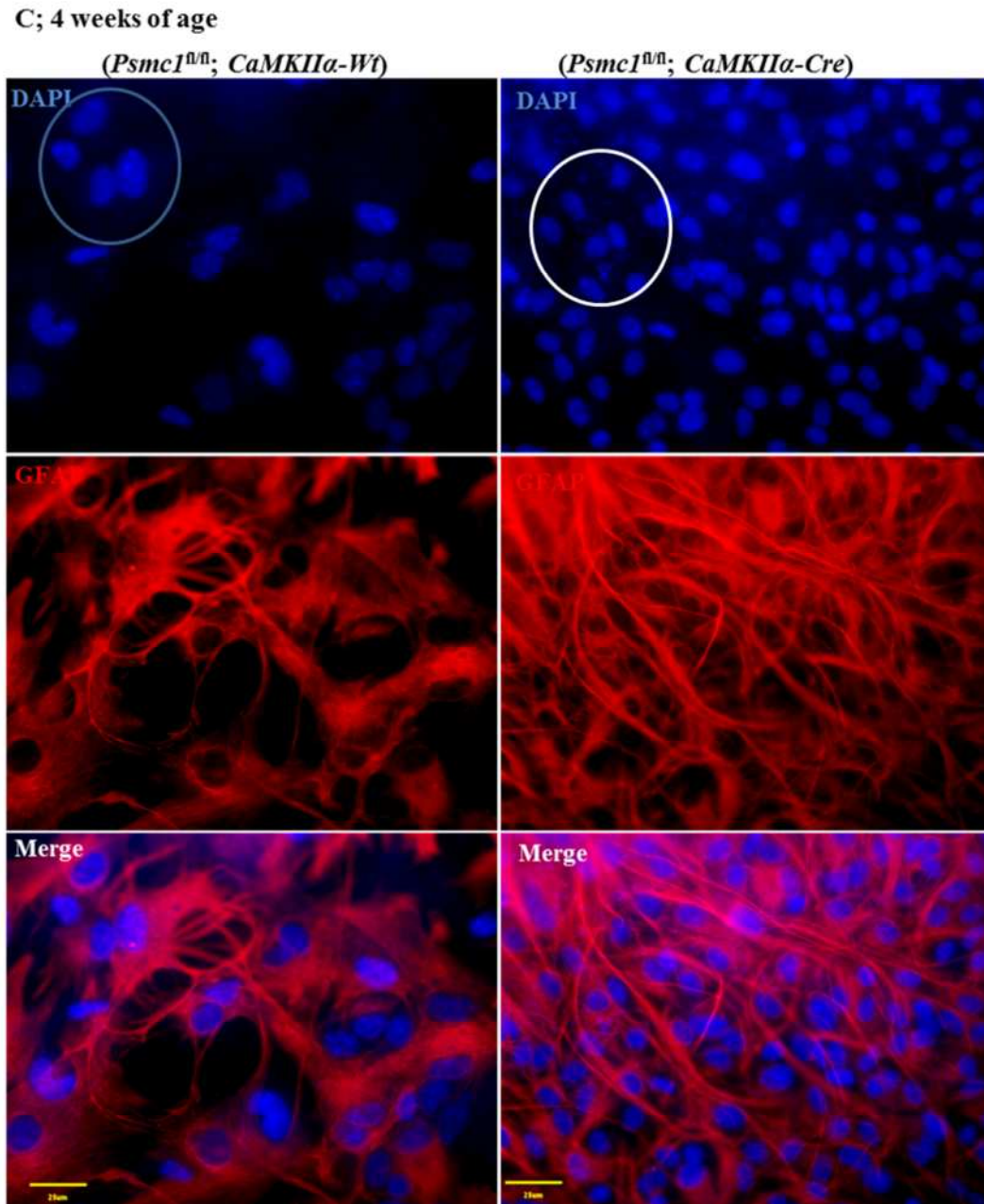


Figure 8-13 Organotypic slice cultures of brains from mutant and wild-type mice at 4 weeks of age.

C; Mouse brain sections at four weeks of age were grown in an organotypic slice culture system. Immunohistochemistry performed using anti-GFAP antibodies and Rodamine Red marker. As you can see in the merged micrographs, the numbers of astrocytes increased at this age of culture in mutant slices, compared to control cultures. Micrographs were captured by ordinary fluorescent microscope at magnification 63X.

Astrocytes during the fifth week of culture were also detectable, as the difference in the size of the nuclei between mutant and wild type slices still exists. The differences however, do slowly decline (Figure 8-14).

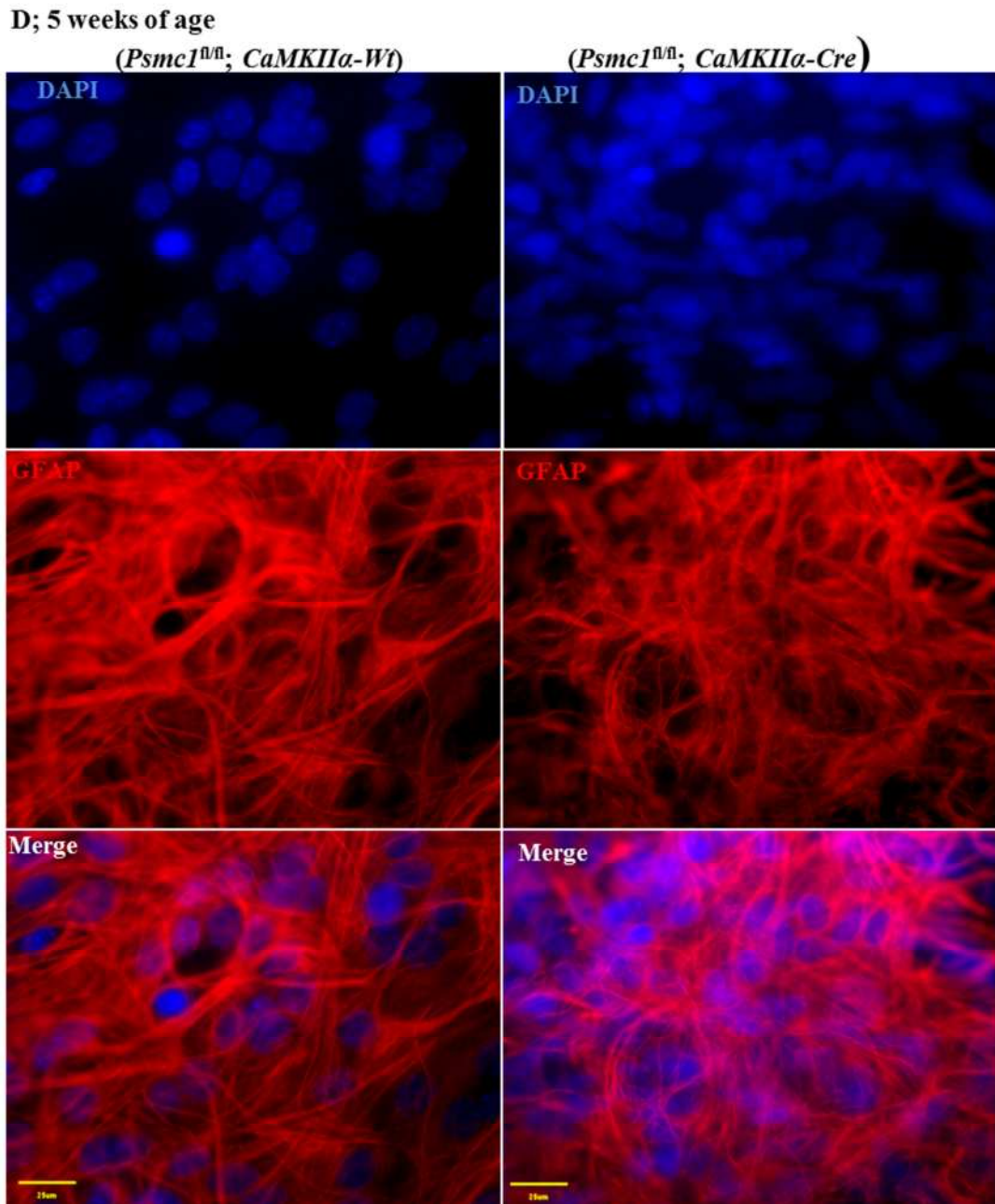


Figure 8-14 Organotypic slice cultures of brains from mutant and wild-type mice at 5 weeks of age.

D; Mouse brain sections at weeks five of age were grown in an organotypic slice culture system. Immunohistochemistry performed using anti-GFAP antibodies and Rodamine Red marker. The micrographs show that there is still a difference in the size of the nuclei between the mutant and wild-type sections, although the magnitude of this difference is declining. Micrographs were captured by ordinary fluorescent microscope at magnification 63X.

One of the most important goals of the study was to investigate whether the slice culture of mutant mice can be cultured up to six weeks (Figure 8-15). Interestingly, by the end of culture week six the nuclei of both mutant and control cultures were found to be of similar size and shape, contrary to what was seen at five weeks in culture.

E; 6 weeks of age

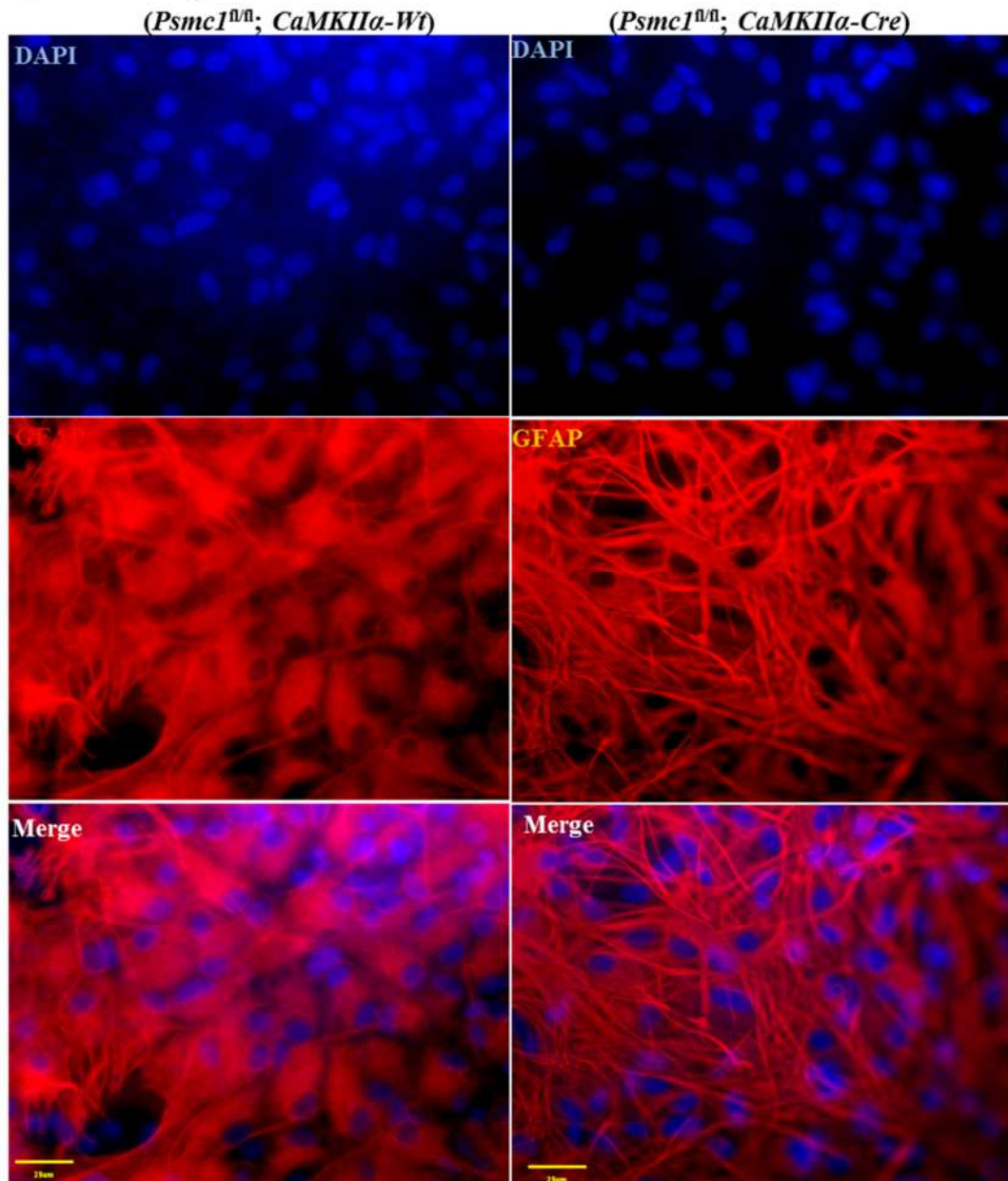


Figure 8-15 Organotypic slice cultures of brain from mutant and wild-type mice at 6 weeks of age.

E; Mouse brain sections at six weeks of age were grown in an organotypic slice culture system. Immunohistochemistry was performed using anti-GFAP antibodies and Rodamine Red marker. Micrographs show comparisons between the nuclei in control and mutant samples, where the nuclei are similar in size and shape. Micrographs were captured by ordinary fluorescent microscope at magnification 63X.

8.5.1 Creating cryostat and paraffin sections from organotypic slice culture

After seeding the organotypic slice cultures for 2 – 6 weeks and fixing at target ages, paraffin and cryostat sections were prepared from control and mutant samples. 5 - 8 slides were obtained, at a section thickness of 8 μm , from each organotypic slice. Immunohistochemistry was performed using anti-GFAP antibodies and Rhodamine Red marker. Astrocytes are clearly detectable in the cryostat sections. The number of astrocytes gradually increased over the period from 4 to 6 weeks (Figure 8-16 & 8-17). However at weeks two and three the difference in astrocyte density is not clear between wild-type and mutant cultures (see Figure 8-16).

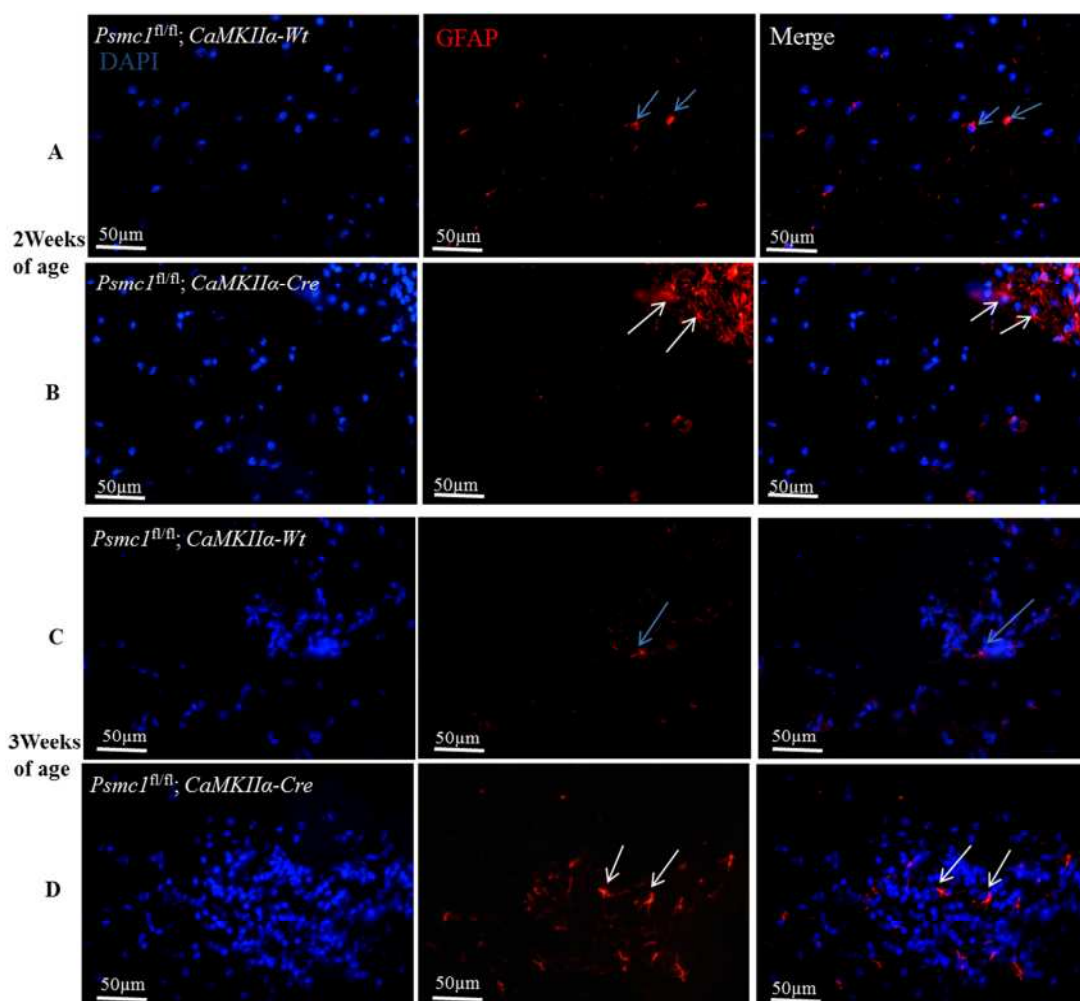


Figure 8-16 Cryostat and paraffin sections of brains created from organotypic brain slice cultures from mutant and wild-type mice at ages 2 and 3 weeks.

Slices were fixed after 2 and 3 weeks of culture. Astrocytes were labeled with Rhodamine RedTM using the immunohistochemistry technique. Micrographs A & C represent cryostat sections created from organotypic slices were harvested from wild-type mice. B & D show micrographs illustrating sections that were harvested from mutant mouse brains. Blue arrows show examples of astrocytes that were detected in the control samples, while **white** arrows indicate astrocytes detected in mutant samples. The differences between the astrocyte density is not clear between control and mutant sections at both week 2 and three of the cultures. Magnification is X20.

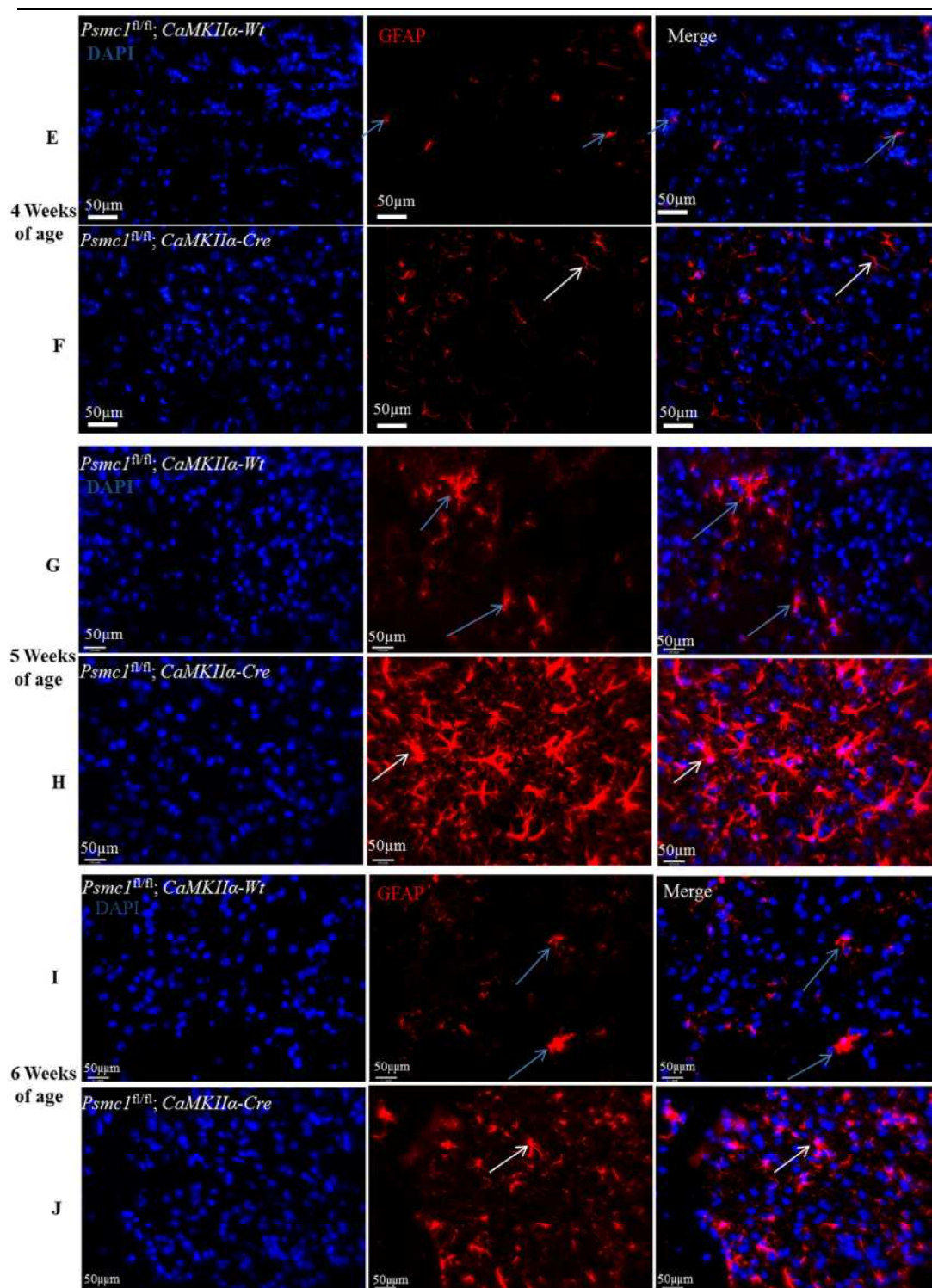


Figure 8-17 Cryostat sections of mice brains were created from organotypic slice cultures at 4, 5 and 6 wks.

Slices were fixed after 4, 5 and 6 weeks of culture. Micrographs E, G and I represent cryostat sections generated from organotypic cultures from wild-type mouse brain. F, H and J were harvested from mutant mouse brain organotypic slice cultures. Blue arrows indicate examples of astrocytes detected in the control samples, and white arrows indicate astrocytes found in mutant samples. There is a higher astrocyte density in the mutant samples, compared to the control samples. Magnification is X20.

Paraffin sections were created from organotypic slice cultures to see whether it was possible to improve the detection of astrocytes using a chromogenic stain. This was particularly important, to enable quantification of astrocyte density from the images, as the fluorescent stain is labile. Paraffin sections were prepared from slice culture from mice aged 2 weeks, stained and labelled with DAB (Figure 8-18). Figure A represents brain tissue of a wild-type mouse. Figure B represents brain tissue of a mutant mouse. The astrocytes were labelled in brown and the nuclei in blue. The results show that both cryostat (Figures 8-16 and 8-17) and paraffin embedded sections (Figure 8-18) can be used. DAB labelling will be used in the next experiments, as this staining enables a better ability to distinguish between astrocytes morphology and their borders, especially in the dentate gyrus region.

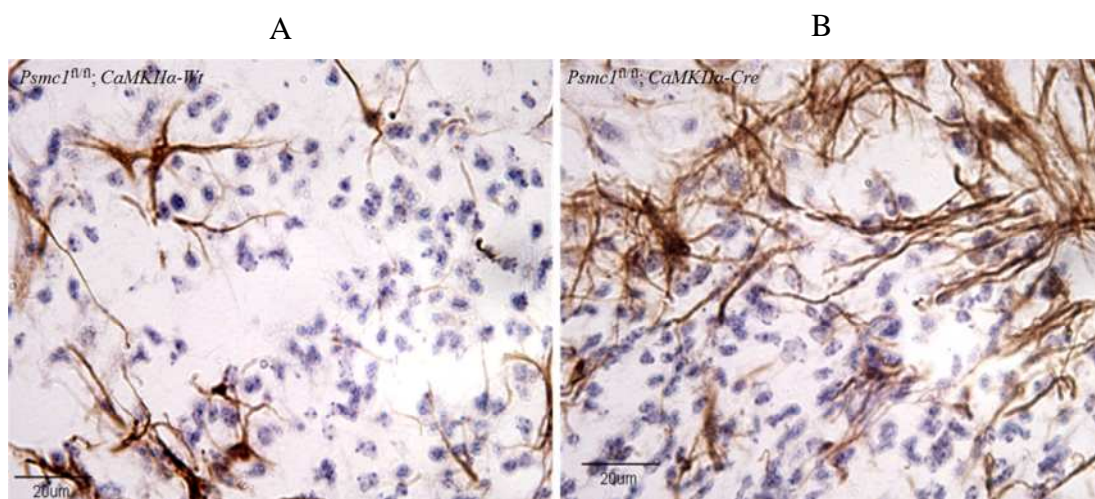


Figure 8-18 Paraffin sections of mutant and wild-type mouse brains created from organotypic slice cultures at 2 weeks of culture.

A; brain tissue of a wild-type mouse, B; brain tissue of a mutant mouse. The astrocytes revealed in brown colour and the nuclei in blue. Magnification is 50 X.

8.5.2 Morphology of brain tissue in paraffin sections using haematoxylin and eosin staining

Haematoxylin and eosin staining is commonly used in histology (Schwartz, Bukshpan et al.). It has been used in this study to determine the structure of the hippocampus and cortex in paraffin wax sections. 5 different thicknesses (5, 6, 7, 8 and 10 μm) were examined to determine which are the most stable on the slide, as they are small. All thicknesses were examined (data not shown). The 8 μm thick coronal slice was chosen as it showed good stability on APES coated slides, in addition to illustrating sufficient penetration by antibodies and markers. All sections were collected and every 11th section was selected for H&E staining. Approximately 16 – 20 slides were obtained for morphometric measurement. The slides were checked under a light microscope to compare morphology between control and mutant tissue within the same age group. Subsequent micrographs (Figure 8-19) showed regions of the cortex and hippocampus in the brains of control and mutant mice at 2 weeks old.

Images showed the size and area chosen, and all astrocytes in this area were counted for each section. For all ages, immunohistochemistry was performed to obtain *in vivo* results. Three random areas were counted in both the cortex and hippocampus (2 CA1, 1 CA2 and 1 CA3) and then the DG zone. Three samples from three different animals would be used.

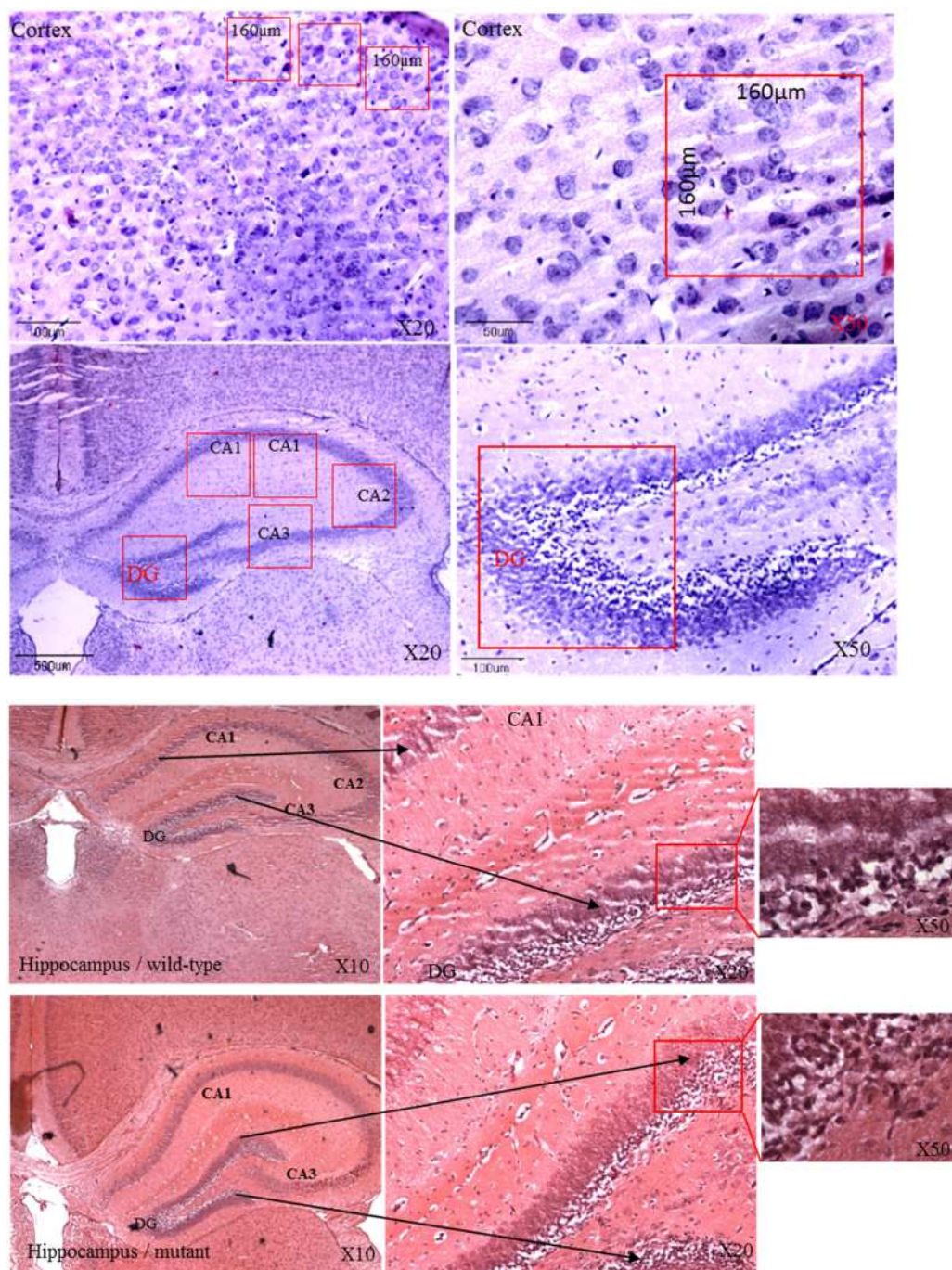


Figure 8-19 Coronal hematoxylin and eosin stained section through the cortex (CTX) and hippocampus.

Micrographs show morphology of wild-type and mutant mouse brain slices at 2 weeks old. Red squares indicate zones in which the number of astrocytes was counted after subsequent immunohistochemical stain. The tissues were sliced at 8 µm thicknesses and shown at magnifications X10, X20 and X 50.

8.6 Neurodegenerative disease

8.6.1 Progression of neurological disease *in vivo*

In order to monitor the progression of disease in the brains of *Psmc1^{fl/fl}; CaMKII α -Cre* (mutant) mice *in vivo*, a set of slides was prepared from each age group, including mutant and control samples. The slides were selected according to the results from H & E staining. An immunohistochemistry technique was used for the detection of astrocytes. However the antigen retrieval time was altered according to the requirements of the experiment (See Materials & Methods p164). The results obtained showed that the number of astrocytes started to increase in the brains of mutant animals at the third week in both the cortex and hippocampus (tables 8-1, 8-2 and 8-3). The population of astrocytes was greater in the fourth week. Therefore, the disease was more pronounced when the mutant animal entered the fourth week of age. It was noted that the difference in the number of astrocytes was greater in the area of the cortex than in the hippocampus, especially at weeks 4, 5 and 6 (Figures; 8-20, 8-22 and 8-24).

In conclusion, reactive gliosis was observed by the third week of age in mutant animals, and gradually increased to the sixth week of age, especially in the cortex. Subsequent statistical analysis showed the results of each week separately represented graphically.

The histograms and figures of each age group will now be analysed. Figure 8-23 is comparison GFAP⁺ cells in the cortex, CA1 and dentate gyrus.

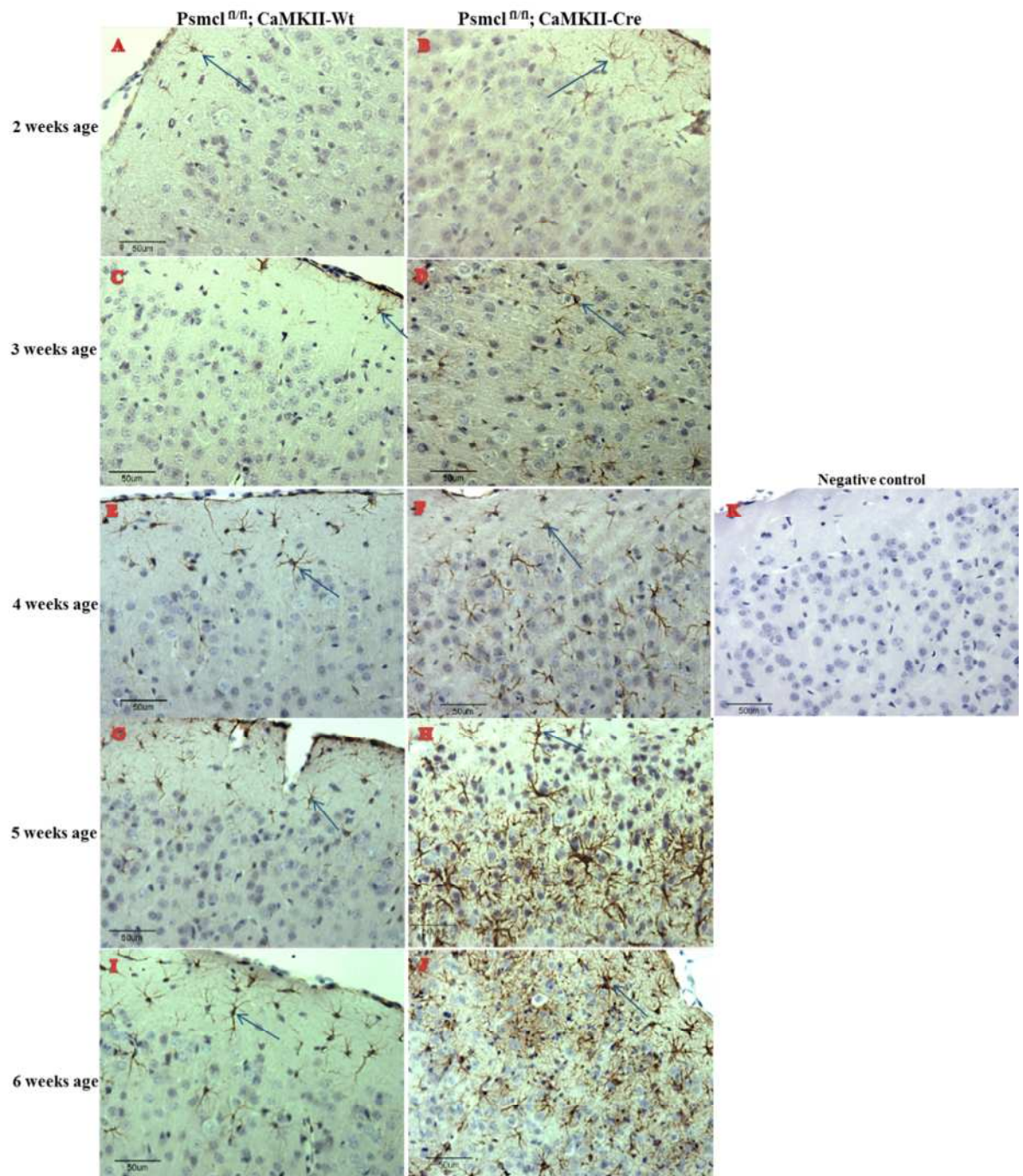


Figure 8-20; Detection of astrogliosis in mouse brain using GFAP⁺ cells in the cortex.

Micrographs showing GFAP⁺ cells; A, C, E, G and I display coronal sections from *Psmc1^{fl/fl};CaMKIIα-Wt* (wild-type). B, D, F, H and J show *Psmc1^{fl/fl};CaMKIIα-Cre* mutant mouse brains at 2 to 6 weeks of age in cortex region. K represents negative control; arrows refer to the GFAP⁺ cells. The number of GFAP⁺ cells increased at 3 weeks of age and was significantly greater at 4, 5 and 6 weeks of age in mutant mice. Neurodegeneration begins in the third week in this mouse model then increasingly progressively in subsequent weeks. Micrographs were captured by a light microscope. Scale bar 50 μm.

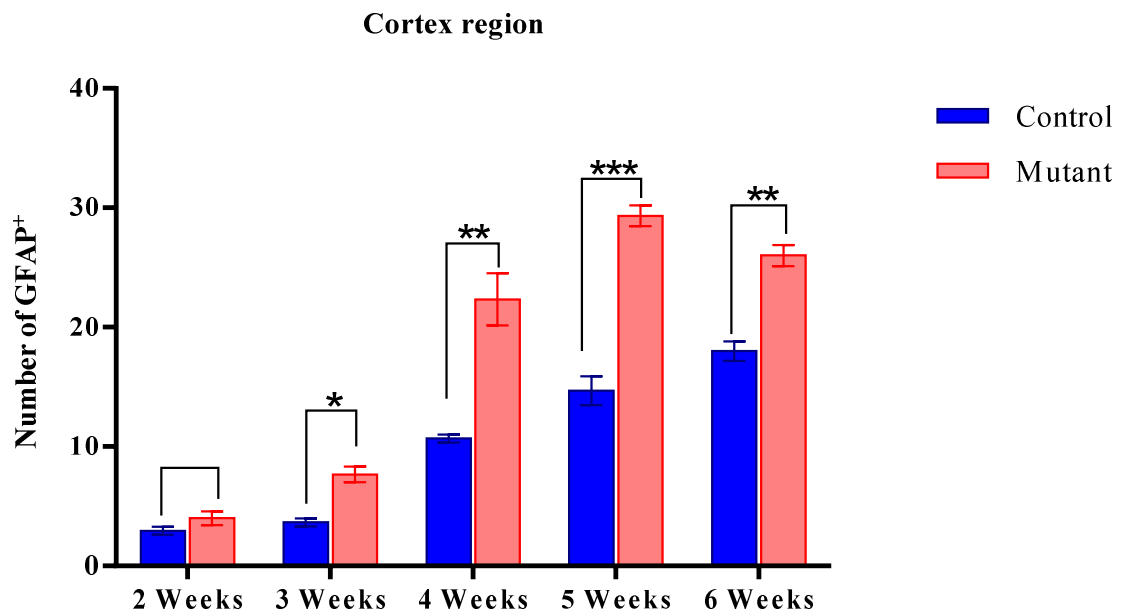


Figure 8-21 Number of astrocytes in wild-type and mutant mice between 2 and 6 weeks of ages in the dentate gyrus.

Bar graph showing GFAP⁺ cells in the cortex of control and mutant mice. The mean (\pm SD) number of the GFAP⁺ cells per control (n=3) or mutant (n=3) was determined from three coronal sections per mouse. Asterisks refer to the results of 2-way ANOVA using original cell counts. There was an increase in GFAP⁺ cells in the cortex of mutant mice. Analysis shows a statistically significant difference using unpaired Student's t-tests between control and mutant at 3, 4, 5 and 6 weeks of age. P* < 0.05, P** < 0.001 and P*** < 0.0001

Table 8-1 Number of astrocytes in the cortex

Age	Wild-type mean	Mutant mean	P value
2 weeks	2.66 \pm 0.33	4.0 \pm 0.57	P < 0.05 (NS)
3 weeks	3.66 \pm 0.33	8.66 \pm 0.66	*P < 0.015
4 weeks	10.6 \pm 0.3	22.3 \pm 2.0	**P < 0.004
5 weeks	14.6 \pm 1.03	29.3 \pm 0.8	***P < 0.0004
6 weeks	17.6 \pm 1.5	26.3 \pm 1.6	**P < 0.0057

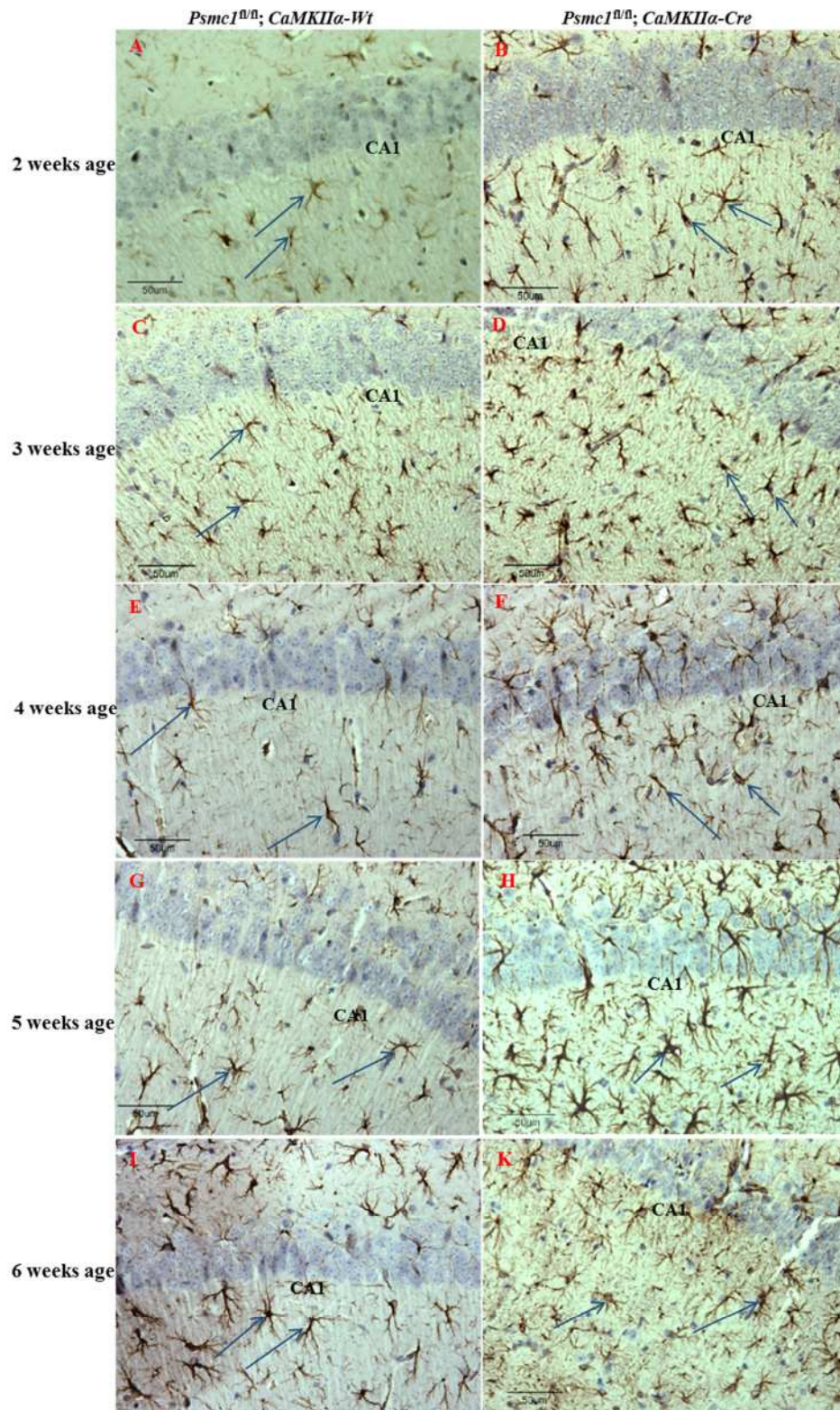


Figure 8-22; Detection of astrogliosis via GFAP⁺ cells in the CA1 area of the hippocampus, in mouse brain.

Micrographs showing GFAP⁺ cells in the cortex. A, C, E, G and I show coronal sections from *Psmc1^{fl/fl};CaMKIIα-Wt* (wild-type) mouse brain and B, D, F, H and j show coronal sections from *Psmc1^{fl/fl};CaMKIIα-Cre* mutant mouse brains at 2 weeks to 6 weeks of ages. Arrows refer to the GFAP⁺ cells. The number of GFAP⁺ cells increased at 4 weeks of age in both mutant and wild-type mice. The number of GFAP⁺ cells in the mutant sections was significantly greater at 5 weeks of age compared to control mice. Scale bar 50 μm.

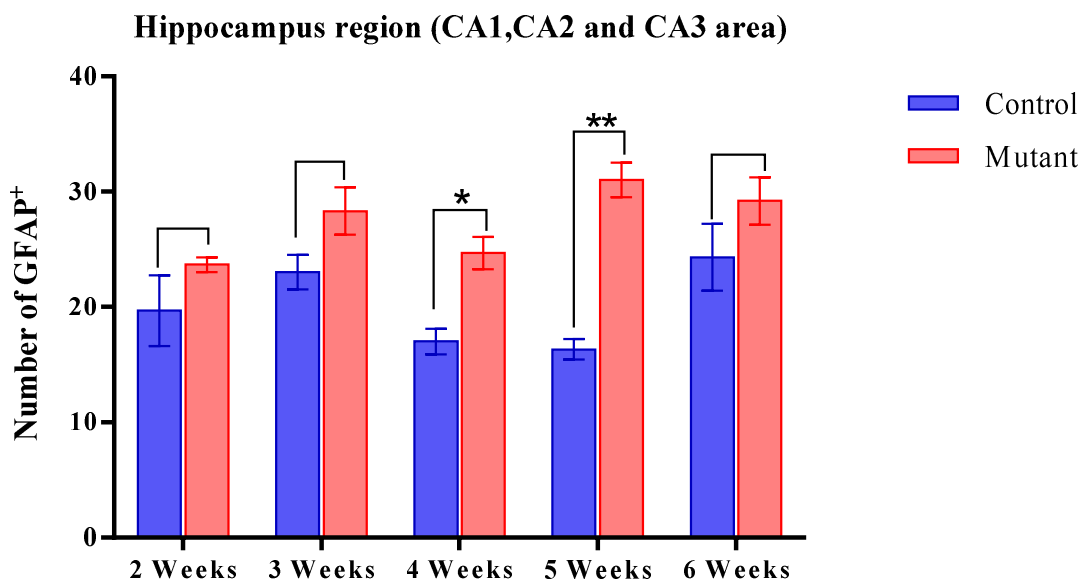


Figure 8-23 Number of astrocytes in wild-type and mutant mice between 2 weeks and 6 weeks of age in the CA1 area of the hippocampus.

Bar graph showing GFAP⁺ cells in the hippocampal region of control and mutant mice. The mean (\pm SD) number of the GFAP⁺ cells in the control (n=3) or mutant (n=3) animals was determined from three coronal sections per mouse. Asterisks refer to the results of 2-way ANOVA using original cell counts. There was a significant increase in GFAP⁺ cells in the hippocampal region of mutant mice, compared to the controls, at 4 and 5 weeks of age Where $P^* < 0.05$ and $P^{**} < 0.001$, respectively in an unpaired Student's test.

Table 8-2 Number of astrocytes in the CA1 area of the hippocampus

Age	Wild-type mean	Mutant mean	P value
2 weeks	19.8 \pm 2.33	24.0 \pm 0.4	P < 0.15 (NS)
3 weeks	23.7 \pm 0.88	28.66 \pm 1.8	P < 0.068 (NS)
4 weeks	18.0 \pm 1.8	25.5 \pm 1.2	*P < 0.025
5 weeks	16.6 \pm 1.1	31.3 \pm 1.4	**P < 0.0012
6 weeks	22.6 \pm 2.0	28.0 \pm 1.8	P < 0.0115(NS)

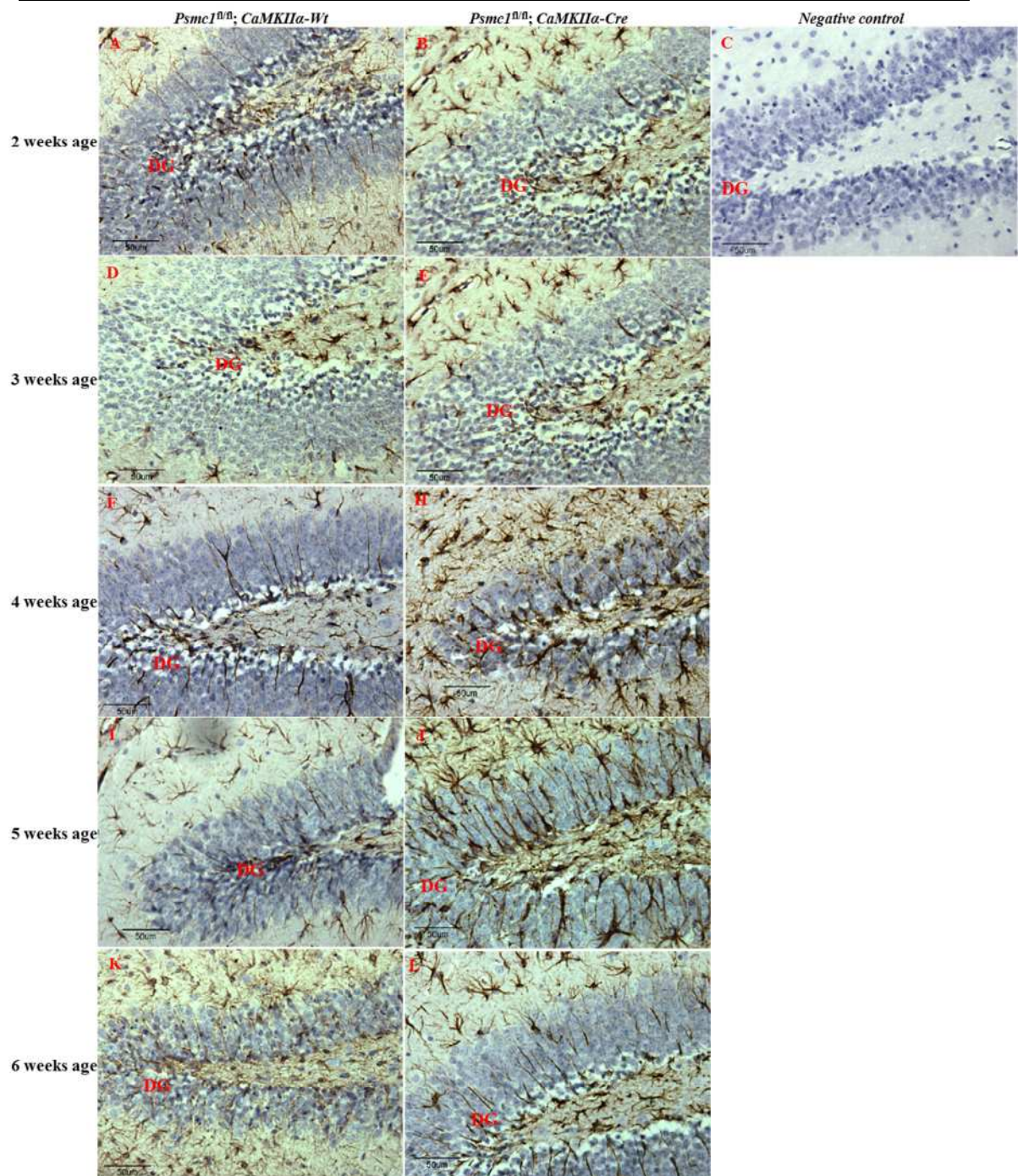


Figure 8-24; Using GFAP⁺ cells to detect astrogliosis in the dentate gyrus of the mouse brain.

Micrographs showing GFAP⁺ cells. A, C, E, G and I display coronal sections from *Psmc1^{fl/fl};CaMKIIα-Wt* (wild-type) mice. B, D, F, H and J display coronal sections from *Psmc1^{fl/fl};CaMKIIα-Cre* mutant mice, between 2 and 6 weeks of age in the cortex. K represents negative control. Arrows refer to the GFAP⁺ cells. The number of GFAP⁺ cells increased at 3 weeks of age and was significantly greater at 4, 5 and 6 weeks of age in mutant mice, compared to control mice. Scale bar 50 μm.

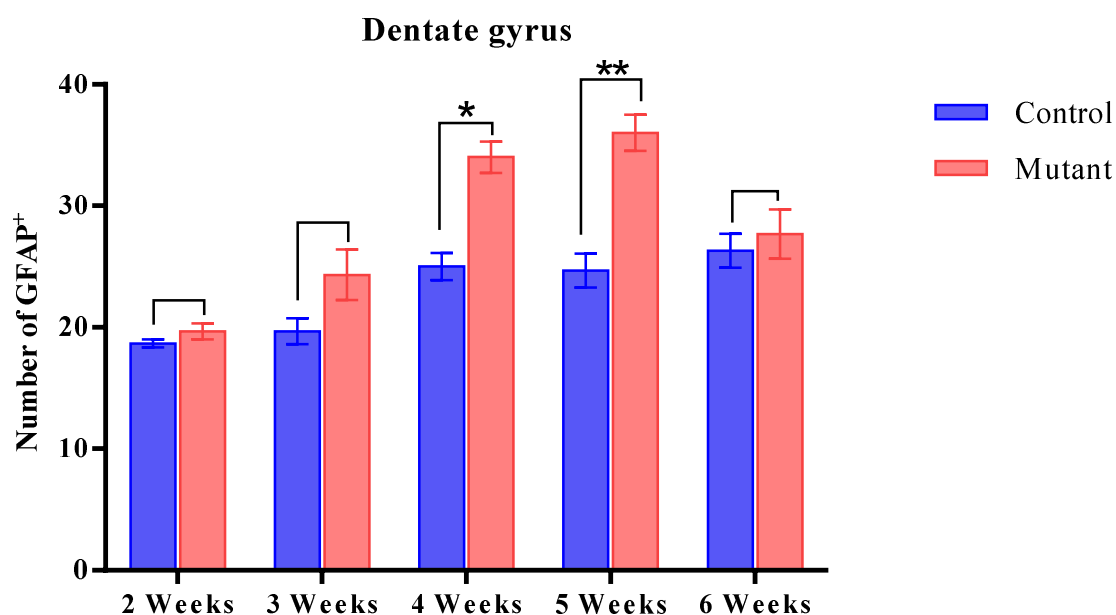


Figure 8-25 Number of GFAP⁺ cells in wild-type and mutant mice between 2 weeks and 6 weeks of age in dentate gyrus area.

Bar graph showing GFAP⁺ cells in the cortex of control and mutant mice. The mean (\pm SD) number of GFAP⁺ cells in control (n=3) or mutant (n=3) mice was determined from three coronal sections per mouse. Asterisks refer to the results of 2-way ANOVA using original cell counts. There was an increase in GFAP⁺ cells in the cortex of mutant mice, which is significantly different to control mice at 4 and 5 weeks of age, where $P^* < 0.05$ and $P^{**} < 0.001$ using an unpaired Student's test.

Table 8-3 Number of astrocytes in the DG area of the hippocampal

Age	Wild-type mean	Mutant mean	P value
2 weeks	18.6 \pm 0.33	20.0 \pm 0.67	P < 0.21 (NS)
3 weeks	20.7 \pm 1.4	23.0 \pm 1.8	P < 0.25 (NS)
4 weeks	23.60 \pm 1.4	33.0 \pm 1.5	*P < 0.010
5 weeks	23.7 \pm 1.5	35.0 \pm 1.6	**P < 0.0067
6 weeks	24.5 \pm 1.5	25.7 \pm 1.8	P < 0.63 (NS)

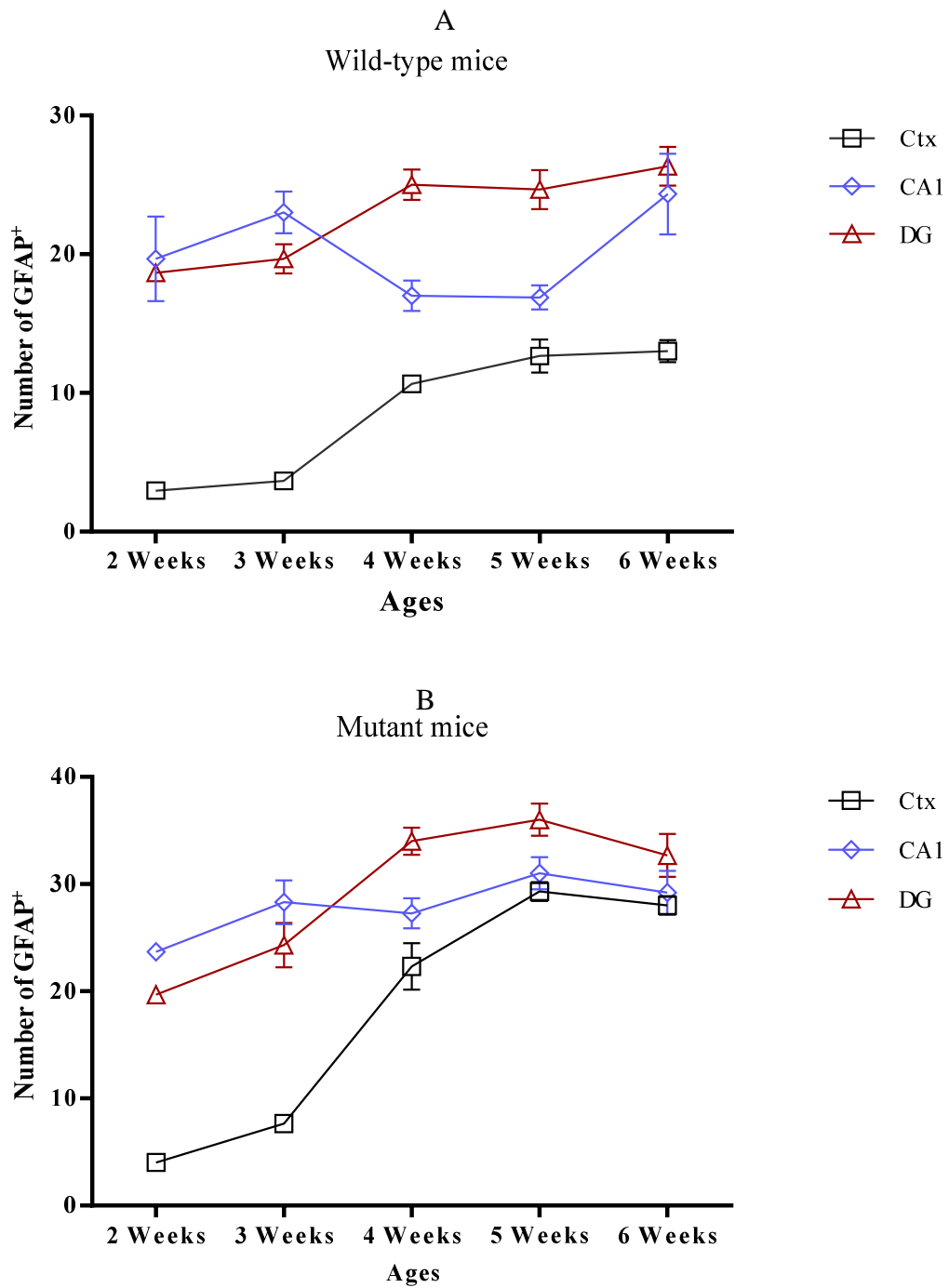
 Comparison of GFAP⁺ cells in the cortex, CA1 and dentate gyrus


Figure 8-26; Comparison of the number of GFAP⁺ cells in the cortex, CA1 and dentate gyrus, in wild type and mutant mice up to 6 weeks of age.

A; GFAP⁺ cells in the brains of *Psmc^{1fl/fl};CaMKII α -Wt* wild-type mice in three different areas of the brain B; GFAP⁺ cells in the brains of *Psmc^{1fl/fl};CaMKII α -Cre* mutant mice in three different areas of the brain. Data is expressed as mean \pm SD, based on three animals per region.

8.6.2 Effect of PPAR- γ agonist on astrocyte population in Dementia with Lewy Body Model

8.6.2.1 Resazurin assay to investigate a non-toxic dose of Rosiglitazone (PPAR- γ agonist)

Before investigating the actual effects of the agonist, a preliminary assessment was carried out to determine the toxic levels of the drug. This was necessary to determine whether any potential reduction of cell number was not due to toxicity. For this purpose, 3T3 cells (fibroblast cell line) were grown in a 96-well plate. The cells were grown to densities of 1K, 5K, 10K, 20K and 50K. This type of cells was chosen instead of brain tissue, for three reasons. They only require 24 hours to grow; they grow in a uniform manner, and are highly sensitive to toxic materials. The cells were grown in several 96-well plates for 24 and 72 hours. The medium was changed every other day. Rosiglitazone was dissolved in DMSO at the following concentrations: 25 μ M, 50 μ M and 100 μ M. The medium was removed and the cells were treated with either Rosiglitazone, or the same concentrations of DMSO vehicle for 24 and 72 hours. Once the time points were reached, Resazurin was added and the plates were subsequently re- incubated from 2 hours, up to 1 week. The results were analysed by a FLUOstar Galaxy software reader Results showed that Rosiglitazone was non-toxic at the concentrations used in this study. Subsequent bar charts represent the cell viability after treatment with Rosiglitazone, (Figures 8.27 – 8.30).

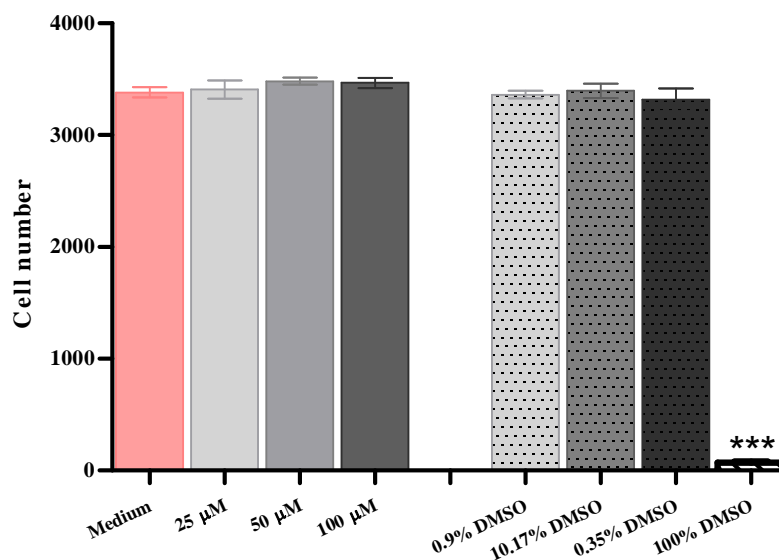


Figure 8-27 Cell viability of 3T3 cells treated with rosiglitazone (PPAR γ agonist) for 24h.

The Resazurin assay was performed and fluorescent cells were checked 2 h later. Results of a one way ANOVA (post-hoc Dunnett's multiple comparison tests) show that all three concentrations are not toxic. Data are expressed as mean \pm SD (n=6) 100% DMSO positive control showed a significant difference from the control medium, indicated with an asterisk ($P < 0.05$).

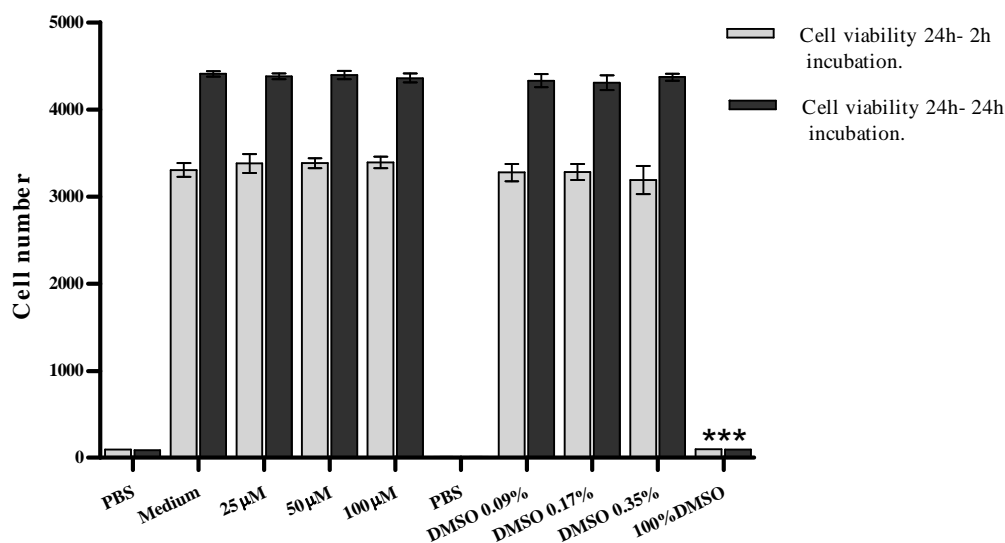


Figure 8-28 Bar chart shows the results obtained when reading the plates after 2 and 24 hours (24 hours post-seeding).

Cell viability of 3T3 cells was measured after 2 and 24 hours, using the Resazurin assay, after being treated with Rosiglitazone (PPAR γ agonist) for 24 hours. Two ways ANOVA shows all three concentrations are not toxic. Data are expressed as mean \pm SD (n=6). The 100% DMSO positive control showed significant difference from the control medium indicated with an asterisk ($P < 0.001$).

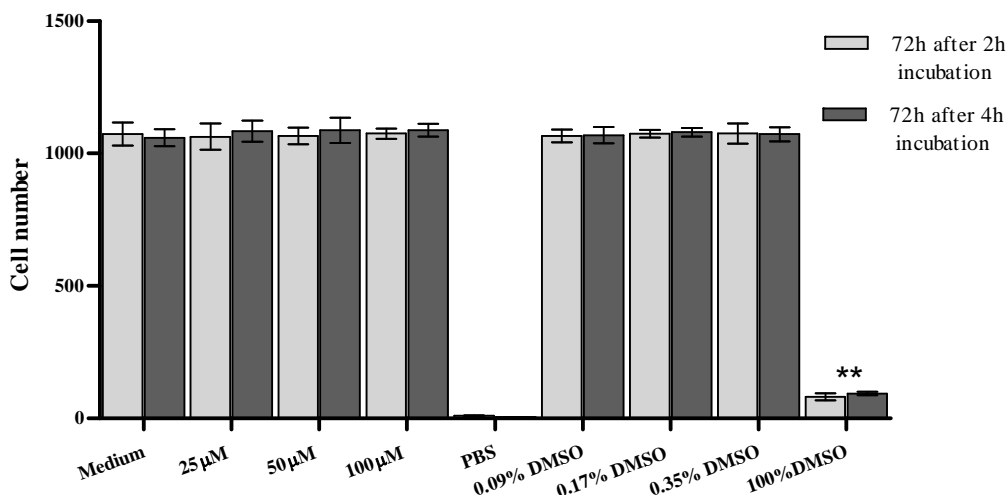


Figure 8-29 Bar chart shows the results obtained after reading the plates after 2 and 4 hr, (72 hours post-seeding).

Cell viability of 3T3 cells was measured after 2 and 24 hours, using the Resazurin assay, after being treated with Rosiglitazone (PPAR- γ agonist) for 72h. Two way ANOVA shows all three concentrations are not toxic. Data are expressed as mean \pm SD (n=6.100% DMSO positive control showed significant difference from the control medium, indicated with an asterisk (P < 0.001).

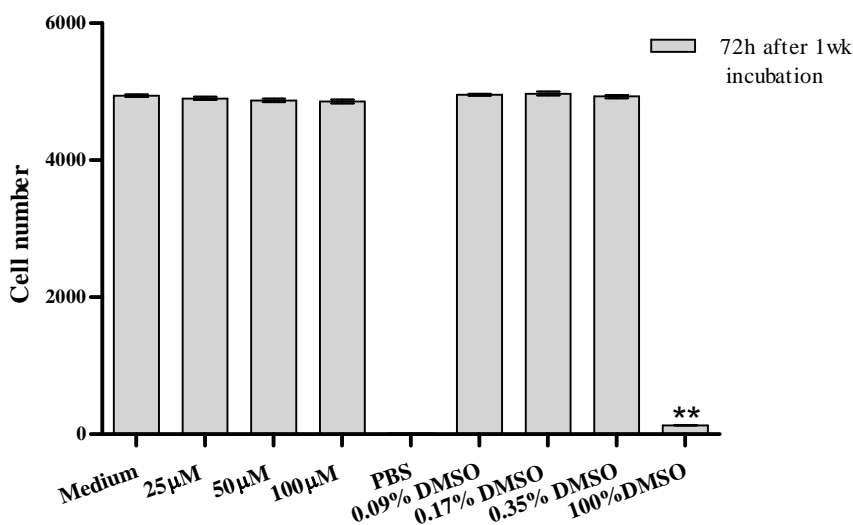


Figure 8-30 Bar chart shows the results of the survival of the cells after seeding for 72 hours.

Cell viability of 3T3 cells after 1 week incubation was measured using the Resazurin assay, after being treated with Rosiglitazone (PPAR- γ agonist) for 72h. Two way ANOVA shows all three concentrations are not toxic. All data are expressed as mean \pm SD (n=6) 100% DMSO positive control showed significant difference from the control medium, indicated with an asterisk (P < 0.001).

8.6.2.2 Effects of PPAR- γ agonist on astrocyte population during astrocyte reactivation

In order to, Organotypic slice cultures of the transgenic mouse model of dementia with lewy body disease were used to assess the effect of peroxisomal proliferation on pathological injury *in vitro* (Bianco, Ridet et al. 2002).

The brains of four day old mice were sliced to a thickness of 350 μm and cultured on membrane inserts (See materials and methods, page; 148 for details). The hippocampus was separated from the cortex before culturing organotypic slice cultures of the mutant and wild-type mice. Four different control brain slice cultures were used; DMSO vehicle, antagonist (T0070907), antagonist with agonist and untreated medium. The slices were grown for 6 weeks and treatment was started by the end of the fifth week. Three different doses of Rosiglitazone PPAR- γ agonist were used on the slices: (25 μM , 50 μM and 100 μM) every other day for a one week. The culture medium was changed every other. At the end of the sixth week, brain slices were fixed and paraffin sections were prepared in preparation for immunohistochemistry staining.

Since there is no published data on volume-dose ratio in slice culture technique, we anticipated that 25 μM , 50 μM and 100 μM would be suitable to study organotypic slice cultures. The doses 50 μM and 100 μM showed a positive result in the cultures, while the 25 μM dose did not. We investigated the effect of PPAR- γ agonist, rosiglitazone, in the cortex and hippocampal areas after a week of treatment. The results showed that PPAR- γ agonist inhibited astrocyte activation in both the cortex and hippocampus of the mutant mice (Figure; 8-35 & 8-40). The number of GFAP positive astrocytes was significantly decreased in mutant mice slices treated with 100 μM rosiglitazone in both areas. 50 μM rosiglitazone caused decreases in the number of astrocytes in both the hippocampus (see histograms; 8-36 to 8-39) and the cortex, yet was only significant compared to controls, in the cortex. (Figures and histograms 8-31 to 8-34).

Investigating the effect of two different concentrations of the PPAR- γ agonist rosiglitazone on astrocyte numbers in cortical organotypic slice cultures of wild-type mice.

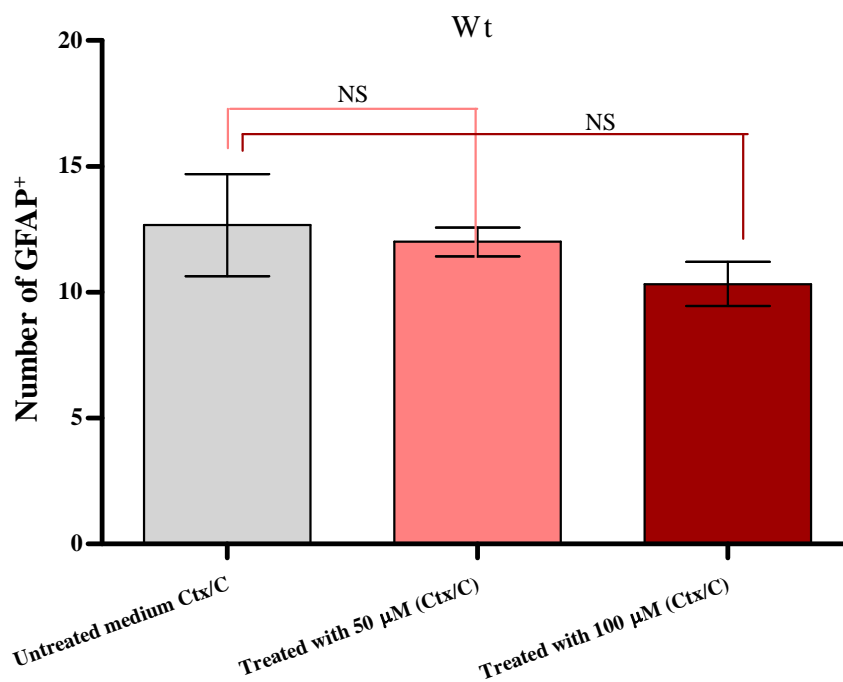


Figure 8-31 Investigation of the effect of the PPAR- γ agonist; rosiglitazone on astrocyte numbers in the cortex region, using wild-type organotypic slice cultures.

The bar chart represents the varying effects of two different concentrations of rosiglitazone on astrocyte numbers in organotypic slice cultures of wild-type mouse cortex. Data are expressed as mean \pm SD. Slices were treated with either 50 μ M or 100 μ M rosiglitazone (PPAR- γ agonist). There is no significant difference between the concentrations and controls when analysed using one way ANOVA with Post-hoc; Dunnett's multiple comparison test, (n=3) $P < 0.05$.

Investigating the effect of two different concentrations of the PPAR- γ agonist; rosiglitazone on astrocyte numbers in cortical organotypic slice cultures from mutant mice.

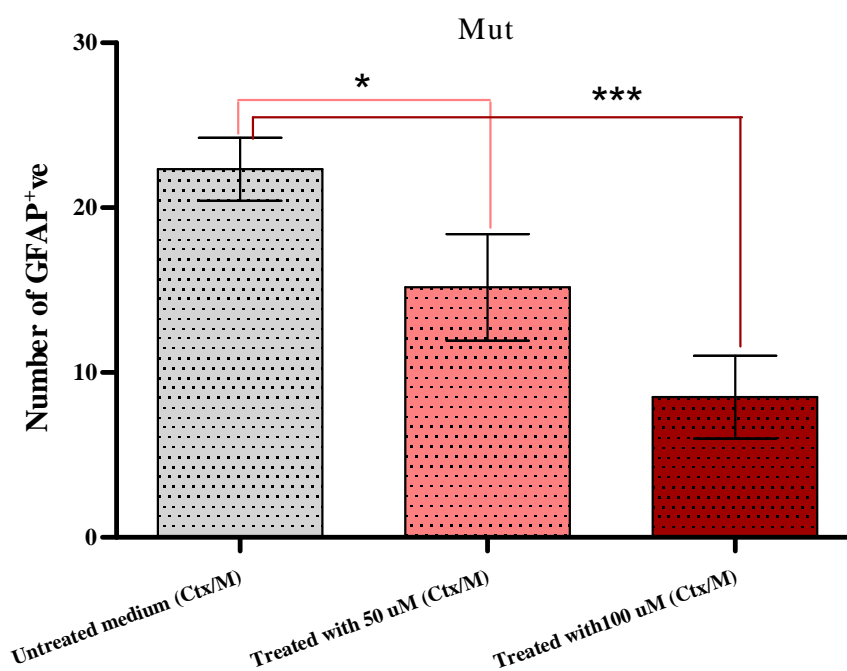


Figure 8-32 Investigation of the effect of the PPAR- γ agonist; rosiglitazone on astrocyte numbers in the cortex region of cultures from mutant mice.

The bar chart represents the varying effects of two different concentrations (50uM and 100uM) of rosiglitazone on astrocyte number in organotypic slice cultures of mutant mouse cortex. Data are expressed as mean \pm SD. A statistically significant difference was seen between control treated cultures and rosiglitazone treated cultures when analysed using ANOVA with post-hoc Dunnett;s multiple comparison test (n=3) *P< 0.01 and ***P< 0.001.

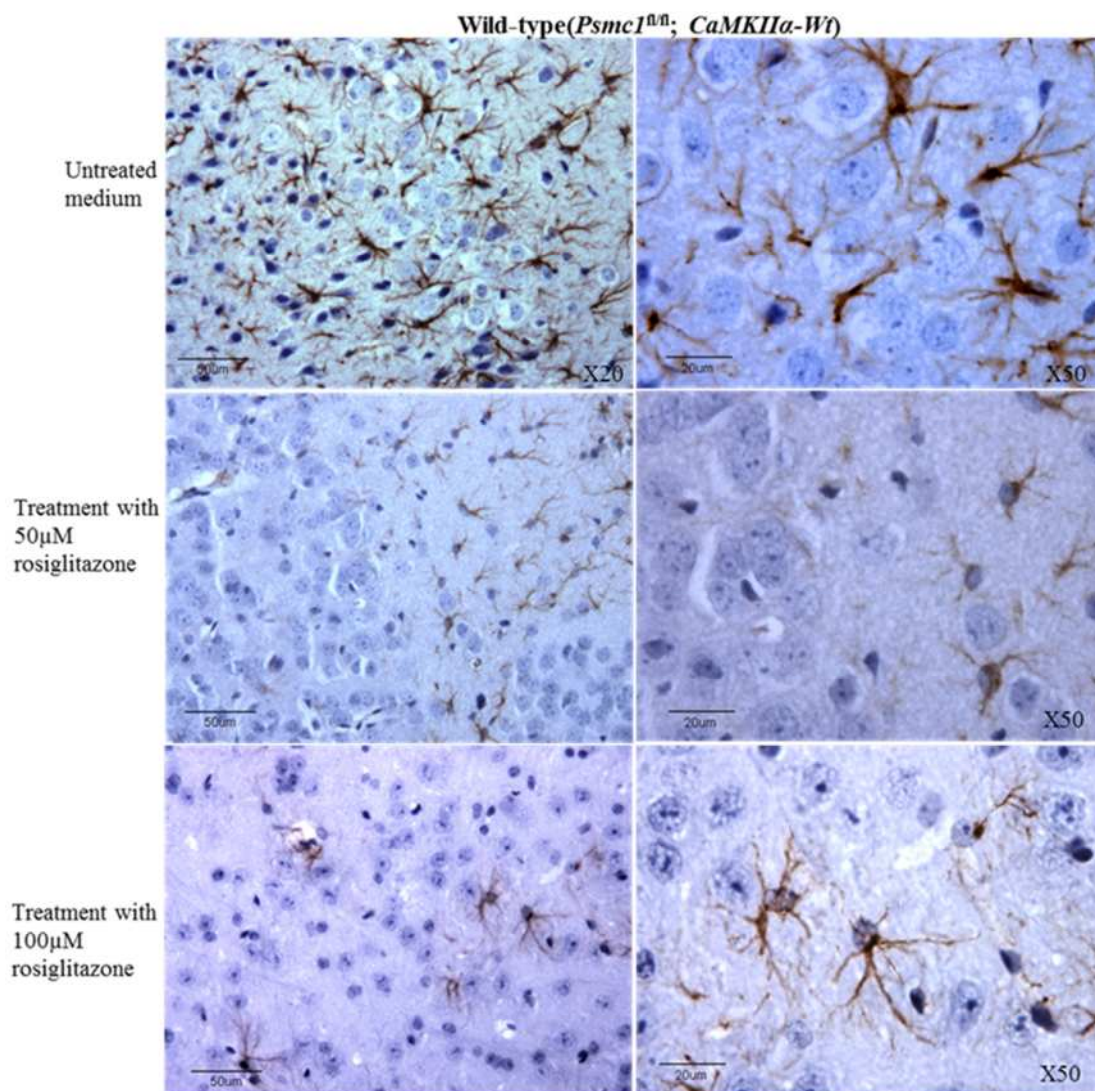


Figure 8-33 Immunohistochemical staining of GFAP through the cortical region of a brain slice from a wild-type mouse, treated with 50 and 100 µM rosiglitazone.

Micrographs illustrate the differences in the number of labelled astrocytes when comparing the control condition with the two concentrations of PPAR- γ agonist, rosiglitazone. Micrographs were captured at two magnifications X20 and X50.

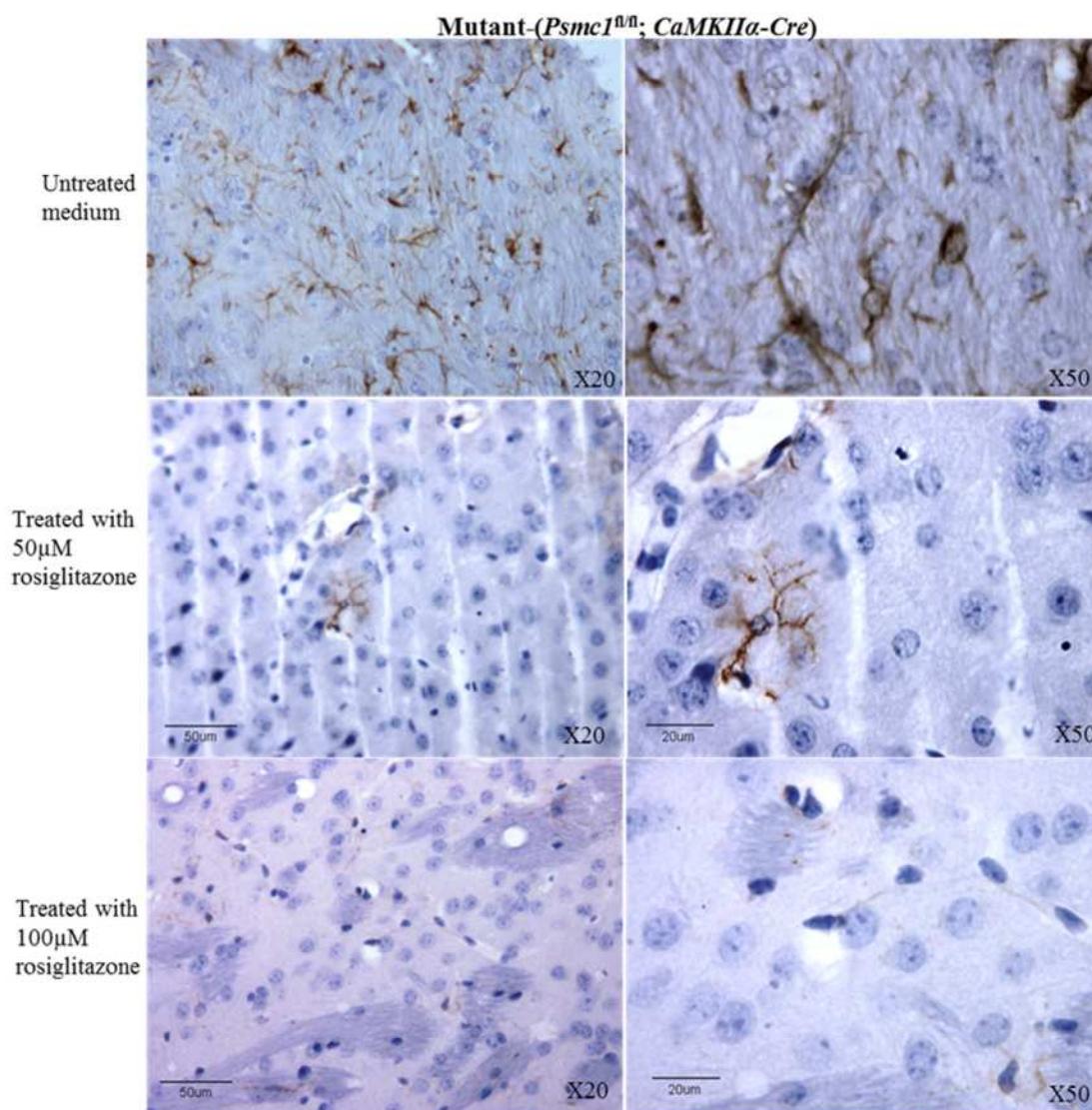


Figure 8-34 Immunohistochemical staining of GFAP through the cortical region of brain slices from a mutant mouse treated with 50 and 100 μ M rosiglitazone.

Micrographs illustrate the differences in the number of labelled astrocytes when comparing the control condition with the two concentrations of PPAR- γ agonist, rosiglitazone, in mutant mouse slices. Micrographs were captured at two magnifications X20 and X50.

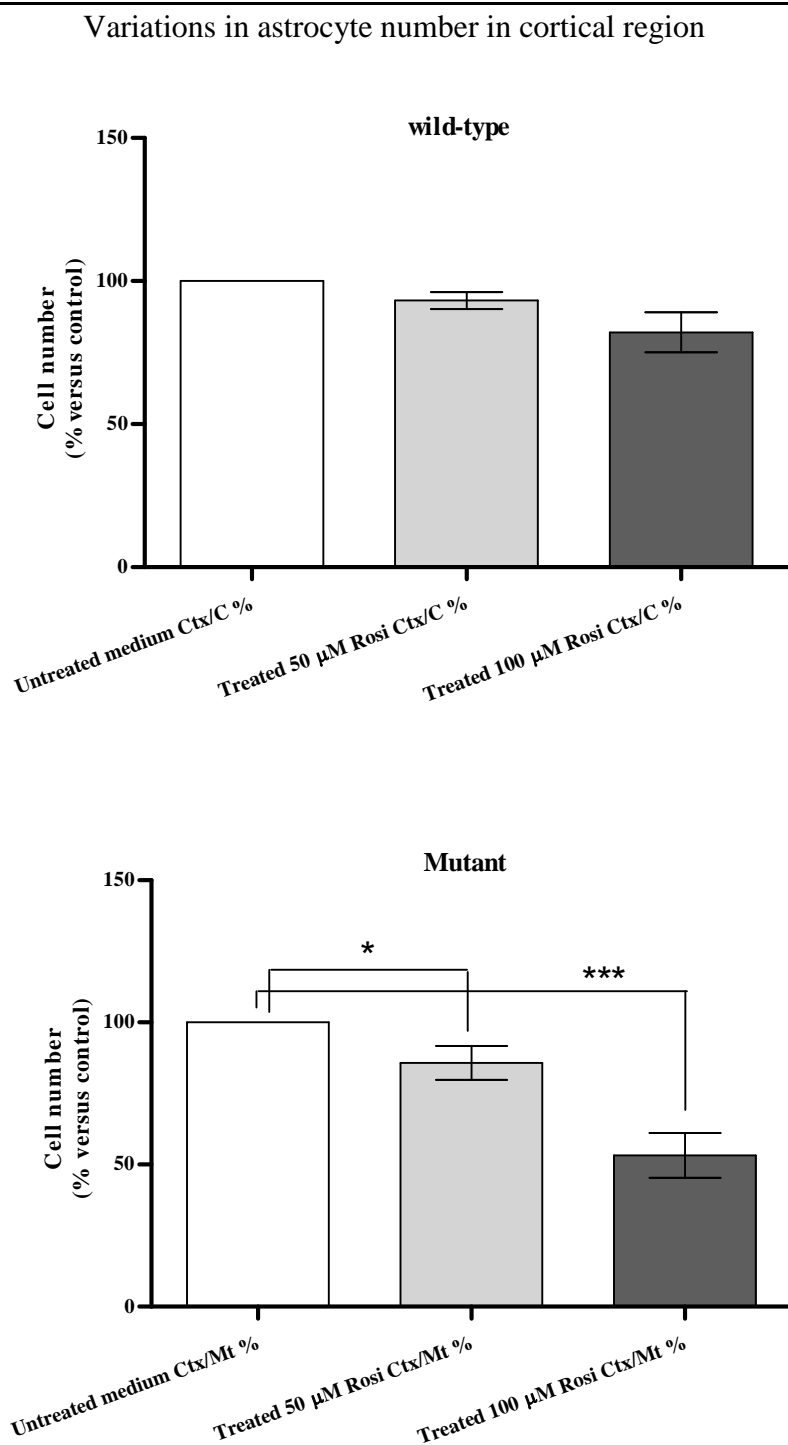


Figure 8-35 Percentages change of GFAP⁺ cells in the cortex of wild type and mutant mouse brain slices after treatment with 50 μM and 100 μM of rosiglitazone.

The bar charts show the reduction in astrocyte number after PPAR-γ agonist treatment as a percentage of the control. Data are expressed as mean ± SD, (n=3). One way ANOVA analysis with post-hoc Dunnett's multiple comparison test found no significance in the wild-type animals, however both concentrations on rosiglitazone caused a significant reduction in GFAP⁺ cells compared to controls, (n=3) P < 0.05 and ***P < 0.001.

Investigating the effect of two different concentrations of the PPAR- γ agonist rosiglitazone on astrocyte numbers in hippocampal organotypic slice cultures of wild-type mice.

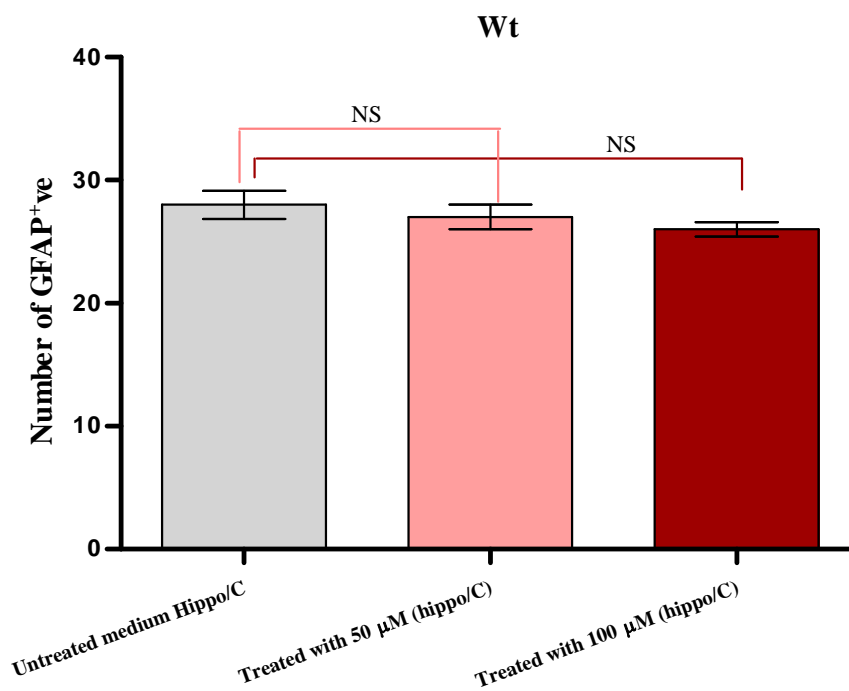


Figure 8-36 Investigating the effect of the PPAR- γ agonist; rosiglitazone on astrocyte numbers in the hippocampal region of wild-type mice.

The bar chart represents the effects of two different concentrations (50 μ M and 100 μ M) of rosiglitazone on astrocyte numbers in organotypic slice cultures of wild-type mouse hippocampus. Data are expressed as mean \pm SD). One way ANOVA analysis; Dunnett's multiple comparison test, (n=3) showed no significance.

Investigating the effects of two different concentrations of the PPAR- γ agonist; rosiglitazone on astrocyte numbers in hippocampal organotypic slice cultures of mutant mice.

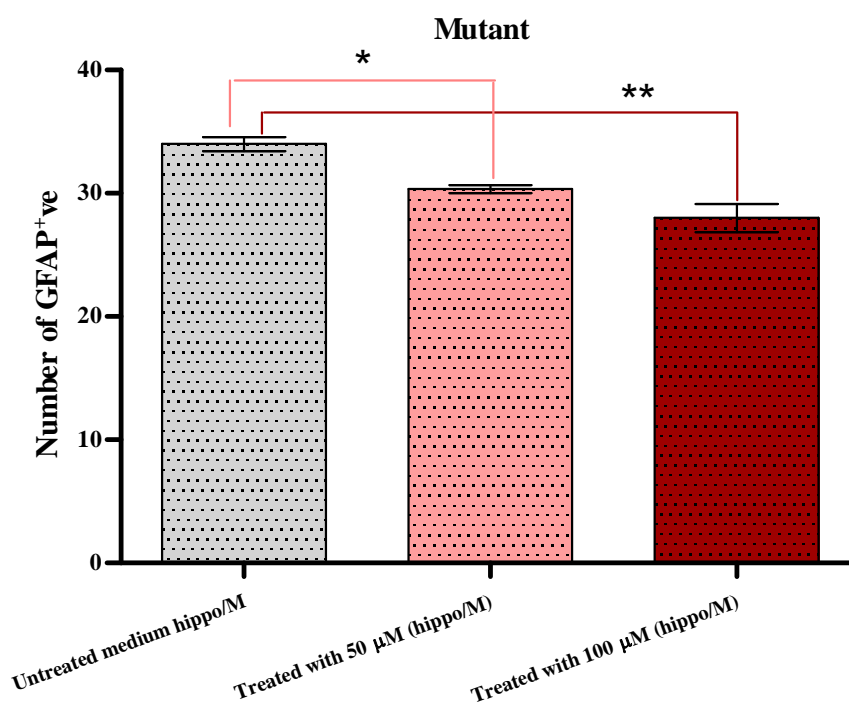


Figure 8-37 Investigating the effect of the PPAR- γ agonist; rosiglitazone on astrocyte numbers in hippocampal region of mutant mice slices.

The bar chart represents to the varying effect of two different concentrations of rosiglitazone (50 μ M and 100 μ M) on astrocyte numbers in hippocampal organotypic slice cultures of mutant mice. Data are expressed as mean \pm SD One way ANOVA with Dunnett's multiple comparison test (n =3) revealed a significant difference between control and treated cultures, where *P< 0.01 and ***P< 0.001.

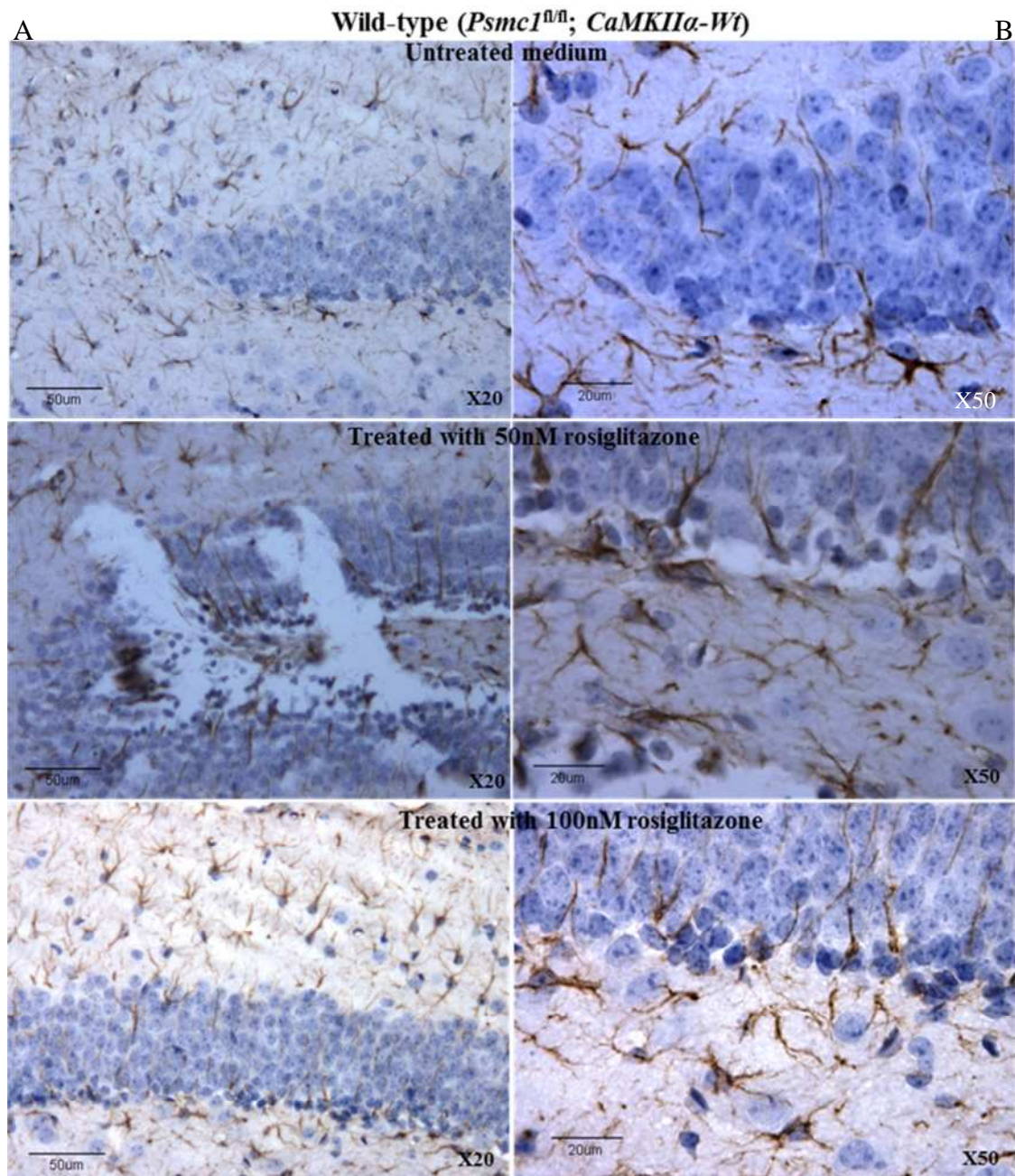


Figure 8-38 Immunohistochemical staining of GFAP in the hippocampal region of slices from wild-type mouse brain treated with 50 and 100 μM rosiglitazone.

Micrographs show the abundance of labelled astrocytes in untreated slices compared to slices treated with two different concentrations of PPAR- γ agonist, rosiglitazone. Micrographs were captured at two magnifications X20 (column A) and X50 (column B).

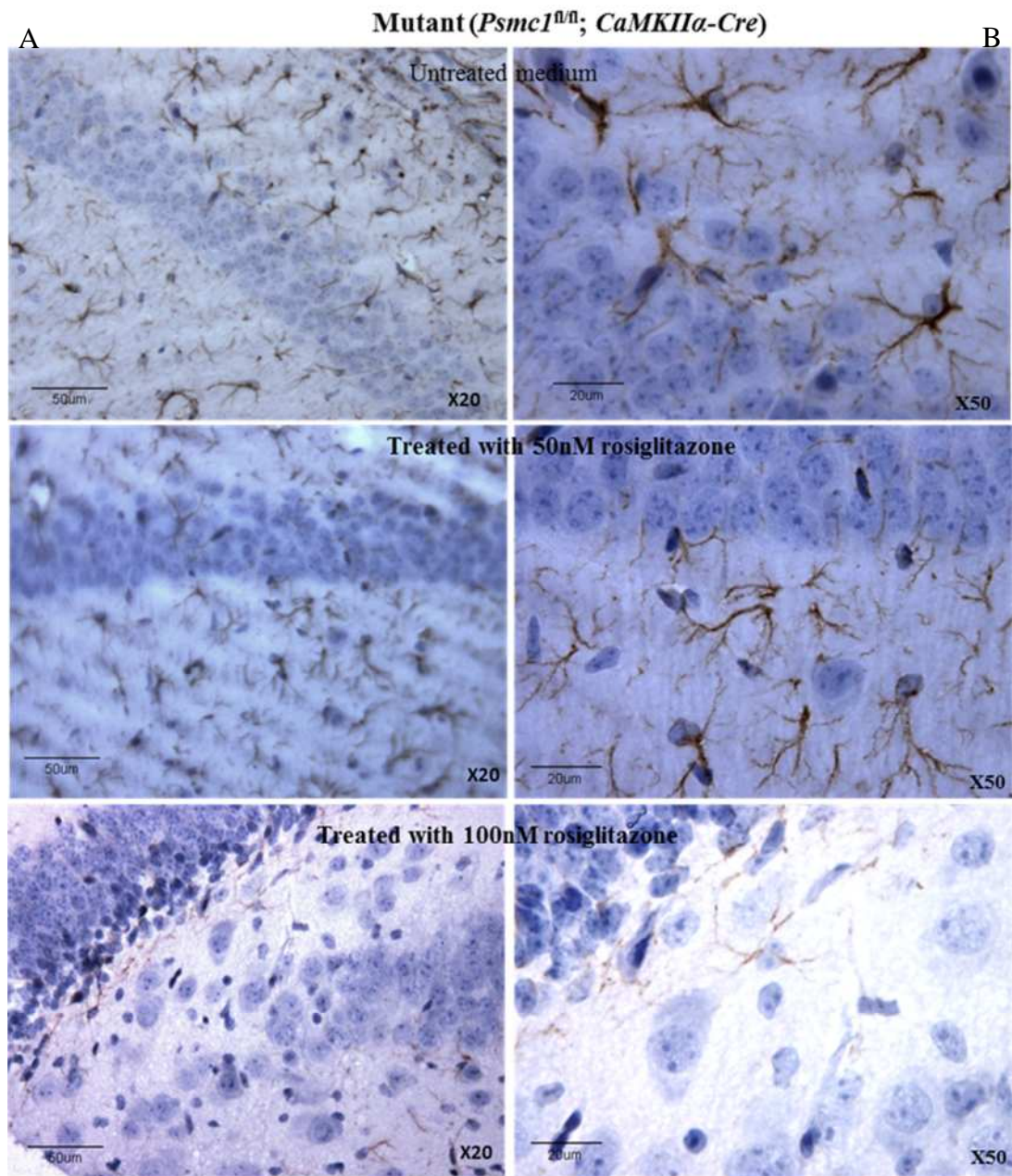


Figure 8-39 Immunohistochemistry staining of GFAP in the hippocampal region of mutant mouse brain slices treated with 50 and 100 μ M rosiglitazone.

Micrographs show the abundance of labelled astrocytes in untreated slices compared to slices treated with two different concentrations of PPAR- γ agonist, rosiglitazone. Micrographs were captured at two magnifications X20 (column A) and X50 (column B).

Percentage difference of the number of astrocytes in the hippocampal region of wild-type and mutant mice

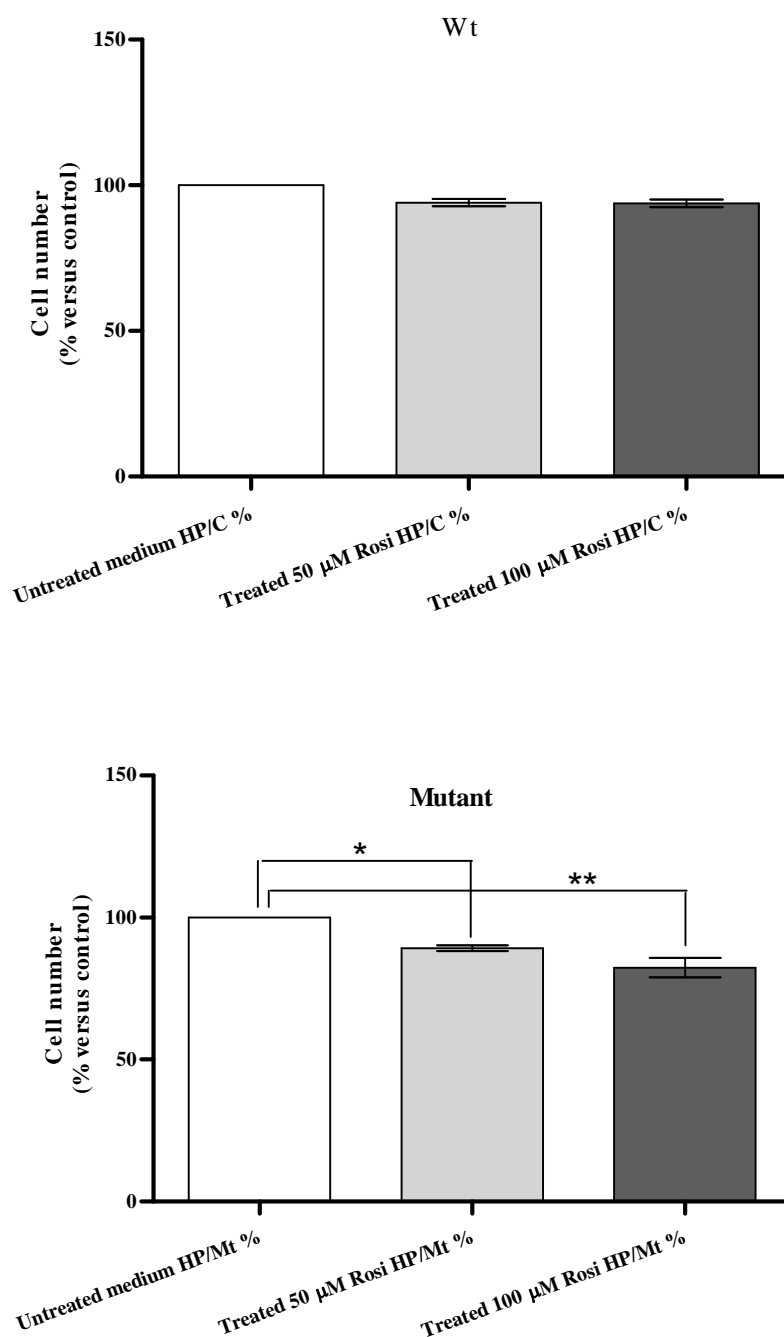


Figure 8-40 The number of GFAP⁺ cells expressed in the hippocampal region of wild-type and mutant mice brains after treatment with 50 μM or 100 μM rosiglitazone, expressed as a percentage of control.

The bar chart shows the percentage reduction of astrocyte number as a result of PPAR-γ agonist treatment. One way ANOVA analysis; Dunnett's multiple comparison test, revealed that although wild-type results showed no significance, the mutant results indicate significant declines in astrocyte count compared to the controls. Data are expressed as mean ± SD, (n=3) *P < 0.01 and **P < 0.001.

8.6.2.3 Effect of the PPAR- γ antagonist, T0070907, on PPAR - γ agonist activity.

It was necessary to confirm that PPAR- γ activation is the mechanism by which rosiglitazone (PPAR- γ agonist) regulates its effects in slice cultures of mutant mice. Therefore, PPAR- γ antagonist, T0070907 was added to the culture medium as concentrations of 75 μ M and 150 μ M, 6 hours prior to adding rosiglitazone. When rosiglitazone was added at concentrations of 50 and 100 μ M, the same concentrations of the antagonist were added, so the slices were exposed to both reagents. The results indicated that PPAR- γ antagonist has attenuated the effect of rosiglitazone. The difference in the number of astrocytes between the untreated slices and antagonist treated slices used in this study was not significant, (Fig 8-41& 8-43).

There was a significant difference ($P < 0.001$) in astrocyte number between the slices treated with rosiglitazone and controls (Figure 8-42 & 8-44).

Interestingly, PPAR- γ agonist has shown a minimal effect between the samples prepared from control mice. Therefore, peroxisome proliferators may be considered as potential therapeutic agents against the disease.

Investigating the ability of the PPAR- γ antagonist; T0070907 in blocking PPAR- γ agonist activity, represented by astrocyte numbers in cortical organotypic slice cultures from wild-type mice.

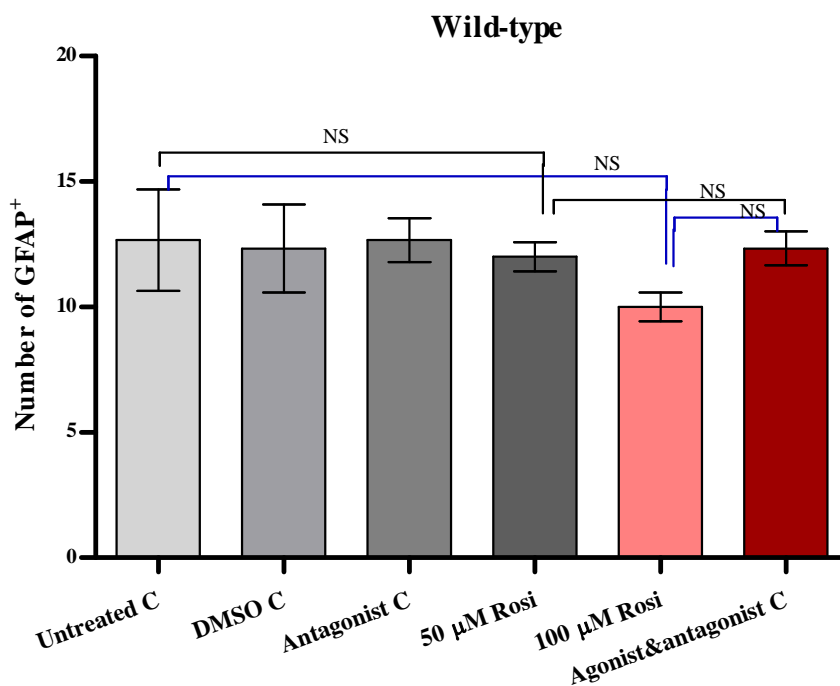


Figure 8-41 Bar chart representing the effects of 50 μ M and 100 μ M rosiglitazone treatment in control mouse slices, compared with controls and combined agonist/antagonist treatment.

Data are expressed as mean \pm SD. The number of astrocytes is similar in all four controls. Rosiglitazone caused no significant difference in GFAP⁺ cell number, when one way ANOVA analysis with Tukey's multiple comparison test, (n=3) was performed, $P < 0.05$.

Investigating the ability of the PPAR- γ antagonist; T0070907 in blocking PPAR- γ agonist activity, represented by astrocyte numbers in cortical organotypic slice cultures from mutant mice.

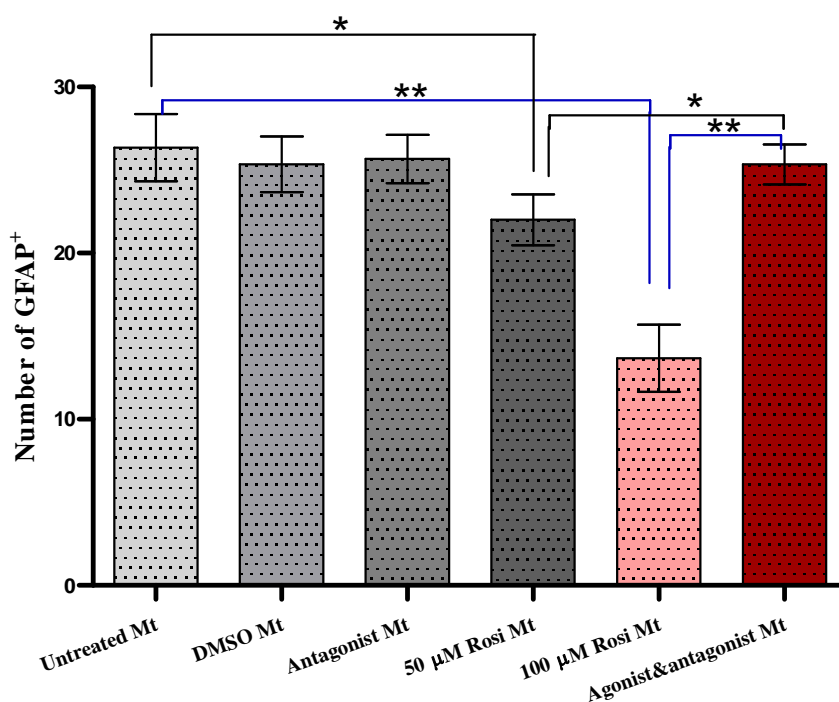


Figure 8-42 Bar chart represents the effects of 50 μ M and 100 μ M rosiglitazone treatment in mutant mouse slices, compared with controls and combined agonist/antagonist treatment.

Data are expressed as Rosiglitazone caused significant decreases in the number of GFAP⁺ cells at both concentrations. Administration of the antagonist alongside the agonist, showed no reduction in GFAP⁺ cell number, indicating that the antagonist blocks the agonist effects. One way ANOVA analysis; Tukey's multiple comparison test, (n=3) *P< 0.01 and **P< 0.001 .

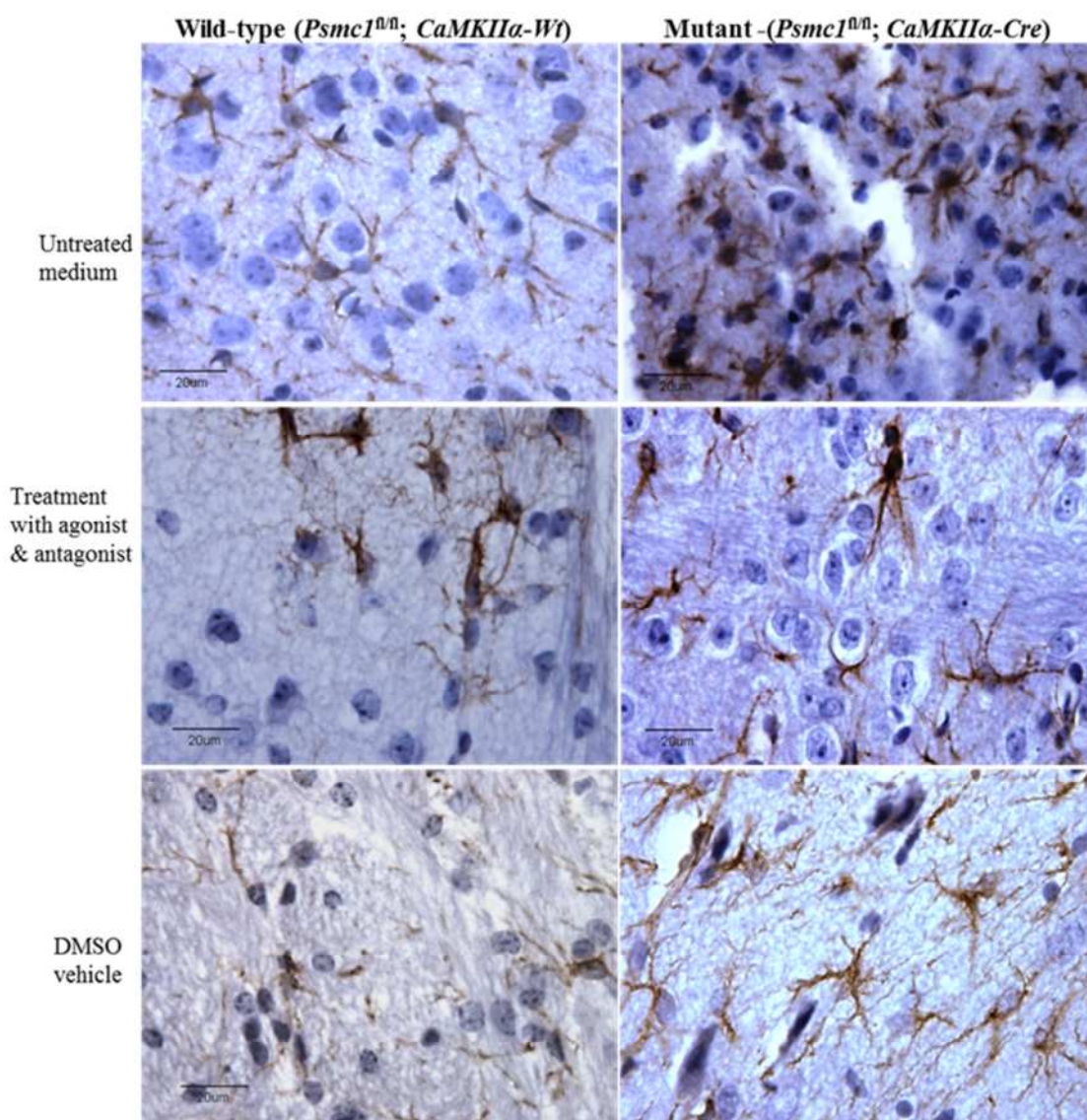


Figure 8-43 Comparison of astrocyte number in the cortex of paraffin sections created from control and mutant mouse organotypic slice cultures.

Micrographs represent labelled astrocytes in wild-type and mutant mouse brains. Sections were either untreated or treated with a DMSO control, or with a combination of agonist and antagonist. Slices were stained with DAB that reacted positively for GFAP⁺ cells. The images were captured at two magnifications X20 and X50.

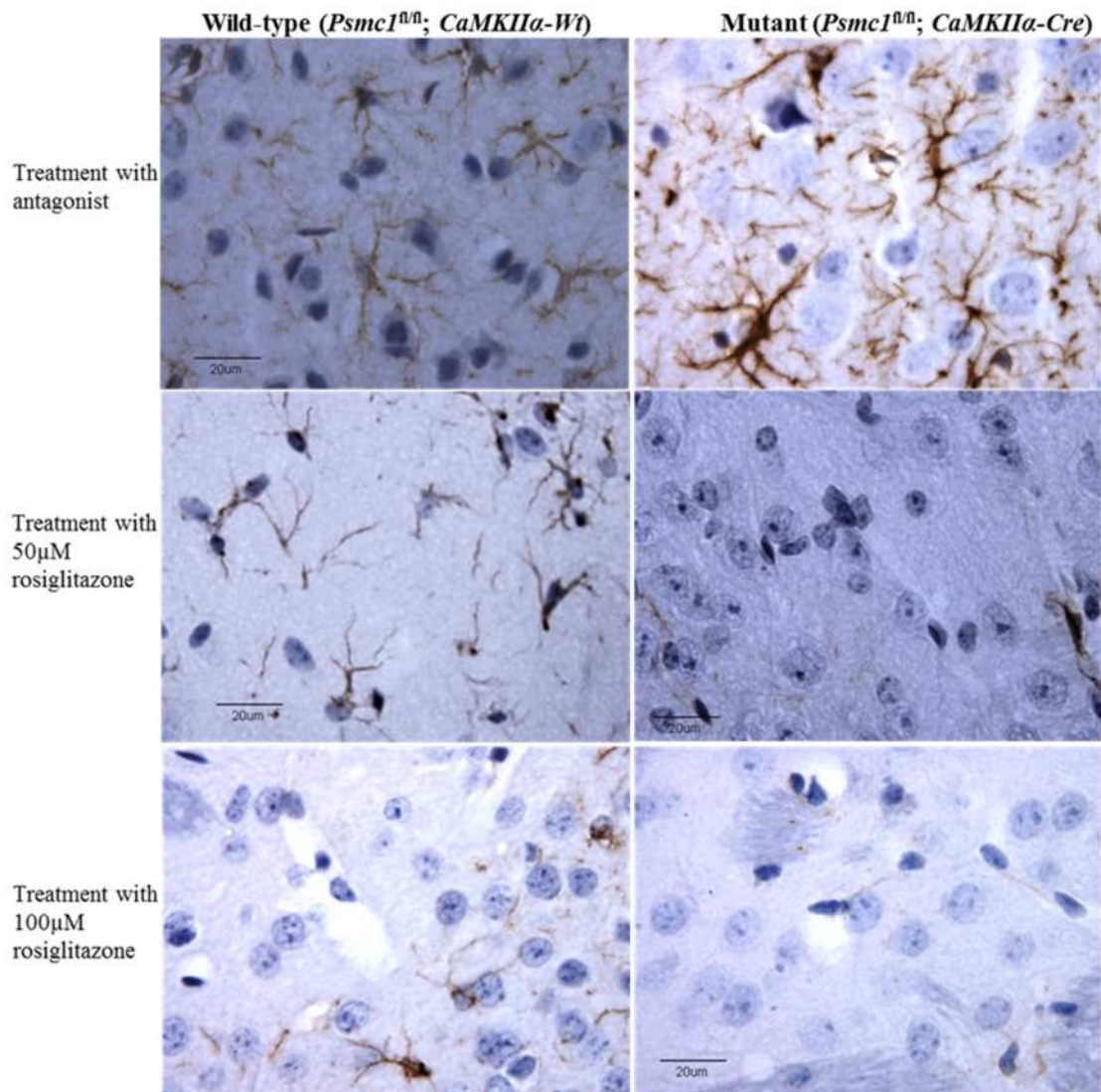


Figure 8-44 Comparison of astrocyte number in the cortex of paraffin sections created from treated organotypic slice cultures from wild type and mutant mouse brain.

Micrographs represent labelled astrocytes in wild-type and mutant mouse brains. Sections were treated with a PPAR-gamma antagonist, or with either 50 μ m or 100 μ m rosiglitazone. Micrographs were captured at two magnifications X20 and X50.

8.6.3 Expressing astrocyte numbers as a percentage of the controls

The number of astrocytes counted in each condition was expressed as a percentage of the controls (drug free medium). Results were analysed using a one way ANOVA, with an unpaired student's t-test.

The results showed that in the mutant mouse slices, there was a dose-dependent decline in the number of astrocytes compared to controls, when treated with rosiglitazone, in both the cortex and hippocampus (Figure 8-48). The drugs had no effect on astrocyte number in the wild-type mouse slices (Figure 8-47).

In the cortex of wild-type mice, the percentage reduction of astrocytes was 4.7 ± 2.1 % and 5.2 ± 4.3 % for the 50 μM and 100 μM PPAR- γ agonist, respectively. In contrast, in mutant slices there was a significant decline in the number of astrocytes; 19.1 ± 5.7 % and 43.2 ± 7.4 % for the PPAR- γ agonist, at concentrations of 50 μM and 100 μM , respectively (Figure 8-41).

In the hippocampus of wild-type mice, number of astrocytes decreased by 3.0 ± 1.1 % and 3.7 ± 2.9 % for the 50 μM and 100 μM PPAR- γ agonist, respectively. In contrast, the number of astrocytes was significantly lower in the mutant mice; 15.1 ± 0.7 % and 27.2 ± 2.4 % for the PPAR- γ agonist 50 μM and 100 μM , respectively (Figure 8-42). (Figure 8-42).

Effect of rosiglitazone on astrocyte number, expressed as a percentage of control in the cortex and hippocampus of wild-type and mutant mice

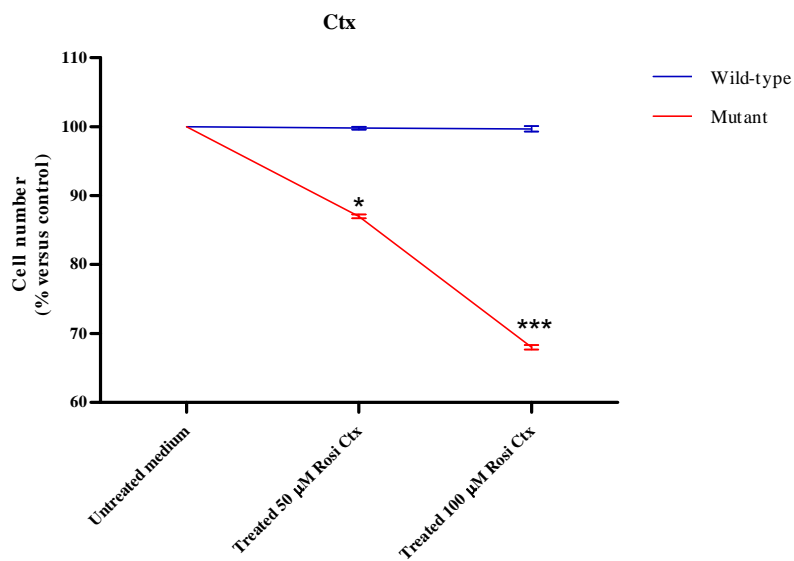


Figure 8-45 The change in the number of GFAP⁺ cells in 50 µM and 100 µM rosiglitazone treated mutant and wild-type mouse brain slices, compared to controls.

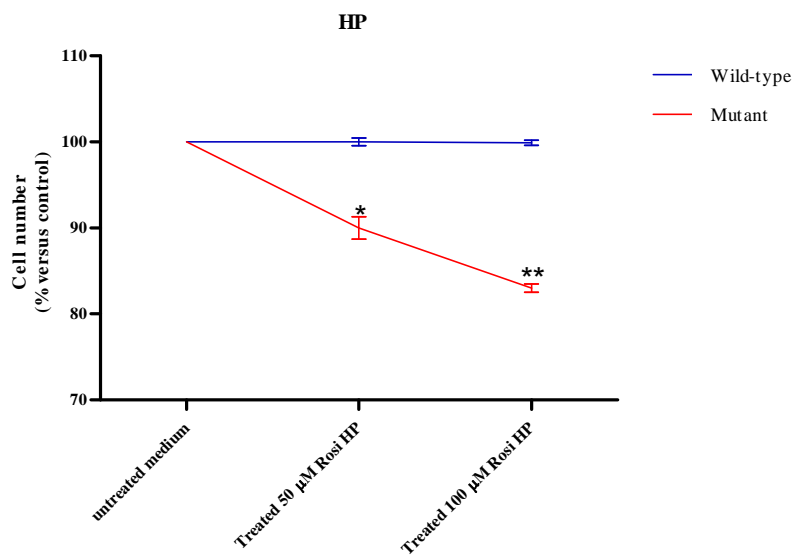


Figure 8-46 The change in the number of GFAP⁺ cells in 50 µM and 100 µM rosiglitazone treated wild-type and mutant mouse brain slices.

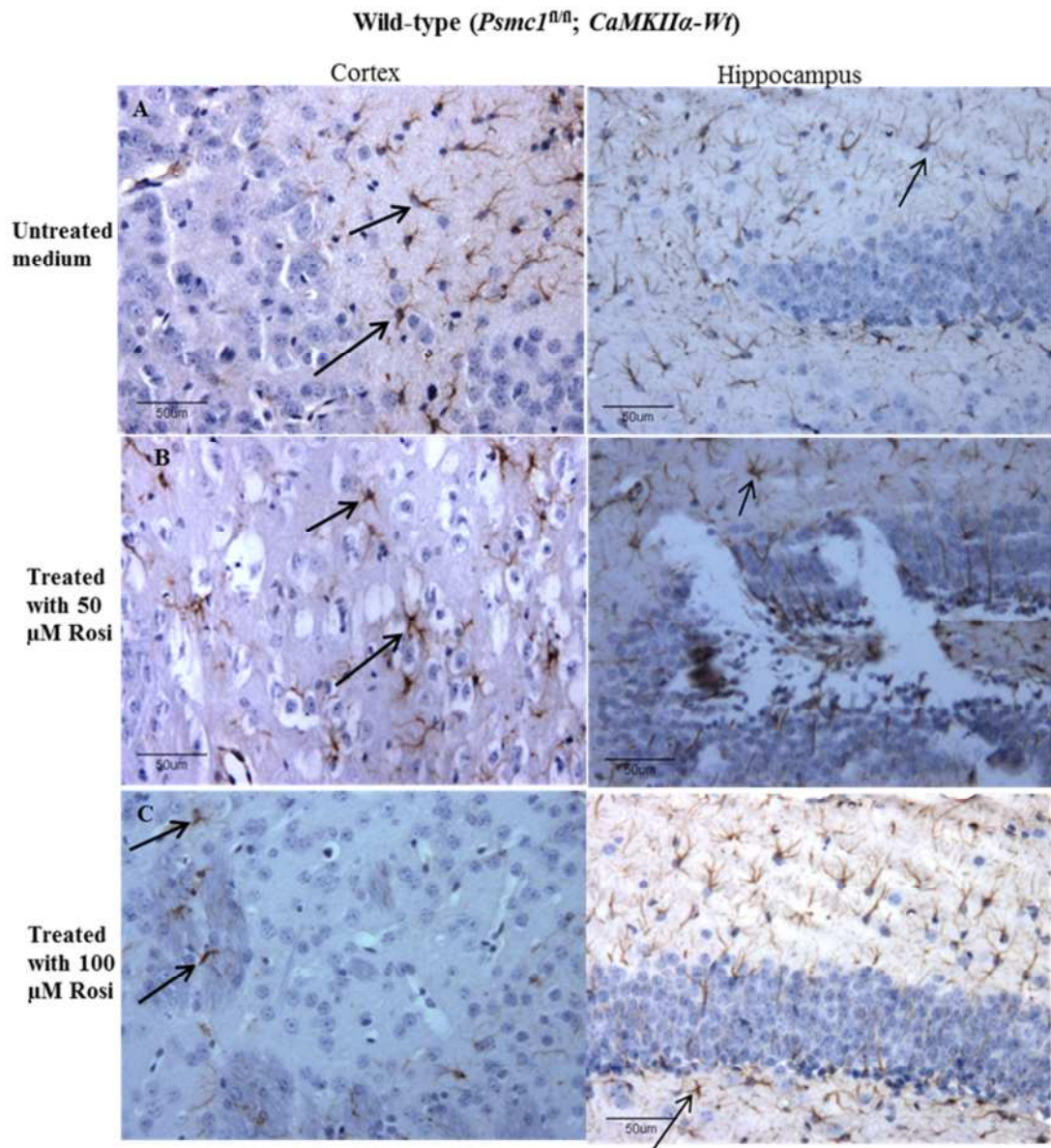


Figure 8-47 Effect of two different concentrations of rosiglitazone on the expression of astrocytes in the cortex and hippocampus in the brains of wild-type mice.

The micrographs represent immunohistochemistry staining of GFAP⁺ cells (astrocytes) in the cortex and hippocampus of wild-type mice after treatment with either 50 μ M or 100 μ M rosiglitazone. Investigating the reduction of astrocytes number. The PPAR- γ agonist caused a reduction in astrocytes number in the cortical areas at a concentration of 100 μ M but showed very little effect in the hippocampus in wild-type brain mice with no effect seen at a concentration of 50 μ M. Magnification is X20.

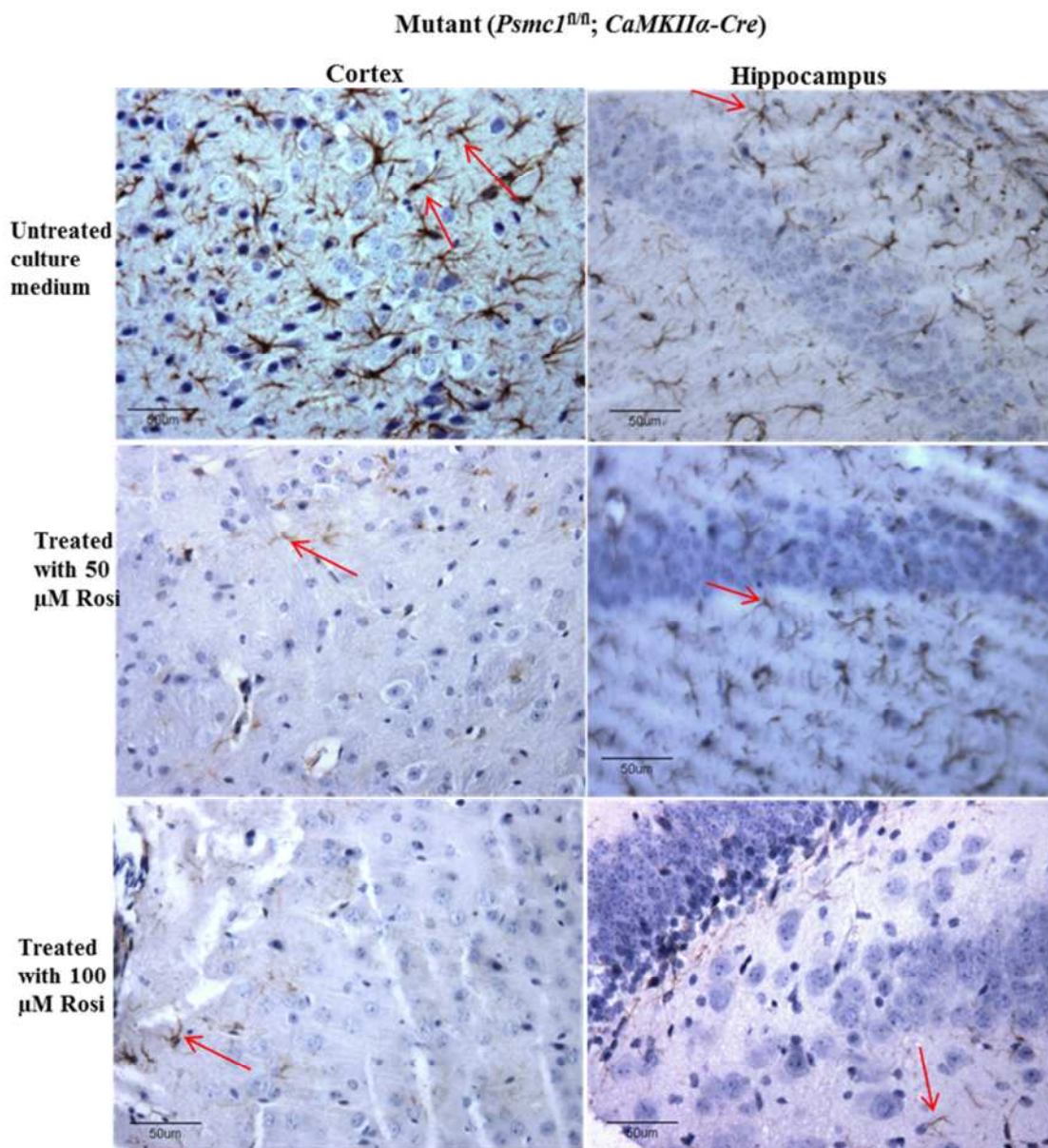


Figure 8-48 Effect of two different concentrations of rosiglitazone on the expression of astrocytes in the cortex and hippocampus in the brains of mutant mice.

The micrographs represent immunohistochemical staining of GFAP⁺ cells (astrocytes) in the cortex and hippocampus of mutant mice after treatment with either 50µM or 100 µM rosiglitazone. The PPAR- γ agonist has a potent effect on astrocyte number at 100 µM in both the cortex and hippocampus. Magnification is X20.

9. Discussion

9.1 Methodology validation

9.1.1 Assessment of the use of immunohistochemistry to detect astrocytes

There is an increasing number of studies investigating the involvement of astrocyte proliferation in neurodegenerative disorders (McGeer and McGeer 1995, Bolaños, Almeida et al. 1997, Chiarugi and Moskowitz 2003). This study has evaluated the role of PPAR- γ agonist, Rosiglitazone, in inhibiting astrocyte proliferation. To this end, it was necessary to optimise the tools and materials of the experiments:

- Validating the GFAP in staining the astrocytes.

In this process, several steps were optimised. These include determining the thickness of the paraffin sections of brain tissues, of which 5, 6, 7, 8, and 10 μm , were tested. 8 μm was the most suitable, as it showed better stability on the slide during immunohistochemical staining. Furthermore, this thickness enabled thorough penetration of the primary and secondary antibodies, particularly the fluorescent marker, Rhodamine red. If thinner slices were used, such as 5 μm , the brightness of the fluorescent marker was compromised after a week. A previous study cut 7 – 10 μm slices, which were double-stained successfully using immunohistochemistry. In this study a 10 μm was used for a double staining which provided enough penetration (Dickson, Farlo *et al.* 1988).

- The procedure required an optimised concentration of the GFAP primary antibody, to yield a good signal-to-noise ratio, prior to Rhodamine Red labelling. The ratio of the GFAP antibody (Thermo Scientific) to diluent used was 1:150, and this enabled better detection of astrocytes when compared to another GFAP antibody (Abcam) whereby the ratio was 1:100. The former yielded better results at a lower cost than that of the latter. The diluent ratio of 1:150 for the GFAP antibody (Thermo Scientific) is identical to that used by Ferriero and Aurora (Bergeron, Ferriero *et al.* 1997, Flax, Aurora *et al.* 1998). It was different to that of Zhang (2001) who used a ratio of 1:100. others used 1:50 concentration from Sigma. The use of normal goat

serum to prevent nonspecific binding was more effective at concentrations of 10% than 5% if, incubated for 1 hour for paraffin sections. Previous studies indicate varying concentrations of blocker have been used with paraffin sections. Clark et al. (2001) used between 3% - 50%, and concluded that concentrations between 3% and 10% were most suitable (Zhang, Wernig *et al.* 2001, Kaneko, Kawakami *et al.* 2006; Ozzello, De Rosa *et al.* 1987, Clark, Ding *et al.* 2001). The incubation time was extended to 3 hours in organotypic slice cultures using 10% bovine serum albumin in PBS (pH 7.4) to enable better penetration. Three concentrations were used in this study; 5, 10 and 15%. Of these 10% was the most effective, supported by Gulubova and Vlaykova (2008) who used 8% (Gulubova and Vlaykova 2008).

It was necessary to use antigen retrieval reagents to break the protein cross-links formed by fixation, to uncover hidden antigens. This procedure was optimised by increasing the vapour exposure time from 20 to 45 minutes. Longer exposure times resulted in a greater improvement in the clarity of the micrograph. Although Fiala, Liu et al. (2002) heated paraffin brain tissue sections for 25 mins, their tissue sections were at a thickness of 6 μ m which could account for the difference in vapour exposure time (Fiala, Liu *et al.* 2002).

9.1.2 The development of neurodegenerative diseases *in vivo*

A transgenic mouse model of neurodegeneration with 26S proteasome dysfunction was used. The model depends on a system known as *Cre-loxP* recombination which allows the DNA modifications to be targeted to a specific cell type. This model represents Lewy Body Dementia (LBD) in humans.

Paraffin sections were prepared from the brains of *Psmc1^{fl/fl}; CaMKII α -Cre* (mutant) (Ardley and Robinson) and *Psmc1^{fl/fl}; CaMKII α -Wt* (control) mice. Immunohistochemistry was performed for GFAP, to determine at which age astrocyte activation is triggered, following 26S proteasome dysfunction. This is the hallmark of the onset of neurodegeneration.

Identification of the age of disease onset was vital so that it could be correlated with start of drug administration. There was a gradual increase in number of astrocytes in the mutant mice, compared to the control mice at three weeks of age which became significant at four and six weeks. This correlates well with the reports of Bedford, Hay *et al.* (2008) who used the same mouse model to study 26S proteasomes in neurodegeneration (Bedford, Hay *et al.* 2008).

9.1.3 Evaluating the use of organotypic slice cultures study neurodegenerative diseases

Organotypic slice cultures proved to be a useful tool for understanding aspects of neurodegenerative disorders. The major advantage is that the glia cell grows in a 3-D configuration, helping to maintain both microcircuitry connections and relationships between neurons, glia and the extra cellular matrix (ECM). It closely resembles the *in vivo* state and is a relatively simple to prepare. However, the slices need to be treated carefully to avoid damage to the slice when transferring to the trans-well inserts.

9.1.3.1 Establishing the optimal conditions when conducting organotypic Slice Culture

The organotypic slice culture technique is fast becoming the favoured technique to study many CNS disorders, including neuronal death and other neurotoxic effects, such as oxidative stress. Nevertheless, slice culture studies present several difficulties. For example, some researches have experienced issues with secondary-antibody stimulated neurotransmitter release from astrocytes (Hamilton and Attwell 2010). When comparing the numbers of astrocytes in wild-type and mutant mice, there was still reliable detection of astrocytes (Section 8.4.2).

In order to determine the most appropriate slice culture conditions, many options have been considered, as shown in the results chapter (section 8.4.1). Postnatal

derived slice cultures are commonly used in the study of neurodegenerative disorders (Zimmer, Kristensen *et al.* 2000). In this study, slice cultures were derived from early postnatal mice (P1-P5) which helps to conserve the cytoarchitectural state of the slice, so that arrangement of cell bodies in their tissue is similar to that of the whole brain, *in vivo* (Gähwiler, Capogna *et al.* 1997)

In the current study, slices were cultured in two different inserts, of which the membranes were 0.4 μm and 3.0 μm in diameter. The 0.4 μm inserts provide sufficient oxygen and medium to the slice, as well as providing sufficient adhesion for the tissues compared to 3.0 μm pore. This is consistent with earlier studies, such as Lein, Barnhart *et al.* (2011) who provided the protocol of preparing hippocampal slices using the same system, and A. Alshehri (2010) who used an organotypic slice system (PhD thesis 2011) (Lein, Barnhart *et al.* 2011).

In terms of thickness, it was found that a typical thickness of 200 μm was optimal for detecting nerve cells under confocal microscope. However, for paraffin or cryostat sections from organotypic slice cultures, a thickness of 325-350 μm is preferred. 400 μm was not ideal, due to hypoxia of the slices, which resulted in the loss of in long-term cultures. Muller, (1996) reported that long-term culturing requires specific medium and a lower temperature of incubation, whereby 33°C is recommended (Muller, Wang *et al.* 1996).

Others have found 400 μm sections acceptable but it depends on the period of culture. Park, (2009) recommended slices between 300 and 400 μm thickness harvested from rat for ideal conditions for up to three weeks successful culture. In the present study the period of culture was six weeks, which would limit the use of 400 μm thick slices (Cho, Park *et al.* 2009).

The above circumstances have led to better survival of tissue culture in older animals. Nevertheless, the use of neonatal pups instead of adults remains the favourable option. However in situations where an adult brain slice (neuronal cell bodies) is desirable then it would be possible to use these specialised conditions. Cryostat sections were created at thickness 8 μm using coated glutamate slides, which was ideal for this study, while others used 12 μm thickness (Gao, Stieger *et al.* 1999).

9.1.3.2 Astrocytes nuclei modification in organotypic slice cultures

As another aspect of this work, it was observed that nuclei in the astrocytes of the brains of mutant animals were smaller and more oval, compared to those in the wild-type animals, which were larger and round. It was hypothesised that the astrocytes in mutant mouse brain should have undergone hypertrophy and hyperplasia. It has been suggested that cell division is dependent on nuclear size (Webster, Witkin *et al.* 2009). Villena *et al.*, (1997) suggested that nuclei did not shrink, but rather adapted to conditions, causing small nuclei to grow faster, until a suitable ratio is achieved (Villena, Diaz *et al.* 1997). In reference to Figure 8.13 the nuclei return to their normal size in the fifth week. An extra week was required in the organotypic slices cultures (Figure 8.14). This finding may support the notion raised by Bedford. Hay *et al.* (2008), noting that brains of mutant pups were smaller than those of the control pups (Bedford, Hay *et al.* 2008).

9.2 Peroxisome proliferator activated receptor- γ agonists

9.2.1 Rosiglitazone (Peroxisome proliferator activated receptor- γ agonist) may be effective in the treatment of human diseases

Evidence indicates that astrocyte activation is implicated in the pathogenesis of some neurodegenerative disorders. Astrocytes undergo changes during the process of neurodegeneration, including altered morphology, gene expression and cellular function. These can be collectively encompassed by the term 'reactive astrogliosis'. However, it is still not fully understood when and how proliferation arises in the developmental course of a neurodegenerative disorder (Sun, Xu *et al.* 2004).

9.2.1.1 Abolishing the actions of a PPAR- γ agonist

Many studies have implicated the T0070907 antagonist, as it potently abolishes PPAR- γ activity. The PPAR- γ antagonist T0070907 has the opposite effect to PPAR- γ agonists, as it causes anti-proliferative dose-response effects. Most researchers emphasize that it is necessary to have a higher antagonist concentration than agonist, in order to acquire a revoked effect (Burton, Goldenberg *et al.* 2008). The antagonist: agonist ratio is dependent on several conditions: the site of administration (i.e. oral or i.p dose), whether the study is *in vitro* or *in vivo*, and the origin of the tissue/cells.

In this study, the ratio of antagonist: agonist was (1:0.7) which was effective in reversing the effects of the agonist. Antagonist T0070907 abolished the effect seen with rosiglitazone treatment alone. The concentration used is lower than that in another study *in vivo*, whereby the ratio was 0.1:1.5 (Adabi Mohazab, Javadi-Paydar *et al.* 2012).

It has been reported that 10 – 20 μ M of the PPAR- γ antagonist were unable to inhibit the anti-inflammatory effects seen with 10 μ M of the PPAR- γ agonist rosiglitazone (Brody, Mandelkern *et al.* 2004, Ray, Akbiyik *et al.* 2006).

Lee *et al.* (2002) identified a potent of PPAR- γ function with T0070907 as PPAR- γ antagonists. She found that effects of rosiglitazone were blocked by 50% upon administration of T0070907

For optimal effects, an antagonist should be given prior to the agonist, however this is also subject to tissue/cell type. For example, in isolated glia cells *in vitro*, the T0070907 antagonist was added 30 minutes prior to the agonist; to be effective *in vivo*, it was necessary to add the antagonist 24 hours earlier (Ou, Zhao *et al.* 2006). As the organotypic slice cultures were thicker in this study, the antagonist was added 6 hr prior to the agonist, as well as using agonist treatment.

9.2.1.2 Dose-dependent effects of rosiglitazone, a PPAR- γ agonist

It was necessary to focus on the role of PPAR- γ agonists in reducing astrocyte proliferation, as this may contribute to knowledge for the future therapy of neurological degeneration. Rosiglitazone is an agonist of PPAR- γ , also known as thiazolidinedione (TZD). It is classified as a non-steroidal anti-inflammatory compound and is widely used in recent neurodegenerative experiments. Few studies have addressed the development of therapeutic strategy, with regards to inhibiting astrocyte activation in an attempt to reduce inflammation and neurotoxic effects in the CNS.

More recently, PPAR- γ agonists have been shown to affect production of pro-inflammatory molecules by primary microglia and astrocytes (Lovett-Racke, Hussain *et al.* 2004, Storer, Xu *et al.* 2005). Likewise, PPAR- γ agonists have also been shown to reduce disease pathology in animal models that previously presented neurodegenerative disorders (Racke and Drew 2008).

The mouse model chosen for this study has a proteasome deletion that causes neurodegeneration. In this model, astrocyte number increases in response to the neurodegenerative disorder. In this study, the finding that astrocyte activation was high at week 4 was interpreted as proteasome deletion in neurons, causing neuronal death. This is consistent with the findings of Bedford, (2008). At week 4, the neurons may send a signal to astrocytes, causing them to enter proliferation (Bedford, Hay *et al.* 2008). Another possibility is that as a result of neuronal death, the astrocytes increase in number to fill the gaps left by the neurons.

Three different concentrations of rosiglitazone were administered. The high concentrations (50 μM and 100 μM) have shown significant reduction in astrocyte activation in mutant animals. It is known from the literature that, PPAR- γ regulates gene transcription heterodimers with the retinoic acid receptor (RXR), by binding to a precise site of DNA sequences, termed peroxisome proliferator response elements (PPREs). The mechanism of PPAR- γ agonists rely on the increase in the binding of PPAR- γ to PPRE's, resulting in enhanced translational activity of PPAR- γ (Yi, Park *et al.* 2007).

It was expected that rosiglitazone would reduce proliferating cell number in brain slices, as shown by GFAP⁺ cells staining. Rosario Luna *et al.* (2005) reported that PPAR- γ receptor played a vital role in the regulation of cellular proliferation and inflammation. The majority of the results from the present study agreed with this, as it showed that rosiglitazone did alter proliferation in the hippocampus. This may be consistent with another finding, that a 50 μM dose did not cause a reduction in proliferation in the hippocampus, while increasing the dose to 100 μM , caused a significant effect. The number of astrocytes was decreased and statistically different in mutant brains, compared to wild-type brains in both the cortex and hippocampus. However, lower doses of 25 μM had no effect on the astrocyte number in mutant mice in either regions (Luna-Medina, Cortes-Canteli *et al.* 2005).

9.3 Conclusion

Peroxisome proliferator-activated receptor gamma is protective against neurodegeneration, by its action in preventing astrocyte proliferation. Rosiglitazone acts as an agonist for PPAR- γ and inhibits secretion of pro-inflammatory molecules (Sastre, Klockgether *et al.* 2006). This effect could be reversed by administration of the antagonist T0070907. In the current study, it was hypothesized that treatment with the PPAR- γ agonist rosiglitazone could be used to inhibit astrocyte proliferation, and therefore enhance neuro-protection against neurodegenerative disorders. Organotypic slice cultures were treated with 25 μ M, 50 μ M and 100 μ M doses of Rosiglitazone after five weeks of culture for 7 days. This experiment showed a therapeutic effect of rosiglitazone, after it was bound to PPAR- γ . Rosiglitazone is capable of reducing astrocyte proliferation, which could reduce the effects of neurodegeneration in this particular model. The current study produced similar findings to studies that have also utilized this PPAR- γ agonist. For example, rosiglitazone has also been shown to prevent cognitive impairment by inhibiting astrocyte activation and oxidative stress in a rat epilepsy model of neurodegenerative disease (Chuang, Lin *et al.* 2012). Similar to the current study it was concluded that the PPAR- γ agonist caused decreased numbers of immune cells, astrocytes, oligodendrocytes, neurons and microglia and may therefore be effective as a therapeutic drug used to inhibit neurodegeneration (Chuang, Lin *et al.* 2012).

Part 3

GENERAL DISCUSSION

Future work

10. General discussion

Peroxisome proliferators are a class of chemicals that have diverse effects in rats and mice including the induction of increased DNA synthesis and peroxisome proliferation. These chemicals act through ligand activation of nuclear membrane receptors termed ‘peroxisome-proliferator-activated receptors’ (PPARs), which themselves act as nuclear transcription factors. This project focused on an investigation of the biological roles of PPs, covering two aspects: a follow on from previous work to investigate the role of the PPs in the liver growth, and investigation of the role of this chemical class in the treatment of neurodegeneration. This ironically involved an examination of both the detrimental aspects of PPs in causing disease, but also the beneficial aspects in their possible use for medical treatment.

10.1 Role of peroxisome proliferators in liver growth

Peroxisome proliferators include herbicides, plasticisers, hypolipidemic drugs and synthetic fatty acids. However, the mechanism of action of increased hepatocyte growth is not currently understood. It was hoped that gaining understanding relating to the mechanism by which increased liver growth is induced by PPs in rodents would hopefully provide insights into how natural liver growth occurs and have medical benefits for human health if the mechanism of PP toxicity can be overcome. Knowledge gained from the mechanism of PP activation might also then be applied to other chemical carcinogens. Experimental work was undertaken to determine if the same, of different hepatocyte cells, were induced to divide during the two rounds of cell division following ciprofibrate treatment revealed. The two histochemical stains used were EdU and BrdU, which are both base-pair analogues that stain nuclei undergoing DNA replication.

The results showed that the cells undergoing division at 24 hr were not related to those that undergoing division at 48 hr following repeat treatment with ciprofibrate.

This is of medical significance as it suggests that there are not hepatic cells that are especially sensitive to repeated PP treatment, but that different cells can respond and therefore there is a more general risk of increased cell division and carcinogenesis from such non-genotoxic carcinogenic compounds.

In related studies, previous work had investigated the effects of the genotoxic carcinogen; cyproterone acetate (CPA) on hepatocyte growth of male rats treated with 100 mg/kg CPA. In the present study female rats were treated with CPA, to firstly evaluate whether differences in labelling indices were present compared to male rats. Female F-344/NHsd rats, aged 14-15 weeks, were treated at time 0 with CPA and then injected i.p with BrdU at 22 hr, and rats were killed 2 hr later. Results showed that the female rats were found to indeed have a considerably higher labelling index (38.9%) compared to male rats (6%), confirming the results of Amer (2011). This finding suggested that upregulation of gene expression in female rats should be much higher as well, which might provide an exciting opportunity to identify sets of genes involved in carcinogenic response, with overlap with those involved PP response, including those of possible low transcript number.

This study then made a preliminary investigation of whether genes induced by chemical treatment are largely the same or different between ciprofibrate and CPA i.e. whether they might share some underlying mechanisms of action. This followed previous work undertaken by Amer (2011) at Nottingham who used microarray analysis to identify global sets of genes that are upregulated by CPA and ciprofibrate treatment. Due to time restriction only preliminary work could be undertaken using real-time PCR methodology to study changes in expression in three target genes, *Scd1*, *Ccnd1* and *G0s2* (together with the *CY3A1* control) previously identified by Amer (2011). Of these genes, only *Ccnd1* showed a similar pattern of induction between CPA and ciprofibrate. Thus, overall there was little evidence of shared pathways between CPA and ciprofibrate activity and therefore different mechanism of cell toxicity are likely to be present, albeit with some potential overlap as shown by the *Ccnd1* gene. So to conclude, although ciprofibrate and CPA are chemicals which both cause liver growth and possible cancer, they appear to do so by completely difference mechanisms.

10.2 Role of peroxisome proliferators in neurodegenerative disorders

The second part of research project presented in this thesis aimed to use a mouse model to investigate the role of peroxisome proliferators (primarily rosiglitazone) in causing neurodegenerative disorder, using Parkinson's disease (PD) as an example. Organotypic slice cultures were used to discover whether rosiglitazone is involved in inhibiting astrocytes activation. To this end, a series of experiments were performed to optimise the tools and materials for the experiments in order to test the hypothesis that PPs have the ability to reduce astrocyte proliferation.

Studies were made using an organotypic slice system, an animal model system which allowed neurodegeneration progression to be monitored *in vitro* in particular, this system enabled a closed study to be made of the effect of rosiglitazone in reducing the progression of disease, by tracking the evolution of astrocytes activation. Given that PPARs bind DNA as heterodimers with RXR, it was considered possible that therefore PPAR- γ activation by anti-inflammatory drug ligands might regulate the activation of macrophages and astrocytes.

Preliminary results showed that development of disease was apparent at 4, 5 and 6 weeks of growth in organotypic slice cultures harvested from brain mutant pups. Based on this disease progression it was decided to commence drug treatment of the agonist rosiglitazone at 5 weeks of age, with the drug being given for 7 days. This was found to result in extensive astrogliosis activity in both areas of interest, namely the hippocampus and cortex.

From the literature review chapter, it is known that the dementia with lewy bodies is associated with proteasome 26S deletion. One possible scenario is that PPAR- γ agonists might alter/enhance proteasome 26S activity in such a way that this results in a reduction in proliferation of astrocytes in both the hippocampus and cortex regions, compared to wild-type mice. This was consistent with observations from the present study that treatment with rosiglitazone resulted in a significant reduction in the number of astrocytes at concentrations of both 50 and 100 μM . This finding suggests that the PP rosiglitazone can be considered for potential use as a therapeutic drug to inhibit neurodegeneration.

11. Future work

11.1 Studies on PP and CPA toxicity and mode of action

Due to time restrictions and changes in supervision, only a very limited pilot study of changes in expression in three target genes (together with the *CY3A1* control) in response to CPA treatment was made. But ideally a far larger number of genes should be assayed to determine whether similar sets of genes are induced in female rat liver cells by the genotoxic carcinogen cyproterone acetate (CPA) as are induced by ciprofibrate. This work might be achieved for instance by RNA seq studies. Should it then be found that particular genes were identified with clear differential expression following treatment by both carcinogens, then this raises the question of what is their function and how do they work? Is the protein associated with the RNA? To investigate these questions it would be worthwhile exploring the possibility of using a knock out mouse which lacks that gene to determine possible physiological effects (Aleshin, Grabeklis *et al.* 2009).

11.2 Studies on role of PPs in neurodegenerative disorders

In this part of study we wished to use *in vitro* methods, due to the benefits of this technique in reducing the number of animals used and increasing the ability to control experimental parameters. It is also important to compare the results with those *in vivo* to confirm the relevance of the results in a whole animal

In this work, we have demonstrated the neuroprotective potential of a peroxisome proliferator activated receptor gamma agonist, rosiglitazone in an *ex vivo* model of dementia with lewy body model. It would be beneficial to further these studies by the administration of rosiglitazone to mice *in vivo* and assess its beneficial effects. In addition, it would be important to include other neurodegenerative disease models such as Alzheimer disease, which will also benefit from rosiglitazone treatment where the focus is on inflammatory processes, such as microgliosis.

Further studies are required to elucidate the molecular mechanism by which PPAR- γ agonist attach to the proliferation sites of astrocytes.

12. References

- Abeles, M. (1991). Corticomics: Neural circuits of the cerebral cortex, Cambridge University Press.
- Abrous, D. N., M. Koehl and M. Le Moal (2005). "Adult neurogenesis: from precursors to network and physiology." Physiological Reviews **85**(2): 523-569.
- Adabi Mohazab, R., M. Javadi-Paydar, B. Delfan and A. R. Dehpour (2012). "Possible involvement of PPAR-gamma receptor and nitric oxide pathway in the anticonvulsant effect of acute pioglitazone on pentylenetetrazole-induced seizures in mice." Epilepsy Research **101**(1): 28-35.
- Aggarwal, B. B. and K. B. Harikumar (2009). "Potential therapeutic effects of curcumin, the anti-inflammatory agent, against neurodegenerative, cardiovascular, pulmonary, metabolic, autoimmune and neoplastic diseases." The International Journal of Biochemistry & Cell Biology **41**(1): 40-59.
- Akaike, A., Y. Takada-Takatori, T. Kume and Y. Izumi (2010). "Mechanisms of neuroprotective effects of nicotine and acetylcholinesterase inhibitors: role of $\alpha 4$ and $\alpha 7$ receptors in neuroprotection." Journal of Molecular Neuroscience **40**(1-2): 211-216.
- Al Kholaiifi, A., A. Amer, B. Jeffery, T. Gray, R. Roberts and D. Bell (2008). "Species-specific kinetics and zonation of hepatic DNA synthesis induced by ligands of PPAR {alpha}." Toxicological Sciences **104**(1): 74.
- Aleshin, S., S. Grabeklis, T. Hanck, M. Sergeeva and G. Reiser (2009). "Peroxisome proliferator-activated receptor (PPAR)- γ positively controls and PPAR α negatively controls cyclooxygenase-2 expression in rat brain astrocytes through a convergence on PPAR β/δ via mutual control of PPAR expression levels." Molecular Pharmacology **76**(2): 414-424.
- Allaman, I., M. Bélanger and P. J. Magistretti (2011). "Astrocyte–neuron metabolic relationships: for better and for worse." Trends In Neurosciences **34**(2): 76-87.
- Allen, N. J. and B. A. Barres (2009). "Neuroscience: glia—more than just brain glue." Nature **457**(7230): 675-677.
- Altmann, G. and C. Leblond (1982). "Changes in the size and structure of the nucleolus of columnar cells during their migration from crypt base to villus top in rat jejunum." Journal of Cell Science **56**(1): 83.
- Amer, A. H. (2011). Mechanism of action of liver growth induced by peroxisome proliferators, University of Nottingham.

Amer, A. H. A. (2011). Mechanism of action of liver growth induced by peroxisome proliferators, University of Nottingham.

Ardley, H. C. and P. A. Robinson (2004). "The role of ubiquitin-protein ligases in neurodegenerative disease." Neurodegener Dis **1**(2-3): 71-87.

Ashby, J., A. Brady, C. R. Elcombe, B. M. Elliott, J. Ishmael, J. Odum, J. D. Tugwood, S. Kettle and I. F. Purchase (1994). "Mechanistically-based human hazard assessment of peroxisome proliferator-induced hepatocarcinogenesis." Hum Exp Toxicol **13 Suppl 2**: S1-117.

Bailey, I., G. G. Gibson, K. Plant, M. Graham and N. Plant (2011). "A PXR-mediated negative feedback loop attenuates the expression of CYP3A in response to the PXR agonist pregnenolone-16 α -carbonitrile." PLoS One **6**(2): e16703.

Baker, V. A., H. M. Harries, J. F. Waring, C. M. Duggan, H. A. Ni, R. A. Jolly, L. W. Yoon, A. T. De Souza, J. E. Schmid and R. H. Brown (2004). "Clofibrate-induced gene expression changes in rat liver: a cross-laboratory analysis using membrane cDNA arrays." Environmental Health Perspectives **112**(4): 428.

Barbeito, L. H., M. Pehar, P. Cassina, M. R. Vargas, H. Peluffo, L. Viera, A. G. Estévez and J. S. Beckman (2004). "A role for astrocytes in motor neuron loss in amyotrophic lateral sclerosis." Brain Research Reviews **47**(1): 263-274.

Bartholdi, D. and M. E. Schwab (2006). "Expression of pro-inflammatory cytokine and chemokine mRNA upon experimental spinal cord injury in mouse: An in situ hybridization study." European Journal of Neuroscience **9**(7): 1422-1438.

Bartus, R. T. and R. L. Dean III (2009). "Pharmaceutical treatment for cognitive deficits in Alzheimer's disease and other neurodegenerative conditions: exploring new territory using traditional tools and established maps." Psychopharmacology **202**(1-3): 15-36.

Bear, M. F., B. W. Connors and M. A. Paradiso (2006). Neuroscience: Exploring the brain, Lippincott Williams & Wilkins.

Bedford, L., D. Hay, A. Devoy, S. Paine, D. G. Powe, R. Seth, T. Gray, I. Topham, K. Fone and N. Rezvani (2008). "Depletion of 26S proteasomes in mouse brain neurons causes neurodegeneration and Lewy-like inclusions resembling human pale bodies." The Journal of Neuroscience **28**(33): 8189-8198.

Bergeron, M., D. M. Ferriero, H. J. Vreman, D. K. Stevenson and F. R. Sharp (1997). "Hypoxia-ischemia, but not hypoxia alone, induces the expression of heme oxygenase-1 (HSP32) in newborn rat brain." Journal of Cerebral Blood Flow & Metabolism **17**(6): 647-658.

Bernardo, A. and L. Minghetti (2006). "PPAR-agonists as regulators of microglial activation and brain inflammation." Current Pharmaceutical Design **12**(1): 93-109.

Bianco, C. L., J. Ridet, B. Schneider, N. Deglon and P. Aebischer (2002). " α -Synucleinopathy and selective dopaminergic neuron loss in a rat lentiviral-based model of Parkinson's disease." Proceedings of the National Academy of Sciences **99**(16): 10813-10818.

Bignami, A. and D. Dahl (2008). "The astroglial Response to Stabbing. Immunofluorescence studies with antibodies to astrocyte-specific protein (gfa) in mammalian and submammalian vertebrates." Neuropathology and Applied Neurobiology **2**(2): 99-110.

Blackburn, D., S. Sargsyan, P. N. Monk and P. J. Shaw (2009). "Astrocyte function and role in motor neuron disease: a future therapeutic target?" Glia **57**(12): 1251-1264.

Bliss, T. V. and G. L. Collingridge (1993). "A synaptic model of memory: long-term potentiation in the hippocampus." Nature **361**(6407): 31-39.

Boenisch, T. (2001). "Formalin-fixed and heat-retrieved tissue antigens: a comparison of their immunoreactivity in experimental antibody diluents." Applied Immunohistochemistry & Molecular Morphology **9**(2): 176.

Boenisch, T., A. Farmilo and R. Stead (2001). Handbook, Immunochemical Staining Methods, Dako Corporation.

Bolaños, J. P., A. Almeida, V. Stewart, S. Peuchen, J. M. Land, J. B. Clark and S. J. Heales (1997). "Nitric oxide-mediated mitochondrial damage in the brain: Mechanisms and implications for neurodegenerative diseases." Journal of Neurochemistry **68**(6): 2227-2240.

Brambilla, G. and A. Martelli (2002). "Are some progestins genotoxic liver carcinogens?" Mutation Research/Reviews in Mutation Research **512**(2): 155-163.

Brody, A. L., M. A. Mandelkern, M. E. Jarvik, G. S. Lee, E. C. Smith, J. C. Huang, R. G. Bota, G. Bartzokis and E. D. London (2004). "Differences between smokers and nonsmokers in regional gray matter volumes and densities." Biological Psychiatry **55**(1): 77-84.

Brown, C. M., B. Reisfeld and A. N. Mayeno (2008). "Cytochromes P450: a structure-based summary of biotransformations using representative substrates." Drug Metabolism Reviews **40**(1): 1-100.

Buffo, A., C. Rolando and S. Ceruti (2010). "Astrocytes in the damaged brain: molecular and cellular insights into their reactive response and healing potential." Biochemical Pharmacology **79**(2): 77-89.

Bulera, S. J., S. M. Eddy, E. Ferguson, T. A. Jatko, J. F. Reindel, M. R. Bleavins and F. A. De La Iglesia (2001). "RNA expression in the early characterization of

hepatotoxicants in Wistar rats by high-density DNA microarrays." Hepatology **33**(5): 1239-1258.

Bünger, M., G. J. E. J. Hooiveld, S. Kersten and M. Müller (2007). "Exploration of PPAR functions by microarray technology--a paradigm for nutrigenomics." Biochimica et Biophysica Acta (BBA)-Molecular and Cell Biology of Lipids **1771**(8): 1046-1064.

Burton, J. D., D. M. Goldenberg and R. D. Blumenthal (2008). "Potential of peroxisome proliferator-activated receptor gamma antagonist compounds as therapeutic agents for a wide range of cancer types." PPAR research **2008**.

Bustin, S. A., V. Benes, J. A. Garson, J. Hellemans, J. Huggett, M. Kubista, R. Mueller, T. Nolan, M. W. Pfaffl and G. L. Shipley (2009). "The MIQE guidelines: minimum information for publication of quantitative real-time PCR experiments." Clinical Chemistry **55**(4): 611-622.

Cappella, P., F. Gasparri, M. Pulici and J. Moll (2008). "A novel method based on click chemistry, which overcomes limitations of cell cycle analysis by classical determination of BrdU incorporation, allowing multiplex antibody staining." Cytometry Part A **73**(7): 626-636.

Carta, A. (2013). "PPAR- γ : Therapeutic Prospects in Parkinson's Disease." Current Drug Targets.

Carta, A. R. and A. Pisanu (2012). "Modulating Microglia Activity with PPAR- γ Agonists: A Promising Therapy for Parkinson's Disease?" Neurotoxicity Research: 1-12.

Cattley, R. C. (2003). "Regulation of cell proliferation and cell death by peroxisome proliferators." Microsc Res Tech **61**(2): 179-184.

Cattley, R. C., D. S. Marsman and J. A. Popp (1991). "Age-related susceptibility to the carcinogenic effect of the peroxisome proliferator WY-14,643 in rat liver." Carcinogenesis **12**(3): 469-473.

Cavalieri, E., K. Frenkel, J. G. Liehr, E. Rogan and D. Roy (2000). "Estrogens as endogenous genotoxic agents—DNA adducts and mutations." JNCI Monographs **2000**(27): 75-94.

Chang, M. S. (2009). Anti-IL-20 antibody and its use in treating IL-20 associated inflammatory diseases, Google Patents.

Chiarugi, A. and M. A. Moskowitz (2003). "Poly (ADP-ribose) polymerase-1 activity promotes NF- κ B-driven transcription and microglial activation: implication for neurodegenerative disorders." Journal of Neurochemistry **85**(2): 306-317.

Chinetti, G., J.-C. Fruchart and B. Staels (2000). "Peroxisome proliferator-activated receptors (PPARs): nuclear receptors at the crossroads between lipid metabolism and inflammation." Inflammation Research **49**(10): 497-505.

Cho, J.-S., H.-W. Park, S.-K. Park, S. Roh, S.-K. Kang, K.-S. Paik and M.-S. Chang (2009). "Transplantation of mesenchymal stem cells enhances axonal outgrowth and cell survival in an organotypic spinal cord slice culture." Neuroscience letters **454**(1): 43-48.

Chuang, Y.-C., T.-K. Lin, H.-Y. Huang, W.-N. Chang, C.-W. Liou, S.-D. Chen, A. Y. Chang and S. H. Chan (2012). "Peroxisome proliferator-activated receptors γ /mitochondrial uncoupling protein 2 signaling protects against seizure-induced neuronal cell death in the hippocampus following experimental status epilepticus." Journal of Neuroinflammation **9**(1): 1-18.

Ciechanover, A. (2005). "Intracellular protein degradation: from a vague idea thru the lysosome and the ubiquitin-proteasome system and onto human diseases and drug targeting*." Cell Death & Differentiation **12**(9): 1178-1190.

Clark, D. A., J.-W. Ding, G. Yu, G. A. Levy and R. M. Gorczynski (2001). "Fgl2 prothrombinase expression in mouse trophoblast and decidua triggers abortion but may be countered by OX-2." Molecular Human Reproduction **7**(2): 185-194.

Coleman, W. B. and D. H. Best (2005). "Cellular responses in experimental liver injury: Possible cellular origins of regenerative stem-like progenitor cells." Hepatology **41**(5): 1173-1176.

Connolly, K. and M. Bogdanffy (1993). "Evaluation of proliferating cell nuclear antigen (PCNA) as an endogenous marker of cell proliferation in rat liver: a dual-stain comparison with 5-bromo-2'-deoxyuridine." Journal of Histochemistry & Cytochemistry **41**(1): 1-6.

Constan, A. A., C. S. Sprankle, J. M. Peters, G. L. Kedderis, J. I. Everitt, B. A. Wong, F. L. Gonzalez and B. E. Butterworth (1999). "Metabolism of chloroform by cytochrome P450 2E1 is required for induction of toxicity in the liver, kidney, and nose of male mice." Toxicology and Applied Pharmacology **160**(2): 120-126.

Cristiano, L., A. Bernardo and M. P. Cerù (2001). "Peroxisome proliferator-activated receptors (PPARs) and peroxisomes in rat cortical and cerebellar astrocytes." Journal of Neurocytology **30**(8): 671-683.

Crunkhorn, S. E., K. E. Plant, G. G. Gibson, K. Kramer, J. Lyon, P. G. Lord and N. J. Plant (2004). "Gene expression changes in rat liver following exposure to liver growth agents: role of Kupffer cells in xenobiotic-mediated liver growth." Biochemical Pharmacology **67**(1): 107-118.

Cullingford, T. E., K. Bhakoo, S. Peuchen, C. T. Dolphin, R. Patel and J. B. Clark (1998). "Distribution of mRNAs Encoding the Peroxisome Proliferator-Activated

-
- Receptor α , β , and γ and the Retinoid X Receptor α , β , and γ in Rat Central Nervous System." Journal of Neurochemistry **70**(4): 1366-1375.
- Culman, J., Y. Zhao, P. Gohlke and T. Herdegen (2007). "PPAR- γ : therapeutic target for ischemic stroke." Trends in Pharmacological Sciences **28**(5): 244-249.
- Dahlstrand, J., M. Lardelli and U. Lendahl (1995). "Nestin mRNA expression correlates with the central nervous system progenitor cell state in many, but not all, regions of developing central nervous system." Developmental Brain Research **84**(1): 109-129.
- Dehm, S. and D. Tindall (2005). "Regulation of androgen receptor signaling in prostate cancer." Expert Review of Anticancer Therapy **5**(1): 63-74.
- Del Cul, A., S. Dehaene, P. Reyes, E. Bravo and A. Slachevsky (2009). "Causal role of prefrontal cortex in the threshold for access to consciousness." Brain **132**(9): 2531-2540.
- Dementia, C. I. N. and M. C. I. MCI "AAGP Position Statement: Principles of Care for Patients With Dementia Resulting From Alzheimer Disease."
- Deml, E., L. Schwarz and D. Oesterle (1993). "Initiation of enzyme-altered foci by the synthetic steroid cyproterone acetate in rat liver foci bioassay." Carcinogenesis **14**(6): 1229.
- Dhaunsi, G. S., I. Singh, J. K. Orak and A. K. Singh (1994). "Antioxidant enzymes in ciprofibrate-induced oxidative stress." Carcinogenesis **15**(9): 1923-1930.
- Di Napoli, M. and B. A. McLaughlin (2005). "The proteasome ubiquitin system as a drug target in cerebrovascular disease: The therapeutic potential of proteasome inhibitors." Current opinion in Investigational Drugs (London, England: 2000) **6**(7): 686.
- Dickson, D., J. Farlo, P. Davies, H. Crystal, P. Fuld and S.-H. Yen (1988). "Alzheimer's disease. A double-labeling immunohistochemical study of senile plaques." The American Journal of Pathology **132**(1): 86.
- Djebaili, M., Q. Guo, E. H. Pettus, S. W. Hoffman and D. G. Stein (2005). "The neurosteroids progesterone and allopregnanolone reduce cell death, gliosis, and functional deficits after traumatic brain injury in rats." Journal of Neurotrauma **22**(1): 106-118.
- Egolf, D. B. (2012). Human Communication and the Brain: Building the Foundation for the Field of Neurocommunication, Lexington Books.
- El-Sankary, W., G. G. Gibson, A. Ayrton and N. Plant (2001). "Use of a reporter gene assay to predict and rank the potency and efficacy of CYP3A4 inducers." Drug Metabolism and Disposition **29**(11): 1499-1504.
-

-
- Emerit, J., M. Edeas and F. Bricaire (2004). "Neurodegenerative diseases and oxidative stress." Biomedicine & Pharmacotherapy **58**(1): 39-46.
- Ezaki, H., Y. Yoshida, Y. Saji, T. Takemura, J. Fukushima, H. Matsumoto, Y. Kamada, A. Wada, T. Igura and S. Kihara (2009). "Delayed liver regeneration after partial hepatectomy in adiponectin knockout mice." Biochemical and Biophysical Research Communications **378**(1): 68-72.
- Fahl, W., N. Lalwani, T. Watanabe, S. Goel and J. Reddy (1984). "DNA damage related to increased hydrogen peroxide generation by hypolipidemic drug-induced liver peroxisomes." Proceedings of the National Academy of Sciences of the United States of America **81**(24): 7827.
- Fausto, N. (2000). "Liver regeneration." Journal of hepatology **32**: 19-31.
- Fausto, N. and E. Webber (1993). "Control of liver growth." Critical Reviews in Eukaryotic Gene Expression **3**(2): 117.
- Fiala, M., Q. Liu, J. Sayre, V. Pop, V. Brahmandam, M. Graves and H. Vinters (2002). "Cyclooxygenase-2-positive macrophages infiltrate the Alzheimer's disease brain and damage the blood-brain barrier." European Journal of Clinical Investigation **32**(5): 360-371.
- Finn, R. D., C. J. Henderson, C. L. Scott and C. R. Wolf (2009). "Unsaturated fatty acid regulation of cytochrome P450 expression via a CAR-dependent pathway." Biochemical Journal **417**(Pt 1): 43.
- Fischl, B. and A. M. Dale (2000). "Measuring the thickness of the human cerebral cortex from magnetic resonance images." Proceedings of the National Academy of Sciences **97**(20): 11050-11055.
- Fiskerstrand, T., D. H'Mida-Ben Brahim, S. Johansson, A. M'Zahem, B. I. Haukanes, N. Drouot, J. Zimmermann, A. J. Cole, C. Vedeler, C. Bredrup, M. Assoum, M. Tazir, T. Klockgether, A. Hamri, V. M. Steen, H. Boman, L. A. Bindoff, M. Koenig and P. M. Knappskog (2010). "Mutations in ABHD12 cause the neurodegenerative disease PHARC: An inborn error of endocannabinoid metabolism." Am J Hum Genet **87**(3): 410-417.
- Flax, J. D., S. Aurora, C. Yang, C. Simonin, A. M. Wills, L. L. Billingham, M. Jendoubi, R. L. Sidman, J. H. Wolfe and S. U. Kim (1998). "Engraftable human neural stem cells respond to development cues, replace neurons, and express foreign genes." Nature biotechnology **16**(11): 1033-1039.
- Fraenkel, J. R., N. E. Wallen and H. H. Hyun (1993). "How to design and evaluate research in education."
-

-
- Franke, H., U. Krügel, J. Grosche and P. Illes (2003). "Immunoreactivity for glial fibrillary acidic protein and P2 receptor expression on astrocytes in vivo." Drug Development Research **59**(1): 175-189.
- Gähwiler, B., M. Capogna, D. Debanne, R. McKinney and S. Thompson (1997). "Organotypic slice cultures: a technique has come of age." Trends in Neurosciences **20**(10): 471-477.
- Gao, B., B. Stieger, B. Noé, J.-M. Fritschy and P. J. Meier (1999). "Localization of the organic anion transporting polypeptide 2 (Oatp2) in capillary endothelium and choroid plexus epithelium of rat brain." Journal of Histochemistry & Cytochemistry **47**(10): 1255-1263.
- Gavériaux-Ruff, C. and B. L. Kieffer (2007). "Conditional gene targeting in the mouse nervous system: Insights into brain function and diseases." Pharmacology & Therapeutics **113**(3): 619-634.
- Gilbert, P. E., R. P. Kesner and I. Lee (2001). "Dissociating hippocampal subregions: a double dissociation between dentate gyrus and CA1." Hippocampus **11**(6): 626-636.
- Gill, J. H., N. H. James, R. A. Roberts and C. Dive (1998). "The non-genotoxic hepatocarcinogen nafenopin suppresses rodent hepatocyte apoptosis induced by TGFbeta1, DNA damage and Fas." Carcinogenesis **19**(2): 299-304.
- Glöckner, R., J. Wagener, A. Lieder and D. Müller (2003). "< i> In vitro</i> induction of cytochrome P4503A1-mRNA and testosterone hydroxylation in precision-cut liver slices from male and female rats." Experimental and Toxicologic Pathology **54**(5): 411-415.
- Gluck, M. A., M. Meeter and C. E. Myers (2003). "Computational models of the hippocampal region: linking incremental learning and episodic memory." Trends in Cognitive Sciences **7**(6): 269-276.
- Goedert, M., F. Clavaguera and M. Tolnay (2010). "The propagation of prion-like protein inclusions in neurodegenerative diseases." Trends in Neurosciences **33**(7): 317-325.
- Goodwin, B., M. R. Redinbo and S. A. Kliewer (2002). "Regulation of CYP3A Gene Transcription by the Pregnane X Receptor*." Annual review of Pharmacology and Toxicology **42**(1): 1-23.
- Gournay, J., I. Auvigne, V. Pichard, C. Ligeza, M. Bralet and N. Ferry (2002). "In vivo cell lineage analysis during chemical hepatocarcinogenesis in rats using retroviral-mediated gene transfer: evidence for dedifferentiation of mature hepatocytes." Laboratory Investigation **82**(6): 781-788.
-

-
- Grisham, J. (1962). "A morphologic study of deoxyribonucleic acid synthesis and cell proliferation in regenerating rat liver; autoradiography with thymidine-H3." Cancer research **22**(7 Part 1): 842.
- Gulubova, M. and T. Vlaykova (2008). "Chromogranin A-, serotonin-, synaptophysin- and vascular endothelial growth factor-positive endocrine cells and the prognosis of colorectal cancer: An immunohistochemical and ultrastructural study." Journal of Gastroenterology and Hepatology **23**(10): 1574-1585.
- Guzelian, J., J. Barwick, L. Hunter, T. Phang, L. Quattrochi and P. Guzelian (2006). "Identification of genes controlled by the pregnane X receptor by microarray analysis of mRNAs from pregnenolone 16 {alpha}-carbonitrile-treated rats." Toxicological Sciences **94**(2): 379.
- Guzelian, J., J. L. Barwick, L. Hunter, T. L. Phang, L. C. Quattrochi and P. S. Guzelian (2006). "Identification of Genes Controlled by the Pregnane X Receptor by Microarray Analysis of mRNAs from Pregnenolone 16 α -Carbonitrile-Treated Rats." Toxicological Sciences **94**(2): 379-387.
- Halliwell, B. (2006). "Oxidative stress and neurodegeneration: where are we now?" Journal of Neurochemistry **97**(6): 1634-1658.
- Hamilton, N. B. and D. Attwell (2010). "Do astrocytes really exocytose neurotransmitters?" Nature Reviews Neuroscience **11**(4): 227-238.
- Handschin, C. and U. Meyer (2005). "Regulatory network of lipid-sensing nuclear receptors: roles for CAR, PXR, LXR, and FXR." Archives of Biochemistry and Biophysics **433**(2): 387-396.
- Hanisch, U. K. and H. Kettenmann (2007). "Microglia: active sensor and versatile effector cells in the normal and pathologic brain." Nature Neuroscience **10**(11): 1387-1394.
- Hara, T., K. Nakamura, M. Matsui, A. Yamamoto, Y. Nakahara, R. Suzuki-Migishima, M. Yokoyama, K. Mishima, I. Saito and H. Okano (2006). "Suppression of basal autophagy in neural cells causes neurodegenerative disease in mice." Nature **441**(7095): 885-889.
- Hartley, D. P., X. Dai, Y. D. He, E. J. Carlini, B. Wang, W. H. Su-er, R. G. Ulrich, T. H. Rushmore, R. Evers and D. C. Evans (2004). "Activators of the rat pregnane X receptor differentially modulate hepatic and intestinal gene expression." Molecular Pharmacology **65**(5): 1159-1171.
- Hashimoto, K., E. Ishida, A. Miura, A. Ozawa, N. Shibusawa, T. Satoh, S. Okada, M. Yamada and M. Mori (2013). "Human Stearoyl-CoA Desaturase 1 (SCD-1) Gene Expression Is Negatively Regulated by Thyroid Hormone without Direct Binding of Thyroid Hormone Receptor to the Gene Promoter." Endocrinology **154**(1): 537-549.
-

Hasmall, S. C. and R. A. Roberts (1999). "The perturbation of apoptosis and mitosis by drugs and xenobiotics." Pharmacology & Therapeutics **82**(1): 63-70.

Hauwel, M., E. Furon, C. Canova, M. Griffiths, J. Neal and P. Gasque (2005). "Innate (inherent) control of brain infection, brain inflammation and brain repair: the role of microglia, astrocytes, "protective" glial stem cells and stromal ependymal cells." Brain Research reviews **48**(2): 220-233.

Heuvel, J. P. V., J. T. Thompson, S. R. Frame and P. J. Gillies (2006). "Differential activation of nuclear receptors by perfluorinated fatty acid analogs and natural fatty acids: a comparison of human, mouse, and rat peroxisome proliferator-activated receptor- α , - β , and - γ , liver X receptor- β , and retinoid X receptor- α ." Toxicological Sciences **92**(2): 476-489.

Heuvel, V. (1999). "Peroxisome proliferator-activated receptors (PPARS) and carcinogenesis." Toxicological Sciences **47**(1): 1.

Hilgetag, C. C. and H. Barbas (2009). "Are there ten times more glia than neurons in the brain?" Brain Structure and Function **213**(4): 365-366.

Hirsch, E., T. Breidert, E. Rousselet, S. Hunot, A. Hartmann and P. Michel (2003). "The role of glial reaction and inflammation in Parkinson's disease." Annals of the New York Academy of Sciences **991**(1): 214-228.

Hirsch, E., T. Breidert, E. Rousselet, S. Hunot, A. Hartmann and P. Michel (2006). "The role of glial reaction and inflammation in Parkinson's disease." Annals of the New York Academy of Sciences **991**(1): 214-228.

Holden, P. and J. Tugwood (1999). "Peroxisome proliferator-activated receptor alpha: role in rodent liver cancer and species differences." Journal of Molecular endocrinology **22**(1): 1.

Hosoe, T., T. Nakahama and Y. Inouye (2005). "Divergent Modes of Induction of Rat Hepatic and Pulmonary CYP3A1 by Dexamethasone and Pregnenolone 16 α -Carbonitrile." Journal of Health Science **51**(1): 75-79.

Ijpenberg, A., E. Jeannin, W. Wahli and B. Desvergne (1997). "Polarity and specific sequence requirements of peroxisome proliferator-activated receptor (PPAR)/retinoid X receptor heterodimer binding to DNA A functional analysis of the malic enzyme gene PPAR response element." Journal of Biological Chemistry **272**(32): 20108-20117.

Issemann, I. and S. Green (1990). "Activation of a member of the steroid hormone receptor superfamily by peroxisome proliferators." Nature **347**(6294): 645.

Jacobs, M. (2004). "In silico tools to aid risk assessment of endocrine disrupting chemicals." Toxicology **205**(1): 43-53.

-
- Jacobs, M., M. Dickins and D. Lewis (2003). "Homology modelling of the nuclear receptors: human oestrogen receptor β (hER β), the human pregnane-X-receptor (PXR), the Ah receptor (AhR) and the constitutive androstane receptor (CAR) ligand binding domains from the human oestrogen receptor α (hER α) crystal structure, and the human peroxisome proliferator activated receptor α (PPAR α) ligand binding domain from the human PPAR γ crystal structure." The Journal of Steroid Biochemistry and Molecular Biology **84**(2): 117-132.
- Jessen, K. R. and R. Mirsky (2005). "The origin and development of glial cells in peripheral nerves." Nature Reviews Neuroscience **6**(9): 671-682.
- Jones, S. A., L. B. Moore, J. L. Shenk, G. B. Wisely, G. A. Hamilton, D. D. McKee, N. C. O. Tomkinson, E. L. LeCluyse, M. H. Lambert and T. M. Willson (2000). "The pregnane X receptor: a promiscuous xenobiotic receptor that has diverged during evolution." Molecular Endocrinology **14**(1): 27-39.
- Kamath, P., R. Wiesner, M. Malinchoc, W. Kremers, T. Therneau, C. Kosberg, G. D'Amico, E. Dickson and W. Kim (2003). "A model to predict survival in patients with end-stage liver disease." Hepatology **33**(2): 464-470.
- Kaneko, S., S. Kawakami, Y. Hara, M. Wakamori, E. Itoh, T. Minami, Y. Takada, T. Kume, H. Katsuki and Y. Mori (2006). "A critical role of TRPM2 in neuronal cell death by hydrogen peroxide." Journal of Pharmacological Sciences **101**(1): 66-76.
- Kapitulnik, J., O. Pelkonen, U. Gundert-Remy, S. G. Dahl and A. R. Boobis (2009). "Effects of pharmaceuticals and other active chemicals at biological targets: mechanisms, interactions, and integration into PB-PK/PD models." Expert Opinion on Therapeutic Targets **13**(7): 867-887.
- Kasper, P. (2001). "Cyproterone acetate: a genotoxic carcinogen?" Pharmacology & Toxicology **88**(5): 223-231.
- Kesner, R. P. (2007). "Behavioral functions of the CA3 subregion of the hippocampus." Learning & Memory **14**(11): 771-781.
- Kettenmann, H., U. K. Hanisch, M. Noda and A. Verkhratsky (2011). "Physiology of microglia." Physiological Reviews **91**(2): 461-553.
- Kimelberg, H. K. and M. Nedergaard (2010). "Functions of astrocytes and their potential as therapeutic targets." Neurotherapeutics **7**(4): 338-353.
- Kimura, Y. and K. Tanaka (2010). "Regulatory mechanisms involved in the control of ubiquitin homeostasis." Journal of Biochemistry **147**(6): 793-798.
- Klaunig, J. E., M. A. Babich, K. P. Baetcke, J. C. Cook, J. C. Corton, R. M. David, J. G. DeLuca, D. Y. Lai, R. H. McKee and J. M. Peters (2003). "PPAR α agonist-induced rodent tumors: modes of action and human relevance." CRC Critical Reviews in Toxicology **33**(6): 655-780.
-

-
- Klegeris, A., E. G. McGeer and P. L. McGeer (2007). "Therapeutic approaches to inflammation in neurodegenerative disease." Current Opinion in Neurology **20**(3): 351-357.
- Kliwer, S., B. Goodwin and T. Willson (2002). "The nuclear pregnane X receptor: a key regulator of xenobiotic metabolism." Endocrine Reviews **23**(5): 687.
- Kliwer, S. A., B. Goodwin and T. M. Willson (2002). "The nuclear pregnane X receptor: a key regulator of xenobiotic metabolism." Endocrine Reviews **23**(5): 687-702.
- Kobliakov, V. (2010). "Mechanisms of tumor promotion by reactive oxygen species." Biochemistry (Moscow) **75**(6): 675-685.
- Kodama, S., C. Koike, M. Negishi and Y. Yamamoto (2004). "Nuclear receptors CAR and PXR cross talk with FOXO1 to regulate genes that encode drug-metabolizing and gluconeogenic enzymes." Molecular and Cellular Biology **24**(18): 7931-7940.
- Koves, T. R., J. R. Ussher, R. C. Noland, D. Slentz, M. Mosedale, O. Ilkayeva, J. Bain, R. Stevens, J. R. Dyck and C. B. Newgard (2008). "Mitochondrial overload and incomplete fatty acid oxidation contribute to skeletal muscle insulin resistance." Cell Metabolism **7**(1): 45-56.
- Krebs, O., B. Schäfer, T. Wolff, D. Oesterle, E. Deml, M. Sund and J. Favor (1998). "The DNA damaging drug cyproterone acetate causes gene mutations and induces glutathione-S-transferase P in the liver of female Big Blue transgenic F344 rats." Carcinogenesis **19**(2): 241-245.
- Krishnamurthy, G. and S. Krishnamurthy (2009). Nuclear Hepatology: a textbook of hepatobiliary diseases, Springer Verlag.
- Kuhn, R. and R. M. Torres (2002). "Cre/loxP recombination system and gene targeting." Methods In Molecular Biology-Clifton Then Totowa- **180**: 175-206.
- Kullmann, D. M. (2011). "Interneuron networks in the hippocampus." Current Opinion in Neurobiology **21**(5): 709-716.
- Lake, B. G., A. B. Renwick, M. E. Cunnighame, R. J. Price, D. Surry and D. C. Evans (1998). "Comparison of the effects of some CYP3A and other enzyme inducers on replicative DNA synthesis and cytochrome P450 isoforms in rat liver." Toxicology **131**(1): 9-20.
- Lalancette-Hébert, M., G. Gowing, A. Simard, Y. C. Weng and J. Kriz (2007). "Selective ablation of proliferating microglial cells exacerbates ischemic injury in the brain." The Journal of Neuroscience **27**(10): 2596-2605.
-

-
- Lamas, E., D. Chassoux, J. Decaux, C. Brechot and P. Debey (2003). "Quantitative fluorescence imaging approach for the study of polyploidization in hepatocytes." Journal of Histochemistry and Cytochemistry **51**(3): 319.
- Latruffe, N., C. Pacot, P. Passilly, M. Petit, O. Bardot, F. Caira, M. Malki, B. Jannin, M. Clemencet and P. Deslex (1995). "Peroxisomes and hepatotoxicity." Comparative Haematology International **5**(3): 189-195.
- LeCluyse, E. L. (2001). "Pregnane X receptor: Molecular basis for species differences in CYP3A induction by xenobiotics." Chemico-biological Interactions **134**(3): 283-289.
- Lee, S., T. Pineau, J. Drago, E. Lee, J. Owens, D. Kroetz, P. Fernandez-Salguero, H. Westphal and F. Gonzalez (1995). "Targeted disruption of the alpha isoform of the peroxisome proliferator-activated receptor gene in mice results in abolishment of the pleiotropic effects of peroxisome proliferators." Molecular and Cellular Biology **15**(6): 3012.
- Lehmann, J. M., D. D. McKee, M. A. Watson, T. M. Willson, J. T. Moore and S. A. Kliewer (1998). "The human orphan nuclear receptor PXR is activated by compounds that regulate CYP3A4 gene expression and cause drug interactions." Journal of Clinical Investigation **102**(5): 1016.
- Lein, P. J., C. D. Barnhart and I. N. Pessah (2011). Acute hippocampal slice preparation and hippocampal slice cultures. In Vitro Neurotoxicology, Springer: 115-134.
- Lindroos, P. M., R. Zarnegar and G. K. Michalopoulos (1991). "Hepatocyte growth factor (hepatopoinetin A) rapidly increases in plasma before DNA synthesis and liver regeneration stimulated by partial hepatectomy and carbon tetrachloride administration." Hepatology **13**(4): 743-750.
- Lipton, S. A. (2005). "The molecular basis of memantine action in Alzheimer's disease and other neurologic disorders: low-affinity, uncompetitive antagonism." Current Alzheimer Research **2**(2): 155-165.
- Logan, A., M. Berry, A. M. Gonzalez, S. A. Frautschy, M. B. Sporn and A. Baird (2006). "Effects of Transforming Growth Factor β 1, on Scar Production in the Injured Central Nervous System of the Rat." European Journal of Neuroscience **6**(3): 355-363.
- Lovett-Racke, A. E., R. Z. Hussain, S. Northrop, J. Choy, A. Rocchini, L. Matthes, J. A. Chavis, A. Diab, P. D. Drew and M. K. Racke (2004). "Peroxisome proliferator-activated receptor α agonists as therapy for autoimmune disease." The Journal of Immunology **172**(9): 5790-5798.
- Lucier, G. W., A. Tritscher, T. Goldsworthy, J. Foley, G. Clark, J. Goldstein and R. Maronpot (1991). "Ovarian hormones enhance 2, 3, 7, 8-tetrachlorodibenzo-p-
-

dioxin-mediated increases in cell proliferation and preneoplastic foci in a two-stage model for rat hepatocarcinogenesis." Cancer research **51**(5): 1391-1397.

Luna-Medina, R., M. Cortes-Canteli, M. Alonso, A. Santos, A. Martínez and A. Perez-Castillo (2005). "Regulation of inflammatory response in neural cells in vitro by thiadiazolidinones derivatives through peroxisome proliferator-activated receptor γ activation." Journal of Biological Chemistry **280**(22): 21453-21462.

Luna-Medina, R., M. Cortes-Canteli, S. Sanchez-Galiano, J. A. Morales-Garcia, A. Martinez, A. Santos and A. Perez-Castillo (2007). "NP031112, a thiadiazolidinone compound, prevents inflammation and neurodegeneration under excitotoxic conditions: potential therapeutic role in brain disorders." The Journal of Neuroscience **27**(21): 5766-5776.

Malinowski, J. M. and S. Bolesta (2000). "Rosiglitazone in the treatment of type 2 diabetes mellitus: a critical review." Clinical Therapeutics **22**(10): 1151-1168.

Mandard, S., M. Müller and S. Kersten (2004). "Peroxisome proliferator-activated receptor α target genes." Cellular and Molecular Life Sciences CMLS **61**(4): 393-416.

Mandrekar-Colucci, S., A. Sauerbeck, P. G. Popovich and D. M. McTigue (2013). "PPAR agonists as therapeutics for CNS trauma and neurological diseases." ASN neuro **5**(5): 347-362.

Mannaerts, G. and P. Van Veldhoven (1993). "Metabolic pathways in mammalian peroxisomes." Biochimie **75**(3-4): 147-158.

Martelli, A., G. B. Campart, M. Ghia, A. Allavena, E. Mereto and G. Brambilla (1996). "Induction of micronuclei and initiation of enzyme-altered foci in the liver of female rats treated with cyproterone acetate, chlormadinone acetate or megestrol acetate." Carcinogenesis **17**(3): 551-554.

Martin, H. (2009). "Role of PPAR-gamma in inflammation. Prospects for therapeutic intervention by food components." Mutation Research/Fundamental and Molecular Mechanisms of Mutagenesis **669**(1): 1-7.

Matheson, L., S. Hanton and F. Brandizzi (2006). "Traffic between the plant endoplasmic reticulum and Golgi apparatus: to the Golgi and beyond." Current Opinion in Plant Biology **9**(6): 601-609.

McCaffery, P., J. Zhang and J. E. Crandall (2006). "Retinoic acid signaling and function in the adult hippocampus." Journal of Neurobiology **66**(7): 780-791.

McGeer, P., S. Itagaki, B. Boyes and E. McGeer (1988). "Reactive microglia are positive for HLA-DR in the substantia nigra of Parkinson's and Alzheimer's disease brains." Neurology **38**(8): 1285-1285.

-
- McGeer, P. L. and E. G. McGeer (1995). "The inflammatory response system of brain: implications for therapy of Alzheimer and other neurodegenerative diseases." Brain Research Reviews **21**(2): 195-218.
- McGinley, J., K. Knott and H. Thompson (2000). "Effect of fixation and epitope retrieval on BrdU indices in mammary carcinomas." Journal of Histochemistry and Cytochemistry **48**(3): 355.
- McGowan, K., M. Kurtis, L. Lottman, D. Watson and R. Sah (2002). "Biochemical quantification of DNA in human articular and septal cartilage using PicoGreen® and Hoechst 33258." Osteoarthritis and Cartilage **10**(7): 580-587.
- Menegazzi, M., A. Carcereri-De Prati, H. Suzuki, H. Shinozuka, M. Pibiri, R. Piga, A. Columbano and G. M. Ledda-Columbano (1997). "Liver cell proliferation induced by nafenopin and cyproterone acetate is not associated with increases in activation of transcription factors NF- κ B and AP-1 or with expression of tumor necrosis factor α ." Hepatology **25**(3): 585-592.
- Miguel-Hidalgo, J. J., C. Baucom, G. Dilley, J. C. Overholser, H. Y. Meltzer, C. A. Stockmeier and G. Rajkowska (2000). "Glial fibrillary acidic protein immunoreactivity in the prefrontal cortex distinguishes younger from older adults in major depressive disorder." Biological Psychiatry **48**(8): 861-873.
- Mikamo, E., S. Harada, J.-i. Nishikawa and T. Nishihara (2003). "Endocrine disruptors induce cytochrome P450 by affecting transcriptional regulation via pregnane X receptor." Toxicology and Applied Pharmacology **193**(1): 66-72.
- Minagar, A., P. Shapshak, R. Fujimura, R. Ownby, M. Heyes and C. Eisdorfer (2002). "The role of macrophage/microglia and astrocytes in the pathogenesis of three neurologic disorders: HIV-associated dementia, Alzheimer disease, and multiple sclerosis." Journal of the Neurological Sciences **202**(1): 13-23.
- Moore, L. B., D. J. Parks, S. A. Jones, R. K. Bledsoe, T. G. Consler, J. B. Stimmel, B. Goodwin, C. Liddle, S. G. Blanchard and T. M. Willson (2000). "Orphan nuclear receptors constitutive androstane receptor and pregnane X receptor share xenobiotic and steroid ligands." Journal of Biological Chemistry **275**(20): 15122-15127.
- Moreau, K., S. Luo and D. C. Rubinsztein (2010). "Cytoprotective roles for autophagy." Current Opinion in Cell Biology **22**(2): 206-211.
- Moreno, S., S. Farioli-Vecchioli and M. Ceru (2004). "Immunolocalization of peroxisome proliferator-activated receptors and retinoid X receptors in the adult rat CNS." Neuroscience **123**(1): 131-145.
- Muller, D., C. Wang, G. Skibo, N. Toni, H. Cremer, V. Calaora, G. Rougon and J. Z. Kiss (1996). "PSA-NCAM is required for activity-induced synaptic plasticity." Neuron **17**(3): 413-422.
-

-
- Muskhelishvili, L., J. Latendresse, R. Kodell and E. Henderson (2003). "Evaluation of cell proliferation in rat tissues with BrdU, PCNA, Ki-67 (MIB-5) immunohistochemistry and in situ hybridization for histone mRNA." Journal of Histochemistry and Cytochemistry **51**(12): 1681.
- Nagy, L., P. Tontonoz, J. G. Alvarez, H. Chen and R. M. Evans (1998). "Oxidized LDL regulates macrophage gene expression through ligand activation of PPAR γ ." Cell **93**(2): 229-240.
- Nedergaard, M., B. Ransom and S. A. Goldman (2003). "New roles for astrocytes: Redefining the functional architecture of the brain." Trends in Neurosciences **26**(10): 523-530.
- Neves, G., S. F. Cooke and T. V. P. Bliss (2008). "Synaptic plasticity, memory and the hippocampus: a neural network approach to causality." Nature Reviews Neuroscience **9**(1): 65-75.
- Nieuwenhuys, R., J. Voogd and C. Van Huijzen (2007). The human central nervous system, Springer.
- Norman, R., H. Urich and G. E. Woods (1958). "The relationship between prenatal porencephaly and the encephalomalacias of early life." The British Journal of Psychiatry **104**(436): 758-771.
- Ntambi, J. M. (1995). "The regulation of stearyl-CoA desaturase (SCD)." Progress in Lipid Research **34**(2): 139.
- Nwe, K. and M. W. Brechbiel (2009). "Growing applications of "click chemistry" for bioconjugation in contemporary biomedical research." Cancer Biotherapy and Radiopharmaceuticals **24**(3): 289-302.
- O'Brien, M. L., B. T. Spear and H. P. Glauert (2005). "Role of oxidative stress in peroxisome proliferator-mediated carcinogenesis." CRC Critical Reviews in Toxicology **35**(1): 61-88.
- Oddo, S. (2008). "The ubiquitin-proteasome system in Alzheimer's disease." Journal of Cellular and Molecular Medicine **12**(2): 363-373.
- Olanow, C. W., K. Kieburtz and A. H. Schapira (2008). "Why have we failed to achieve neuroprotection in Parkinson's disease?" Annals of Neurology **64**(S2): S101-S110.
- Olson, J. K., S. S. Zamvil and S. D. Miller (2003). "Efficient technique for immortalization of murine microglial cells relevant for studies in murine models of multiple sclerosis." Journal of Neuroscience Methods **128**(1): 33-43.
-

Otteneider, M. and W. K. Lutz (1999). "Correlation of DNA adduct levels with tumor incidence: carcinogenic potency of DNA adducts." Mutation Research/Fundamental and Molecular Mechanisms of Mutagenesis **424**(1): 237-247.

Ou, Z., X. Zhao, L. A. Labiche, R. Strong, J. C. Grotta, O. Herrmann and J. Aronowski (2006). "Neuronal expression of peroxisome proliferator-activated receptor-gamma (PPAR γ) and 15d-prostaglandin J₂—Mediated protection of brain after experimental cerebral ischemia in rat." Brain research **1096**(1): 196-203.

Ozzello, L., C. De Rosa, D. Habif and R. Lipton (1987). Antiestrophilin monoclonal antibodies as immunocytochemical probes of estrogen receptor in tissue sections of breast carcinomas. New Frontiers in Mammary Pathology 1986, Springer: 99-111.

Pakkenberg, B. and H. Gundersen (2011). "Total number of neurons and glial cells in human brain nuclei estimated by the disector and the fractionator." Journal of Microscopy **150**(1): 1-20.

Pascussi, J., S. Gerbal-Chaloin, L. Drocourt, P. Maurel and M. Vilarem (2003). "The expression of CYP2B6, CYP2C9 and CYP3A4 genes: a tangle of networks of nuclear and steroid receptors." Biochimica et Biophysica Acta (BBA)-General Subjects **1619**(3): 243-253.

Passilly, P., H. Schohn, B. Jannin, M. Cherkaoui Malki, D. Boscoboinik, M. Dauça and N. Latruffe (1999). "Phosphorylation of peroxisome proliferator-activated receptor [α] in rat Fao cells and stimulation by ciprofibrate." Biochemical Pharmacology **58**(6): 1001-1008.

Pekny, M. and M. Nilsson (2005). "Astrocyte activation and reactive gliosis." Glia **50**(4): 427-434.

Peters, A., D. Leahu, M. B. Moss and K. J. McNally (1994). "The effects of aging on area 46 of the frontal cortex of the rhesus monkey." Cerebral Cortex **4**(6): 621-635.

Petrucci, L. and M. Dawson (2004). "Mechanism of neurodegenerative disease: role of the ubiquitin proteasome system." Annals of Medicine **36**(4): 315-320.

Pichard, V. and N. Ferry (2005). "Long term phenobarbital administration does not promote the multiplication of hepatocytes replicating after single cyproterone acetate administration." Life Sciences **76**(26): 3057-3068.

Piekema, C., R. P. Kessels, R. B. Mars, K. M. Petersson and G. Fernández (2006). "The right hippocampus participates in short-term memory maintenance of object–location associations." Neuroimage **33**(1): 374-382.

Plant, N. (2008). "Can systems toxicology identify common biomarkers of non-genotoxic carcinogenesis?" Toxicology **254**(3): 164-169.

Plant, N. J., N. J. Horley, R. L. Savory, C. R. Elcombe, T. Gray and D. R. Bell (1998). "The peroxisome proliferators are hepatocyte mitogens in chemically-defined media: glucocorticoid-induced PPAR alpha is linked to peroxisome proliferator mitogenesis." Carcinogenesis **19**(5): 925-931.

Pryce, G., Z. Ahmed, D. J. Hankey, S. J. Jackson, J. L. Croxford, J. M. Pocock, C. Ledent, A. Petzold, A. J. Thompson and G. Giovannoni (2003). "Cannabinoids inhibit neurodegeneration in models of multiple sclerosis." Brain **126**(10): 2191-2202.

Quattrochi, L. C. and P. S. Guzelian (2001). "CYP3A regulation: from pharmacology to nuclear receptors." Drug metabolism and disposition **29**(5): 615-622.

Racke, M. K. and P. D. Drew (2008). "PPARs in neuroinflammation." PPAR research **2008**.

Ray, D. M., F. Akbiyik and R. P. Phipps (2006). "The peroxisome proliferator-activated receptor γ (PPAR γ) ligands 15-deoxy- Δ 12, 14-prostaglandin J2 and ciglitazone induce human B lymphocyte and B cell lymphoma apoptosis by PPAR γ -independent mechanisms." The Journal of Immunology **177**(8): 5068-5076.

Roberts, R. (1999). "Peroxisome proliferators: mechanisms of adverse effects in rodents and molecular basis for species differences." Archives of Toxicology **73**(8): 413-418.

Roberts, R., N. James, S. Cosulich, S. Hasmall and G. Orphanides (2001). "Role of cytokines in non-genotoxic hepatocarcinogenesis: cause or effect?" Toxicology Letters **120**(1-3): 301-306.

Roberts, R. A. (1996). "Non-genotoxic Hepatocarcinogenesis: Suppression of Apoptosis by Peroxisome Proliferators." Annals of the New York Academy of Sciences **804**(1): 588-611.

Robinson, R. G. (1998). The clinical neuropsychiatry of stroke: Cognitive, behavioral and emotional disorders following vascular brain injury, Cambridge University Press.

Rogers, N., S. Paine, L. Bedford and R. Layfield (2010). "Review: The ubiquitin-proteasome system: contributions to cell death or survival in neurodegeneration." Neuropathology and Applied Neurobiology **36**(2): 113-124.

Romero, F. J. and C. Rodríguez Luque (2011). Research on neurodegenerative diseases: Epistemological and methodological problems. Conceptual revolutions: From cognitive science to medicine.

Ross, J., S. M. Plummer, A. Rode, N. Scheer, C. C. Bower, O. Vogel, C. J. Henderson, C. R. Wolf and C. R. Elcombe (2010). "Human constitutive androstane receptor (CAR) and pregnane X receptor (PXR) support the hypertrophic but not the

hyperplastic response to the murine nongenotoxic hepatocarcinogens phenobarbital and chlordane in vivo." Toxicological Sciences **116**(2): 452-466.

Rotroff, D. M., A. L. Beam, D. J. Dix, A. Farmer, K. M. Freeman, K. A. Houck, R. S. Judson, E. L. Lecluyse, M. T. Martin and D. M. Reif (2010). "Xenobiotic-metabolizing enzyme and transporter gene expression in primary cultures of human hepatocytes modulated by ToxCast chemicals." Journal of Toxicology and Environmental Health, Part B **13**(2-4): 329-346.

Saavedra, J. M., E. Sánchez-Lemus and J. Benicky (2011). "Blockade of brain angiotensin II AT₁ receptors ameliorates stress, anxiety, brain inflammation and ischemia: Therapeutic implications." Psychoneuroendocrinology **36**(1): 1-18.

Sadeghi, N., N. D'Haene, C. Decaestecker, M. Levivier, T. Metens, C. Maris, D. Wikler, D. Balériaux, I. Salmon and S. Goldman (2008). "Apparent diffusion coefficient and cerebral blood volume in brain gliomas: relation to tumor cell density and tumor microvessel density based on stereotactic biopsies." American Journal of Neuroradiology **29**(3): 476-482.

Salic, A. and T. Mitchison (2008). "A chemical method for fast and sensitive detection of DNA synthesis in vivo." Proceedings of the National Academy of Sciences **105**(7): 2415.

Sarker, S. D., L. Nahar and Y. Kumarasamy (2007). "Microtitre plate-based antibacterial assay incorporating resazurin as an indicator of cell growth, and its application in the *in vitro* antibacterial screening of phytochemicals." Methods **42**(4): 321-324.

Sastre, M., T. Klockgether and M. T. Heneka (2006). "Contribution of inflammatory processes to Alzheimer's disease: molecular mechanisms." International Journal of Developmental Neuroscience **24**(2): 167-176.

Schintu, N., L. Frau, M. Ibba, P. Caboni, A. Garau, E. Carboni and A. R. Carta (2009). "PPAR-gamma-mediated neuroprotection in a chronic mouse model of Parkinson's disease." European Journal of Neuroscience **29**(5): 954-963.

Schneider, J., R. Wilson, E. Cochran, J. Bienias, S. Arnold, D. Evans and D. Bennett (2003). "Relation of cerebral infarctions to dementia and cognitive function in older persons." Neurology **60**(7): 1082-1088.

Schulte-Hermann, R., V. Hoffman, W. Parzefall, M. Kallenbach, A. Gerhardt and J. Schuppler (1980). "Adaptive responses of rat liver to the gestagen and anti-androgen cyproterone acetate and other inducers. II. Induction of growth." Chemico-biological Interactions **31**(3): 287-300.

-
- Schutte, B., M. Reynders, F. Bosman and G. Blijham (1987). "Effect of tissue fixation on anti-bromodeoxyuridine immunohistochemistry." Journal of Histochemistry & Cytochemistry **35**(11): 1343-1345.
- Schwartz, M., S. Bukshpan and G. Kunis (2008). "Application of glatiramer acetate to neurodegenerative diseases beyond multiple sclerosis: the need for disease-specific approaches." BioDrugs **22**(5): 293-299.
- Seidman, M., S. Hogan, R. Wendland, S. Worgall, R. Crystal and P. Leopold (2001). "Variation in adenovirus receptor expression and adenovirus vector-mediated transgene expression at defined stages of the cell cycle." Molecular Therapy **4**(1): 13-21.
- Seiler, A., A. Visan, R. Buesen, E. Genschow and H. Spielmann (2004). "Improvement of an in vitro stem cell assay for developmental toxicity: the use of molecular endpoints in the embryonic stem cell test." Reproductive Toxicology **18**(2): 231-240.
- Semendeferi, K., E. Armstrong, A. Schleicher, K. Zilles and G. W. Van Hoesen (2001). "Prefrontal cortex in humans and apes: a comparative study of area 10." American Journal of Physical Anthropology **114**(3): 224-241.
- Severino, V., J. Locker, G. M. Ledda-Columbano, A. Columbano, A. Parente and A. Chambery (2011). "Proteomic characterization of early changes induced by triiodothyronine in rat liver." Journal of Proteome Research **10**(7): 3212-3224.
- Sherlock, S. and J. Dooley (2002). Diseases of the Liver and Biliary System, Wiley-Blackwell.
- Shoelson, S. E., J. Lee and A. B. Goldfine (2006). "Inflammation and insulin resistance." Journal of Clinical Investigation **116**(7): 1793-1801.
- Shukla, S. J., S. Sakamuru, R. Huang, T. A. Moeller, P. Shinn, D. VanLeer, D. S. Auld, C. P. Austin and M. Xia (2011). "Identification of clinically used drugs that activate pregnane X receptors." Drug Metabolism and Disposition **39**(1): 151-159.
- Siddique, Y. H., G. Ara, T. Beg, M. Faisal, M. Ahmad and M. Afzal (2008). "Antigenotoxic role of *Centella asiatica* L. extract against cyproterone acetate induced genotoxic damage in cultured human lymphocytes." Toxicology in vitro **22**(1): 10-17.
- Singh, I. (1997). "Biochemistry of peroxisomes in health and disease." Molecular and Cellular Biochemistry **167**(1): 1-29.
- Smith, M. L., P. Fries, F. Gosselin, R. Goebel and P. Schyns (2009). "Inverse mapping the neuronal substrates of face categorizations." Cerebral Cortex **19**(10): 2428-2438.
-

-
- Sofroniew, M. V. and H. V. Vinters (2010). "Astrocytes: biology and pathology." Acta Neuropathologica **119**(1): 7-35.
- Song, H., C. F. Stevens and F. H. Gage (2002). "Astroglia induce neurogenesis from adult neural stem cells." Nature **417**(6884): 39-44.
- Storer, P. D., J. Xu, J. Chavis and P. D. Drew (2005). "Peroxisome proliferator-activated receptor-gamma agonists inhibit the activation of microglia and astrocytes: implications for multiple sclerosis." Journal of Neuroimmunology **161**(1): 113-122.
- Stuchbury, G. and G. Münch (2005). "Alzheimer's associated inflammation, potential drug targets and future therapies." Journal of Neural Transmission **112**(3): 429-453.
- Sueyoshi, S., M. Mitsumata, Y. Kusumi, M. Niihashi, M. Esumi, T. Yamada and I. Sakurai (2010). "Increased expression of peroxisome proliferator-activated receptor (PPAR)- α and PPAR- γ in human atherosclerosis." Pathology-Research and Practice **206**(7): 429-438.
- Sueyoshi, T. and M. Negishi (2001). "Phenobarbital Response Elements of Cytochrome P450 Genes and Nuclear Receptors 1." Annual Review of Pharmacology and Toxicology **41**(1): 123-143.
- Sun, G. Y., J. Xu, M. D. Jensen and A. Simonyi (2004). "Phospholipase A2 in the central nervous system implications for neurodegenerative diseases." Journal of Lipid Research **45**(2): 205-213.
- Tabak, H., J. Murk, I. Braakman and H. Geuze (2003). "Peroxisomes start their life in the endoplasmic reticulum." Traffic **4**(8): 512-518.
- Takamiya, Y., S. Kohsaka, S. Toya, M. Otani and Y. Tsukada (1988). "Immunohistochemical studies on the proliferation of reactive astrocytes and the expression of cytoskeletal proteins following brain injury in rats." Developmental Brain Research **38**(2): 201-210.
- Taub, R. (2004). "Liver regeneration: from myth to mechanism." Nature Reviews Molecular Cell Biology **5**(10): 836-847.
- Thomas, J. H. (2007). "Rapid birth-death evolution specific to xenobiotic cytochrome P450 genes in vertebrates." PLoS genetics **3**(5): e67.
- Ueda, J., H. Saito, H. Watanabe and B. M. Evers (2005). "Novel and quantitative DNA dot-blotting method for assessment of in vivo proliferation." American Journal of Physiology-Gastrointestinal and Liver Physiology **288**(4): G842-G847.
- Van Praag, H., T. Shubert, C. Zhao and F. H. Gage (2005). "Exercise enhances learning and hippocampal neurogenesis in aged mice." The Journal of Neuroscience **25**(38): 8680-8685.
-

Villena, A., F. Diaz, V. Requena, I. Chavarria, F. Rius and I. Perez de Vargas (1997). "Quantitative morphological changes in neurons from the dorsal lateral geniculate nucleus of young and old rats." The Anatomical Record **248**(1): 137-141.

Volterra, A., P. Bezzi, B. L. Rizzini, D. Trotti, K. Ullensvang, N. C. Danbolt and G. Racagni (2006). "The competitive transport inhibitor L-trans-pyrrolidine-2, 4-dicarboxylate triggers excitotoxicity in rat cortical neuron-astrocyte co-cultures via glutamate release rather than uptake inhibition." European Journal of Neuroscience **8**(9): 2019-2028.

Volterra, A. and J. Meldolesi (2005). "Astrocytes, from brain glue to communication elements: the revolution continues." Nature Reviews Neuroscience **6**(8): 626-640.

Wallenius, V., K. Wallenius and J.-O. Jansson (2000). "Normal pharmacologically-induced, but decreased regenerative liver growth in interleukin-6-deficient (IL-6^{-/-}) mice." Journal of Hepatology **33**(6): 967-974.

Wan, Y. J. Y., D. An, Y. Cai, J. J. Repa, T. H. P. Chen, M. Flores, C. Postic, M. A. Magnuson, J. Chen and K. R. Chien (2000). "Hepatocyte-specific mutation establishes retinoid X receptor α as a heterodimeric integrator of multiple physiological processes in the liver." Molecular and Cellular Biology **20**(12): 4436-4444.

Warren, M., K. Puskarczyk and S. Chapman (2009). "Chick embryo proliferation studies using EdU labeling." Dev Dyn **238**: 944-949.

Warren, M., K. Puskarczyk and S. C. Chapman (2009). "Chick embryo proliferation studies using EdU labeling." Developmental Dynamics **238**(4): 944-949.

Waxman, S. and A. Booth (2003). "The origins and evolution of links between word learning and conceptual organization: new evidence from 11-month-olds." Developmental Science **6**(2): 128-135.

Webster, M., K. L. Witkin and O. Cohen-Fix (2009). "Sizing up the nucleus: nuclear shape, size and nuclear-envelope assembly." Journal of Cell Science **122**(10): 1477-1486.

Widmann, J. J. and H. Fahimi (1975). "Proliferation of mononuclear phagocytes (Kupffer cells) and endothelial cells in regenerating rat liver. A light and electron microscopic cytochemical study." The American journal of Pathology **80**(3): 349.

Woodyatt, N., K. Lambe, K. Myers, J. Tugwood and R. Roberts (1999). "The peroxisome proliferator (PP) response element upstream of the human acyl CoA oxidase gene is inactive among a sample human population: significance for species differences in response to PPs." Carcinogenesis **20**(3): 369-372.

Wyss-Coray, T. and L. Mucke (2002). "Inflammation in neurodegenerative disease—a double-edged sword." Neuron **35**(3): 419-432.

Yang, I., S. J. Han, G. Kaur, C. Crane and A. T. Parsa (2010). "The role of microglia in central nervous system immunity and glioma immunology." Journal of Clinical Neuroscience **17**(1): 6-10.

Yano, J. K., M.-H. Hsu, K. J. Griffin, C. D. Stout and E. F. Johnson (2005). "Structures of human microsomal cytochrome P450 2A6 complexed with coumarin and methoxsalen." Nature structural & Molecular Biology **12**(9): 822-823.

Yi, J.-H., S.-W. Park, R. Kapadia and R. Vemuganti (2007). "Role of transcription factors in mediating post-ischemic cerebral inflammation and brain damage." Neurochemistry International **50**(7): 1014-1027.

Yoshida, T., S. Arii and T. Tobe (1992). "Cell Kinetics Of Regenerating Liver After 70% Hepatectomy In Rats 2-Color Flow Cytometric Analysis." HPB Surgery **5**: 103-115.

Yu, S., K. Matsusue, P. Kashireddy, W. Q. Cao, V. Yeldandi, A. V. Yeldandi, M. S. Rao, F. J. Gonzalez and J. K. Reddy (2003). "Adipocyte-specific gene expression and adipogenic steatosis in the mouse liver due to peroxisome proliferator-activated receptor γ 1 (PPAR γ 1) overexpression." Journal of Biological Chemistry **278**(1): 498-505.

Yuan, F., J. Chen, W. Wu, S. Chen, X. Wang, Z. Su and M. Huang (2010). "Effects of matrine and oxymatrine on catalytic activity of cytochrome P450s in rats." Basic & Clinical Pharmacology & Toxicology **107**(5): 906-913.

Zandbergen, F., S. x. e. p. Mandard, P. Escher, N. x. a. s. Tan, D. Patsouris, T. Jatkoje, S. Rojas-Caro, S. Madore, W. Wahli and S. Tafuri (2005). "The G0/G1 switch gene 2 is a novel PPAR target gene." Biochem. J **392**: 313-324.

Zecca, L., M. B. Youdim, P. Riederer, J. R. Connor and R. R. Crichton (2004). "Iron, brain ageing and neurodegenerative disorders." Nature Reviews Neuroscience **5**(11): 863-873.

Zhang, B., W. Xie and M. D. Krasowski (2008). "PXR: a xenobiotic receptor of diverse function implicated in pharmacogenetics." Pharmacogenomics **9**(11): 1695-1709.

Zhang, P., J. Li, Y. Liu, X. Chen and Q. Kang (2009). "Transplanted human embryonic neural stem cells survive, migrate, differentiate and increase endogenous nestin expression in adult rat cortical peri-infarction zone." Neuropathology **29**(4): 410-421.

Zhang, S.-C., M. Wernig, I. D. Duncan, O. Brüstle and J. A. Thomson (2001). "In vitro differentiation of transplantable neural precursors from human embryonic stem cells." Nature Biotechnology **19**(12): 1129-1133.

Zimmer, J., B. W. Kristensen, B. Jakobsen and J. Noraberg (2000). "Excitatory amino acid neurotoxicity and modulation of glutamate receptor expression in organotypic brain slice cultures." *Amino Acids* **19**(1): 7-21.

13. Appendixes

Table(1) Immunohistochemistry technique for BrdU paraffin sections.

No.	Solution	Time <i>if the number of the slides are small you may give them less timing at stage 17-30</i>
1-	Xylene I	5 min after heating in microwave (40°C
2-	Xylene II	
3-	ethanol 100%	8 min.
4-	ethanol 70%	4 min.
5-	ethanol 50%	3 min.
6-	Distal H ₂ O	2 min.
7-	H ₂ O ₂ (1)	15 min.
8-	PBS (2)	5 min.
9-	PBS	5 min.
10-	Citric acid (ph 6)(3)	10 min. at 3 (warm)
11-	PBS	5 min.
12-	BSA 5% (4)	15min.
13-	Primary antibodies (5)	45 min. 1ml lab dilute+1 µL anti-pri
14-	Distal H ₂ O	5 min.
15-	Secondary antibodies(6)	30 min. 2 µL:100 µL
16-	PBS *	9 min.
17-	Staining solution DAB(7)	8 min.
18-	Distal H ₂ O	3 min.
19-	Haematoxyline sol.(8)	30 sec.
20-	Tape water	3 min.
21-	Acid alcohol(9)	5 sec.
22-	Rinse in running Tape water	1 min.
23-	Ammonia in water(10)	1 sec.
24-	Tape water	3 min.
25-	ethanol 50%	2 min.
26-	ethanol 70%	2 min.
27-	ethanol 95%	2 min.
28-	ethanol 100%	2 min.
29-	Xylene	2 min.
30-	Mount with DPX	
31-	Put cover slide	

Table (2) Histochemistry technique for Hoechst dye and EdU paraffin sections.

No.	Solution	<i>Time if the number of the slides are small you may give them less timing at stage 17-30</i>
1-	Xylene I	5 min after heating in microwave (40°C for 2 min)
2-	Xylene II	5 min
3-	Ethanol 100%	8 min.
4-	ethanol 70%	4 min.
5-	ethanol 50%	3 min.
6-	Distal H ₂ O	2 min.
7-	H ₂ O ₂ (1)	15 min.
8-	PBS (2)	5 min.
9-	1 X Hoechst (500-1000) μ L per slide	- in dark 5 min.
10-	PBS	5 min
11-	PBS	5 min.
12-	H ₂ O distal	3 min
13-	ethanol 50%	1 min.
14-	ethanol 70%	1 min.
15-	ethanol 95%	1 min.
16-	ethanol 100%	1 min.
17-	Xylene	1 min.
18-	Mount with DPX	
19-	Put cover slide	

Table (3) Immunohistochemistry technique for BrdU paraffin sections and histochemistry for EdU paraffin section.

No.	solution	<i>Time if the number of the slides are small you may give them less timing at stage</i>
1-	Xylene I	5 min after heating in microwave (40°C for 2 min)
2-	Xylene II	
3-	ethanol 100%	8 min.
4-	ethanol 70%	4 min.
5-	ethanol 50%	3 min.
6-	Distal H2O	2 min.
7-	H2O2 (1)	15 min.
8-	PBS (2)	5 min.
9-	PBS	5 min.
10-	Citric acid (ph 6)(3)	10 min. at 3 (warm)
11-	PBS	5 min.
12-	BSA 5% (4)	15min.
13-	Primary antibodies (5)	45 min.
14-	Distal H2O	5 min.
15-	Secondary antibodies(6)*	30 min.
16-	PBS **	9 min.
17-	Staining solution DAB(7)	8 min.
18-	Distal H2O	3 min.
19-	Haematoxylin sol.(8)	30 sec.
20-	Tape water	3 min.
21-	Acid alcohol(9)	5 sec.
22-	Rinse in running Tape water	1 min.
23-	Ammonia in water(10)	1 sec.
24-	Tape water	3 min.
25-	PBS	5 min
26-	3% BSA in PBS(1) use pipette	10 min
27-	Click-iT reaction cocktail (250µl/ 1 slide)	30 min (room temp.) in dark
28-	3% BSA in PBS(II) wash use pipette	5 min
29-	PBS I	5 min
30-	I X Hoechst dye (250 µl per slide)	30 min (in dark)
31-	PBS I	5 min
32-	PBS II	5 min
33-	H2O distal	3 min
34-	Mount with DPX	
35-	Put cover slide	Over night 5 hrs

*remove the mark at this point

**put on a shaker

Table (4): Immunohistochemical staining of paraffin sections. Mouse primary antibody; mouse on mouse (M.O.M) kit-Vector labs PK-2200

No.	Solution	Time if the number of sides are small you may give them less timing -At stage 17-30
1-	Xylene I	15-20 min before de-wax and rehydrate in oven or heating in microwave (40 ° C for 2 min)
2-	Xylene II	
3-	Ethanol 100%	10 min
4-	Ethanol 95%	10 min
5-	Ethanol 70%	10 min
6-	Running water (gently)	10 min
7-	Place in hot antigen retrieval solution at~100 °C (PH 6)	20 min
8-	Remove beaker to a shaker set	20 min
9-	Wash in running water (gently)	10 min
10-	Incubate in 3% H ₂ O ₂ (5ml H ₂ O ₂ +45ml methanol) in a coplin jar	5 min
11-	PBS**	5-10 min
12-	<u>1 drop</u> of M O M Ig blocking reagent in <u>1.25ml</u> PBS	30 min-1 hrs incubate in <u>humid</u> chamber
13-	PBS** X3	5-10min
14-	Working solution of M O M diluent	5 min
15-	Primary antibody 1 µl/100 µl of M O M diluent	30min-1hrs in <u>humid</u> chamber
16-	PBS** X3	5-10 min
17-	Secondary antibody (1 µl/250 µl of M O M diluents)	30min-1hrs in <u>humid</u> chamber
18-	PBS**X3	5-10 min
19-	ABC reagents (1 drop of A to 1.25ml PBS mix gently then add 1 drop of B and mix gently)	15 min in humid chamber
20-	PBS**	5-10 min
21-	DAB reaction (3, 3' diaminobenzidine)	30 sec-10 min / in coplin jar
22-	Running water (gently)	10 min
23-	Harris haematoxylin	5 min
24-	Rinse in running water until water runs clear	-
25-	Dip in 1% acid alcohol (Hcl in 70% ethanol)	15 sec
26-	Rinse in running water tape water	5 min
27-	Dehydrate: 70% ethanol	10 sec
28-	Ethanol 95%	10 sec
29-	Ethanol 100%	10 sec
30-	Ethanol 100%	10 sec
31-	Xylene	5 min
32-	Mount with DPX	1 min
33-	Put cover slide	

* Remove the mark at this point

** put on a shaker

Table (5): Immunohistochemical staining of paraffin section anti-GFAR with fluorescent rhodamine redtm – X goat anti-mouse igG: marken

NO.	Solution	Time
1-	Dewax and rehydrate	-
2-	Xylene I	10 min
3-	Xylene II	5 min
4-	Ethanol 100% I	8 min
5-	Ethanol 100% II	4 min
6-	Ethanol 95%	5 min
7-	Ethanol 70%	5 min
8-	Running water (gently)	5 min
9-	Wash in PBS I	5 min
10-	Wash in PBS II	5 min
11-	Wash with PBS (use pipette gently)	1-2 min
12-	* Antigen retrieval steamer	40 min+20 min cool down
13-	**Block with 5% normal goat serum (NGS) with 0.5% triton X-100 in PBS	2 hrs incubate in <u>humid</u> chamber at room temperature
14-	PBS X 2	5-10 min
15-	PBS (use pipette gently)	1-2 min
16-	***Incubate primary antibody 1 µl/100 µl in solution of 2% (NGS) in PBS	Overnight (18 hr) at 4°C in <u>humid</u> chamber
17-	PBS X 2	5-10 min
18-	PBS (use pipette gently)	1-2 min
19-	Incubate secondary antibody , Rhodamine red goat anti-mouse 1µ /1000 µl of 2% (NGS) in PBS	1 hrs in <u>humid</u> chamber at room temperature. (with little boiling water)
20-	PBS X 3	5-10 min
21-	PBS (use pipette gently)	1-2 min
22-	Incubate with DAPI stain	20 min at room temperature
23-	Wash in PBS X 2	5 min
24-	PBS (using pipette gently)	1-2 min
25-	Wash with sterile distal water	2 min (in hood)
26-	Drop of mounting	-
27-	Cover slip	-
28-	Sealed with nail varnish	-

*cooking pot with water and place the beaker of antigen retrieval in it until it reaches the temperature of antigen retrieval solution up to 100°C then places the slides for 40 min as above.

**Prepare 0.25% triton in PBS mix well the add 5% of NGS.

***2 µl of NGS in 982 µl of PBS (100 µl total)

Table (6): immunohistochemistry staining of paraffin section. Mouse primary antibody; mouse on mouse (M.O.M) kit-vector labs PK-2200. 14.08.12

NO.	Solution	Time
1.	Xylene I	10 min
2.	Xylene II	
3.	Ethanol 100%	10 min
4.	Ethanol 95%	10 min
5.	Ethanol 70%	10 min
6.	Running water (gently)	10 min
7.	Place in hot * antigen retrieval solution at~100° c (PH6)	20 min
8.	Remove beaker to a shaker set	20 min
9.	Wash in running water (gently)	20 min
10.	Incubate in 3% H ₂ O ₂ (5ml H ₂ O ₂ + 45ml methanol) in coplin jar-wash in tap water running	5 min
11.	PBS**	5-10 min
12.	1 drop of M.O.M Ig blocking reagent in 3.6µl in 100 µl 1.25 PBS /150µl/9µl	30 min- 1hrs incubate in humid chamber /125µl 400µl PBS + 14.5µl
13.	PBS** X3	5-10 min
14.	** working solution of M O M diluent	5 min
15.	Primary antibody 1 µl/100 µl of M O M diluent	1hrs in humid chamber
16.	PBS** X3	5-10 min
17.	Secondary antibody (1 µl/250 µl of M O M diluents)	1hrs in humid chamber
18.	PBS** X3	5-10 min
19.	ABC reagents (1 drop of A to 1.25ml PBS mix gently then add 1 drop of B and mix gently)	30 min in humid chamber
20.	PBS**	5-10 min
21.	DAB reaction (3,3' diaminobenzidine)	30 sec-10 min/in coplin jar
22.	Running water (gently)	10 min
23.	Harris haematoxylin	5 min
24.	Rinse in running water until water runs clear	-
25.	Dip in 1% acid alcohol (HCL in 70% ethanol)	15 sec
26.	Rinse in running tap water	5 min
27.	Dehydrate: 70% ethanol	10 sec
28.	Ethanol 95%	10 sec
29.	Ethanol 100%	10 sec
30.	Ethanol 100%	10 sec
31.	Xylene	5 min
32.	Mount with DPX	1 min
33.	Put cover slide	

*sodium citrate retrieval/ 10mM sodium citrate buffer PH 6:

2.35g sodium citrate in 800 ml of water - add 400 µl of tween-20 (0.05%).

**prepare enough M O M diluent for primary and secondary antibody steps [80 µl of protein concentrate in 1ml PBS]

Table (7): Immunohistochemical staining of organotypic slice cultures

No.	Solution	Time
1.	Wash with PBS (use pipette)	10 min
2.	Permeabilize in 1% triton X-100 in PBS	Overnight at 4°C
3.	Wash with PBS (use pipette)	10 min
4.	Block with 20% bovine serum albumin with 0.1% triton X-100 in PBS	1.30hrs incubate in <u>humid</u> chamber at room temperature
5.	PBS X2	5-10 min
6.	Incubate primary antibody 1µl/100µl in solution of 1% (NGS) with 0.1% triton X-100 in PBS	Overnight (16-18hr) at 4°C in <u>humid</u> chamber
7.	Wash with PBS	1-2 min
8.	Incubate secondary antibody red goat anti-mouse (1µl/400µl of 5% (NGS) with 0.5% triton -100 in PBS)	3hrs in <u>humid</u> chamber at room temperature
9.	PBS (use pipette gently)	10 min
10	Incubate with DAPI stain	45 min at room temperature
11	Wash with PBS (use pipette gently)	10 min
12	Drop 5µl of mounting medium	-
13	Cover slip	-
14	Sealed with nail varnish	-
15	Stored in the dark	At 4°C for 12hr

Table (8): Immunohistochemical staining of organotypic slice cultures

No.	Solution	Time
1.	Wash with PBS X3	10 min
2.	Permeabilize in 0.5% triton X-100 in PBS	1hr incubate in <u>humid</u> chamber at room temperature
3.	Block with 10% bovine serum albumin with 0.5% triton X-100 in PBS	Overnight at 4°C
4.	PBS X3	5-10 each time
5.	Incubate primary antibody 1µl/150µl of 10% (NGS) with 0.5% triton-X100 in PBS (200µl for each well) 100µl/1ml (NGS)	Overnight (6-18hr) at 4°C in <u>humid</u> chamber
6.	Wash with PBS	20 min each time
7.	Incubate secondary antibody-rhodamin red goat anti-mouse (1 µl/200 µl of 10% (NGS) with 0.5% triton-X100 in PBS)	3hrs in <u>humid</u> chamber at room temperature
8.	PBS X3	20 min each
9.	Incubate with DAPI stain	20 min at room temperature
10	Wash in PBS X3	10 min each time
11	Drop 5 µl or so of mounting medium	-
12	Cover slip	-
13	Sealed with nail varnish	-
14	Stored in the dark	At 4°C for 12hr
15	All steps from 1-10 will perfume in wells inserts	-